Aminergic GPCR-Ligand Interactions

Vass, Márton; Podlewska, Sabina; De Esch, Iwan J.P.; Bojarski, Andrzej J.; Leurs, Rob; Kooistra, Albert J.; De Graaf, Chris

published in
Journal of Medicinal Chemistry
2019

DOI (link to publisher)
10.1021/acs.jmedchem.8b00836

document version
Publisher's PDF, also known as Version of record

Journal of Medicinal Chemistry

Perspective

Cite This: J. Med. Chem. 2019, 62, 3784−3839

pubs.acs.org/jmc

Aminergic GPCR−Ligand Interactions: A Chemical and Structural Map of Receptor Mutation Data

Márton Vass,[†,⊥] Sabina Podlewska,[‡,⊥] Iwan J. P. de Esch,[†] Andrzej J. Bojarski,[‡] Rob Leurs,[†] Albert J. Kooistra,[†,§] and Chris de Graaf*[,†,∥]

[†]Division of Medicinal Chemistry, Faculty of Sciences, Amsterdam Institute for Molecules, Medicines and Systems (AIMMS), VU University Amsterdam, 1081HZ Amsterdam, The Netherlands

[‡]Department of Medicinal Chemistry, Institute of Pharmacology, Polish Academy of Sciences, Smętna 12, PL31-343 Kraków, Poland

[§]Department of Drug Design and Pharmacology, University of Copenhagen, Universitetsparken 2, 2100 Copenhagen, Denmark

[∥]Sosei Heptares, Steinmetz Building, Granta Park, Great Abington, Cambridge CB21 6DG, U.K.

Supporting Information

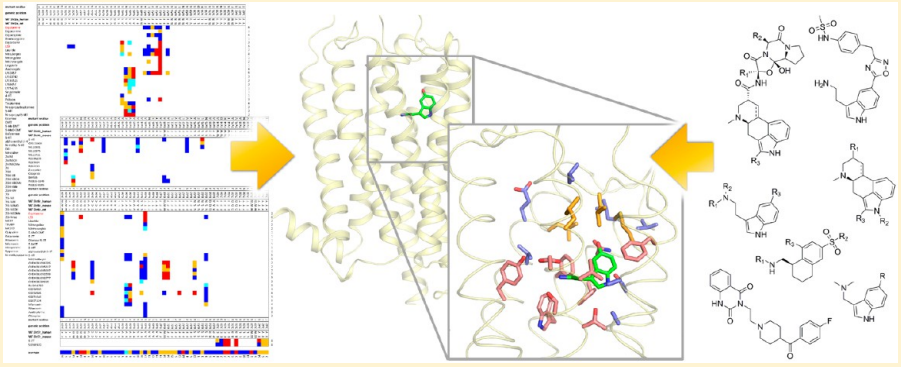

ABSTRACT: The aminergic family of G protein-coupled receptors (GPCRs) plays an important role in various diseases and represents a major drug discovery target class. Structure determination of all major aminergic subfamilies has enabled structure-based ligand design for these receptors. Site-directed mutagenesis data provides an invaluable complementary source of information for elucidating the structural determinants of binding of different ligand chemotypes. The current study provides a comparative analysis of 6692 mutation data points on 34 aminergic GPCR subtypes, covering the chemical space of 540 unique ligands from mutagenesis experiments and information from experimentally determined structures of 52 distinct aminergic receptor−ligand complexes. The integrated analysis enables detailed investigation of structural receptor−ligand interactions and assessment of the transferability of combined binding mode and mutation data across ligand chemotypes and receptor subtypes. An overview is provided of the possibilities and limitations of using mutation data to guide the design of novel aminergic receptor ligands.

1. INTRODUCTION

G protein-coupled receptors (GPCRs) are an important family of signal-transducing membrane proteins capable of binding various types of ligands from the extracellular space and activating various signaling pathways inside the cell, rendering them one of the largest protein target families in pharmaceutical research.[1] In 2007, the first nonrhodopsin GPCR was crystallized.[2] Currently, stabilizing mutations,[3,4] fusion constructs,[5,6] and the use of antibodies[7] allowed the crystallization of more than 50 different GPCR subtypes with various interacting partners and in different functional states, covering more than 183 unique receptor−ligand complexes.[8] This growing amount of structural information is invaluable for understanding GPCR function and the structural determinants of ligand binding and for structure-based design of novel ligands. Receptors of the aminergic GPCR family are particularly rewarding drug targets as they are implicated in neurotransmission, cognition, memory, mood and circadian cycle regulation, muscle, and broncho- and vasoconstriction. However, for the desired mode of action, often a specific selectivity or polypharmacological profile of the drug is needed (see Figure 1 for drugs known to act on multiple GPCRs discussed in this study). Among GPCRs, the aminergic family is the most extensively covered by structural biology studies, including crystal structures of 13 receptor subtypes and 40 different aminergic receptor−ligand complexes. Despite the availability of such structural data, these structures still

Received: May 26, 2018
Published: October 17, 2018

DOI: 10.1021/acs.jmedchem.8b00836
J. Med. Chem. 2019, 62, 3784−3839

Figure 1. Heat map of bioactivity profiles of multiaminergic GPCR drugs (compounds in rows with at least three activity values including K_D, K_i, IC_{50}, and EC_{50} at aminergic receptors in ChEMBL which have mutation data discussed in this paper) at all aminergic GPCRs (in columns). Heat map colors run from red (pAct = 13) to white (no measured activity, pAct = 0), no measurement is shown as gray cells.

represent only a fraction of the large number of known aminergic ligands (1−12 cocrystallized ligands vs 19−4758 ligands in ChEMBL[9] per receptor, see Table 1). Furthermore, the cocrystallized ligands in these complexes are chemically similar to only 10% of all known active ligands of aminergic receptors, rendering additional information necessary to uncover their binding modes.[10] The combination of crystal structure information with analyses of ligand structure−activity relationships (SAR), and receptor mutagenesis data can provide complementary information to enrich the knowledge on structural receptor−ligand information and to facilitate computational binding mode prediction of chemically dissimilar ligands as well.[11]

Site-directed mutagenesis (SDM) is a versatile and frequently employed tool in pharmacological investigations used to infer structural features of protein−ligand interactions. GPCR research has especially benefited from the large body of available mutational data.[12] Mutation studies complement structural information provided by crystal structures by defining the roles and relative importance of residues involved in binding, functional activity, and selectivity of a variety of receptor−ligand combinations, and thus an integrated analysis of these data is crucial.[13] Much of the early mutational data on GPCRs was collected in the TinyGRAP database,[14] but today the largest resource of GPCR sequence, structure, and mutation data is the GPCR database (GPCRdb, http://gpcrdb.org).[12,15−17] The GPCRdb also features structure-based sequence alignments[18] that enable the identification of structurally equivalent positions for large-scale analysis of data related to GPCR sequence. This database is constantly being improved by community contributions of manually curated and annotated mutagenesis data sets. The Pocketome database[19] also contains information about single-point mutations of crystallized proteins grouped by binding pocket homology. These data sources provide valuable information for medicinal chemists, molecular biologists, and computational chemists for various types of analyses. Community-wide GPCR structure modeling challenges (GPCR Dock 2008,[20] 2010,[21] and 2013[22]) have shown that the best models could be constructed by careful incorporation of mutation and SAR data relating to ligand binding.[23−25] However, a receptor family wide analysis is required to provide insights on a structural chemogenomics level and to complement available data in order to fill gaps in mutant−ligand matrices for single receptors. Such an analysis has been carried out for adenosine receptors[13] but not yet for the aminergic GPCR family. Although a large body of mutagenesis data has already been accumulated for the aminergic GPCRs, this information is still sparse considering all unexplored combinations of receptors, amino acid positions, mutations, and ligands. Through an exhaustive database and literature search, 6692 mutational data points were collected for 34 aminergic GPCR subtypes of eight species. This review provides a systematic overview of all mutation data of aminergic GPCRs, mapped on all currently available crystal structure information. The mutation data are described per binding pocket region observed in the different GPCR crystal structures: amine and major pocket, minor pocket, and extracellular vestibule (ECV) and are discussed in relation to ligand chemotypes and SAR (where sufficient ligands are available). This integrated analysis and presentation provides new insights into receptor regions more or less well characterized and allows translation of mutation data between aminergic receptors. To bridge the gap between crystal structures and mutation data for ligands for which no binding mode information is available, we have combined docking and interaction fingerprint (IFP) scoring approaches[26] to map the mutation data on validated binding modes of the ligands involved in mutation studies in complexes with crystallized aminergic receptors. We hypothesized that mutational effects may be transferable between ligands of similar binding modes in the increasingly complex cases of (i) the same receptor subtype, (ii) between receptor subtypes in the same subfamily with X-ray structures, or (iii) using homology models. By mapping the mutation effects on structure-based generic amino acid positions, we were able to identify interesting mutations that are missing from the current mutational repertoire of aminergic GPCR investigations and show that prediction of mutation effects is feasible, albeit with limitations.

2. MUTATIONAL DATA COLLECTION AND ANALYSIS

2.1. Mutational Data Collection. Data from equilibrium ligand binding experiments (saturation or displacement) on single amino acid mutants of 34 aminergic receptors were collected using references from the TinyGRAP database,[14] GPCRdb,[12,15−17] and PubMed search (with keywords "mutant(s)", "mutation(s)", "mutagenesis", "site-directed", and the respective receptor names). For the adrenergic α_{2C} and the trace amine TAAR1 receptors, no such data was found. For the sake of interpretability, our analysis: i) primarily focused on the annotation of the effects of single residue mutations on ligand binding affinity; ii) did not consider the effects of multiple simultaneous (double, triple, etc.) mutations; iii) did not systematically annotate mutational

DOI: 10.1021/acs.jmedchem.8b00836
J. Med. Chem. 2019, 62, 3784−3839

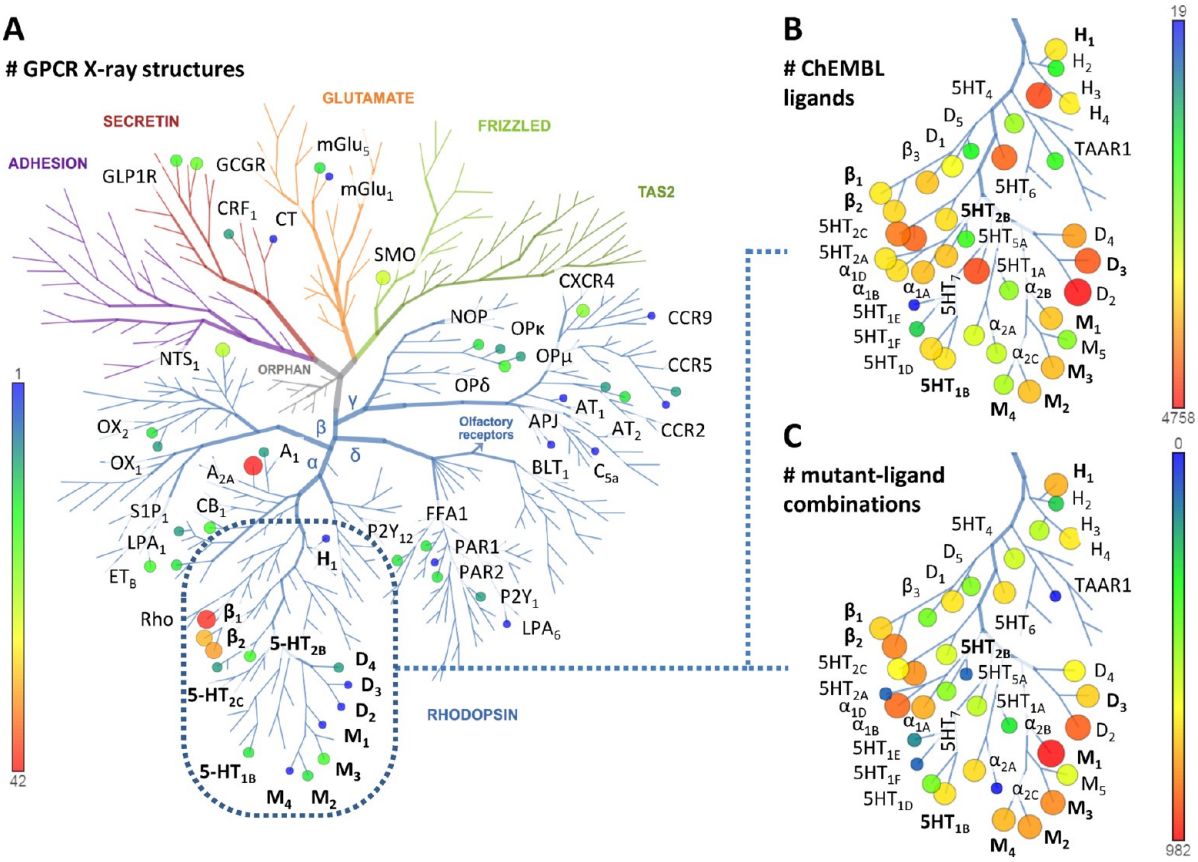

Figure 2. Structural and mutation data available for aminergic GPCRs. (A) Full GPCR phylogenetic tree color coded according to the number of unique crystal structure complexes. (B,C) The aminergic branch of the GPCR phylogenetic tree with mutation data statistics, circle sizes, and color coding according to the different data types. (B) Number of active ligands in ChEMBL (pAct > 6, activity types considered: EC_{50}, IC_{50}, K_D, K_i). (C) Number of unique mutant–ligand combinations in mutation studies.

effects on functional activity, but includes a description of similarities and differences between mutational effects on functional activity and binding affinity (e.g., section 8.5).

2.2. Mutational Data Annotation. The mutational effects on ligand binding were manually annotated in the mutation data submission format developed by GPCRdb,[12,15−17] including mutation position and type, ligand name and identifier, assay type and radioligand, mutational effect on ligand binding (expressed as wild-type and mutant ligand binding affinity or inhibitory constant, or fold effect, or qualitative effect), and, if available, receptor expression data (expressed as wild-type and mutant surface expression or fold expression, or qualitative effect). The collected data set was deposited in Zenodo[27] and uploaded to GPCRdb.[12,15−17] Statistics of the data set are shown in Figure 2 and Table 1. All mutational effects were then converted to mutant activity/wild-type activity and were discretized into four classes: <0.3 (increased), 0.3−3 (no effect), 3−10 (decreased), >10 (abolished). If more data points were available for a given point mutation−ligand pair, the geometric mean of the fold effect value was taken. To facilitate systematic comparison of structurally equivalent positions over multiple receptor subtypes, receptor residue numbers were annotated by their UniProt[28] numbers (for specific receptors) as well as their structure-based generic class A GPCR (Ballesteros−Weinstein[29]) residue number (as superscript).[18] This generic GPCRdb residue numbering scheme accounts for bulges and constrictions in the transmembrane helices, and defines residue numbers by their helix number, an "×" separator, and the residue number in the helix (50 denotes the most conserved residue).[18] $D^{3\times32}$, for example, is the characteristic aspartate in aminergic receptors, which is located in TM3, 18 positions before the most conserved residue in TM3 ($R^{3\times50}$). Bulges are denoted by an additional number after the preceding residue number, such as 5×461, and constrictions are skipped numbers relative to a normal helix. The most conserved residues of ECL1 and ECL2 are denoted as $W^{23\times50}$ and $C^{45\times50}$, respectively. As this review focuses on mutation effects on ligand binding, a consensus binding site was defined as a collection of residues annotated as ligand contacting residues in any aminergic receptor crystal structure by GPCRdb (see Figure 3).[15−17] This resulted in the following set of generic residue positions:

- amine pocket: 3×32, 3×36, 6×48, 6×51, 7×38, 7×42
- major pocket: 3×33, 3×37, 3×40, 4×56, 4×57, 5×39, 5×40, 5×43, 5×44, 5×461, 5×47, 6×44, 6×52, 6×55, 6×56
- minor pocket: 2×53, 2×56, 2×59, 2×60, 3×28, 3×29, 7×34, 7×35, 7×39, 7×41
- extracellular vestibule: 2×63, 2×64, 23×50, 45×50, 45×51, 45×52, 5×36, 5×37, 6×58, 6×59, 7×31.

Data points were annotated using the generic numbering system and selected for the consensus binding pocket, which allowed construction of heat maps of the mutation effects across receptor subtypes and even across the whole aminergic receptor family. Data analysis was carried out using a

DOI: 10.1021/acs.jmedchem.8b00836
J. Med. Chem. 2019, 62, 3784−3839

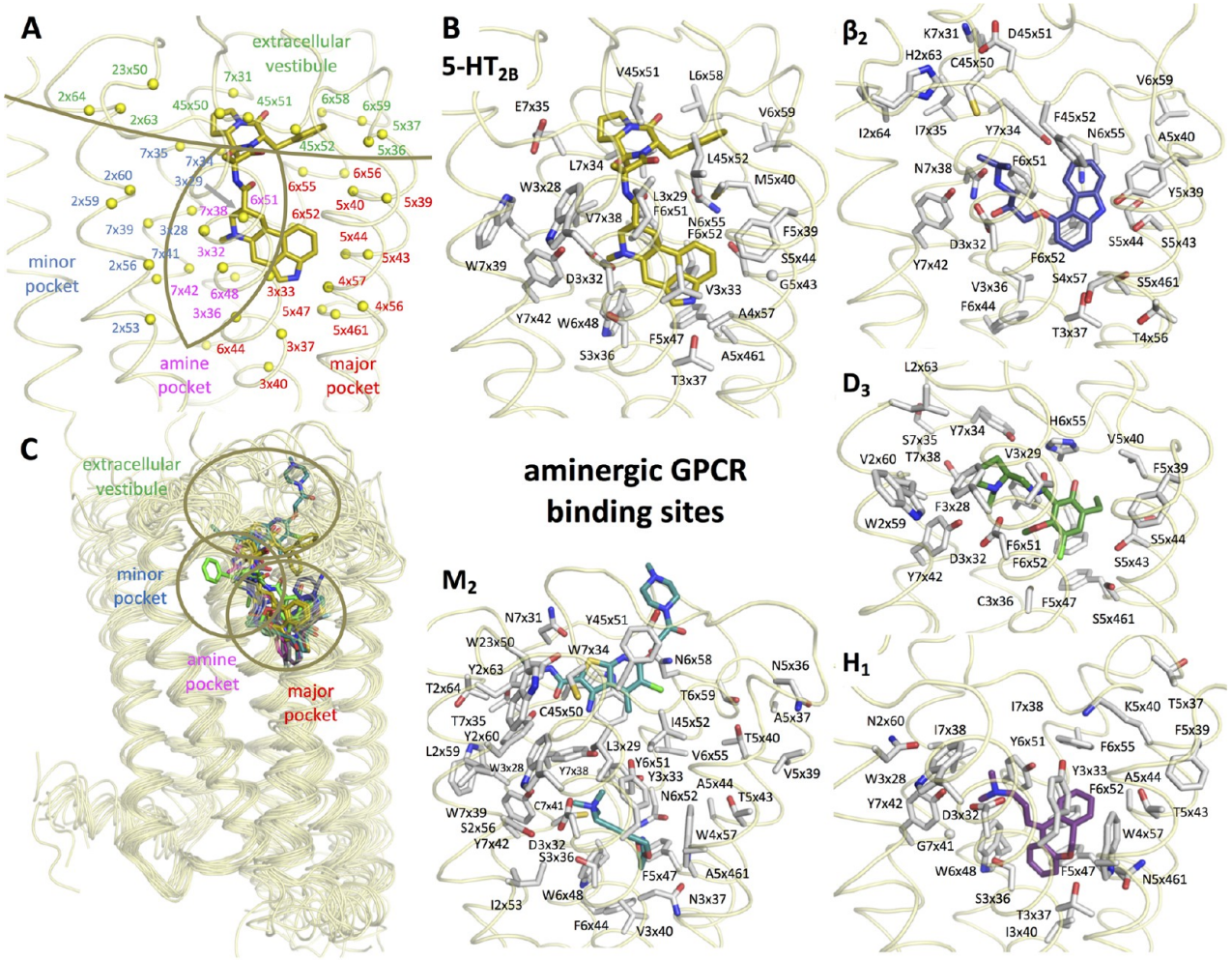

D

	2x53	2x56	2x59	2x60	2x63	2x64	23x50	3x28	3x29	3x32	3x33	3x36	3x37	3x40	4x56	4x57	45x50	45x51	45x52	5x36	5x37	5x39	5x40	5x43	5x44	5x461	5x47	6x44	6x48	6x51	6x52	6x55	6x56	6x58	6x59	7x31	7x34	7x35	7x38	7x39	7x41	7x42
human 5-HT$_{1B}$	V	V	I	S	Y	T	W	W	L	D	I	C	T	I	I	S	C	V	V	H	I	Y	T	S	T	A	F	F	W	F	F	S	L	M	P	L	F	D	T	W	G	Y
human 5-HT$_{2B}$	V	V	I	A	T	I	W	W	L	D	V	S	T	I	I	A	C	V	L	F	G	F	M	G	S	A	F	F	W	F	F	N	I	L	V	Q	L	E	V	W	G	Y
human 5-HT$_{2C}$	V	V	L	S	A	I	W	W	I	D	V	S	T	I	V	S	C	V	L	D	P	F	V	G	S	A	F	F	W	F	F	N	I	S	V	E	L	N	V	W	G	Y
human M$_1$	I	S	L	Y	Y	L	W	W	L	D	Y	S	N	V	L	W	C	Y	I	Q	P	I	T	T	A	A	F	F	W	Y	N	V	L	S	T	E	W	E	Y	W	C	Y
human M$_2$	I	S	L	Y	Y	T	W	W	L	D	Y	S	N	V	L	W	C	Y	I	N	A	V	T	T	A	A	F	F	W	Y	N	V	L	N	T	N	W	T	Y	W	C	Y
rat M$_3$	I	S	L	F	Y	I	W	W	L	D	Y	S	N	V	L	W	C	F	I	E	P	I	T	T	A	A	F	F	W	Y	N	V	L	N	T	K	W	N	Y	W	C	Y
human M$_4$	I	S	L	Y	Y	I	W	W	L	D	Y	S	N	V	L	W	C	F	I	N	P	V	T	T	A	A	F	F	W	Y	N	V	L	N	T	D	W	S	Y	W	C	Y
turkey β$_1$	M	V	F	G	L	V	W	W	T	D	V	V	T	I	V	S	C	D	F	N	R	Y	A	S	S	S	F	F	W	F	F	N	I	N	V	D	F	V	N	W	G	Y
human β$_2$	M	V	F	G	H	I	W	W	T	D	V	V	T	I	T	S	C	D	F	N	Q	Y	A	S	S	S	F	F	W	F	F	N	I	H	V	K	Y	I	N	W	G	Y
human D$_2$	V	V	W	V	L	E	W	F	V	D	V	C	T	I	I	S	C	I	I	N	P	F	V	S	S	S	F	F	W	F	F	H	I	N	I	P	Y	S	T	W	G	Y
human D$_3$	V	V	W	V	L	E	W	F	V	D	V	C	T	I	V	S	C	S	I	N	P	F	V	S	S	S	F	F	W	F	F	H	V	N	T	P	Y	S	T	W	G	Y
human D$_4$	L	V	L	F	S	E	W	L	M	D	V	C	T	I	V	A	C	R	L	D	R	Y	V	S	S	S	F	F	W	F	F	H	I	Q	A	P	V	S	T	W	G	Y
human H$_1$	V	V	M	N	Y	L	W	W	L	D	Y	S	T	I	-	W	C	E	T	V	T	F	K	T	A	N	F	F	W	Y	F	F	M	I	A	E	H	M	I	W	G	Y

Figure 3. (A) Location of the 42 consensus binding site amino acid residues analyzed in the present paper, spheres indicating Cα positions, the structure depicted is 5-HT$_{2B}$ 4IB4. (B) Binding site amino acids involved in mutation studies in serotonin, muscarinic acetylcholine, adrenergic, dopamine, and histamine receptors, the structures depicted are 5-HT$_{2B}$ (PDB: 4IB4[31]), M$_2$ (PDB: 4MQT[34]), β_2 (PDB: 2RH[12]), D$_3$ (PDB: 3PBL[38]), and H$_1$ (PDB: 3RZE[40]). (C) Location of ligand binding pockets (amine pocket, minor pocket, major pocket, extracellular vestibule) in aminergic GPCRs (PDB: 5-HT$_{1B}$ 4IAQ,[30] 5-HT$_{2B}$ 4IB4,[31] 5-HT$_{2C}$ 6BQH,[32] M$_1$ 5CXV,[33] M$_2$ 4MQT,[34] M$_3$ 4DAJ,[34] M$_4$ 5DSG,[33] β_1 4BVN,[36] β_2 2RH1,[2] D$_2$ 6CM4,[37] D$_3$ 3PBL,[38] D$_4$ 5WIU,[39] H$_1$ 3RZE[40]). (D) Ligand binding site residue alignment of crystallized aminergic GPCRs. Generic GPCRdb residue numbers[18] are colored according to the binding pockets defined in panel A, and residue positions in contact with a ligand in any crystal structure of the given receptor are marked gray.

customizable KNIME workflow, making use of the 3D-e-Chem[41,42] KNIME[43] nodes communicating with GPCRdb.[12,15−17] This workflow fetches the available mutation data and the mapping between UniProt and generic numbering for aminergic GPCRs from GPCRdb, calculates the fold effect and binning of the data, and then constructs the heat maps after customized data filters are applied. The KNIME workflow

DOI: 10.1021/acs.jmedchem.8b00836
J. Med. Chem. 2019, 62, 3784−3839

Table 1. Overview of the Collected Aminergic GPCR Mutation Data Set

Receptors[a]	Number of active ligands in ChEMBL[a]	Number of data points	Number of mutants (orthologs aggregated)[b]	Number of positions[c]	Number of unique ligands	Unique mutant-ligand combinations (orthologs aggregated)[b]	Redundancy (%)[d]	Completeness (%)[e]
All	26515	6692	1306 (748)	316	540	5445 (4934)	19 (26)	0.8 (1.2)
Serotonin	11034	1026	206 (137)	83	146	889 (797)	13 (22)	3 (4)
5-HT_{1A} (h,r)	3271	68	19 (19)	14	23	49 (49)	28 (28)	11 (11)
5-HT_{1B}	966	159	25	21	26	123	23	19
5-HT_{1D} (h,d,g)	1063	28	9 (9)	8	13	24 (24)	14 (14)	21 (21)
5-HT_{1E}	19	3	1	1	3	3	0	100
5-HT_{1F}	104	2	1	1	2	2	0	100
5-HT_{2A} (h,r)	3113	350	52 (48)	32	73	306 (295)	13 (16)	8 (8)
5-HT_{2B} (h,m)	1122	69	29 (28)	28	3	65 (64)	6 (7)	75 (76)
5-HT_{2C} (h,r)	2298	117	16 (15)	11	31	96 (95)	18 (19)	19 (20)
5-HT_4 (h,m)	464	63	16 (16)	14	14	58 (58)	8 (8)	26 (26)
5-HT_{5A}	191	2	2	2	1	2	0	100
5-HT_6 (h,m,r)	2694	135	21 (18)	15	29	131 (131)	3 (3)	22 (25)
5-HT_7 (h,m)	1387	30	15 (15)	10	7	30 (30)	0 (0)	29 (29)
Muscarinic	2654	2333	533 (392)	235	106	1877 (1602)	20 (31)	3 (4)
M_1 (h,m,r)	1312	1214	265 (240)	182	70	1023 (982)	16 (19)	6 (6)
M_2 (h,p,r)	1336	335	61 (57)	42	42	269 (257)	20 (23)	10 (11)
M_3 (h,r)	1384	383	102 (97)	64	27	318 (314)	17 (18)	12 (12)
M_4 (h,m)	466	303	47 (47)	43	10	196 (196)	35 (35)	42 (42)
M_5	326	71	58	16	3	71	0	41
Adrenergic	4280	1593	314 (260)	134	125	1315 (1247)	17 (22)	3 (4)
α_{1A} (h,r)	1435	273	23 (22)	19	45	215 (215)	21 (21)	21 (22)
α_{1B} (h,ham)	1089	500	144 (141)	70	34	433 (427)	13 (15)	9 (9)
α_{1D}	1051	2	1	1	2	2	0	100
α_{2A} (h,m,p)	623	220	21 (19)	11	39	138 (136)	37 (38)	17 (18)
α_{2B}	359	8	1	1	8	8	0	100
β_1	888	149	27	20	21	149	0	26
β_2 (h,ham,r)	1099	414	90 (86)	58	42	347 (343)	16 (17)	9 (9)
β_3 (h,m)	1324	27	7 (7)	7	9	23 (23)	15 (15)	37 (37)
Dopamine	6698	1274	154 (128)	70	131	982 (931)	23 (27)	5 (6)
D_1 (h,mac,r)	758	138	29 (28)	24	21	123 (122)	11 (12)	20 (21)
D_2 (h,m,r)	4758	751	83 (78)	52	80	537 (528)	28 (30)	8 (8)
D_3	3436	249	29	21	48	196	21	14
D_4 (h,r)	1982	106	9 (9)	9	34	98 (98)	8 (8)	32 (32)
D_5	142	30	4	3	12	28	7	58
Histamine	4910	466	99 (83)	45	60	382 (368)	18 (21)	6 (7)
H_1 (h,g)	963	251	53 (49)	28	35	214 (208)	15 (17)	12 (12)
H_2	125	6	4	3	2	6	0	75
H_3	3255	60	9	9	11	46	23	46
H_4	936	149	33	22	16	116	22	22

[a]Receptor orthologues: h = human, r = rat, m = mouse, d = dog, g = guinea pig, *p* = pig, ham = hamster, mac = macaque. Number of active ligands in ChEMBL (pAct > 6, activity types considered: EC_{50}, IC_{50}, K_D, K_i) determined for the human orthologue. [b]Number of mutants defined as the number of unique combinations of the generic position number from GPCRdb[18] (or UniProt number when that is not defined) and the amino acid type in the mutant, in brackets the number of mutants are aggregated for the orthologues; note that in this case the wild-type residues may differ. [c]Number of positions defined as the number of unique generic position numbers from GPCRdb[18] (or UniProt numbers when that is not defined). [d]Redundancy defined as the percentage of data points exceeding the number of unique mutant−ligand combinations. [e]Completeness defined as the number of unique mutant−ligand combinations divided by the product of the number of mutants and the number of ligands for that receptor.

and workflow scheme are included in the Supporting Information.

2.3. Mutation Data Analysis. The obtained collection of mutational data points was analyzed to provide insights into the extent of mutational coverage of all receptors, amino acid positions, and ligands. Altogether, 6692 data points were collected for the 34 aminergic receptor subtypes. Data for the human orthologue was available for all of these receptors. For 12 receptors, data for one additional species and for eight receptors data for two additional species could also be incorporated (see Table 1). Although bioactivity data or mutational effects might vary for different species, in this study these data have been combined because crystal structures used for docking for solely one species per receptor were available. The distribution of the amount of information available for particular receptor subtypes (Table 1) showed that the highest

DOI: 10.1021/acs.jmedchem.8b00836
J. Med. Chem. 2019, 62, 3784−3839

number of data points was available for muscarinic acetylcholine receptors (2333 data points), with the M_1R providing the highest contribution to this number (1214 data points). The number of mutants these data correspond to was assessed in two ways. First, mutants were defined by the receptor, species, sequence-specific position, and introduced amino acid. Second, mutants were defined by receptor, generic position (from GPCRdb),[18] and introduced amino acid. The former allowed for simple summation of mutants in subfamilies and the whole data set, while the latter allows for the assessment of the number of different types of mutations carried out across receptor subtypes and subfamilies. From the comparison of the two numbers, it can be seen that the same mutations for different species have rarely been introduced (0−14% overlap). From the inspection of the original publications, it is also seen that research groups often work only with a single species throughout several publications and the overlap between efforts of different groups working on different species is understandably small. However, often exactly those positions are mutated that make up the difference between sequences of different species. For the different aminergic receptor subfamilies, 16−42% of the mutations defined by generic position have been performed on more than one subtype. Also, the number of generic positions regardless of introduced amino acid were enumerated. For most subtypes, the average number of mutations per position was between one and two, but for M_5R, for example, this ratio was 3.6. For the whole data set, the average number of introduced amino acids was 2.3. In the whole set, mutational data for 316 unique positions were found, accounting for 71% of the average length of the aminergic receptor sequences. The number of unique ligands was assessed based on the unique ligand identifiers in the data set (ChEMBL ID,[9] PubChem CID,[44] FASTA sequence, or SMILES string). The overlap between ligand sets of the different subtypes within subfamilies was 30−38% for the serotonin, muscarinic, adrenergic, and dopamine receptors, but it was only 6% for histamine receptors (histamine, thioperamide, and clobenpropit were used for multiple receptors). The number of mutants assessed in both described ways and the number of unique ligands were combined to obtain the number of unique mutant-ligand combinations. A ratio of this number and the number of data points allowed for the estimation of the redundancy of data points for each subtype and subfamily, which ranged from 0% to 38% (for the α_{2A} receptor). These redundant data points either come from the same publication (66%) being different data types (radioligand K_D and competition K_i) or multiple data points for the same measurement (e.g., low and high-affinity receptor states), or they come from different publications (34%), being again different data types or using a different radioligand. The ratio of the number of unique mutant−ligand combinations and the product of the number of mutants and ligands was also calculated, that is, what percent of the heat maps for each receptor subtype is filled with known mutation effect data, which we call the completeness of the data subsets. Except for some receptors with very few data points, the completeness varied from 8% to 76%. When completeness for the subfamilies was assessed, this dropped to 3−7% because of the low overlap of the employed mutations for the different subtypes. Finally, this further drops to about 1% completeness when the whole data set is considered, meaning that the full GPCR mutation heat map is very sparse, with small well-filled areas and large empty areas.

In the whole data set of 5445 unique receptor mutation−ligand combinations, there are 862 mutant−ligand combinations for which multiple data points are available. Out of these, 230 cases (116 in the binding site and 114 in another region of the receptor) covered mutational effects across different classes (fold <0.3 increased effect, 0.3−3 no effect, 3−10 decreased effect, >10 lost effect). Only 47 mutant−ligand combinations cover nonadjacent classes. The highest discrepancy is observed for acetylcholine and *N*-methylscopolamine (NMS) in human and rat M_1 receptors, for which both increased an decreased effects are reported for specific mutant−ligand combinations. The highest number of mutant−ligand combinations with multiple data points were observed for human M_1 (117 of which 67 assigned to different classes), human M_4 (104 of which 1 in different classes), and rat D_2 (93 of which 32 in different classes) receptors. Uncertain data points with multiple class effects are indicated with a cross in the heatmaps, but the geometric mean of all data is used for depiction. Data discrepancy may originate from several factors: intra- and interlaboratory variation in assay conditions, different radioligands used, and different receptor constructs used. For some receptor mutants, different effects were reported for different radioligands. For example, $F185^{4\times61}A$ and $S344^{6\times55}A$ mutants of human 5-HT_{1B} result in a 6-fold decrease and a 4-fold increase of 5-HT affinity in [^{3}H]5-HT radioligand displacement assays but do not affect 5-HT affinity in [^{3}H]GR125743 displacement studies.[45,46] In [^{3}H]5-CT and [^{3}H]5-HT radioligand displacement studies, the $T362^{7\times38}N$ mutant of 5-HT_{1B} caused the same 8-fold decrease of methysergide affinity but resulted in 6- vs 15-fold decrease in sumatriptan affinity, respectively.[47,48] The $S196^{5\times38}L$ mutant of 5-HT_{1D} resulted in 3- vs 7-fold decrease in ketanserin binding in [^{3}H]5-CT and [^{3}H]GR125744 displacement studies, respectively.[49] Different radioligands gave similar mutational effects for rat 5-HT_{2A} ([^{125}I]DOI, [^{3}H]ketanserin),[50] rat 5-HT_{2C} ([^{3}H]5-HT, [^{3}H]mesulergine), human muscarinic M_1 ([^{3}H]QNB, [^{3}H]NMS),[51−53] and human adrenergic α_{1A} studies ([^{3}H]prazosin, [^{3}H]KMD-3213).[54]

The residues involved in mutational data points were labeled either as ligand-contacting or noncontacting residues. In total 49% of the whole mutational effect data set (3338 data points) covers residues that are involved in protein−ligand interactions in currently available crystal structures of the corresponding aminergic receptor subfamilies (Figure 3). It should be noted however, that at the time of the original publications, these positions were mostly hypothesized. Using the consensus binding pocket definition, 55% of the data set was classified as representing protein−ligand interaction data. The most mutated amino acid positions outside the ligand binding pocket were 6×34 in the intracellular end of TM6 with 369 data points, then 2×50, 3×49, and 3×50 with over a hundred data points each (section 8.4). The number of known crystal contacts is 305 (gray cells in Figure 3), of which 153 (50%) have already been investigated in mutational studies. No observed ligand binding amino acid positions have yet been mutated in the 5-$HT_{1E/1F}$ and H_2 receptors, and only one of those positions have been mutated for the 5-HT_{1D}, α_{1D}, and β_3 receptors. The obtained mutagenesis data were mapped to the amino acid residues making contacts in crystallized aminergic GPCRs, presented in the form of heat maps (Figures 5, 8, 11, 14, 17), and the ligands involved in mutation studies are shown in Figures 6, 9, 12, 15, and 18. The color codes in the heat maps refer to the fold mutation effects, that is, the ratio of K_i

DOI: 10.1021/acs.jmedchem.8b00836
J. Med. Chem. 2019, 62, 3784−3839

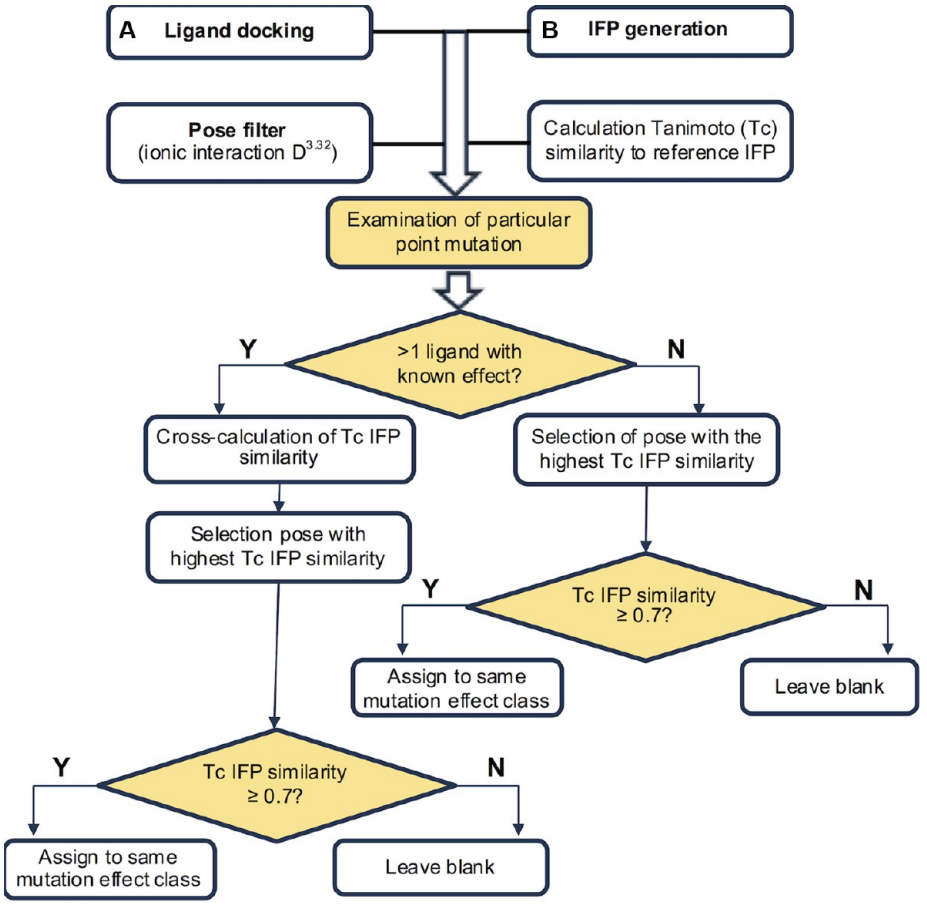

Figure 4. Structural receptor−ligand interaction fingerprint (IFP) similarity based receptor mutation data mapping flowchart for the prediction of receptor mutation effects. (a) PLANTS[58,59] docking; (b) structural interaction fingerprint (IFP) analysis.[26]

MUT/K_i WT (wild type) below 0.3 (cyan), between 0.3 and 3 (blue), between 3 and 10 (yellow), and above 10 (red). For selected examples, mutation effects were mapped on structures including a cocrystallized ligand (or a very similar ligand), the modeled binding mode of the endogenous ligand, and the modeled binding mode of a drug-like ligand with relative high number of mutation data points for each receptor subfamily (Figures 7, 10, 13, 16, 19).

2.4. Structure-Based Extrapolation of Mutational Data. Opportunities to map and extrapolate mutational data across different receptor−ligand complexes were assessed by combining mutation data mining with structural interaction fingerprint based binding mode prediction based on aminergic receptor crystal structures.

2.4.1. Docking. All available crystal structures for aminergic GPCRs were fetched from the PDB database[55] and manually cleaned from additional entities so that only the protein and the cocrystallized ligand remained. Sets of ligands used in mutational studies associated with particular receptor subtypes and species were prepared for docking: their possible tautomeric and protonation states were calculated with the Calculator[56] from the ChemAxon package. Three-dimensional conformations of the structures were then generated with the use of Molecular Networks' Corina[57] software. Docking was performed using PLANTS[58,59] (version 1.2), and for each ligand 25 poses were produced (speed setting 2) and were scored using the ChemPLP scoring function. The binding pockets were defined in a consensus way taking into account all amino acid positions contacting any cocrystallized ligands in the aminergic GPCR crystal structures within 5 Å. This selection resulted in 53 amino acid positions for all considered targets (1×35, 1×39, 2×53, 2×551, 2×56, 2×59−64, 3×25, 3×28, 3×29, 3×32, 3×33, 3×36, 3×37, 3×40, 4×56, 4×57, 4×59, 4×60, 45×50−52, 5×39−45, 5×461, 5×47, 6×44, 6×48, 6×51, 6×52, 6×54−56, 6×58, 6×59, 7×30, 7×31, 7×33−35, 7×38, 7×39, 7×41, 7×42 in generic GPCRdb numbering[18]). For muscarinic receptors, orthosteric ligands were distinguished from allosteric ones, and additional docking to the allosteric site was performed based on amino acids contacting the allosteric ligand in the M_2 structure with PDB 4MQT.[34] All obtained ligand−receptor complexes were represented using interaction fingerprints (IFP),[26] with bits characterizing interaction of ligands with each of the amino acids of the binding pocket (7 bits per position: hydrophobic, aromatic (2 bits), H-bond (2 bits), ionic (2 bits)) allowing for a fingerprint of 371 bits. The poses that did not possess a required H-bond or ionic interaction with the conserved aspartate $D^{3\times32}$ in aminergic receptors were filtered out, and the remaining ones were ranked according to descending Tanimoto coefficient (Tc) values to the reference IFP (calculated for the ligand cocrystallized with particular crystal structure). Thereafter, IFPs of ligands with a Tc value over a certain cutoff were used in a second round as reference IFPs, and poses with IFP similarity to any of these reference IFPs above the same Tc value cutoff were also selected (the grid search-based optimization of the Tc value cutoff for the procedure was carried out in the range of 0.6−0.9 with a step of 0.05; the lower bound was set on the basis of generally the

DOI: 10.1021/acs.jmedchem.8b00836
J. Med. Chem. 2019, 62, 3784−3839

accepted cutoff for overall pose similarity).[26] This two-step pose selection protocol allowed identification of plausible poses for most docked orthosteric ligands even when the IFP similarity to the cocrystallized ligand was lower than the predefined cutoff due to, e.g., size difference of the ligands. After the sensitivity assessment part in the subtype specific studies, an IFP similarity cutoff of 0.7 was used for all steps (Figure 4).

2.4.2. Prediction of Mutational Effects. After construction of the mutation effect heat maps for all receptor subtypes, retrospective studies were conducted using leave-one-out experiments, in which all data points were separately removed and predicted from the remaining data set. From each mutant−ligand pair, the examined ligand was assigned to the mutational effect class of the compound which had a known effect at the examined mutant and to which it had the highest IFP similarity unless the similarity coefficient was lower than the assigned similarity threshold (Figure 4). The prediction power of the protocol was evaluated by accuracy expressed as the ratio of the number of correct mutational effect class predictions and the number of predictions plus the number of cases where a prediction could not be made (blank fields) due to lack of ligands with a known mutational effect and IFP similarity above the imposed threshold. Leave-one-out accuracy of the method was assessed, and mutational effects were prospectively predicted in the same manner as for the retrospective evaluation.

3. SEROTONIN RECEPTORS

3.1. Structural Serotonin Receptor−Ligand Interactions. Serotonin receptors are activated by the small neurotransmitter serotonin or 5-hydroxytryptamine (5-HT). In humans, there are 12 5-HT receptor subtypes, of which three (5-HT_{1B}, 5-HT_{2B}, and 5-HT_{2C}) have currently been crystallized.[30,31,60,61] The ergotamine and dihydroergotamine bound 5-HT_{1B} (PDB: 4IAR, 4IAQ[30]), the ergotamine and lysergic acid diethylamide (LSD) bound 5-HT_{2B} (PDB: 4IB4,[31] 4NC3,[60] 5TUD,[62] 5TVN[61]), and the ergotamine bound 5-HT_{2C} (PDB: 6BQG[32]) crystal structures show a conserved binding mode of the ergoline scaffold in the orthosteric pocket, covering residues in the amine pocket ($D^{3\times32}$, $C/S^{3\times36}$, $W^{6\times48}$, $F^{6\times51}$, $T/V^{7\times38}$, $Y^{7\times42}$) and major pocket ($I/V^{3\times33}$, $T^{3\times37}$, $I^{3\times40}$, $I/V^{4\times56}$, $F/Y^{5\times39}$, $T/M/V^{5\times40}$, $G/S^{5\times43}$, $S/T^{5\times44}$, $A^{5\times461}$, $F^{6\times52}$, $S/N^{6\times55}$). The butterfly shaped diaromatic scaffolds of methiothepin in 5-HT_{1B} (PDB: 5V54[63]) and ritanserin in 5-HT_{2C} (PDB: 6BQH[32]) mainly contact the same residues, only the *p*-fluorophenyl moiety of ritanserin reaches into a deeper pocket additionally forming aromatic interactions with $F223^{5\times47}$ and $F320^{6\times44}$ in the major pocket in 5-HT_{2C}. The interaction patterns with different residues targeted in the minor pocket and extracellular vestibule ($A/S^{2\times60}$, $Y/T/A^{2\times63}$, $W^{3\times28}$, $L/I^{3\times29}$, $V^{45\times51}$, $V/L^{45\times52}$, $M/L/S^{6\times58}$, $P/V^{6\times59}$, $L/Q/E^{7\times31}$, $F/L^{7\times34}$, $D/E/N^{7\times35}$) of 5-HT_{1B}, 5-HT_{2B}, and 5-HT_{2C} by the tripeptide appendages of cocrystallized ergotamine and dihydroergotamine, the thiazolopyrimidinon appendage of ritanserin, as well as other dualsteric ligands (i.e., ligands interacting with both the orthosteric binding pocket and the extracellular vestibule), determine the ligand-dependent structure−affinity, −function, and −selectivity relationships of serotonin receptors.[64] Serotonin receptor crystal structures are generally similar to each other per subtype, but there is some variation among subtypes seen in the extracellular tips of TM helices and ECL2 conformation. The average heavy atom RMSD for 5-HT_{1B}, 5-HT_{2B}, and 5-HT_{2C} receptor subtypes are 1.3, 0.9, and 1.4 Å, respectively. The average backbone RMSD for these subtypes are 0.8, 0.5, and 1.0 Å, respectively. The average backbone RMSD for all 5-HT receptors is 1.2 Å, with the largest difference of 1.9 Å between the methiothepin-bound 5-HT_{1B} and the LSD-bound 5-HT_{2B} (Figures 3, 7, 20). In this case, the extracellular tips of helices TM4−7 are shifted about 2−2.5 Å relative to each other. The structures with ergoline derivatives show a conserved binding mode of the ergoline scaffold, only LSD is shifted 1.5 Å higher in the binding site relative to the other ligands. The upper aromatic moieties of methiothepin and ritanserin overlap with that of the ergoline scaffold, and their lower aromatic moiety reaches further toward the hydrophobic core of the receptors, facilitated by a rotamer change of $I^{3\times40}$. In the ECV, the benzyl appendage of ergotamine and dihydroergotamine adopts different orientations in 5-$HT_{1B/2B}$ due to divergent amino acids $T/M^{5\times40}$ and $M/L^{6\times58}$. The ECV appendage of ritanserin is shifted toward TM7 relative to ergotamine due to ECL2 protruding more toward the binding site. In the amine pocket, $D^{3\times32}$ forms an ionic interaction with the amine group of basic ligands including tryptamine derivatives, phenylethylamine derivatives, and arylpiperazines. Residues $C/S^{3\times36}$ and $Y^{7\times42}$ stabilize the conformation of $D^{3\times32}$ and residues $W^{6\times48}$ and $F^{6\times51}$ form cation−π interaction with basic ligands. These findings are consistent with mutation studies (section 3.3.1) and SAR studies showing the essential role of the cationic properties of the amine group of ergoline ligands and other serotonin receptor ligands. The ergoline scaffold of the cocrystallized ligands ergotamine, dihydroergotamine, and LSD, and the diaromatic scaffolds of methiothepin and ritanserin, make hydrophobic interactions with $I/V^{3\times33}$, $I^{4\times56}$, $F^{5\times47}$, $F^{6\times44}$, $F^{6\times51}$, $F^{6\times52}$, $F/Y^{5\times39}$, and $T/M^{5\times40}$ and form H-bond interactions with $T^{3\times37}$ or the backbone carbonyl of $G/S^{5\times43}$ in the major pocket between TM3−6. Mutation studies demonstrate the important role of these hydrophobic and polar residues (section 3.3.2) and SAR studies demonstrate the preference of serotonin receptors for ligands with aromatic moieties substituted optionally with a polar H-bond interaction functionality, mimicking the 5-hydroxy-indole group of the endogenous ligand. In 5-HT_6, the mutation of $S/N^{6\times55}$ underlines the important role of this residue in recognizing prototypical sulfonamide ligands, including SB258585, CHEMBL1085617 and CHEMBL1086326. In the minor pocket and extracellular vestibule, the tripeptidic appendage of the cocrystallized ergoline ligands forms H-bonds with the backbone of $V/L^{45\times52}$ and other polar residues such as $Y/T^{2\times63}$, $L/Q^{7\times31}$, and $D/E^{7\times35}$ are available for polar interactions with appendages of dualsteric ligands including ketanserin, buspirone, ipsapirone, and risperidone. However, such mutant−ligand combinations have not yet been investigated experimentally.

3.2. Chemical Space of Serotonin Receptor Ligands in Crystal Structures and Mutation Studies. The cocrystallized serotonin receptor agonists ergotamine (44 mutants, Figure 7), dihydroergotamine (1 mutant), LSD (50 mutants), the antagonists methiothepin (24 mutants), and ritanserin (9 mutants), as well as the endogenous 5-HT (138 mutants, Figure 7) have been extensively investigated in mutation studies of serotonin receptors 5-$HT_{1A/1B/2A/2B/2C/6/7}$ (Figure 5) covering 30 different residues in total, of which 24 are within the binding site as observed in serotonin receptor

DOI: 10.1021/acs.jmedchem.8b00836
J. Med. Chem. 2019, 62, 3784−3839

crystal structures (Figure 3).[30] Sixteen (11%) of the ligands investigated in mutation studies are chemically similar (defined throughout this paper as having a MACCS[65] Tanimoto similarity ≥0.8 or an ECFP-4[66] Tanimoto similarity ≥0.4) and 20 (14%) are pharmacophorically similar (ROCS[67] ComboScore ≥1.5) to any of the cocrystallized ligands (Figure 6). Nine ligands investigated in serotonin receptor mutation studies contain the endogenous 5-hydroxytryptamine scaffold, and 31 further ligands contain the tryptamine substructure that is also part of the ergoline scaffold of the cocrystallized ligands. 5-Hydroxytryptamine and other tryptamine agonists cover 176 (20%) and 270 (31%) ligand mutant combinations, respectively. Methoxyphenyl-ethanamines (including mescaline analogues DOM, DOB, DOI, and 2,4- and 2,5-dimethoxyphenyl-ethanamines) and aminergic sulfonamides (L-694,247 and SB269970) have been investigated at 146 ligand mutant combinations in total (17%). Most of these compounds do not share 2D chemical or 3D shape/pharmacophore-based similarity with cocrystallized serotonin receptor ligands but represent combined ligand and receptor SAR data sets that provide detailed information on the structural determinants of serotonin receptor binding. Moreover, 14 ligands are chemically similar to cocrystallized ligands in adrenergic $\beta_{1/2}$ complexes (section 5), including antagonist methoxyphenyl-ethanamines, iodocyanopindolol, penbutolol, alprenolol, propranolol, pindolol, and labetalol.[47,68−72] The serotonin receptor agonists cisapride and zacopride are similar to cocrystallized nemonapride[39] in dopamine D_4, and risperidone[37] is cocrystallized in dopamine D_2 (section 6). The serotonin receptor antagonist/inverse agonist amitriptyline is furthermore similar to cocrystallized doxepin in the H_1 crystal structure[40] (section 7), whereas the serotonin receptor agonists MCPP, TFMPP, quizapine, and MK-121 are similar to the cocrystallized fragment-like piperazine ligands of the β_1 adrenergic receptor (section 5).[73] Several nonselective aminergic receptor ligands including clozapine, spiperone, ketanserin, chlorpromazine, lisuride, and haloperidol have been investigated altogether at 44 different serotonin receptor mutants as well as mutants at other receptor subfamilies. For example, clozapine has been investigated in serotonin, muscarinic, dopamine, and histamine receptor mutation studies, providing insights into the receptor specific determinants of binding of these ligands by different aminergic GPCRs.

3.3. Structural Determinants of Serotonin Receptor−Ligand Interactions. *3.3.1. Amine and Major Pocket Mutations in Serotonin Receptors.* Mutation of conserved $D^{3\times32}$ to nonacidic residues ($D^{3\times32}$A/N/Q) has been shown to diminish binding of 12 cationic ligands to three different serotonin receptors, including 5-HT (5-HT_{1A}, 5-HT_{2A} 5-HT_4), LSD (5-HT_4), gramine (5-HT_{1A}), DMT (5-HT_{1A}), DOI (5-HT_{2A}), ketanserin (5-HT_{2A}, Figure 7), mianserin (5-HT_{2A}), spiperone (5-HT_{2A}), ML10302 (5-HT_4), ML10375 (5-HT_4), RO116-1148 (5-HT_4), and CHEMBL1086326 (5-HT_6).[68,74−81] The $D155^{3\times32}$E mutation conserving the acidic feature does not significantly affect rat 5-HT_{2A} binding affinity of the agonists 5-HT and gramine and the antagonist spiperone, indicating that an ionic interaction with the anionic carboxylate group of $D155^{3\times32}$ is required and sufficient for ligand binding.[77] The $D106^{3\times32}$A mutant diminishes 5-HT_6 binding affinity for the basic sulfonyl-tetrahydronaphtalene amines CHEMBL1085617, CHEMBL1086326, and CHEMBL10825037 but does not affect binding of the neutral amide analogues CHEMBL1082508 and CHEMBL1087777, confirming the important role of the cationic amine moieties on the ligand side and their interaction with the anionic $D^{3\times32}$ residue.[80] 5-HT_{1A} affinity of the partial agonist pindolol is not affected by the $D116^{3\times32}$N mutant but is decreased by the $N^{7\times38}$V mutant,[68−70] indicating that this residue is an important interaction partner for the ethanolamine moiety of pindolol, consistent with the binding mode of pindolol and cyanopindolol in β_1 adrenergic and β_2 adrenergic receptor crystal structures (section 5.1). The binding affinity of antagonist GR113808 for 5-HT_4 is not affected by the $D100^{3\times32}$A or $D100^{3\times32}$N mutants but is significantly decreased by the $Y302^{7\times42}$F mutant. The same mutant decreases the affinity of RS395604, which shares a piperidine-ethyl-sulfonamide substructure with GR113808 but does not affect binding of other ligands (ML11411, RS100235), suggesting that $Y302^{7\times42}$ may play a role in an alternative H-bond interaction network with the amine or sulfonamide groups of GR113808 and RS395604.[82,83] The $D106^{3\times32}$A mutant increases the affinity of agonist BIMU8 for 5-HT_6,[79] indicating that this mutation may create space for binding of the bulky methyl-aza-bicyclo-octane moiety of this ligand. Mutations of the conserved aromatic $W^{6\times48}$, $F^{6\times51}$, and $F^{6\times52}$ residues lining the major pocket have variable, ligand-dependent effects on binding to serotonin receptors.[72,84] Whereas the affinity of ligands such as lisuride, mesulergine, LY53857, 5-MeO-DMT, ketanserin, substituted dimethoxyphenyl-ethanamines (5-HT_{2A}), LSD, and 5-HT (5-HT_{2B}), substituted sulfonyl-tetrahydronaphtalene amines (5-HT_6) is diminished by mutation of $W^{6\times48}$/$F^{6\times51}$/$F^{6\times52}$, the binding of ligands ergotamine, LSD, 5-HT, RO116-1148 (5-HT_{1B}, 5-HT_4), and ergotamine (5-HT_{2B}) is not affected or is even increased by mutation of these residues, respectively. The $V136^{3\times33}$A mutation on the other face of the indole ring of the cocrystallized ligands is detrimental to LSD and 5-HT binding in 5-HT_{2B}.[30] Mutation of the aromatic residue F/$Y^{5\times39}$ located above $V^{3\times33}$ to alanine also reduces binding of LSD and 5-HT to 5-HT_{2B} but increases that of ergotamine.[30] Furthermore, the $M218^{5\times40}$A mutation in 5-HT_{2B} also increases binding of ergotamine. It seems that despite the low nanomolar affinity of ergotamine to 5-HT_{2B}, the fit of the ergoline scaffold is not optimal in this ligand−receptor complex. Furthermore, this residue is phenylalanine in human and rat 5-HT_6 receptors but tyrosine in the mouse orthologue and the $F188^{5\times39}$Y mutation reduces (while the $Y188^{5\times39}$F mutation increases) binding of sulfonamide ligands Ro04-6790, SB258585, SB271046 and SB357134, suggesting that this residue is not involved in H-bonding with these ligands but probably forms only aromatic interaction with their aromatic side chains.[85] The important role of $T^{3\times37}$ in providing an H-bonding partner to the indole NH of 5-HT analogues is underlined by the mutation $T^{3\times37}$A decreasing binding of 5-HT and LSD in 5-HT_{1B} and 5-HT_{2B}; however, from the available crystal structures it is seen that this role can also be fulfilled by the backbone carbonyl group of $G221^{5\times43}$ in 5-HT_{2B}.[30] Mutation of the residue 5×43 generally does not have a pronounced effect on ligand binding except for decreasing binding of 5-HT in 5-HT_{1A}, suggesting an alternative H-bond with 5-HT in this receptor. The $C196^{5\times43}$A mutant of 5-HT_4 furthermore increased binding affinity of the partial agonist ML10302, possibly by enlarging the binding site.[68] Mutation of $A^{5\times461}$ of rat 5-HT_{2A}, 5-HT_{2B}, and 5-HT_{2C} to a serine or threonine increases binding of several ergotamine analogues and 5-MT by providing an extra

DOI: 10.1021/acs.jmedchem.8b00836
J. Med. Chem. 2019, 62, 3784−3839

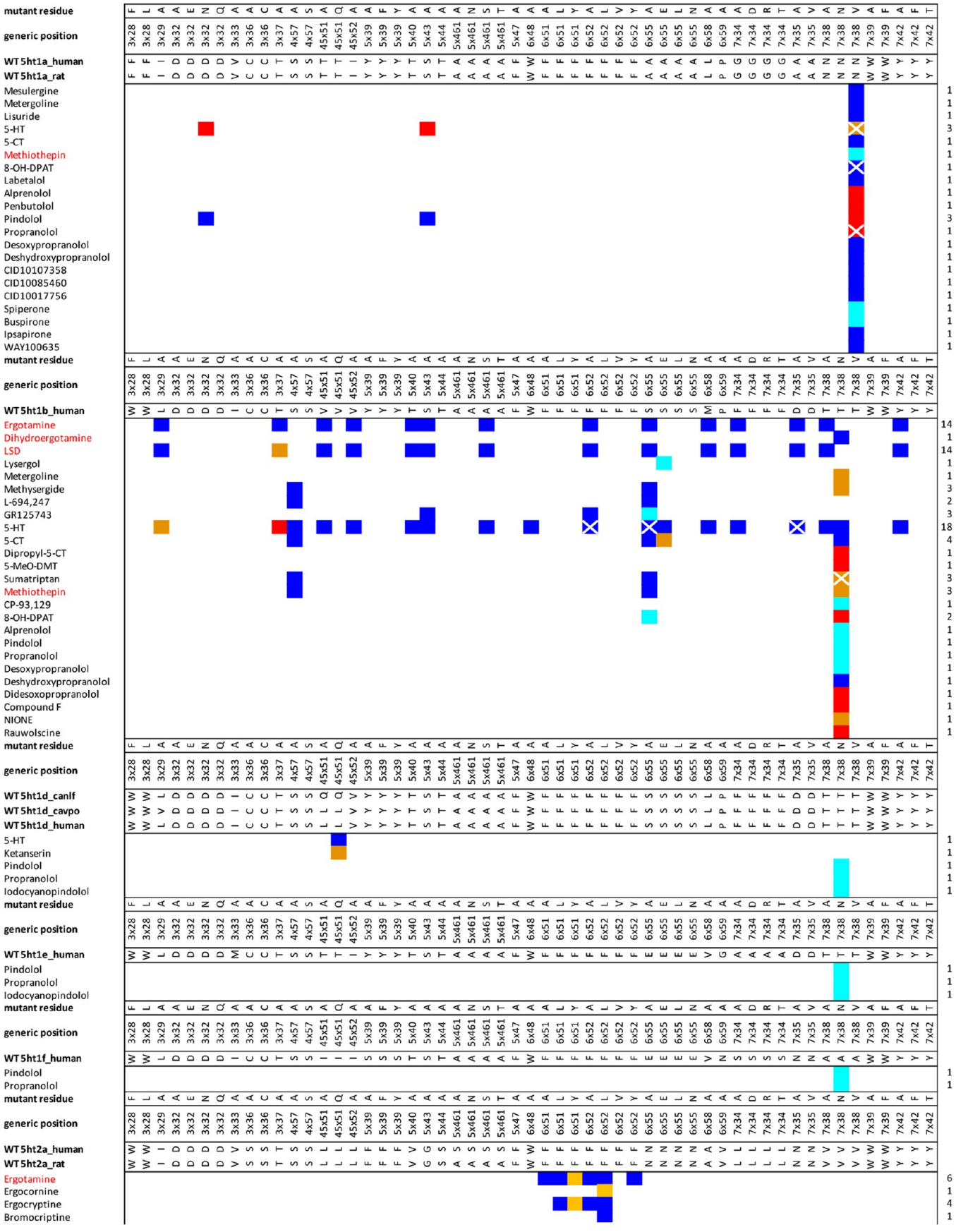

Figure 5. continued

DOI: 10.1021/acs.jmedchem.8b00836
J. Med. Chem. 2019, 62, 3784−3839

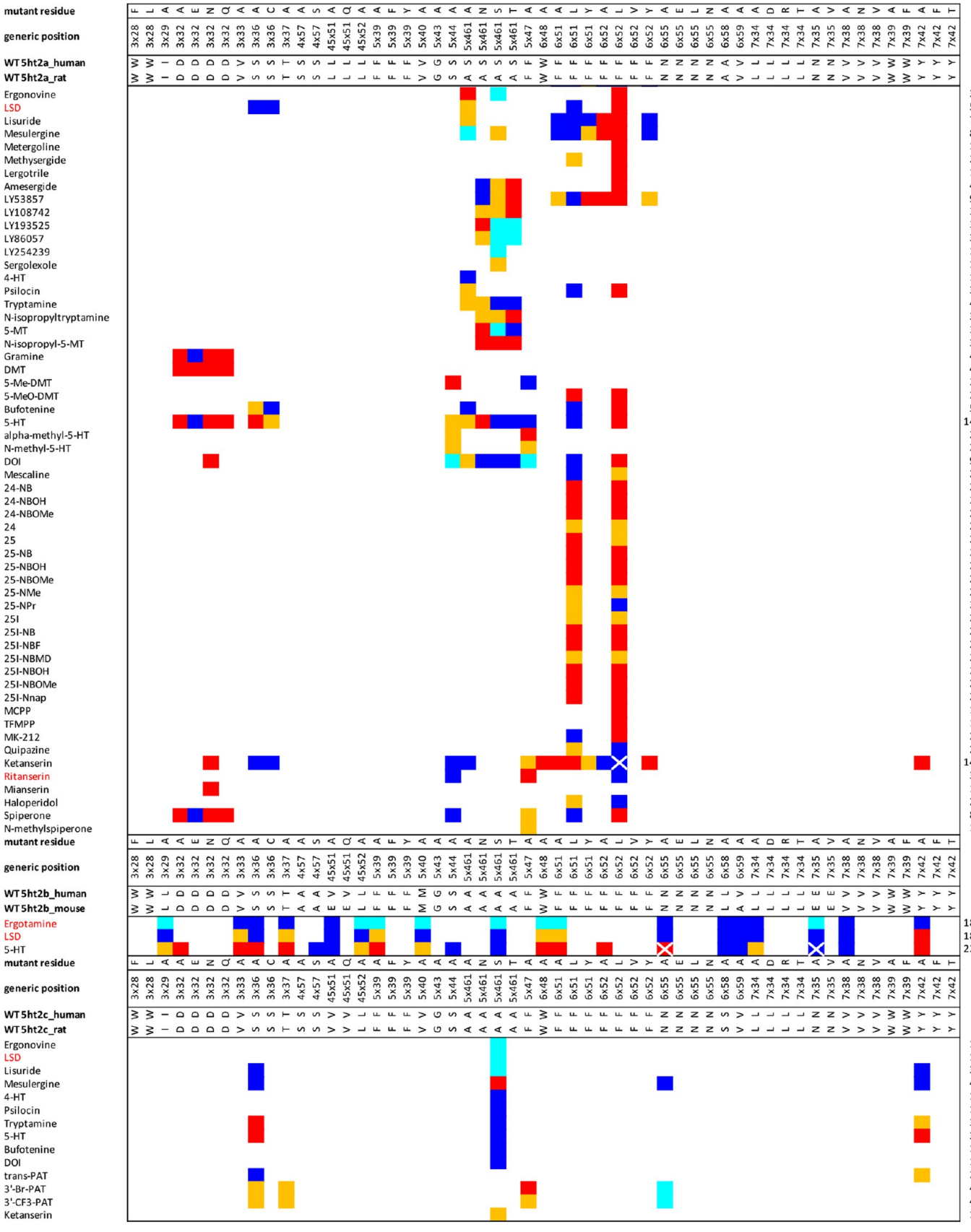

Figure 5. continued

DOI: 10.1021/acs.jmedchem.8b00836
J. Med. Chem. 2019, 62, 3784−3839

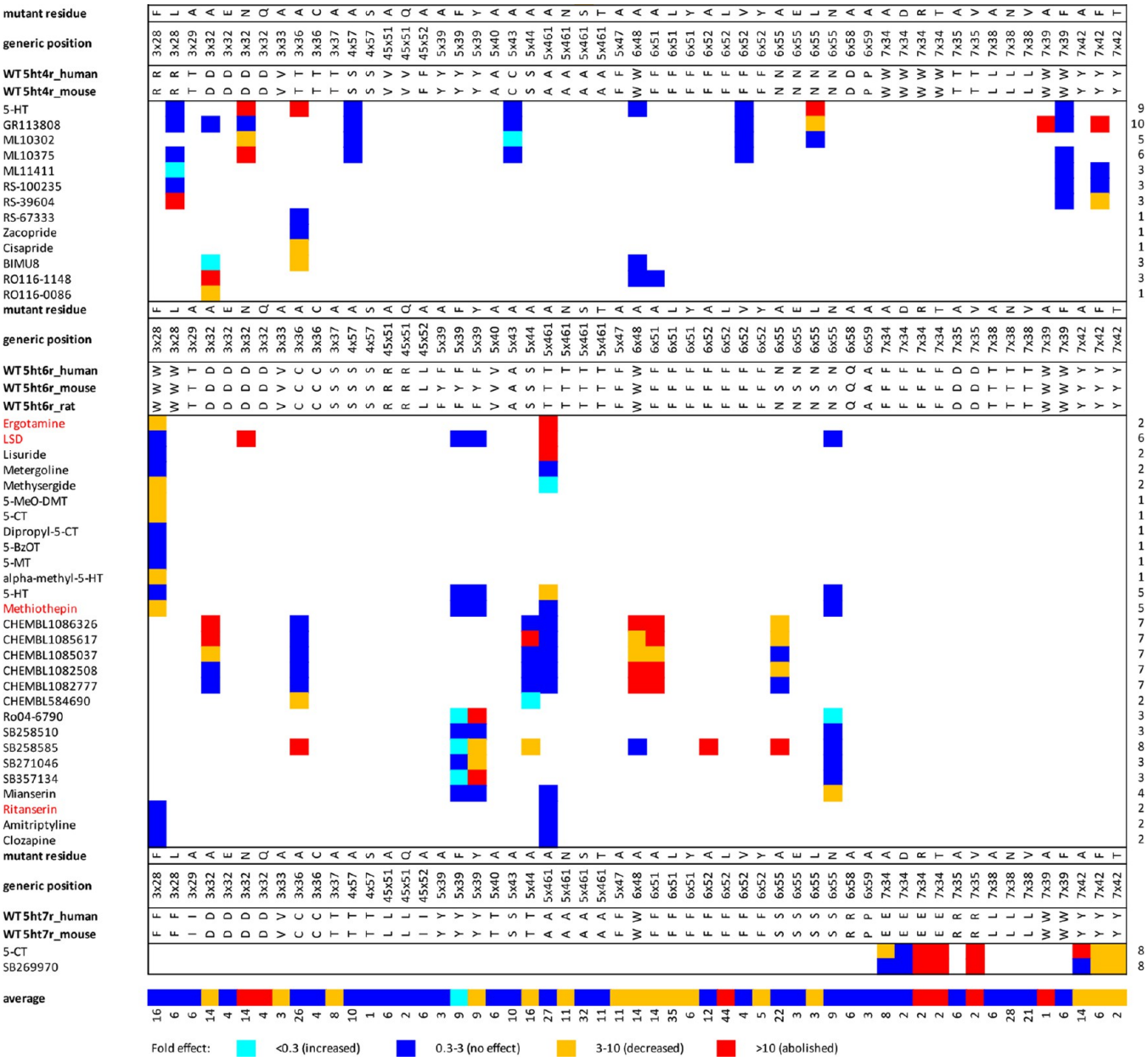

Figure 5. Serotonin receptor mutation data.[30,45−48,50,68−72,74−86,88,89,91−100] Data is shown for the consensus binding pocket defined using structure-based generic position numbers from GPCRdb.[18] Wild-type residues for the orthologues involved in mutation studies, and the mutant residue are shown (note that only the mutations which have a data point shown in the table were actually carried out, the table is organized for comparability among orthologues). Ligands are grouped similarly as in Figure 6. When multiple data points were available for the specific mutant−ligand combination, the geometric mean of the fold effect values was used. Color coding: cyan, fold effect <0.3 (increased), 0.3−3 (no effect), 3−10 (decreased), >10 (abolished). Uncertain data points for which different mutational effect classes have been reported are marked with a cross. Mutant numbers for each ligand and ligand numbers for each mutant are indicated on the right side and the bottom of the heat map, respectively. The average fold effect (geometric mean) for each mutant is also shown at the bottom of the heat map. PDF and Excel versions of the heat map are provided in the Supporting Information.

H-binding partner to the indole NH.[50,86,87] *N*-Alkylated 5HT analogues such as mesulergine, amesergide, *N*-isopropyltryptamine, and *N*-isopropyl-5-MT on the other hand are reversely affected by the $A^{5\times461}S$ mutation. The reverse mutation $S242^{5\times461}A/N$ in human 5-HT_{2A} and $T196^{5\times461}A$ in 5-HT_6 is detrimental to binding of 5-HT analogues but increases binding of *N*-methylated mesulergine and methysergide. Mutation studies indicate that the role of the small or polar residue (A, E, N, or S) at position 6×55 is highly ligand-dependent. The studies suggest that the amide side chain of $N^{6\times55}$ forms important H-bond interactions with several ligands, including the hydroxyl group of 5-HT (5-HT_{2B}, 5-HT_4), the ether group of GR113808 (5-HT_4), and the sulfonyl moieties of CHEMBL1082508, CHEMBL1085617, CHEMBL1086326, and SB258585 (5-HT_6).[30,76,80,88] The larger 5-HT analogues ergotamine and LSD (5-HT_{2B}), mesulergine (5-HT_{2C}), and ML10302 (5-HT_4) are less dependent on interactions with $N^{6\times55}$. Mutation of the smaller $S334^{6\times55}$ does not affect binding of the agonists ergotamine, 5-HT, LSD, and the antagonist methiothepin to 5-HT_{1B}, which is

DOI: 10.1021/acs.jmedchem.8b00836
J. Med. Chem. 2019, 62, 3784−3839

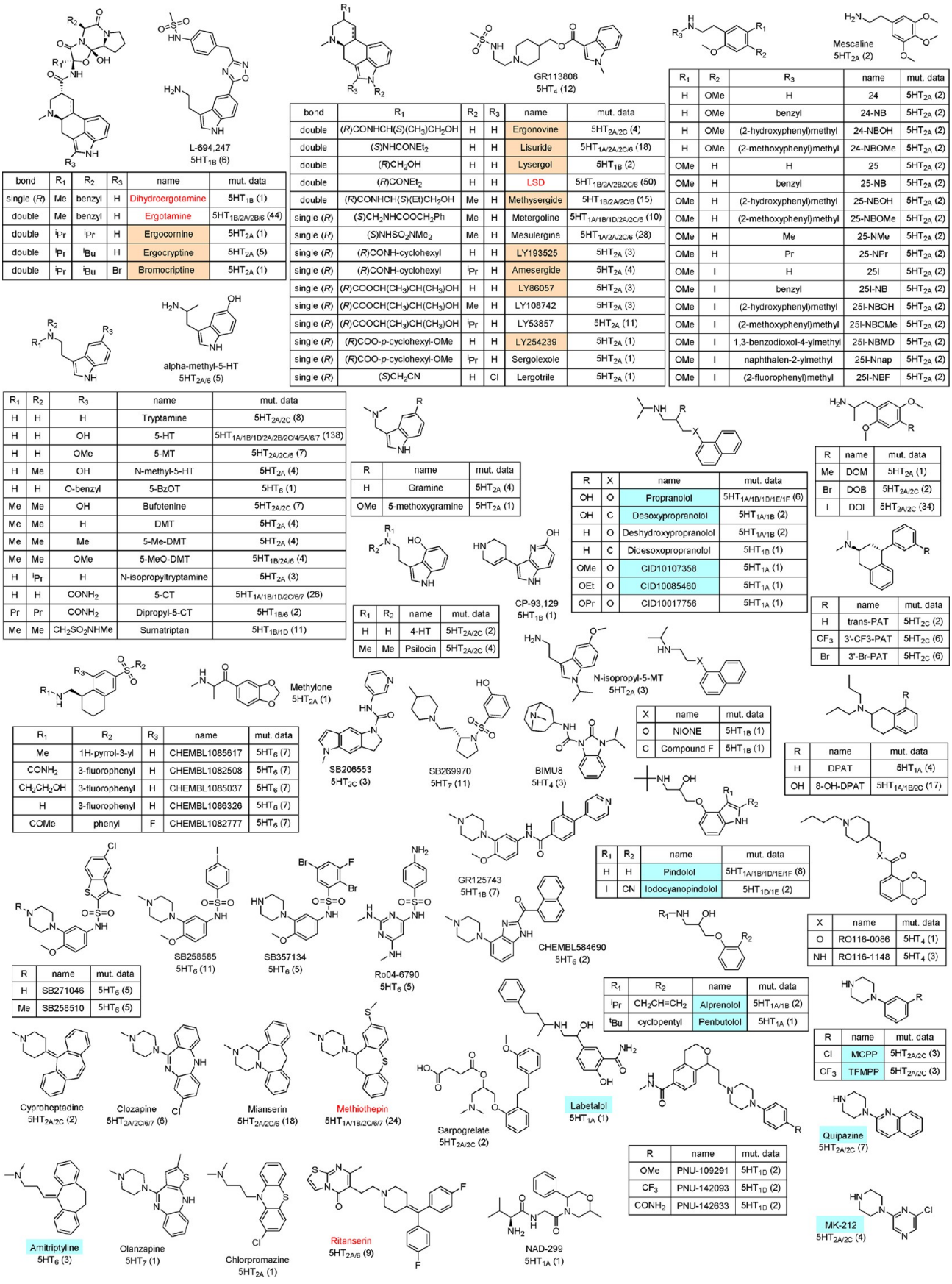

bond	R_1	R_2	R_3	name	mut. data
single (*R*)	Me	benzyl	H	Dihydroergotamine	$5HT_{1B}$ (1)
double	Me	benzyl	H	Ergotamine	$5HT_{1B/2A/2B/6}$ (44)
double	^{i}Pr	^{i}Pr	H	Ergocornine	$5HT_{2A}$ (1)
double	^{i}Pr	^{t}Bu	H	Ergocryptine	$5HT_{2A}$ (5)
double	^{i}Pr	^{i}Bu	Br	Bromocriptine	$5HT_{2A}$ (1)

bond	R_1	R_2	R_3	name	mut. data
double	(*R*)CONHCH(*S*)(CH_3)CH_2OH	H	H	Ergonovine	$5HT_{2A/2C}$ (4)
double	(*S*)$NHCONEt_2$	H	H	Lisuride	$5HT_{1A/2A/2C/6}$ (18)
double	(*R*)CH_2OH	H	H	Lysergol	$5HT_{1B}$ (2)
double	(*R*)$CONEt_2$	H	H	LSD	$5HT_{1B/2A/2B/2C/6}$ (50)
double	(*R*)CONHCH(*S*)(Et)CH_2OH	Me	H	Methysergide	$5HT_{1B/2A/2C/6}$ (15)
single (*R*)	(*S*)$CH_2NHCOOCH_2Ph$	Me	H	Metergoline	$5HT_{1A/1B/1D/2A/2C/6}$ (10)
single (*R*)	(*S*)$NHSO_2NMe_2$	Me	H	Mesulergine	$5HT_{1A/2A/2C/6}$ (28)
single (*R*)	(*R*)CONH-cyclohexyl	H	H	LY193525	$5HT_{2A}$ (3)
single (*R*)	(*R*)CONH-cyclohexyl	^{i}Pr	H	Amesergide	$5HT_{2A}$ (4)
single (*R*)	(*R*)$COOCH(CH_3)CH(CH_3)OH$	H	H	LY86057	$5HT_{2A}$ (3)
single (*R*)	(*R*)$COOCH(CH_3)CH(CH_3)OH$	Me	H	LY108742	$5HT_{2A}$ (3)
single (*R*)	(*R*)$COOCH(CH_3)CH(CH_3)OH$	^{i}Pr	H	LY53857	$5HT_{2A}$ (11)
single (*R*)	(*R*)COO-*p*-cyclohexyl-OMe	H	H	LY254239	$5HT_{2A}$ (1)
single (*R*)	(*R*)COO-*p*-cyclohexyl-OMe	^{i}Pr	H	Sergolexole	$5HT_{2A}$ (1)
single (*R*)	(*S*)CH_2CN	H	Cl	Lergotrile	$5HT_{2A}$ (1)

R_1	R_2	R_3	name	mut. data
H	OMe	H	24	$5HT_{2A}$ (2)
H	OMe	benzyl	24-NB	$5HT_{2A}$ (2)
H	OMe	(2-hydroxyphenyl)methyl	24-NBOH	$5HT_{2A}$ (2)
H	OMe	(2-methoxyphenyl)methyl	24-NBOMe	$5HT_{2A}$ (2)
OMe	H	H	25	$5HT_{2A}$ (2)
OMe	H	benzyl	25-NB	$5HT_{2A}$ (2)
OMe	H	(2-hydroxyphenyl)methyl	25-NBOH	$5HT_{2A}$ (2)
OMe	H	(2-methoxyphenyl)methyl	25-NBOMe	$5HT_{2A}$ (2)
OMe	H	Me	25-NMe	$5HT_{2A}$ (2)
OMe	H	Pr	25-NPr	$5HT_{2A}$ (2)
OMe	I	H	25I	$5HT_{2A}$ (2)
OMe	I	benzyl	25I-NB	$5HT_{2A}$ (2)
OMe	I	(2-hydroxyphenyl)methyl	25I-NBOH	$5HT_{2A}$ (2)
OMe	I	(2-methoxyphenyl)methyl	25I-NBOMe	$5HT_{2A}$ (2)
OMe	I	1,3-benzodioxol-4-ylmethyl	25I-NBMD	$5HT_{2A}$ (2)
OMe	I	naphthalen-2-ylmethyl	25I-Nnap	$5HT_{2A}$ (2)
OMe	I	(2-fluorophenyl)methyl	25I-NBF	$5HT_{2A}$ (2)

R_1	R_2	R_3	name	mut. data
H	H	H	Tryptamine	$5HT_{2A/2C}$ (8)
H	H	OH	5-HT	$5HT_{1A/1B/1D/2A/2B/2C/4/5A/6/7}$ (138)
H	H	OMe	5-MT	$5HT_{2A/2C/6}$ (7)
H	Me	OH	N-methyl-5-HT	$5HT_{2A}$ (4)
H	H	O-benzyl	5-BzOT	$5HT_6$ (1)
Me	Me	OH	Bufotenine	$5HT_{2A/2C}$ (7)
Me	Me	H	DMT	$5HT_{2A}$ (4)
Me	Me	Me	5-Me-DMT	$5HT_{2A}$ (4)
Me	Me	OMe	5-MeO-DMT	$5HT_{1B/2A/6}$ (4)
H	^{i}Pr	H	N-isopropyltryptamine	$5HT_{2A}$ (3)
H	H	$CONH_2$	5-CT	$5HT_{1A/1B/1D/2C/6/7}$ (26)
Pr	Pr	$CONH_2$	Dipropyl-5-CT	$5HT_{1B/6}$ (2)
Me	Me	CH_2SO_2NHMe	Sumatriptan	$5HT_{1B/1D}$ (11)

R	name	mut. data
H	Gramine	$5HT_{2A}$ (4)
OMe	5-methoxygramine	$5HT_{2A}$ (1)

R_1	R_2	name	mut. data
H	H	4-HT	$5HT_{2A/2C}$ (2)
Me	Me	Psilocin	$5HT_{2A/2C}$ (4)

R	X	name	mut. data
OH	O	Propranolol	$5HT_{1A/1B/1D/1E/1F}$ (6)
OH	C	Desoxypropranolol	$5HT_{1A/1B}$ (2)
H	O	Deshydroxypropranolol	$5HT_{1A/1B}$ (2)
H	C	Didesoxopropranolol	$5HT_{1B}$ (1)
OMe	O	CID10107358	$5HT_{1A}$ (1)
OEt	O	CID10085460	$5HT_{1A}$ (1)
OPr	O	CID10017756	$5HT_{1A}$ (1)

X	name	mut. data
O	NIONE	$5HT_{1B}$ (1)
C	Compound F	$5HT_{1B}$ (1)

R	name	mut. data
Me	DOM	$5HT_{2A}$ (1)
Br	DOB	$5HT_{2A/2C}$ (2)
I	DOI	$5HT_{2A/2C}$ (34)

R	name	mut. data
H	trans-PAT	$5HT_{2C}$ (2)
CF_3	3'-CF3-PAT	$5HT_{2C}$ (6)
Br	3'-Br-PAT	$5HT_{2C}$ (6)

R	name	mut. data
H	DPAT	$5HT_{1A}$ (4)
OH	8-OH-DPAT	$5HT_{1A/1B/2C}$ (17)

R_1	R_2	R_3	name	mut. data
Me	1H-pyrrol-3-yl	H	CHEMBL1085617	$5HT_6$ (7)
$CONH_2$	3-fluorophenyl	H	CHEMBL1082508	$5HT_6$ (7)
CH_2CH_2OH	3-fluorophenyl	H	CHEMBL1085037	$5HT_6$ (7)
H	3-fluorophenyl	H	CHEMBL1086326	$5HT_6$ (7)
COMe	phenyl	F	CHEMBL1082777	$5HT_6$ (7)

R	name	mut. data
H	SB271046	$5HT_6$ (5)
Me	SB258510	$5HT_6$ (5)

R_1	R_2	name	mut. data
H	H	Pindolol	$5HT_{1A/1B/1D/1E/1F}$ (8)
I	CN	Iodocyanopindolol	$5HT_{1D/1E}$ (2)

R_1	R_2	name	mut. data
^{i}Pr	$CH_2CH{=}CH_2$	Alprenolol	$5HT_{1A/1B}$ (2)
^{t}Bu	cyclopentyl	Penbutolol	$5HT_{1A}$ (1)

X	name	mut. data
O	RO116-0086	$5HT_4$ (1)
NH	RO116-1148	$5HT_4$ (3)

R	name	mut. data
Cl	MCPP	$5HT_{2A/2C}$ (3)
CF_3	TFMPP	$5HT_{2A/2C}$ (3)

R	name	mut. data
OMe	PNU-109291	$5HT_{1D}$ (2)
CF_3	PNU-142093	$5HT_{1D}$ (2)
$CONH_2$	PNU-142633	$5HT_{1D}$ (2)

Figure 6. continued

DOI: 10.1021/acs.jmedchem.8b00836
J. Med. Chem. 2019, 62, 3784−3839

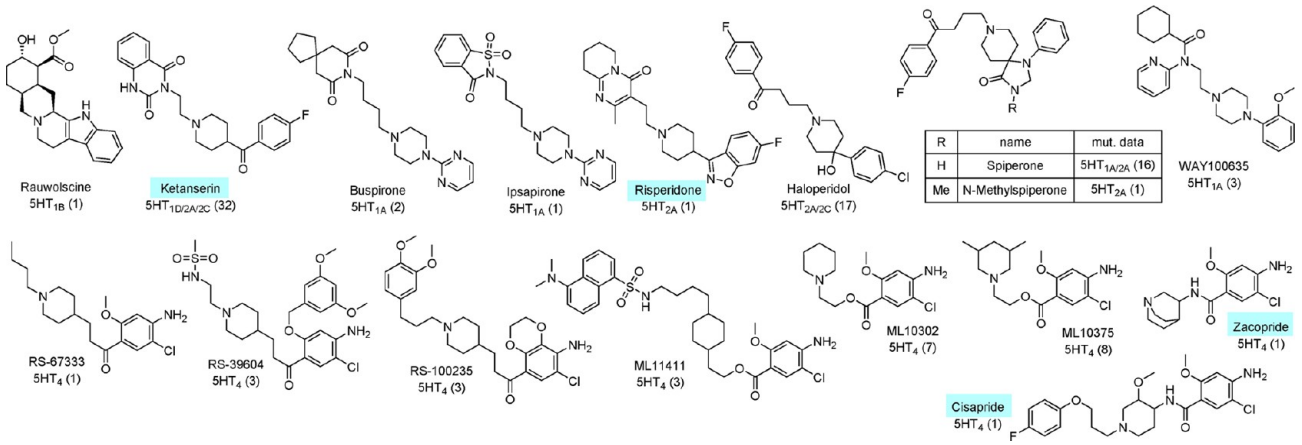

Figure 6. Serotonin receptor ligands used in mutation studies.[30,45−48,50,68−72,74−86,88,89,91−100] Cocrystallized ligands in 5-HT$_{1B}$, 5-HT$_{2B}$, and 5-HT$_{2C}$ structures are shown in red. Chemically similar (MACCS Tanimoto similarity ≥0.8 or ECFP-4 Tanimoto similarity ≥0.4) ligands to any of the cocrystallized ligands in serotonin receptor crystal structures are indicated with orange background and chemically similar ligands to any cocrystallized ligand in aminergic receptor crystal structures are indicated with a cyan background. Receptors with available mutation data for the specific ligand are indicated along with the number of data points in parentheses. A PDF version of the figure is provided in the Supporting Information.

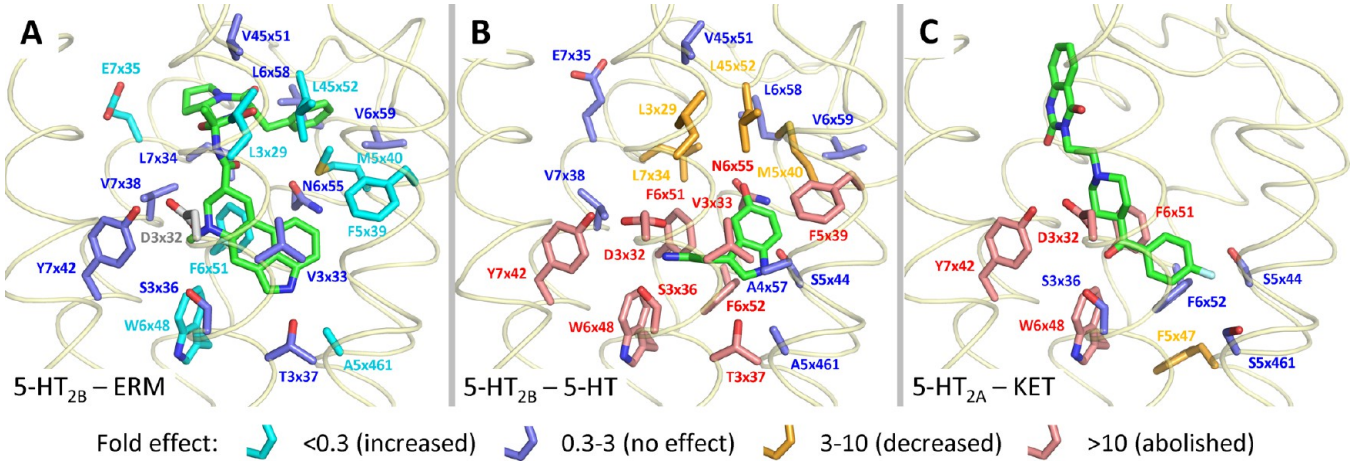

Figure 7. Serotonin receptor ligand binding modes and associated mutation data. (A) 5-HT$_{2B}$ (PDB: 4IB4[31]) with cocrystallized ergotamine, mutation effects mapped on structure for 5-HT$_{2B}$-ergotamine. (B) 5-HT$_{2B}$ (PDB: 5TVN[61]) with docked 5-HT, mutation effects mapped on structure for 5-HT$_{2B}$-5-HT. (C) 5-HT$_{2A}$ homology model from GPCRdb with docked ketanserin, mutation effects mapped on structure for 5-HT$_{2A}$-ketanserin. See Figure 5 for color coding. Mutation effects for alanine mutants were used where available.

consistent with the role of the longer amide side chain of N$^{6\times55}$ in binding of these ligands in 5-HT$_{2B}$, 5-HT$_4$, and 5-HT$_6$.[30,45] The positive effect of the N331$^{6\times55}$A binding of 3′-halo-PAT analogues to 5-HT$_{2C}$ is in line with a binding mode in which the mutation allows these ligands to accommodate their apolar phenyl ring in a subpocket defined by the smaller A331$^{6\times55}$ residue.[88] Similarly, the S334$^{6\times55}$A mutation increases binding of the agonist 8-OH-DPAT and the antagonist GR125743 to 5-HT$_{1B}$,[45] possibly by enlarging the binding pocket for these ligands. The S/T$^{5\times44}$A mutation has ligand-dependent effects, it decreases binding of several 5-HT analogues but increases that for DOI and CHEMBL584690 with large hydrophobic appendages.

3.3.2. Minor Pocket and Extracellular Vestibule Mutations in Serotonin Receptors. Ergotamine analogues possess a large tripeptidic appendage extending into the extracellular vestibule as well as ritanserin with its thiazolopyrimidinon appendage. Several other dualsteric ligands including ketanserin, azapirones, RS39604, and ML11411 also probably interact with the minor pocket in serotonin receptors; however, not many mutation data points are available for these ligands in combination with mutants in the minor pocket (Figure 5). The R$^{3\times28}$L mutation in 5-HT$_4$ receptor reduces binding of the antagonist RS-39604 and increases binding of the antagonist ML11411, suggesting that R$^{3\times28}$ forms an important polar interaction with the sulfonamide moiety of RS-39604, but does not form an essential interaction polar interaction with ML11411.[82] The W102$^{3\times28}$F mutation in 5-HT$_6$ reduces binding of ergotamine, methysergide, and surprisingly of several small 5-HT analogues as well.[75] Also, the L$^{3\times29}$A mutation reduces binding of the small 5-HT in 5-HT$_{1B}$ and 5-HT$_{2B}$ but increases that of ergotamine to 5-HT$_{2B}$ by expanding the minor pocket.[30] The amino acids at positions 7×34 and 7×35 are highly variable among serotonin receptors, therefore, it could be expected that mutation of these residues also has variable effects on ligand binding. No pronounced effect of these mutants is seen in 5-HT$_{1B}$. The L362$^{7\times34}$A mutant surprisingly decreases binding of the small 5-HT, and the E363$^{7\times35}$A mutant increases binding of ergotamine in 5-HT$_{2B}$ while having no effect on the other ligand or on LSD

DOI: 10.1021/acs.jmedchem.8b00836
J. Med. Chem. 2019, 62, 3784−3839

binding.[30] Even more interestingly, the $E^{7\times34}R/T$ and $R^{7\times35}V$ mutants in 5-HT_7 abolish binding of the agonist 5-CT and the antagonist SB269970, although neither ligand is expected to directly interact with these amino acids.[83] The mutation of positions 6×58 and 6×59 contacting the tripeptidic appendage of ergotamine in crystal structures does not affect binding of any probed ligand significantly; however, only six and three data points are available, respectively. Finally, mutations in ECL2 also have variable effects on ligand binding. Binding of the antagonist ketanserin is negatively affected by the $L189^{45\times51}Q$ mutation in 5-HT_{1D}, indicating that this residue cannot form an H-bond with the appendage of ketanserin.[89] The $L209^{45\times52}A$ mutation decreases binding of the small 5-HT but increases binding of ergotamine, while has no effect on LSD in 5-HT_{2B}.[30] These mutations have no effect on the tested ligands in 5-HT_{1B}. From the residues that do not have generic structural numbers assigned, only the R102H mutant in the ECL1 of guinea pig 5-HT_{1D} has a significant positive effect on the binding of the three PNU compounds, suggesting that the isochroman-amide moiety forms a suboptimal interaction with the arginine in the wild-type receptor.[90]

3.4. Structure-Based Extrapolation of Serotonin Receptor Mutation Effects. Mutation data predictions within the serotonin receptor family were performed for human data for 5-HT_{1B} and 5-HT_{2B} receptors with 5-HT_{1B} and 5-HT_{2B} crystal structures (Figure 6). The number of data points that could be used for extrapolation was 128 (20% of all fields) for 5-HT_{1B} and 63 (78% of all fields) for 5-HT_{2B} points available for 28 ligands at 23 mutants for the former serotonin receptor subtype[30,45−48,91,97,99] and just three compounds at 27 mutants for 5-HT_{2B}.[30,78] Due to the relatively low protein−ligand interaction fingerprint (IFP) similarities of ligands to the cocrystallized compounds, no data points were retrieved in retrospective studies for this group of receptors. Only the cocrystallized ergotamine, dihydroergotamine ligands, and metergoline could be docked to 5-HT_{1B} with IFP similarity >0.7, and the available mutation data for these ligands are disjoint (Figure 7). Only ergotamine in 5-HT_{2B} could be docked with the same IFP similarity cutoff. For the same reason, the protocol was only able to make further predictions in prospective studies for ergotamine and dihydroergotamine in 5-HT_{1B}. The heat maps referring to the original data set used for extrapolation, and the retrospective and prospective predictions are provided in the Supporting Information.

4. MUSCARINIC ACETYLCHOLINE RECEPTOR MUTATIONS

4.1. Structural Muscarinic Acetylcholine Receptor−Ligand Interactions. Muscarinic acetylcholine receptors are activated by the small neurotransmitter acetylcholine. In humans, there are five muscarinic acetylcholine receptor subtypes, of which M_1, M_2, M_3, and M_4 have been crystallized,[33−35,101,102] including tiotropium bound M_1 (PDB: 5CXV[33]), iperoxo (PDB: 4MQS), iperoxo/LY2119620 (PDB: 4MQT[34]) and 3-quinuclidinyl benzilate (QNB) (PDB: 3UON[101]) bound M_2, tiotropium (PDB: 4DAJ,[35] 4U14, 4U15) and *N*-methylscopolamine (NMS) (PDB: 4U16[102]) bound M_3, and tiotropium bound M_4 (PDB: 5DSG[33]). The M_2 receptor is unique among the aminergic receptors as it is the only one crystallized in a ternary complex with an orthosteric agonist (iperoxo) and a positive allosteric modulator (LY2119620) bound in the extracellular vestibule. These crystal structures show a conserved binding mode of the quaternary amine scaffold of iperoxo, NMS, and tiotropium and the protonated quinuclidine scaffold of QNB in the orthosteric amine pocket, covering residues in the amine pocket ($D^{3\times32}$, $Y^{3\times33}$, $S^{3\times36}$, $W^{6\times48}$, $Y^{6\times51}$, $Y^{7\times38}$, $C^{7\times41}$, $Y^{7\times42}$). The aromatic and polar residues of the major pocket contact the two aromatic rings of QNB and tiotropium and the single cyclic moieties of iperoxo and NMS ($Y^{3\times33}$, $N^{3\times37}$, $V^{3\times40}$, $W^{4\times57}$, $T^{5\times40}$, $T^{5\times43}$, $A^{5\times44}$, $A^{5\times461}$, $F^{5\times47}$, $N^{6\times52}$, $V^{6\times55}$). The $N^{6\times52}$ residue forms concerted characteristic H-bonds with the tertiary alcohol and ester groups of the muscarinic receptor antagonists tiotropium, NMS, and QNB and a single H-bond with the isoxazole ring of iperoxo and probably the carbonyl group of acetylcholine. The cocrystallized orthosteric ligands in the muscarinic receptors do not directly interact with residues of the minor pocket and extracellular vestibule. A series of tyrosine residues ($Y^{3\times33}$, $Y^{6\times51}$, $Y^{7\times38}$, $Y^{7\times42}$) closely pack together to form a lid over the orthosteric binding pocket and separating it from the observed allosteric pocket in M_2. Some dualsteric ligands that have high affinity for muscarinic acetylcholine receptors such as aripiprazole or risperidone extend toward these binding pockets; however, dualsteric ligands are not commonly known among muscarinic ligands, and to our knowledge they have not been studied in mutation studies. The LY2119620 positive allosteric modulator, on the other hand, binds entirely in the extracellular vestibule contacting residues $Y/F^{2\times60}$, $Y^{2\times63}$, $L/T/I^{2\times64}$, $W^{3\times28}$, $L^{3\times29}$, $Y/F^{45\times51}$, $I^{45\times52}$, $S/N^{6\times58}$, $T^{6\times59}$, $E/N/K/D^{7\times31}$, $W^{7\times34}$, and $E/T/N/S^{7\times35}$ and furthermore E172 in ECL2 and A414 in ECL3 in M_2. Other allosteric modulators, such as the permanently charged gallamine and W84 or the multiply protonated TBPB, also exploit the aromatic clusters found in the extracellular vestibule to form cation−π interactions. Muscarinic acetylcholine receptor crystal structures are generally similar to each other except for the agonist iperoxo bound structures (4MQS, 4MQT).[34] The average heavy atom RMSD for M_2, M_3, and M_4 receptor subtypes are 1.3, 0.7, and 0.4 Å, respectively. The average backbone RMSD for these subtypes are 1.1, 0.5, and 0.2 Å, respectively. The average backbone RMSD for all muscarinic acetylcholine receptors is 0.8 Å, with the largest difference of 1.7 Å between the tiotropium-bound M_1 and the iperoxo and LY2119620-bound M_2 (Figures 3, 10, 20). In this case, the extracellular tip of TM5 is shifted about 2.5 Å outward and the tips of TM6 and TM7 about 4 and 2.5 Å inward in the agonist and PAM-bound structure relative to the antagonist-bound structure. However, despite this large rearrangement in the ECV by helix tilting, the extracellular loop conformations are well conserved among all muscarinic acetylcholine receptor subtypes. In the orthosteric ligands the aromatic regions, the key acceptor, and the charged basic center overlap almost perfectly among all muscarinic acetylcholine receptor subtypes. For ECV-bound allosteric ligands, however, there is only one available crystal structure, comparison of allosteric ligand binding modes is thus not possible. In the amine pocket, $D^{3\times32}$ forms an ionic interaction, while residues $Y^{3\times33}$, $W^{6\times48}$, $Y^{7\times38}$, and $Y^{7\times42}$ form cation−π interactions with the conserved tertiary and quaternary amine moieties of muscarinic acetylcholine receptor ligands consistent with mutation studies (section 4.3.1) and SAR studies, showing the essential role of the cationic properties of the amine groups of tropane, quinuclidine, 1-azabicyclo[2.2.1]-heptane, piperidine, and piperazine containing ligands and acetylcholine derivatives. Mutation data of these five residues equivocally support their important role in ligand recognition.

DOI: 10.1021/acs.jmedchem.8b00836
J. Med. Chem. 2019, 62, 3784−3839

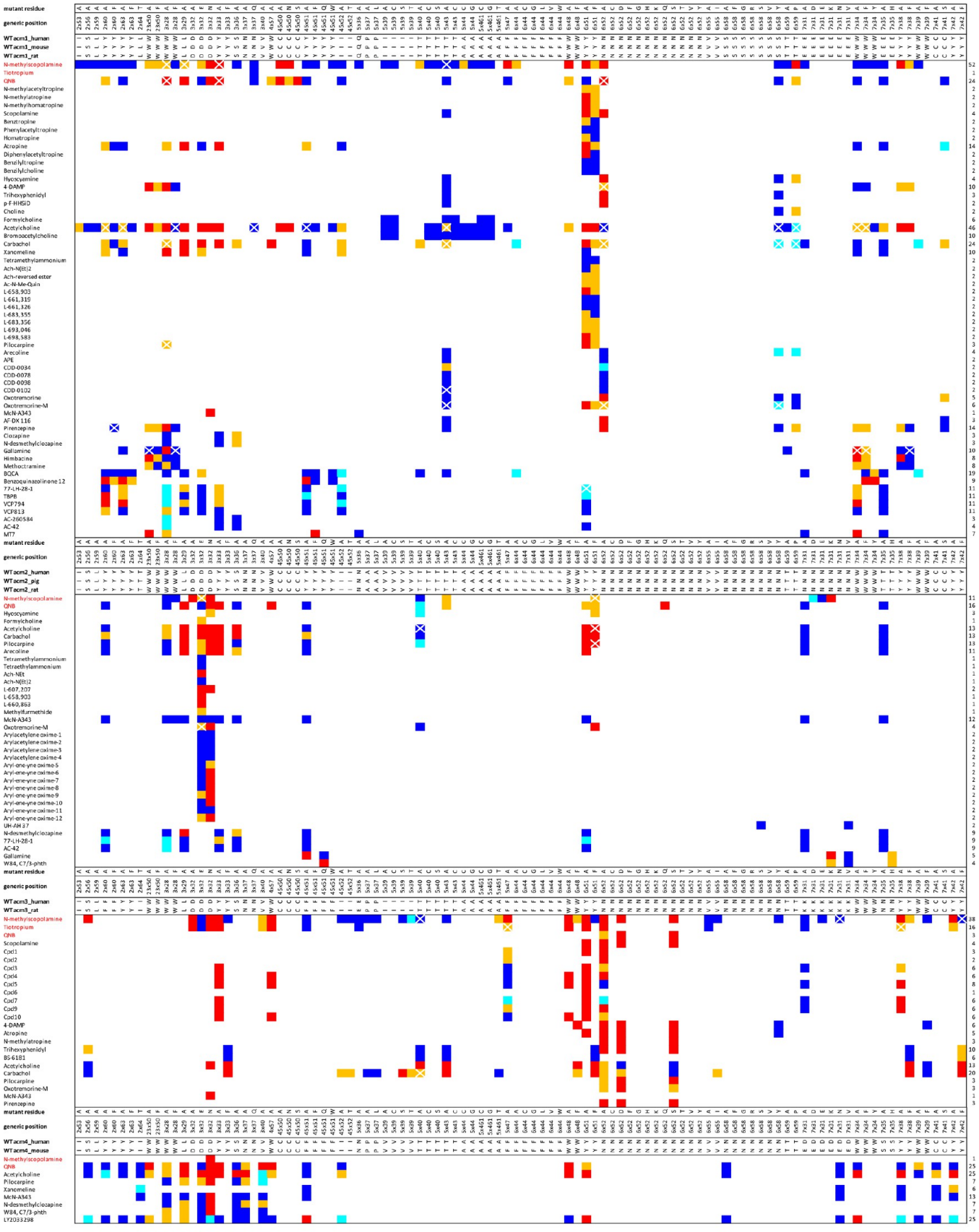

Figure 8. continued

DOI: 10.1021/acs.jmedchem.8b00836
J. Med. Chem. 2019, 62, 3784−3839

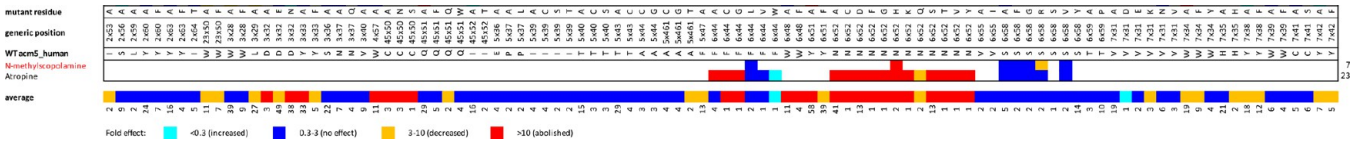

Figure 8. Muscarinic acetylcholine receptor mutation data.[33,51−53,106,109−132,134−151] Data is shown for the consensus binding pocket defined using structure-based generic position numbers from GPCRdb.[18] Wild-type residues for the orthologues involved in mutation studies and the mutant residue are shown (note that only the mutations which have a data point shown in the table were actually carried out, the table is organized for comparability among orthologues). Ligands are grouped similarly as in Figure 9. When multiple data points were available for the specific mutant−ligand combination, the geometric mean of the fold effect values was used. See Figure 5 for color coding. Mutant numbers for each ligand and ligand numbers for each mutant are indicated in the right side and the bottom of the heat map, respectively. The average fold effect (geometric mean) for each mutant is also shown at the bottom of the heat map. PDF and Excel versions of the heat map are provided in the Supporting Information.

The bulky tropane and quinuclidine scaffolds of the cocrystallized ligands tiotropium, QNB, and NMS also make hydrophobic interactions with the aforementioned aromatic residues. The bis-phenyl and bis-tiophenyl moieties of QNB and tiotropium form interactions in the major pocket with $Y^{3\times33}$, $V^{3\times40}$, $W^{4\times57}$, $A^{5\times461}$, $F^{5\times47}$, $W^{6\times48}$, $Y^{6\times51}$, and $V^{6\times55}$. Mutation of most of these hydrophobic residues greatly affects ligand binding. $N^{6\times52}$ forms H-bond interactions with polar scaffold substituents in the major pocket between TM3−6. The importance of this single residue is underlined even by the fact that 78 data points for 12 different mutants of this residue are available. Taken together, mutation and SAR studies demonstrate the preference of muscarinic acetylcholine receptors for ligands with aromatic moieties substituted with at least one polar H-bond interaction functionality, mimicking the ester group of the endogenous acetylcholine or the hydroxyacetate group of the cocrystallized ligands. In the minor pocket and extracellular vestibule, the quaternary ammonium or basic amine and aromatic groups of prototypical muscarinic allosteric modulators (Figure 9) interact with residues including $Y/F^{2\times60}$, $Y^{2\times63}$, $L/T/I^{2\times64}$, $Y/F^{45\times51}$, $E/N/K/D^{7\times31}$, $W^{7\times34}$, and $E/T/N/S^{7\times35}$. Mutation of these residues affect allosteric modulator binding but usually have little or no effect on orthosteric ligands. Mutation of several other amino acids in the minor pocket and extracellular vestibule had little effect on all studied ligands.

4.2. Chemical Space of Muscarinic Acetylcholine Receptor Ligands in Crystal Structures and Mutation Studies. The cocrystallized muscarinic acetylcholine receptor antagonists NMS (investigated in combination with 402 different mutants), QNB (135 mutants), and tiotropium (30 mutants) as well as the endogenous acetylcholine (279 mutants) have been extensively investigated in mutation studies of all muscarinic acetylcholine receptors covering an astounding 135 different residues in total (Figures 8, 9, and 10), including 38 residues that are lining the binding sites in muscarinic receptor crystal structures (Figure 3). On the other hand, cocrystallized ligands iperoxo and LY2119620 have not been involved in mutational studies yet. The most similar ligands to these are oxotremorine-M (with 32 mutants) and LY2033298 (with 42 mutants, Figure 10). Twenty-four (23%) of the ligands investigated in mutation studies are chemically similar, and 41 (39%) are pharmacophorically similar to any of the cocrystallized ligands (Figure 9), covering 626 (33%) and 809 (43%) ligand−mutant combinations, respectively. Quinuclidine derivatives (e.g., QNB, L-698,583, Ac-N-Me-Quin), tropane (e.g., tiotropium, NMS, atropine, benztropine), and tetra-alkyl ammonium containing agonists (e.g., iperoxo, oxotremorine-M, acetylcholine analogues) have been investigated at 1038 ligand−mutant combinations in total (55%). The antagonist pirenzepine and analogues UH-AH 37 and AF-DX 116 and clozapine with *N*-desmethyl analogue (covering 178 different mutants in total) are examples of a ligand series that do not share 2D chemical similarity with cocrystallized muscarinic acetylcholine receptor ligands but that represent combined ligand and receptor SAR data sets that provide detailed information on the structural determinants of muscarinic acetylcholine receptor binding. Allosteric modulators, such as gallamine, W84 and the piperidine benzimidazolinones TBPB and VCP794, the *N*,*N*-dimethyl piperidine VCP813, quinolinone analogues BQCA, benzoquinazolinone 12, AC-260584, and 77-LH-28-1, cover 200 mutant−ligand combinations in total (11%). No ligands are chemically similar to cocrystallized ligands in aminergic receptor complexes from other families. However, the orthosteric ligands clozapine and *N*-desmethylclozapine (altogether 25 mutants) are tricyclic compounds similar to cocrystallized doxepin in the histamine H_1 crystal structure (section 7) and also show a high affinity for the H_1 receptor.[103] Clozapine has been investigated at three muscarinic acetylcholine receptor mutants, as well as mutants at other receptor subfamilies (in serotonin, dopamine, and histamine receptor mutation studies), providing insights into the receptor specific determinants of binding of this ligand by different aminergic GPCRs (see section 9).[104−107]

4.3. Structural Determinants of Muscarinic Acetylcholine Receptor−Ligand Interactions. *4.3.1. Amine and Major Pocket Mutations in Muscarinic Acetylcholine Receptors.* Mutation of conserved $D^{3\times32}$ to nonacidic residues ($D^{3\times32}N/A$) has been shown to diminish muscarinic acetylcholine receptor binding affinity of almost all 38 tested ligands. However, McN-A343 (hypothesized to be a mixed orthosteric−allosteric ligand[108]) and the arylacetylene oxymes are not affected by the $D103^{3\times32}N$ mutation in M_2 and it even increases the affinity of the allosteric modulator LY2033298 binding in the extracellular vestibule. The acidic $D^{3\times32}E$ mutant significantly decreases muscarinic acetylcholine receptor affinity of 21 ligands (mostly quaternary amines, including the agonists acetylcholine, carbachol, oxotremorine-M, and the antagonist NMS) but does not significantly affect the affinity of 17 other ligands (mostly tertiary amines including the antagonists QNB, atoprine, and arylene-ene oxime analogues).[33,51,109−114] These data indicate that both the ionic character of the carboxylate group and the size of the $D^{3\times32}$ side chain are important for ligand binding, consistent with the small, occluded pocket in particular for quaternary amine moieties of tiotropium, NMS, and iperoxo in muscarinic acetylcholine receptor crystal structures (Figure 3). The $S120^{2\times56}A$ mutant in rat M_3 reduces affinity of *N*-

DOI: 10.1021/acs.jmedchem.8b00836
J. Med. Chem. 2019, 62, 3784−3839

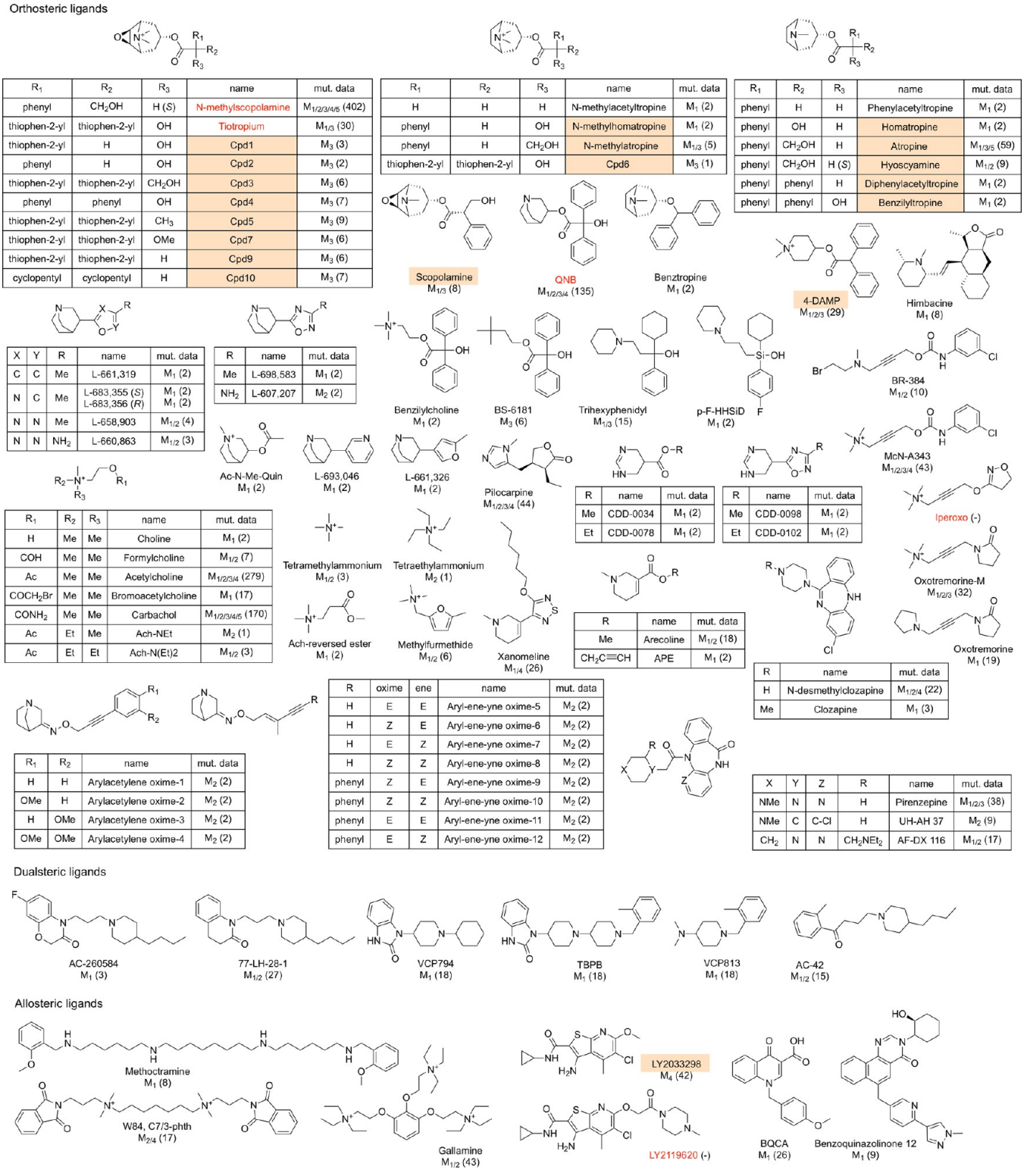

R1	R2	R3	name	mut. data
phenyl	CH_2OH	H (*S*)	N-methylscopolamine	$M_{1/2/3/4/5}$ (402)
thiophen-2-yl	thiophen-2-yl	OH	Tiotropium	$M_{1/3}$ (30)
thiophen-2-yl	H	OH	Cpd1	M_3 (3)
phenyl	H	OH	Cpd2	M_3 (2)
thiophen-2-yl	thiophen-2-yl	CH_2OH	Cpd3	M_3 (6)
phenyl	phenyl	OH	Cpd4	M_3 (7)
thiophen-2-yl	thiophen-2-yl	CH_3	Cpd5	M_3 (9)
thiophen-2-yl	thiophen-2-yl	OMe	Cpd7	M_3 (6)
thiophen-2-yl	thiophen-2-yl	H	Cpd9	M_3 (6)
cyclopentyl	cyclopentyl	H	Cpd10	M_3 (7)

R1	R2	R3	name	mut. data
H	H	H	N-methylacetyltropine	M_1 (2)
phenyl	H	OH	N-methylhomatropine	M_1 (2)
phenyl	H	CH_2OH	N-methylatropine	$M_{1/3}$ (5)
thiophen-2-yl	thiophen-2-yl	OH	Cpd6	M_3 (1)

R1	R2	R3	name	mut. data
phenyl	H	H	Phenylacetyltropine	M_1 (2)
phenyl	OH	H	Homatropine	M_1 (2)
phenyl	CH_2OH	H	Atropine	$M_{1/3/5}$ (59)
phenyl	CH_2OH	H (*S*)	Hyoscyamine	$M_{1/2}$ (9)
phenyl	phenyl	H	Diphenylacetyltropine	M_1 (2)
phenyl	phenyl	OH	Benzilyltropine	M_1 (2)

X	Y	R	name	mut. data
C	C	Me	L-661,319	M_1 (2)
N	C	Me	L-683,355 (*S*) L-683,356 (*R*)	M_1 (2) M_1 (2)
N	N	Me	L-658,903	$M_{1/2}$ (4)
N	N	NH_2	L-660,863	$M_{1/2}$ (3)

R	name	mut. data
Me	L-698,583	M_1 (2)
NH_2	L-607,207	M_2 (2)

R	name	mut. data
Me	CDD-0034	M_1 (2)
Et	CDD-0078	M_1 (2)

R	name	mut. data
Me	CDD-0098	M_1 (2)
Et	CDD-0102	M_1 (2)

R1	R2	R3	name	mut. data
H	Me	Me	Choline	M_1 (2)
COH	Me	Me	Formylcholine	$M_{1/2}$ (7)
Ac	Me	Me	Acetylcholine	$M_{1/2/3/4}$ (279)
$COCH_2Br$	Me	Me	Bromoacetylcholine	M_1 (17)
$CONH_2$	Me	Me	Carbachol	$M_{1/2/3/4/5}$ (170)
Ac	Et	Me	Ach-NEt	M_2 (1)
Ac	Et	Et	Ach-N(Et)2	$M_{1/2}$ (3)

R	name	mut. data
Me	Arecoline	$M_{1/2}$ (18)
$CH_2C{\equiv}CH$	APE	M_1 (2)

R	name	mut. data
H	N-desmethylclozapine	$M_{1/2/4}$ (22)
Me	Clozapine	M_1 (3)

R1	R2	name	mut. data
H	H	Arylacetylene oxime-1	M_2 (2)
OMe	H	Arylacetylene oxime-2	M_2 (2)
H	OMe	Arylacetylene oxime-3	M_2 (2)
OMe	OMe	Arylacetylene oxime-4	M_2 (2)

R	oxime	ene	name	mut. data
H	E	E	Aryl-ene-yne oxime-5	M_2 (2)
H	Z	E	Aryl-ene-yne oxime-6	M_2 (2)
H	E	Z	Aryl-ene-yne oxime-7	M_2 (2)
H	Z	Z	Aryl-ene-yne oxime-8	M_2 (2)
phenyl	Z	E	Aryl-ene-yne oxime-9	M_2 (2)
phenyl	Z	Z	Aryl-ene-yne oxime-10	M_2 (2)
phenyl	E	E	Aryl-ene-yne oxime-11	M_2 (2)
phenyl	E	Z	Aryl-ene-yne oxime-12	M_2 (2)

X	Y	Z	R	name	mut. data
NMe	N	N	H	Pirenzepine	$M_{1/2/3}$ (38)
NMe	C	C-Cl	H	UH-AH 37	M_2 (9)
CH_2	N	N	CH_2NEt_2	AF-DX 116	$M_{1/2}$ (17)

Figure 9. Muscarinic acetylcholine receptor ligands used in mutation studies.[33,51−53,106,109−132,134−151] Cocrystallized ligands in M_1, M_2, M_3, and M_4 structures shown in red. Chemically similar ligands to any of the cocrystallized ligands in muscarinic acetylcholine receptor crystal structures indicated with orange background, chemically similar ligands to any cocrystallized ligand in aminergic receptor crystal structures indicated with a cyan background. Receptors with available mutation data for the specific ligand are indicated along with the number of data points in parentheses. A PDF version of the figure is provided in the Supporting Information.

methylscopolamine and trihexyphenidyl as this residue forms an H-bond with $D^{3\times32}$, stabilizing the conformation of the key acidic anchor. The $S^{3\times36}$ residue forms weak H-bond interactions with the epoxide moiety of tiotropium and NMS in the available muscarinic receptor crystal structures. However, mutation of this residue to alanine does not have a pronounced effect on binding of these and other similar ligands, only on the binding of acetylcholine, carbachol,

DOI: 10.1021/acs.jmedchem.8b00836
J. Med. Chem. 2019, 62, 3784−3839

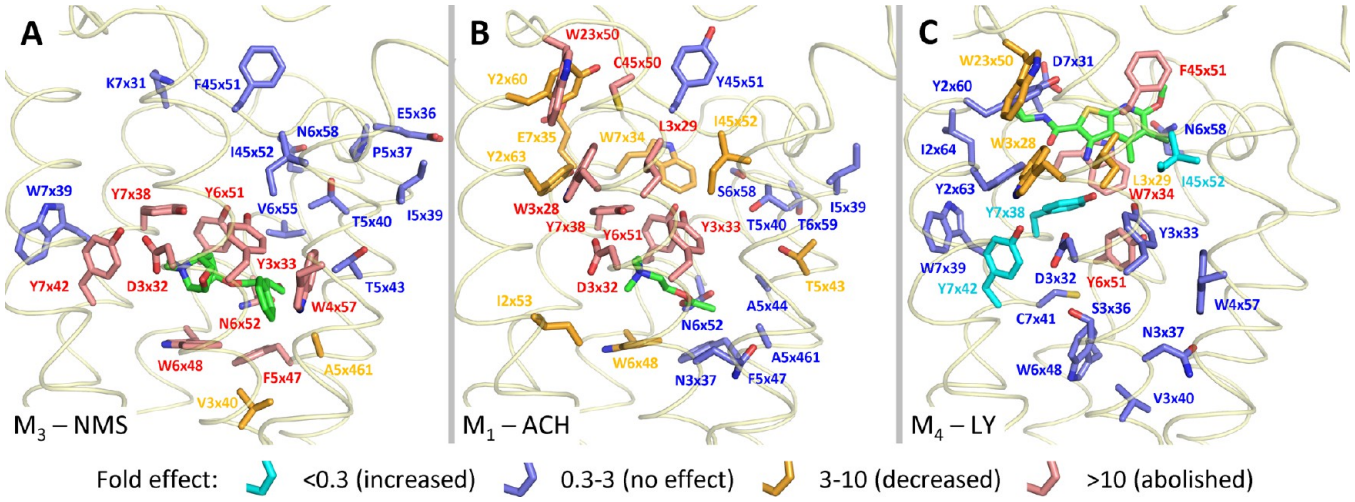

Figure 10. Muscarinic acetylcholine receptor ligand binding modes and associated mutation data. (A) M_3 (PDB: 4U16[102]) with cocrystallized NMS, mutation effects mapped on structure for M_3-NMS. (B) M_1 (PDB: 5CXV[33]) with docked acetylcholine, mutation effects mapped on structure for M_1-acetylcholine. (C) M_4 homology model based on M_2 as a template (PDB: 4MQT[34]) with docked LY2033298, mutation effects mapped on structure for M_4-LY2033298. See Figure 5 for color coding. Mutation effects for alanine mutants were used where available.

clozapine, and *N*-desmethylclozapine.[33,106,114−116] Mutation of the conserved W413$^{6\times48}$ is detrimental to the binding of almost all of 14 evaluated ligands but does not affect LY2033298 affinity to M_4, consistent with the M_2 crystal structure, which showed that this allosteric modulator does not target the major pocket.[33,113,117,118] Y439$^{7\times38}$ and Y443$^{7\times42}$ form H-bonds with D112$^{3\times32}$ to stabilize its conformation and participate in creating an aromatic cage for the quaternary ammonium ligands. Consistently, mutation of these residues to alanine diminishes the binding of several tested orthosteric agonists and antagonists (NMS, tiotropium, 4-DAMP, acetylcholine, pirenzepine, himbacine),[33,53,113,119,120] while mutation to phenylalanine usually has a milder effect consistent with maintaining the cation−π interactions.[53,121,122] The effect on allosteric modulators gallamine, methoctramine, LY2033298, as well as BS-6181 lacking a positively charged group is either nonsignificant or even increasing affinity. Y$^{3\times33}$ and Y$^{6\times51}$ along with the above-mentioned residues form the tyrosine lid over the orthosteric pocket and their mutation is generally detrimental to orthosteric ligand binding. The Y$^{3\times33}$A mutation is employed 33 times in the data set and 24 times it decreases ligand binding. Clozapine, *N*-desmethylclozapine, and allosteric modulators VCP813, AC-42, AC-260584, McN-A343, and LY2033298 are unaffected by this mutation.[121−123] The Y$^{6\times51}$A mutation is employed 58 times, out of which 40 times it decreases or abolishes binding of the tested ligand. Again, this mutation has no or even the opposite effect on five tested allosteric modulators, it increases binding of 77-LH-28-1 and TBPB in M_1 and M_2. Even the Y$^{6\times51}$F mutant decreases ligand binding in 26 of 39 cases, but the effect is generally smaller than for the alanine mutant.[121,122,124−126] The conserved N$^{6\times52}$ residue was identified early on as one of the residues crucial for ligand binding in the muscarinic acetylcholine receptors.[113,123,124,127−129] It is mutated to 12 different amino acids in a total of 78 mutant−ligand combinations, and in 66 out of these, it diminishes or abolishes ligand binding to the M_1, M_2, M_3, and M_5 receptors. The N508$^{6\times52}$A mutant of M3 increases binding affinity for Cpd7 in which the hydroxyacetate scaffold is methylated and therefore the H-bond with N$^{6\times52}$ is expected to be disrupted. The N382$^{6\times52}$A mutant increases CDD-0034 binding affinity for M1, possibly because the tetrahydropyrimidine warhead forms a very strong interaction with D105$^{3\times32}$ and creates an unfavorable H-bond geometry with N382$^{6\times52}$. However, for the CDD agonists, arecoline and APE, the authors report a discrepancy between binding and functional effects: while binding is not affected or even increased by the mutation, receptor activation is diminished in all cases, indicating that the H-bonding potential of N$^{6\times52}$ in muscarinic receptors is required for the activation process.[127] Mutation of the other residues forming the major binding pocket has ligand-dependent effects. The N117$^{3\times37}$A mutant decreases binding of acetylcholine, QNB, pilocarpine, and *N*-desmethylclozapine but expectedly does not have any effect on allosteric ligands.[33,114,115,123,130] The V$^{3\times40}$A mutant decreases binding of QNB, NMS, tiotropium, and *N*-desmethylclozapine in $M_{3/4}$ but increases binding of acetylcholine and pilocarpine and also does not have an effect on allosteric modulators.[33,113−115,130] The W$^{4\times57}$A mutant abolishes binding of all tested orthosteric ligands in $M_{3/4}$ but does not have a significant effect on the allosteric LY2033298.[33,109,113,119,131] Interestingly, the T$^{5\times40}$A mutant located at the top of the orthosteric binding pocket decreases binding of NMS, carbachol, and acetylcholine in M_1 and M_4 but does not have an effect on binding of these ligands to M_2 and even increases binding of QNB, hyoscyamine, and pilocarpine in M_2, indicating that this residue might have differential roles in these receptors.[109,121,122,126,131,132] Mutation of T$^{5\times43}$, A$^{5\times44}$, and A$^{5\times461}$ has little effect on binding of the investigated ligands in $M_{1/2/3}$ except for the T234$^{5\times43}$A mutant on the agonists carbachol and acetylcholine in rat M_3. The F$^{5\times47}$A mutant decreases the binding affinity of N-methylscopolamine for M1 and M3, and the affinities of tiotropium and tiotropoium analogues Cpd1, Cpd2 and Cpd9 for M3. In contrast, the F$^{5\times47}$A mutant does not have a significant effect on the binding of QNB and acetylcholine and even increases binding of Cpd7 with the methylated hydroxyacetate scaffold.[113,117] This residue is located deep in the orthosteric pocket and seems to affect more the ligands with only one aromatic ring through stacking contacts. The V511$^{6\times55}$A/I

DOI: 10.1021/acs.jmedchem.8b00836
J. Med. Chem. 2019, 62, 3784−3839

mutations in the major pocket of M_3 have little effect on the investigated ligands.[113,132]

4.3.2. Minor Pocket and Extracellular Vestibule Mutations in Muscarinic Acetylcholine Receptors. From the current crystal structures, the minor pocket in muscarinic acetylcholine receptors seems to be inaccessible for small molecule ligands. The tyrosine lid almost completely separates the orthosteric binding site and the extracellular vestibule, and the only connection between them in the available crystal structures is a narrow channel at position 4 of the more extracellular thiophene ring of tiotropium. However, for ligand access to and egress from the binding pocket, the lid must be flexible, and it cannot be ruled out that future crystal structures will show alternative arrangements of these residues. Indeed, it has been shown in long-scale molecular dynamics simulations that these tyrosines often change rotameric states but that their flexibility depends also on the quality of polar interactions ligands form with other residues of the binding site, e.g., $N^{6\times52}$.[113,133] As described, the above mutation of the tyrosine lid residues have a detrimental effect on orthosteric ligand binding but variable effect on allosteric modulators, in some cases even increasing allosteric modulator binding and cooperativity. In the extracellular vestibule, the $Y^{2\times60}A$ mutation somewhat reduces binding of several orthosteric ligands such as QNB, atropine, and carbachol possibly through affecting ligand-binding kinetics.[33,51,109,116,134] Interestingly, the binding of acetylcholine is reduced by this mutation in M_1, not affected in M_2, and increased in M_4.[33,52,116] The $Y^{2\times60}A$ mutation decreases M1 binding affinity of the allosteric modulator Benzoquinolinone 12 and dualsteric ligands TBPB, VCP974 and VCP813, but does not have a negative effect on M1/M2 affinity for 77-LH-28-1, AC42, BQCA, and M4 affinity for LY2033298 (despite the fact that the co-crystallized analogue LY2119620 forms an H-bond with this tyrosine).[33,51,52,109,116,135] The $Y^{2\times63}A$ mutation decreases the M1 affinity for Benzoquinolinone 12, TBPB, VCP974 and 77-LH-28-1, but does not affect M_1 affinity for VCP813, and M_4 affinity for LY203329.[33,51−53,109] Mutation of the conserved $W^{23\times50}$ in ECL1 to alanine or even phenylalanine is detrimental to the binding of orthosteric ligands and also to methoctramine in M_1 and LY2033298 in M_4 possibly due to altering receptor dynamics or folding.[33,53] The $W^{3\times28}A/F$ mutation, which is in a stacking interaction with $Y^{2\times60}$ and $W^{23\times50}$ in the crystal structures, is detrimental to the binding of orthosteric ligands but has variable effects on binding affinity of allosteric modulators and dualsteric ligands.[33,51,53,106,109,114−116,123,130,131,135−137] The $W^{3\times28}A$ mutation increases the binding affinity of 77-LH-28-1, TBPB, VCP794, AC-260584, and AC-42 in M_1 and M_2, which might be the result of the increased conformational freedom and accessibility of $Y^{2\times60}$. In M_4, the mutation also decreases binding of W84 and LY2033298. The $L^{3\times29}A$ mutation abolishes or decreases binding of tested orthosteric and allosteric ligands as well.[33,51,109,114−116,130] This residue is located between $W^{3\times28}$ and $I^{45\times52}$ and is probably required for correct packing of ECL2. Mutation of $Y^{45\times51}$ and $I^{45\times52}$ located in ECL2, however, seems to have very selective effects on the tested ligands.[33,51,52,109,116,117,120,135,138,139] In 40 of 58 mutant−ligand combinations, these mutations do not show a significant effect on ligand binding to muscarinic receptors. However, the $Y^{45\times51}A$ mutant abolishes binding of benzoquinazolinone 12 and LY2033298 in $M_{1/4}$ but increases that of TBPB in M_1.[51,52] The $Y177^{45\times51}Q$ mutant furthermore abolishes binding of W84 in M_2.[138] The $I^{45\times52}A$ mutant increases binding of BQCA, 77-LH-28-1, VCP794, and LY2033298 (possibly by increasing the size of the allosteric binding site) but has no effect on TBPB and VCP813 in $M_{1/3/4}$.[33,51,109,117,140] Interestingly, mutation of $N^{6\times58}$ does not have a significant effect on the tested ligands in all muscarinic receptors, even on LY2033298, although it forms an H-bond with the cocrystallized LY2119620.[33,141,142] The $N419^{7\times31}K$ and $T423^{7\times35}H$ mutants decrease binding of gallamine and W84 in M_2 because of the introduced charge repulsion, but mutation to other amino acids does not have a significant effect.[138,143] Mutation of $W^{7\times34}$ equivocally abolishes or decreases binding of all tested allosteric ligands in $M_{1/4}$ in consensus with this residue being an important aromatic stacking or cation−π interaction partner for both first- and second-generation allosteric ligands.[33,51−53] Finally, mutation of several residues that do not have a generic number assigned also has significant effects on ligand binding. The Q181A mutation in human M_1 located after the conserved triad in ECL2 increases binding of BQCA but has no significant effect on other allosteric modulators.[51,53,109,135] The Q427A mutation in human M_4 located in ECL3 increases binding of LY2033298.[33] Several mutations in ECL2 furthermore decrease or abolish binding of orthosteric ligands. The R171A, F182A, and L183A mutants in human M_1 ECL2 as well as the corresponding mutants R171A in rat M_1, R213I/T, F224A, L225A in rat M_3, and L190A in human M_4 decrease binding of acetylcholine, carbachol, atropine, NMS, and QNB. These results are consistent with the fact that the phenylalanine and leucine residues are facing the orthosteric binding site and the arginine is stabilizing the conformation of ECL2 by forming a salt bridge with $D^{3\times26}$ and an H-bond with $Q^{4\times65}$, residues that are conserved in muscarinic receptors.[33,53,109,113,117,131,135,140,144,145]

4.4. Structure-Based Extrapolation of Muscarinic Acetylcholine Receptor Mutation Effects. Mutation data predictions within the muscarinic acetylcholine receptor family were performed for human data for M_1, M_2, M_3, and M_4 receptors with available crystal structures. The original muscarinic acetylcholine receptor data that could be used for extrapolation contained 504 points for the M_1 receptor, 191 for M_2, 193 for M_3, and 174 for M_4, which referred to 16%, 12%, 20%, and 45% mutational data map coverage, respectively. In retrospective studies, on average, 20% of original data points were predicted: 23% (116 data points) for M_1, 28% (54) for M_2, 12% (24) for M_3, and 24% (41) for M_4 with accuracies of 0.20, 0.70, 0.88, and 0.71, respectively. In prospective studies, 748 points could be predicted for M_1 (however, the low accuracy in retrospective studies indicates a potentially lower quality for prospective predictions for this receptor subtype), 154 for M_2, 136 for M_3, and 104 for M_4. The heat maps referring to the original data set used for extrapolation, and the retrospective and prospective predictions are provided in the Supporting Information.

5. ADRENERGIC RECEPTOR MUTATIONS

5.1. Structural Adrenergic Receptor−Ligand Interactions. Adrenergic receptors are activated by the small neurotransmitter adrenaline (epinephrine). In humans, there are nine adrenergic receptor subtypes, of which (turkey) β_1 and β_2 adrenergic receptors have already been crystallized. The antagonists and inverse agonists 7-methylcyanopindolol (PDB: 5A8E[152]), bucindolol (PDB: 4AMI[153]), carazolol (PDB:

DOI: 10.1021/acs.jmedchem.8b00836
J. Med. Chem. 2019, 62, 3784−3839

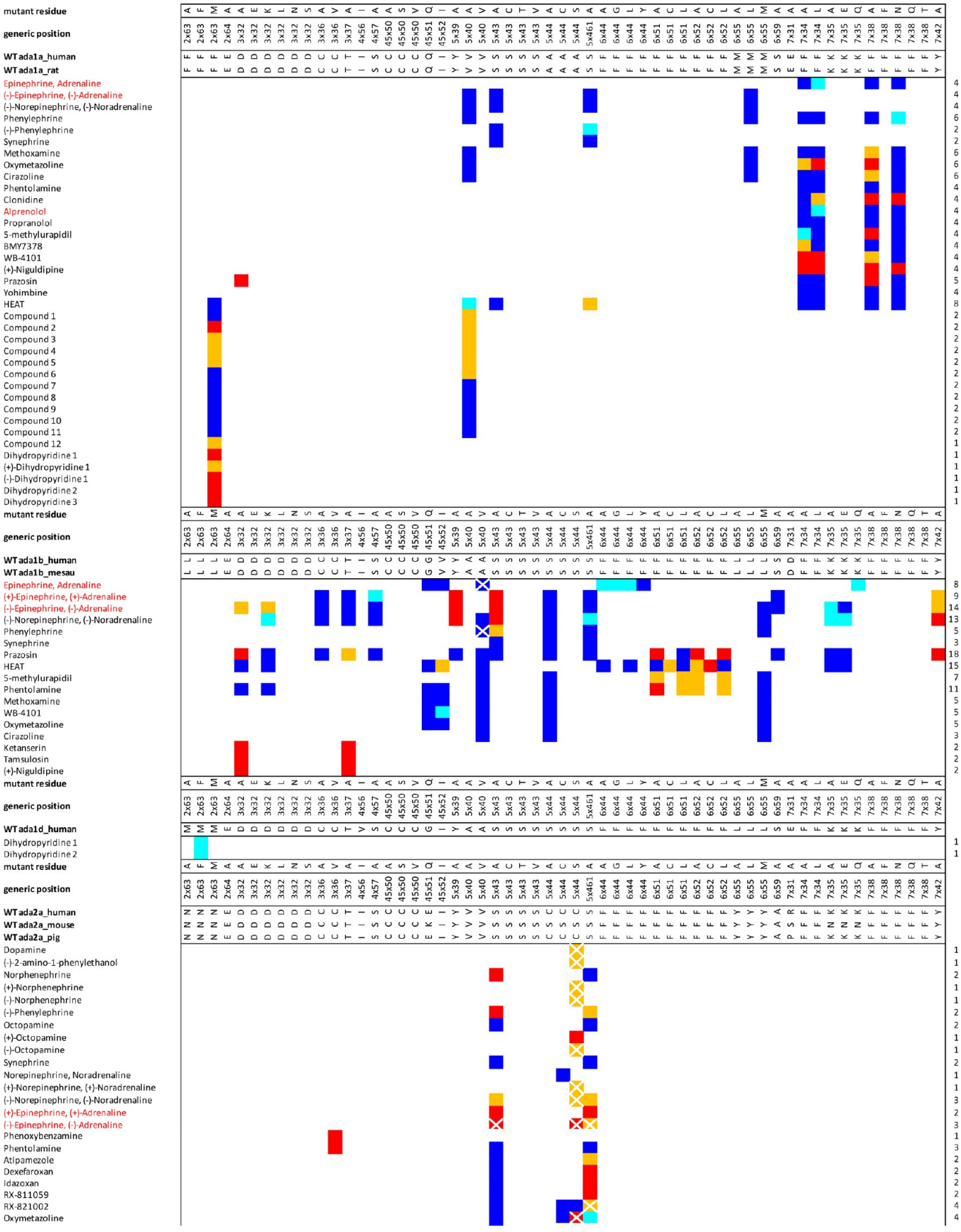

Figure 11. continued

DOI: 10.1021/acs.jmedchem.8b00836
J. Med. Chem. 2019, 62, 3784−3839

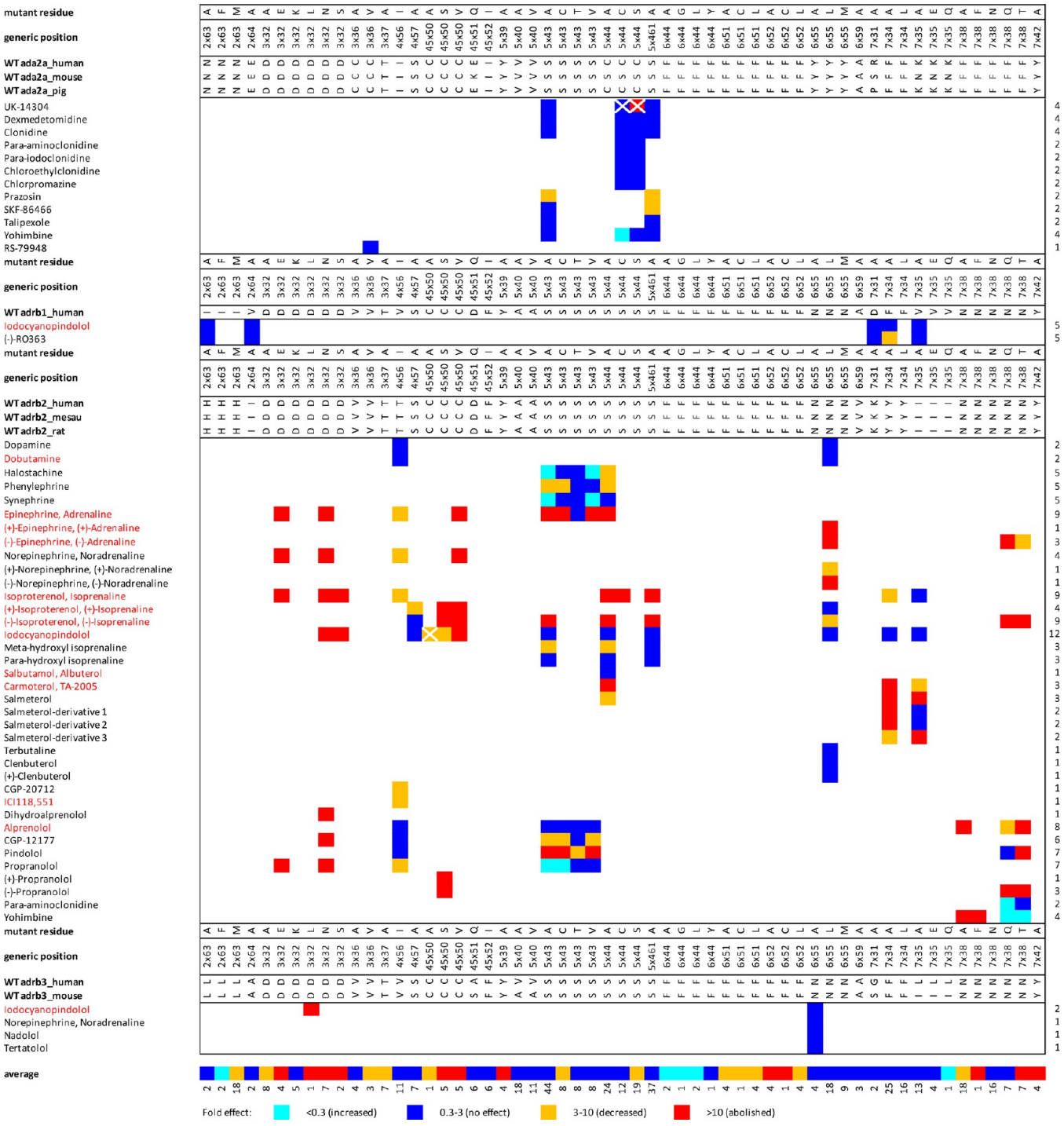

Figure 11. Adrenergic receptor mutation data.[129,174−177,179,182−213] Data is shown for the consensus binding pocket defined using structure-based generic position numbers from GPCRdb.[18] Wild-type residues for the orthologues involved in mutation studies, and the mutant residues are shown (note that only the mutations which have a data point shown in the table were actually carried out, the table is organized for comparability among orthologues). Ligands are grouped similarly as in Figure 12. When multiple data points were available for the specific mutant−ligand combination, the geometric mean of the fold effect values was used. See Figure 5 for color coding. Mutant numbers for each ligand and ligand numbers for each mutant are indicated in the right side and the bottom of the heat map, respectively. The average fold effect (geometric mean) for each mutant is also shown at the bottom of the heat map. PDF and Excel versions of the heat map are provided in the Supporting Information.

2YCW[154]), carvedilol (PDB: 4AMJ[153]), cyanopindolol (PDB: 2VT4,[155] 2YCX, 2YCY,[154] 4BVN,[36] 5F8U[156]), indolylpiperazine (PDB: 3ZPQ[73]), iodocyanopindolol (PDB: 2YCZ[154]), and quinolylpiperazine (PDB: 3ZPR[73]) and the full and partial agonists carmoterol (PDB: 2Y02[157]), dobutamine (PDB: 2Y00, 2Y01[157]), isoprenaline (PDB: 2Y03[157]), and salbutamol (PDB: 2Y04[157]) bound turkey β_1 adrenergic receptor crystal structures, and the antagonists and inverse agonists alprenolol (PDB: 3NYA[158]), an aminopropyloxybenzofurane (PDB: 3NY9[158]), carazolol (PDB: 2RH1,[2] 4GBR,[159] 5D5A, 5D5B,[160] 5D6L,[161] 5JQH,[162] 5X7D[163]), timolol (PDB: 3D4S[164]), and the full and partial agonists adrenaline (PDB:

DOI: 10.1021/acs.jmedchem.8b00836
J. Med. Chem. 2019, 62, 3784−3839

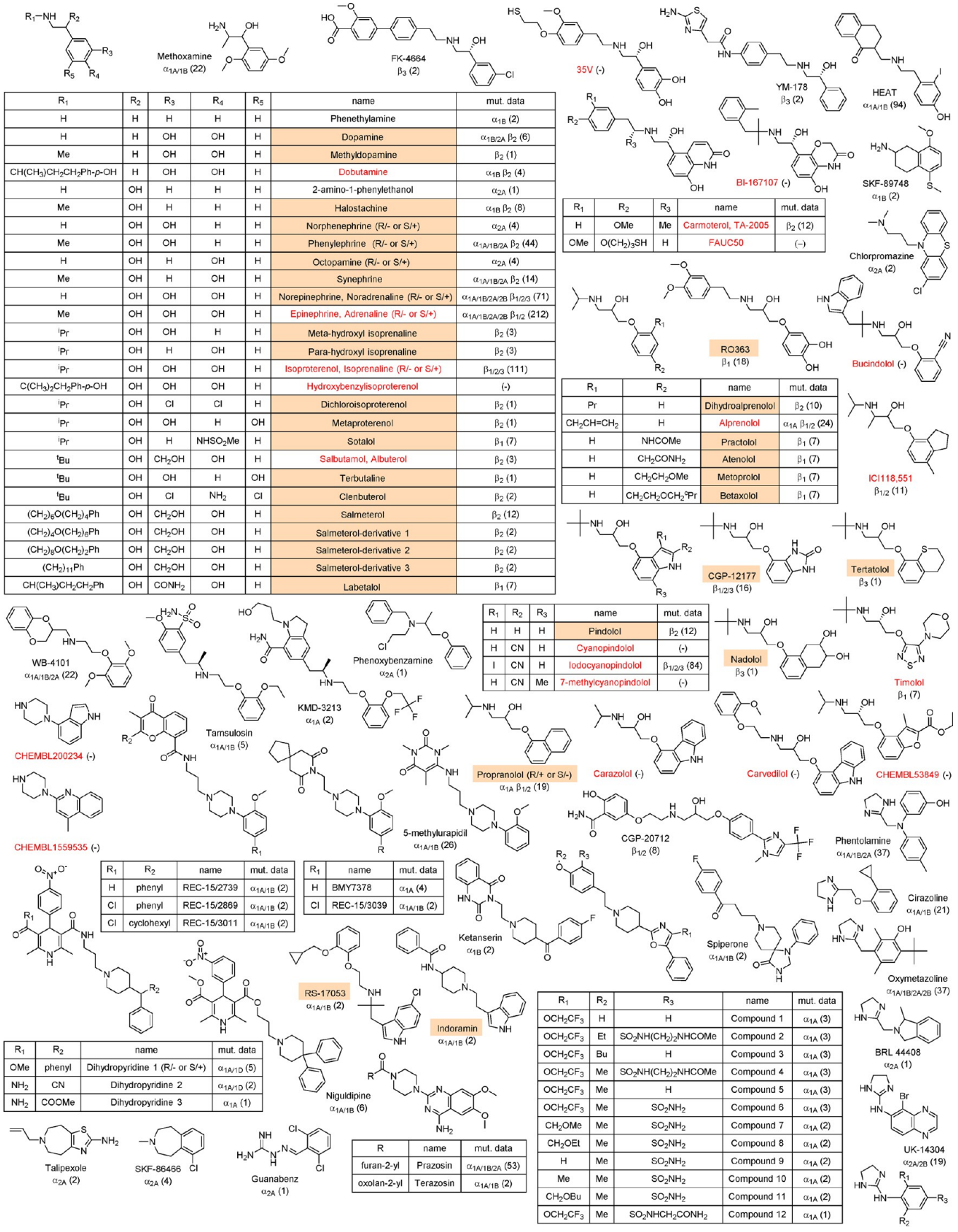

R_1	R_2	R_3	R_4	R_5	name	mut. data
H	H	H	H	H	Phenethylamine	α_{1B} (2)
H	H	OH	OH	H	Dopamine	$\alpha_{1B/2A}$ β_2 (6)
Me	H	OH	OH	H	Methyldopamine	β_2 (1)
$CH(CH_3)CH_2CH_2Ph$-*p*-OH	H	OH	OH	H	Dobutamine	α_{1B} β_2 (4)
H	OH	H	H	H	2-amino-1-phenylethanol	α_{2A} (1)
Me	OH	H	H	H	Halostachine	α_{1B} β_2 (8)
H	OH	OH	H	H	Norphenephrine (R/- or S/+)	α_{2A} (4)
Me	OH	OH	H	H	Phenylephrine (R/- or S/+)	$\alpha_{1A/1B/2A}$ β_2 (44)
H	OH	H	OH	H	Octopamine (R/- or S/+)	α_{2A} (4)
Me	OH	H	OH	H	Synephrine	$\alpha_{1A/1B/2A}$ β_2 (14)
H	OH	OH	OH	H	Norepinephrine, Noradrenaline (R/- or S/+)	$\alpha_{1A/1B/2A/2B}$ $\beta_{1/2/3}$ (71)
Me	OH	OH	OH	H	Epinephrine, Adrenaline (R/- or S/+)	$\alpha_{1A/1B/2A/2B}$ $\beta_{1/2}$ (212)
^{i}Pr	OH	OH	H	H	Meta-hydroxyl isoprenaline	β_2 (3)
^{i}Pr	OH	H	OH	H	Para-hydroxyl isoprenaline	β_2 (3)
^{i}Pr	OH	OH	OH	H	Isoproterenol, Isoprenaline (R/- or S/+)	$\beta_{1/2/3}$ (111)
$C(CH_3)_2CH_2Ph$-*p*-OH	OH	OH	OH	H	Hydroxybenzylisoproterenol	(-)
^{i}Pr	OH	Cl	Cl	H	Dichloroisoproterenol	β_2 (1)
^{i}Pr	OH	OH	H	OH	Metaproterenol	β_2 (1)
^{i}Pr	OH	H	$NHSO_2Me$	H	Sotalol	β_1 (7)
^{t}Bu	OH	CH_2OH	OH	H	Salbutamol, Albuterol	β_2 (3)
^{t}Bu	OH	OH	H	OH	Terbutaline	β_2 (1)
^{t}Bu	OH	Cl	NH_2	Cl	Clenbuterol	β_2 (2)
$(CH_2)_6O(CH_2)_4Ph$	OH	CH_2OH	OH	H	Salmeterol	β_2 (12)
$(CH_2)_4O(CH_2)_6Ph$	OH	CH_2OH	OH	H	Salmeterol-derivative 1	β_2 (2)
$(CH_2)_8O(CH_2)_2Ph$	OH	CH_2OH	OH	H	Salmeterol-derivative 2	β_2 (2)
$(CH_2)_{11}Ph$	OH	CH_2OH	OH	H	Salmeterol-derivative 3	β_2 (2)
$CH(CH_3)CH_2CH_2Ph$	OH	$CONH_2$	OH	H	Labetalol	β_1 (7)

R_1	R_2	R_3	name	mut. data
H	OMe	Me	Carmoterol, TA-2005	β_2 (12)
OMe	$O(CH_2)_3SH$	H	FAUC50	(-)

R_1	R_2	name	mut. data
Pr	H	Dihydroalprenolol	β_2 (10)
$CH_2CH=CH_2$	H	Alprenolol	α_{1A} $\beta_{1/2}$ (24)
H	NHCOMe	Practolol	β_1 (7)
H	CH_2CONH_2	Atenolol	β_1 (7)
H	CH_2CH_2OMe	Metoprolol	β_1 (7)
H	$CH_2CH_2OCH_2{}^cPr$	Betaxolol	β_1 (7)

R_1	R_2	R_3	name	mut. data
H	H	H	Pindolol	β_2 (12)
H	CN	H	Cyanopindolol	(-)
I	CN	H	Iodocyanopindolol	$\beta_{1/2/3}$ (84)
H	CN	Me	7-methylcyanopindolol	(-)

R_1	R_2	name	mut. data
H	phenyl	REC-15/2739	$\alpha_{1A/1B}$ (2)
Cl	phenyl	REC-15/2869	$\alpha_{1A/1B}$ (2)
Cl	cyclohexyl	REC-15/3011	$\alpha_{1A/1B}$ (2)

R_1	name	mut. data
H	BMY7378	α_{1A} (4)
Cl	REC-15/3039	$\alpha_{1A/1B}$ (2)

R_1	R_2	name	mut. data
OMe	phenyl	Dihydropyridine 1 (R/- or S/+)	$\alpha_{1A/1D}$ (5)
NH_2	CN	Dihydropyridine 2	$\alpha_{1A/1D}$ (2)
NH_2	COOMe	Dihydropyridine 3	α_{1A} (1)

R	name	mut. data
furan-2-yl	Prazosin	$\alpha_{1A/1B/2A}$ (53)
oxolan-2-yl	Terazosin	$\alpha_{1A/1B}$ (2)

R_1	R_2	R_3	name	mut. data
OCH_2CF_3	H	H	Compound 1	α_{1A} (3)
OCH_2CF_3	Et	$SO_2NH(CH_2)_2NHCOMe$	Compound 2	α_{1A} (3)
OCH_2CF_3	Bu	H	Compound 3	α_{1A} (3)
OCH_2CF_3	Me	$SO_2NH(CH_2)_2NHCOMe$	Compound 4	α_{1A} (3)
OCH_2CF_3	Me	H	Compound 5	α_{1A} (3)
OCH_2CF_3	Me	SO_2NH_2	Compound 6	α_{1A} (3)
CH_2OMe	Me	SO_2NH_2	Compound 7	α_{1A} (2)
CH_2OEt	Me	SO_2NH_2	Compound 8	α_{1A} (2)
H	Me	SO_2NH_2	Compound 9	α_{1A} (2)
Me	Me	SO_2NH_2	Compound 10	α_{1A} (2)
CH_2OBu	Me	SO_2NH_2	Compound 11	α_{1A} (2)
OCH_2CF_3	Me	$SO_2NHCH_2CONH_2$	Compound 12	α_{1A} (1)

Figure 12. continued

DOI: 10.1021/acs.jmedchem.8b00836
J. Med. Chem. 2019, 62, 3784−3839

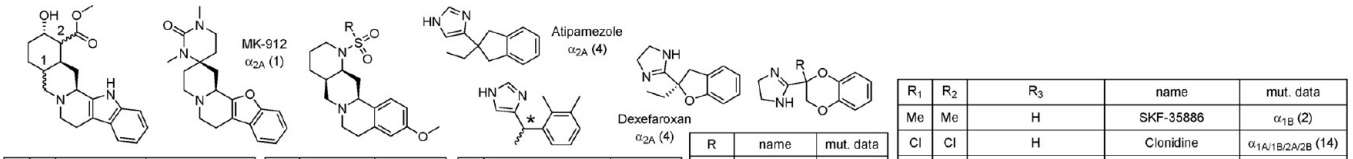

1	2	name	mut. data
R	R	Yohimbine	$\alpha_{1A/1B/2A}$ β_2 (20)
S	S	Rauwolscine	α_{1B} (1)

R	name	mut. data
Me	RS-15385	α_{2A} (1)
Et	RS-79948	α_{2A} (3)

*	name	mut. data
R	Levomedetomidine	α_{2B} (1)
S	Dexmedetomidine	$\alpha_{2A/2B}$ (7)

R	name	mut. data
H	Idazoxan	α_{2A} (6)
OMe	RX-821002	$\alpha_{2A/2B}$ (7)
OEt	RX-811059	α_{2A} (4)

R_1	R_2	R_3	name	mut. data
Me	Me	H	SKF-35886	α_{1B} (2)
Cl	Cl	H	Clonidine	$\alpha_{1A/1B/2A/2B}$ (14)
Cl	Cl	NH_2	Para-aminoclonidine	α_{2A} β_2 (5)
Cl	Cl	I	Para-iodoclonidine	α_{2A} (2)
Cl	Cl	$CH_2N(Me)CH_2CH_2Cl$	Chloroethylclonidine	α_{2A} (2)

Figure 12. Adrenergic receptor ligands used in mutation studies.[129,174−177,179,182−213] Cocrystallized ligands in β_1 and β_2 structures shown in red. Chemically similar ligands to any of the cocrystallized ligands in adrenergic receptor crystal structures indicated with orange background, chemically similar ligands to any cocrystallized ligand in aminergic receptor crystal structures indicated with a cyan background. Receptors with available mutation data for the specific ligand are indicated along with the number of data points in parentheses. A PDF version of the figure is provided in the Supporting Information.

4LDO[165]), BI-167107 (PDB: 3P0G,[166] 3SN6,[167] 4LDE[165]), a covalent agonist (PDB: 4QKX[168]), FAUC50 (PDB: 3PDS[169]), hydroxybenzylisoproterenol (PDB: 4LDL[165]), and ICI-118,551 (PDB: 3NY8[158]) bound human β_2 adrenergic receptor crystal structures show a conserved ligand binding mode in the orthosteric pocket, covering residues in the amine pocket ($D^{3\times32}$, $V^{3\times36}$, $W^{6\times48}$, $F^{6\times51}$, $N^{7\times38}$, $Y^{7\times42}$) and major pocket ($V^{3\times33}$, $T^{3\times37}$, $Y^{5\times39}$, $A^{5\times40}$, $S^{5\times43}$, $S^{5\times44}$, $S^{5\times461}$, $F^{6\times52}$, $N^{6\times55}$). The interaction patterns with different residues targeted in the minor pocket and extracellular vestibule ($G^{2\times60}$, $L/H^{2\times63}$, $V/I^{2\times64}$, $W^{3\times28}$, $T^{3\times29}$, $D^{45\times51}$, $F^{45\times52}$, $D/K^{7\times31}$, $F/Y^{7\times34}$, $V/I^{7\times35}$, $W^{7\times39}$) of β_1 by the cocrystallized ligands dobutamine, carmoterol, bucindolol, and carvedilol and of β_2 by the cocrystallized ligands BI-167107 and hydroxybenzylisoproterenol determine the ligand-dependent structure−affinity, −function, and −selectivity relationships of dualsteric adrenergic receptor ligands. The adrenergic receptor crystal binding site structures are very conserved even among the two different subtypes and active/inactive states. The average heavy atom RMSD for β_1 and β_2 receptor subtypes are 0.8 and 1.0 Å, respectively. The average backbone RMSD for these subtypes are 0.5 and 0.7 Å, respectively. The average backbone RMSD for all adrenergic receptors is 0.6 Å, with the largest difference of 1.2 Å between the antagonist salbutamol-bound β_1 and the agonist hydroxybenzylisoproterenol-bound β_2 (Figures 3, 13, and 20). In this case, the extracellular tip of TM5 is shifted about 1.5 Å outward and the tips of TM6 and TM7 about 1.2 and 2.4 Å inward in the agonist-bound structure relative to the antagonist-bound structure. Ligand binding modes are also very well conserved in adrenergic crystal structures, the orthosteric aromatic moieties, and the key H-bonding ethanolamine moieties almost perfectly overlap among structures. There is some variation in the aromatic moieties used in the minor pocket, the shorter ones interact with $F/Y^{7\times34}$ and $W^{3\times28}$, while the longer ones interact with $W^{7\times39}$ and $Y^{7\times42}$. In the amine pocket, $D^{3\times32}$ and $N^{7\times38}$ form a concerted H-bond interaction network with ethanolamine moieties present in 52 of the 125 β-adrenergic ligands investigated in mutation studies. Ligands lacking the hydroxyl group such as the piperazine moieties of the small, fragment-like indolylpiperazine and quinolylpiperazine ligands do not form concerted H-bonds with the β-adrenergic receptor specific residue $N^{7\times38}$ but target the same amine pocket and form an ionic interaction with $D^{3\times32}$, providing a structural template for piperazine containing ligands in adrenergic receptors consistent with the essential role of the cationic properties of the amine group of ethanolamine ligands in mutational studies and other β-adrenoreceptor ligands (section 5.3.1). The catechol, quinolinone, benzoxazinone, indole, carbazole, and other aromatic scaffolds of the cocrystallized ligands form hydrophobic interactions with $V^{3\times33}$, $F^{45\times52}$, $Y^{5\times39}$, $A^{5\times40}$, $F^{6\times51}$, $F^{6\times52}$ and form H-bond interactions with $S^{5\times43}$ and often with $S^{5\times46}$ and $N^{6\times55}$ in the major pocket between TM3−6. The endogenous ligand adrenaline (in the structure 4LDO, the only aminergic GPCR crystal structure with an endogenous ligand) forms all of the aforementioned H-bonds in the amine and the major pockets. Mutation studies demonstrate the important role of these hydrophobic and polar residues (section 5.3.2), and SAR studies show the preference of adrenergic receptors for ligands with aromatic moieties with at least one polar H-bond interaction functionality, mimicking the catechol group of adrenaline. In the minor pocket and extracellular vestibule, the arylalkyl appendages of the cocrystallized ligands carmoterol, carvedilol, BI-167107, and FAUC50 form hydrophobic/aromatic interactions with $W^{23\times50}$, $W^{3\times28}$, $F/Y^{7\times34}$, $V/I^{7\times35}$, and $W^{7\times39}$ and polar groups of dobutamine, bucindolol, and hydroxybenzylisoproterenol form H-bonds with residues $D^{45\times51}$, $W^{7\times39}$, and the backbone of $C^{45\times50}$ that are also available for polar interactions with minor pocket binding appendages of ligands such as CGP-20712. Furthermore, $S^{2\times60}$ and $K/Q^{7\times35}$ in α-adrenoreceptors, $N^{2\times63}$ in α_2-adrenoreceptors, and the variable $Q/E/K/D^{45\times51}$ and $E/D/R/H/K^{7\times31}$ might provide polar anchor points for dualsteric adrenergic ligands. The β_2 adrenergic receptor is unique among aminergic GPCRs in that it is the only one crystallized in a ternary complex with an orthosteric antagonist (carazolol) and an intracellular allosteric synthetic peptide antagonist (Cmpd-15) (PDB: 5X7D[163]). The data set contains 91 mutation data points associated with residue positions lining the intracellular binding pocket of Cmpd-15, 5-$HT_{1A/2A/2C/7}$, $M_{1/2/3/5}$, $\alpha_{1B/2A}$, and β_2. It should be noted however that all these studies used orthosteric radioligands, and therefore the observed effects possibly originate from differential G protein binding.

5.2. Chemical Space of Adrenergic Receptor Ligands in Crystal Structures and Mutation Studies. Nine of the cocrystallized β-adrenergic receptor ligands, the endogenous agonist epinephrine (212, Figure 13), the partial/full agonists carmoterol (12 mutation data points), dobutamine (4), isoproterenol (111), salbutamol (3), and the antagonists/inverse agonists iodocyanopindolol (84, Figure 13), alprenolol (12), ICI-118,551 (11), and timolol (7) have been extensively investigated in mutation studies of seven receptors, covering 201 mutations of 99 residues in total (Figure 11). Twenty-three of these residues line the binding sites of these ligands in β_1 and β_2 adrenergic receptor crystal structures (Figure 3). The cocrystallized BI-167107, bucindolol, carazolol, carvedilol, 7-methylcyanopindolol, cyanopindolol, FAUC50, hydroxylben-

DOI: 10.1021/acs.jmedchem.8b00836
J. Med. Chem. 2019, 62, 3784−3839

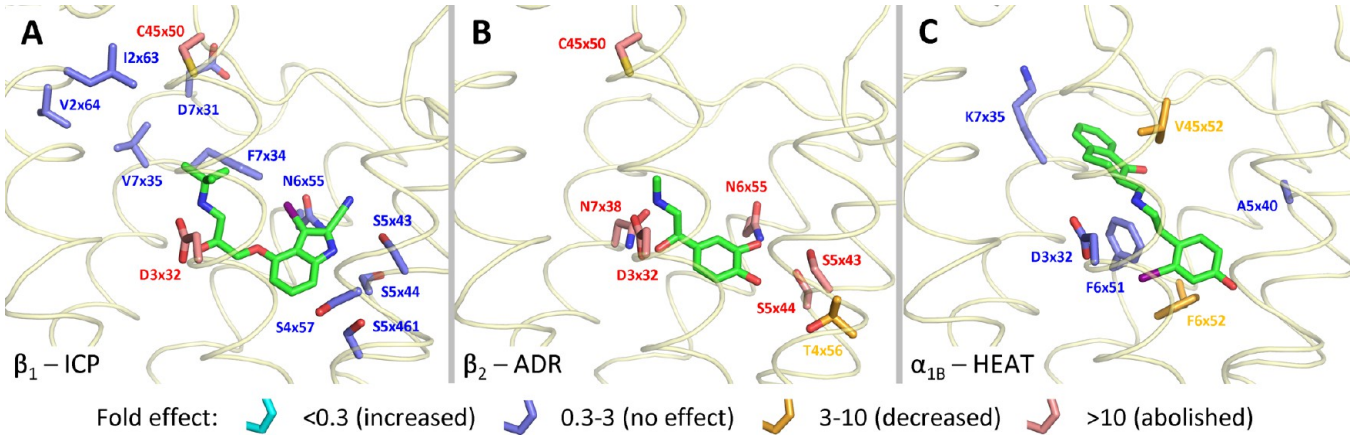

Figure 13. Adrenergic receptor ligand binding modes and associated mutation data. (A) β_1 (PDB: 2YCZ[154]) with cocrystallized iodocyanopindolol, mutation effects mapped on structure for $\beta_{1/2}$-iodocyanopindolol. (B) β_2 (PDB: 4LDO[165]) with cocrystallized adrenaline, mutation effects mapped on structure for β_2-adrenaline. (C) α_{1B} homology model from GPCRdb with docked HEAT, mutation effects mapped on structure for α_{1B}-HEAT. See Figure 5 for color coding. Mutation effects for alanine mutants were used where available.

zylisoprenaline, indolylpiperazine, and quinolylpiperazine ligands in complex with β_1 adrenergic and β_2 adrenergic crystal structures have not yet been investigated in mutation studies but share chemical and binding mode similarity[170] with the crystallized ligands for which mutation data are available. Thirty ligands that share the 2-amino-1-phenylethan-1-ol substructure with cocrystallized (agonist) ligands (including norepinephrine, phenylephrine) and 22 ligands that share the 1-amino-3-phenoxypropan-2-ol substructure with crystallized inverse agonists/antagonists (including CGP-1277, CGP-20712, propranolol) cover 506 (38%) and 290 (22%) ligand−mutant combinations, respectively. Thirty-three (26%) of the ligands investigated in mutation studies (excluding cocrystallized ones) are chemically similar to any of the cocrystallized β_1 and β_2 adrenergic receptor ligands (including nonethanolamines RS-17053 and indoramin) and cover 318 (24%) ligand mutant combinations (Figure 12). Compounds that do not share chemical similarity with any aminergic cocrystallized ligand cover 541 different mutant−ligand combinations, including 2-phenoxyethan-1-amines (e.g., WB-4101, tamsulosin), imidazolines (e.g., phentolamine, oxymetazoline, cirazoline, UK-14304, clonidine), phenylpiperazines (including 5-methylurapidil), aminoquinazoline piperazines (prazosin, terazosin), niguldipine analogues, and tetra/pentacyclic amines (yohimbine). However, 35 (28%) compounds are pharmacophorically similar to any of the cocrystallized ligands. In addition, nonselective aminergic receptor ligands ketanserin, spiperone, and chlorpromazine have been investigated in adrenergic, serotonin, and dopamine receptor mutation studies, and several other ligands including alprenolol, propranolol, labetalol, and pindolol were studied in adrenergic and serotonin receptors and noradrenaline and dopamine were studied in adrenergic and dopamine receptors, providing insights into the receptor specific determinants of binding of these ligands by different aminergic GPCRs.

5.3. Structural Determinants of Adrenergic Receptor−Ligand Interactions. *5.3.1. Amine and Major Pocket Mutations in Adrenergic Receptors.* Mutation of conserved $D^{3\times32}$ to nonacidic residues has been shown to diminish binding of epinephrine, ketanserin, tamsulosin, and niguldipine at the α_{1B} adrenergic receptor ($D125^{3\times32}A$ and $D125^{3\times32}K$) and adrenaline, noradrenaline, isoprenaline, iodocyanopindolol, and propranolol at the β_2 adrenergic receptor ($D113^{3\times32}E/N/S$).[171−173] $Y^{7\times42}$ stabilizes the conformation of $D^{3\times32}$ through a hydrogen bond in adrenergic receptors, and not surprisingly also the $Y338^{7\times42}A$ mutation in hamster α_{1B} abolishes binding of the endogenous ligands and the inverse agonist prazosin.[174,175] The β_2 adrenergic receptor affinities of the β adrenergic selective ligands alprenolol, epinephrine, isoproterenol, and propranolol are decreased for the $N312^{7\times38}Q$ and $N312^{7\times38}T$ mutants and pindolol affinity is decreased by the $N312^{7\times38}T$ mutant (but not by the $N312^{7\times38}Q$ mutant),[176] consistent with the important role of this β adrenergic specific residue in binding the ethanolamine moieties of both agonists and antagonists in β_1 adrenergic and β_2 adrenergic receptor crystal structures. The same $N312^{7\times38}Q$ and $N312^{7\times38}T$ mutants increase β_2 affinity for the α_{2A} antagonists yohimbine and *para*-aminoclodine,[176] confirming $N^{7\times38}$ as an important determinant of β adrenergic receptor selectivity versus $F^{7\times38}$ in α adrenergic receptors. $F^{7\times34}A/L$ or $F^{7\times38}A$ mutations significantly decrease affinity for the α_1 antagonists (BMY7378, 5-methylurapidil, niguldipine, prazosin, and WB4101) and small imidazoline partial agonists (cirazoline, clonidine, and oxymetazoline) but do not affect the affinity for nonselective phenethylamine agonists (epinephrine, methoxamine, phenylephrine) or the more bulky phentolamine.[177] The $F^{7\times34}L$ mutant increases the affinity for the β-adrenergic receptor antagonist alprenolol, but not of propranolol, consistent with the interaction of the ethylene group of alprenolol with the homologous $Y308^{7\times34}$ residue in the β_2 adrenergic receptor crystal structure. $F^{7\times34}A/L$ or $F^{7\times38}A$ mutants also decrease α_1 binding of the small imidazoline-containing partial agonist cirazoline, clonidine, and oxymetazoline but do not have an effect on binding of the bulkier imidazoline antagonist phentolamine, which may be able to compensate the loss of interactions with $F^{7\times34}/F^{7\times38}$ by accommodating two instead of one phenyl ring in the hydrophobic major pocket between $W^{6\times48}$, $F^{6\times51}$, $F^{6\times52}$, and $F^{6\times55}$. This binding mode hypothesis is consistent with the large decrease of phentolamine and 5-methylurapidil binding affinities for the $F310^{6\times51}A/L$ and $F311^{6\times52}A/L$ mutants in α_{1B}.[178] The affinity of prazosin is only affected by the $F310^{6\times51}A$ and $F311^{6\times52}A/L$ mutations and not by the $F310^{6\times51}L$ mutation, whereas the binding affinity of HEAT (Figure 13) is only decreased by the $F310^{6\times51}C$ and $F311^{6\times52}A/C$ mutations.[178] This comparative analysis indicates

DOI: 10.1021/acs.jmedchem.8b00836
J. Med. Chem. 2019, 62, 3784−3839

that the roles of hydrophobic/aromatic interactions with F310$^{6\times51}$ and F311$^{6\times52}$ are ligand-dependent and suggest different binding modes of the aromatic moieties of 5-methylurapidil, phentolamine, prazosin, and HEAT in the major pocket of the α_{1A} adrenergic receptor. Interestingly, although F$^{6\times44}$ is located deep in the binding pocket, mutation of this residue to the smaller residues glycine, alanine, or leucine increases affinity of adrenaline[178,179] by affecting the activation mechanism of GPCRs. Mutation of F303$^{6\times44}$ reduces the hydrophobic hindering mechanism and thereby also increases the constitutive activity of the receptor.[180,181] S$^{5\times43}$A/C/V or S$^{5\times461}$A mutants of α_{1B}, α_{2A}, and β_2 receptors affect binding of phenethylamine agonists with a *meta*-hydroxyl moiety (carmoterol, epinephrine, isoprenaline, *meta*-hydroxyl isoprenaline, norepinephrine, norphenephrine, phenylephrine) and phenoxyethylamine antagonists with polar substituents connected to the phenoxy group (CGP-12177, pindolol).[179,182−187] In contrast, α_{1B}, α_{2A}, and β_2 receptors affinities for phenethylamine agonists that only contain a para-substituted hydroxyl group (*para*-hydroxyl isoprenaline, octopamine, salbutamol) or ligands that do not contain a polar substituent at 5−7 Å from the amine group (alprenolol, clonidine, halostachine, phentolamine, propranolol, synephrine) are not affected by these mutations.[182,183,188,189] The ligand-dependent effects of S$^{5\times43}$ and S$^{5\times461}$ are consistent with the role of these residues as H-bond interaction partners of polar groups in isoproterenol, BI-167107, carmoterol, epinephrine, and pindolol in β_1 and β_2 adrenergic receptor crystal structures. S$^{5\times461}$ mutants furthermore decrease the binding affinities of α_{2A} for ligands that contain polar atoms at 5−7 Å from the imidazoline nitrogen (atipamezole, idazoxan, oxymetazoline, RX-811059, RX-821002, UK-14304),[189] providing useful constraints to construct structural imidazoline bound α adrenergic receptor models. The V$^{5\times40}$A mutant decreases α_{1A} affinity for piperidine oxazole compounds 1−6, but not of compounds 7−11, suggesting that the trifluoro-ethyl substituents of compounds 1−6 interact with this residue. The mutations S$^{5\times44}$A in α_{1B} and β_2, S$^{5\times44}$C in mouse α_{2A} and β_2 and C$^{5\times44}$S in human/pig α_{2A} have a highly receptor subtype and also ligand-dependent effects. For example, the S$^{5\times44}$A mutation has no effect on any ligand binding in α_{1B}[182,188] but negatively affects most ligands in β_2, except for phenethylamines with only a *para*-hydroxyl substituent, suggesting a somewhat altered binding mode for these ligands.[185−187,190] The S201$^{5\times44}$C mutant in mouse α_{2A} has no effect,[191] but the same mutant in β_2 abolishes isoprenaline binding.[185,187,190] The reverse C$^{5\times44}$S in human/pig α_{2A} reduces binding of all adrenaline analogues but generally has no effect on non-phenethylamine ligands,[191−193] implying that this residue might be involved in the polar interaction network around TM3, 5, 6 although it is not seen to form H-bonds with cocrystallized ligands. The same is true for Y$^{5\times39}$ as the Y$^{5\times39}$A mutation abolishes binding of the endogenous ligands, while it does not affect that of prazosin.[188] This residue is seen to form an H-bond with S$^{5\times43}$ in multiple crystal structures, thus it is plausible that this extended network of polar contacts is required for adrenergic receptor function. The N$^{6\times55}$L mutant in the β_2 receptor, which is also seen to form an H-bond with acceptor moieties of cocrystallized ligands, abolishes binding of (nor)adrenaline and isoprenaline but not of several other catechol compounds, therefore it is possibly an important recognition point for the less tight binding ligands but not as important for more optimized ligands.[194] This is underlined by the fact that in α receptors this position features hydrophobic residues and mutation of these does not affect binding of a range of ligands. The T130$^{3\times37}$A mutant of the α_{1B} adrenergic receptor has decreased affinity for the antagonists ketanserin, niguldipine, prazosin, and tamsulosin but unaffected binding affinity for the agonists epinephrine and norepinephrine.[188] The C117$^{3\times36}$V mutant of the α_{2A} adrenergic receptor is not compatible with high affinity binding of the antagonists phenoxybenzamine and phentolamine but does not affect binding of the antagonist RS-79948,[195] suggesting that phenoxybenzamine and phentolamine bind deeper in the major pocket than RS-79948.

5.3.2. Minor Pocket and Extracellular Vestibule Mutations in Adrenergic Receptors. Relatively little mutation data is available for the minor and extracellular vestibule in adrenergic receptors. The F86$^{2\times63}$M mutant in the α_{1A} adrenergic receptor decreases binding of piperidine oxazole compounds 2−5 and 12, suggesting that the phenethyl appendage of this series of ligands interacts with F86$^{2\times63}$.[196,197] This mutation also reduces affinity of dihydropyridines 1−3, indicating that the bulky dihydropyridine moiety contacts TM2 in the extracellular vestibule. The reverse M156$^{2\times63}$F mutant in α_{1D} accordingly increases the affinity of these ligands. Neither the I118$^{2\times63}$A nor the V119$^{2\times64}$A mutants affect binding of the agonist RO363 to β_1.[177] This observation suggests that the appendage of this ligand rather contacts F325$^{7\times34}$ in the same way as carmoterol in the 2Y02 crystal structure.[157] Mutations at positions 45×51 and 45×52 in ECL2 have only been reported for the α_{1B} receptor. This subtype has an unusual G$^{45\times51}$ residue; however, mutation of this to larger polar residues does not affect ligand binding, which is consistent with the conformation pointing away from the ligand binding site in $\beta_{1/2}$ crystal structures.[198] The V$^{45\times52}$I mutation has minor effects on the bulky hydrophobic antagonists HEAT and WB-4101 but not on other tested ligands, including adrenaline, phentolamine, methoxamine, and oxymetazoline.[198] Other mutations in ECL2 include the cysteine bridge between C184 and C190 in the β_2 receptor. Disruption of this link is detrimental to binding of several tested ligands by modifying the structure/dynamics of ECL2. Mutations at positions 6×59 and 7×31 on the tops of TM6 and 7 have no effect on the tested ligands, but it is unlikely that even bitopic ligands would extend toward these residues.[177,188] Finally, the K331$^{7\times35}$A/E/Q mutations in α_{1B} increase binding of (nor)adrenaline, possibly by removing the charge−charge repulsion with these small ligands but have no effect on prazosin and HEAT.[175] Mutation of the analogous hydrophobic residues in the β receptors to alanine reduces binding of ligands with arylalkyl appendages carmoterol and salmeterol but not RO363 and ligands without a large appendage.[177,199,200]

5.4. Structure-Based Extrapolation of Adrenergic Receptor Mutation Effects. Mutation data predictions within the adrenergic receptor family were performed for human data for only the β_2 receptor with available crystal structures. Due to the limited number of data points and low interaction fingerprint similarity of the ligands, no predictions could be made for the β_1 receptor despite having many crystal structures at hand. The original adrenergic receptor data that could be used for extrapolation contained 299 data points (11% coverage); retrospective studies predicted 23% of points (70), and 748 points were a result of the prospective analysis. Accuracy of the retrospective predictions was 0.59. The heat maps referring to the original data set used for extrapolation,

DOI: 10.1021/acs.jmedchem.8b00836
J. Med. Chem. 2019, 62, 3784−3839

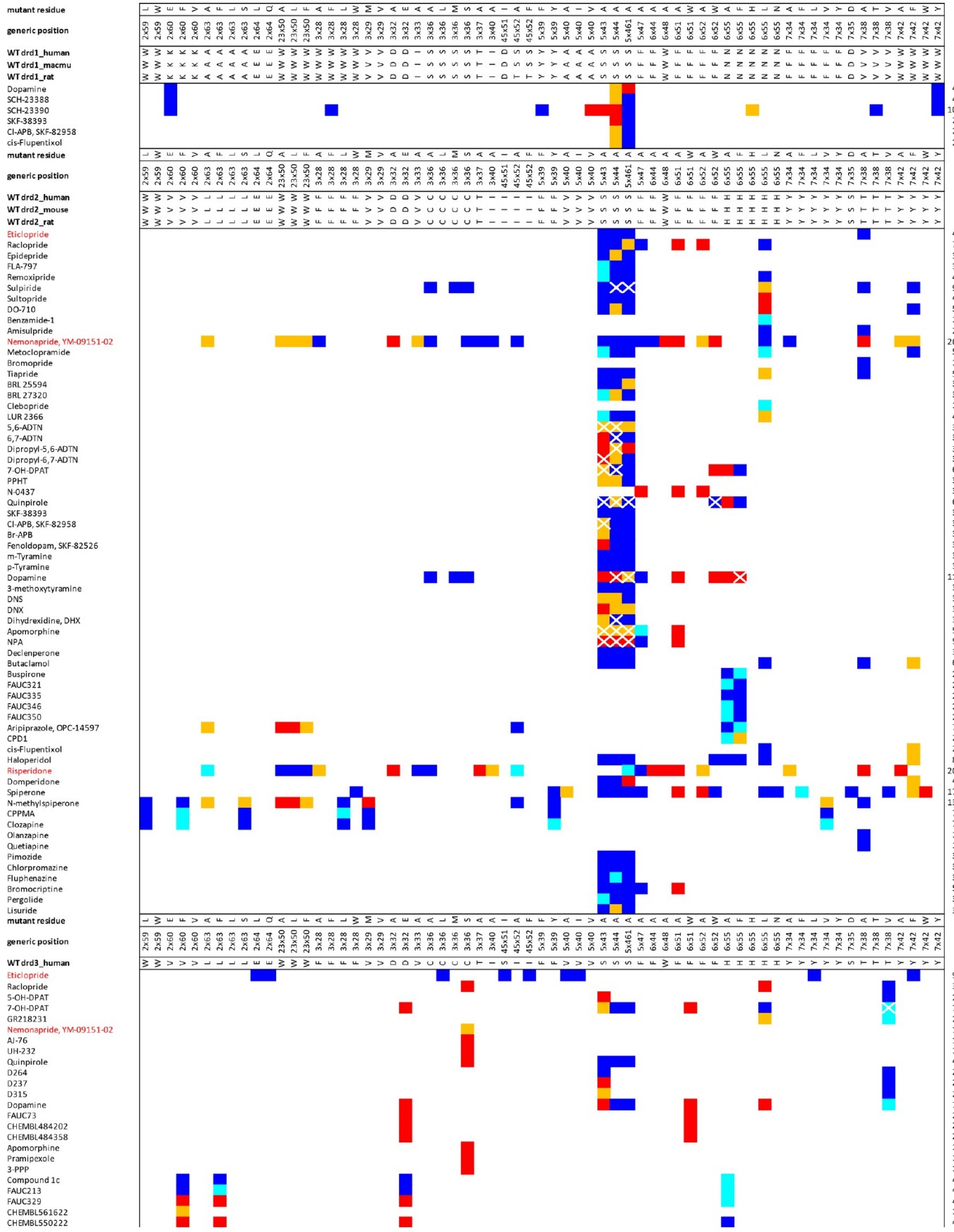

Figure 14. continued

DOI: 10.1021/acs.jmedchem.8b00836
J. Med. Chem. 2019, 62, 3784−3839

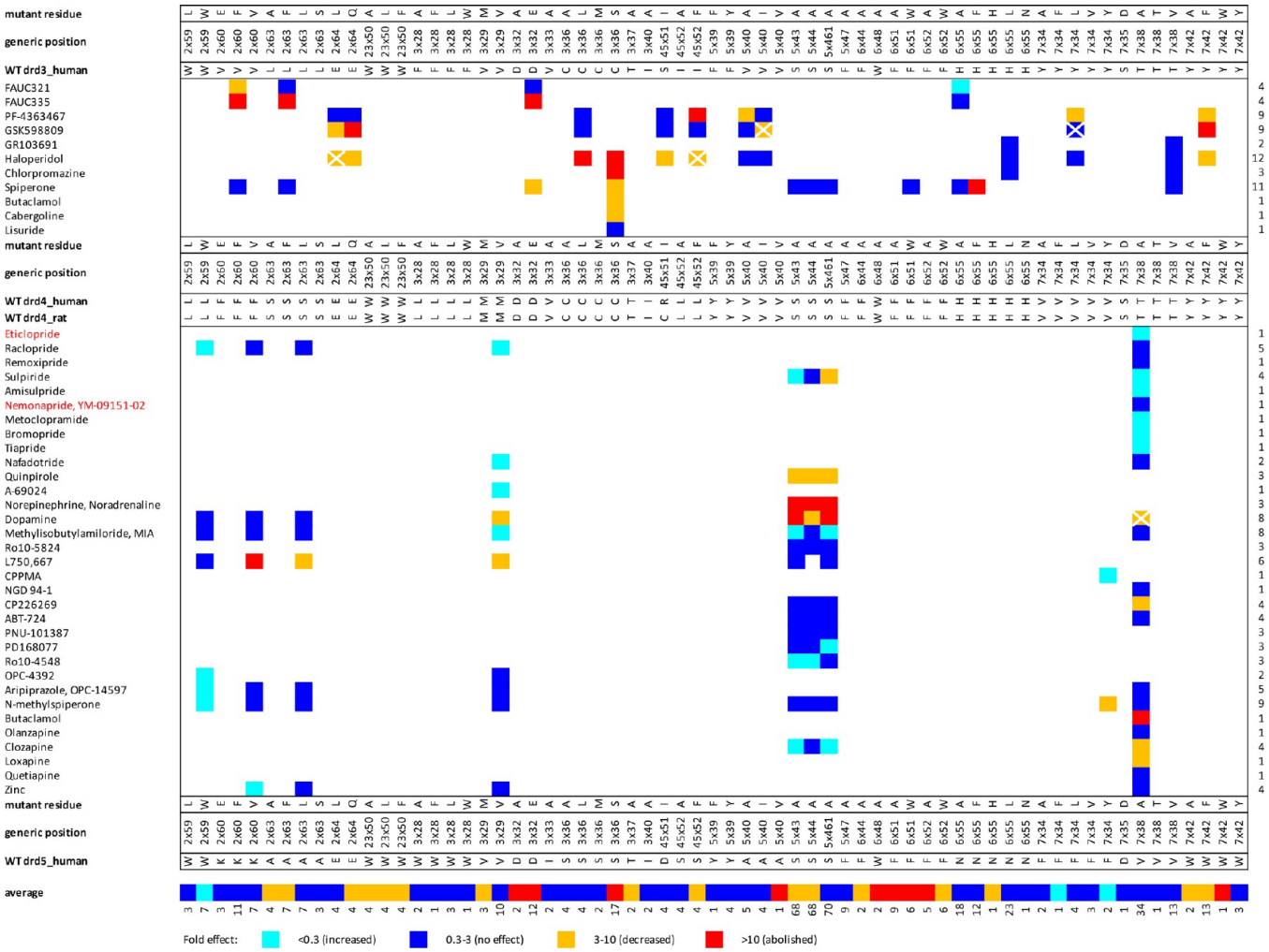

Figure 14. Dopamine receptor mutation data.[214−217,219−241] Data is shown for the consensus binding pocket defined using structure-based generic position numbers from GPCRdb.[18] Wild-type residues for the orthologues involved in mutation studies and the mutant residue are shown (note that only the mutations which have a data point shown in the table were actually carried out, the table is organized for comparability among orthologues). Ligands are grouped similarly as in Figure 15. When multiple data points were available for the specific mutant−ligand combination, the geometric mean of the fold effect values was used. See Figure 5 for color coding. Mutant numbers for each ligand and ligand numbers for each mutant are indicated in the right side and the bottom of the heat map, respectively. The average fold effect (geometric mean) for each mutant is also shown at the bottom of the heat map. PDF and Excel versions of the heat map are provided in the Supporting Information.

and the retrospective and prospective predictions are provided in the Supporting Information.

6. DOPAMINE RECEPTOR MUTATIONS

6.1. Structural Dopamine Receptor−Ligand Interactions. Dopamine receptors are activated by the small neurotransmitter dopamine. In humans, there are five dopamine receptor subtypes of which the D_2, D_3, and D_4 receptors have been crystallized.[38] The antagonist eticlopride bound D_3 (PDB: 3PBL[38]) and antagonist nemonapride bound D_4 (PDB: 5WIU, 5WIV[39]) crystal structures show a conserved binding mode of the pyrrolidinylmethylbenzamide scaffold in the orthosteric pocket, covering residues in the amine pocket ($D^{3\times32}$, $C^{3\times36}$, $W^{6\times48}$, $F^{6\times51}$, $T^{7\times38}$, $Y^{7\times42}$) and major pocket ($V^{3\times33}$, $T^{3\times37}$, $F/Y^{5\times39}$, $V^{5\times40}$, $S^{5\times43}$, $S^{5\times44}$, $S^{5\times461}$, $F^{6\times52}$, $H^{6\times55}$, $I/V^{6\times56}$). Only a few residues are in contact with eticlopride in the minor pocket and extracellular vestibule ($V^{2\times56}$, $F/V^{2\times60}$, $L/S^{2\times63}$, $F/L^{3\times28}$, $M/V^{3\times29}$, $I/L^{45\times52}$, $V/Y^{7\times34}$). The benzyl moiety of nemonapride further opens up a subpocket between TM2 and TM3 between $L^{2\times59}$ and $L^{3\times28}$ in D_4.[39] These residues are $W^{2\times59}$ and $F/W^{3\times28}$ in other dopamine receptors, respectively, and their aromatic rings are oriented away from each other, $W^{2\times59}$ toward the membrane and $F/W^{3\times28}$ toward the binding pocket. Therefore, this subpocket possibly only exists in D_4. A plethora of dualsteric ligands are available for dopamine receptors, such as the cocrystallized antagonist risperidone in D_2 (PDB: 6CM4[37]), which extends toward the extracellular vestibule. The tetrahydropyridopyrimidinone appendage of risperidone forms a water-mediated H-bond with $H^{6\times55}$, aromatic interactions with $W^{23\times50}$, $F^{3\times28}$, $F^{6\times51}$, and $Y^{7\times34}$, and contacts with $V^{2\times60}$, $L^{2\times63}$, and $T^{7\times38}$. Other residues available for polar interactions in the extracellular vestibule include $E^{2\times64}$, $D/S^{7\times35}$, and $T^{7\times38}$, which determine the ligand-dependent structure−affinity, −function, and −selectivity relationships of dopamine receptor ligands. There are only a few dopamine receptor crystal structures, but substantial variations could be seen among the different subtypes in the extracellular tips of TM5−7 helices and all ECL conformations. The average heavy atom RMSD for D_3, and D_4 receptor subtypes is 0.4 Å. The average backbone RMSD for these

DOI: 10.1021/acs.jmedchem.8b00836
J. Med. Chem. 2019, 62, 3784−3839

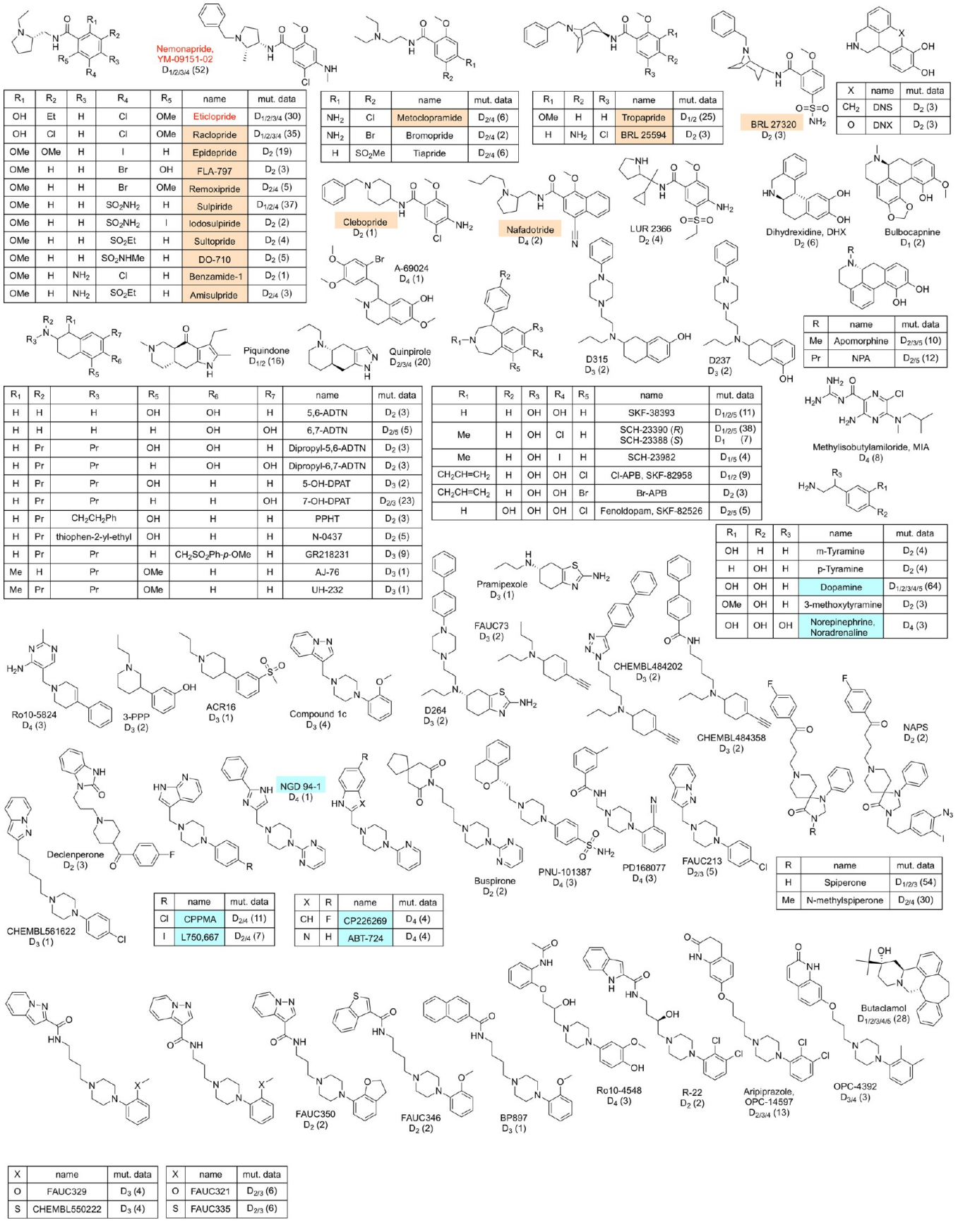

R_1	R_2	R_3	R_4	R_5	name	mut. data
OH	Et	H	Cl	OMe	Eticlopride	$D_{1/2/3/4}$ (30)
OH	Cl	H	Cl	OMe	Raclopride	$D_{1/2/3/4}$ (35)
OMe	OMe	H	I	H	Epidepride	D_2 (19)
OMe	H	H	Br	OH	FLA-797	D_2 (3)
OMe	H	H	Br	OMe	Remoxipride	$D_{2/4}$ (5)
OMe	H	H	SO_2NH_2	H	Sulpiride	$D_{1/2/4}$ (37)
OMe	H	H	SO_2NH_2	I	Iodosulpiride	D_2 (2)
OMe	H	H	SO_2Et	H	Sultopride	D_2 (4)
OMe	H	H	SO_2NHMe	H	DO-710	D_2 (5)
OMe	H	NH_2	Cl	H	Benzamide-1	D_2 (1)
OMe	H	NH_2	SO_2Et	H	Amisulpride	$D_{2/4}$ (3)

R_1	R_2	name	mut. data
NH_2	Cl	Metoclopramide	$D_{2/4}$ (6)
NH_2	Br	Bromopride	$D_{2/4}$ (2)
H	SO_2Me	Tiapride	$D_{2/4}$ (6)

R_1	R_2	R_3	name	mut. data
OMe	H	H	Tropapride	$D_{1/2}$ (25)
H	NH_2	Cl	BRL 25594	D_2 (3)

X	name	mut. data
CH_2	DNS	D_2 (3)
O	DNX	D_2 (3)

R	name	mut. data
Me	Apomorphine	$D_{2/3/5}$ (10)
Pr	NPA	$D_{2/5}$ (12)

R_1	R_2	R_3	R_5	R_6	R_7	name	mut. data
H	H	H	OH	OH	H	5,6-ADTN	D_2 (3)
H	H	H	H	OH	OH	6,7-ADTN	$D_{2/5}$ (5)
H	Pr	Pr	OH	OH	H	Dipropyl-5,6-ADTN	D_2 (3)
H	Pr	Pr	H	OH	OH	Dipropyl-6,7-ADTN	D_2 (3)
H	Pr	Pr	OH	H	H	5-OH-DPAT	D_3 (2)
H	Pr	Pr	H	H	OH	7-OH-DPAT	$D_{2/3}$ (23)
H	Pr	CH_2CH_2Ph	OH	H	H	PPHT	D_2 (3)
H	Pr	thiophen-2-yl-ethyl	OH	H	H	N-0437	D_2 (5)
H	Pr	Pr	H	CH_2SO_2Ph-*p*-OMe	H	GR218231	D_3 (9)
Me	H	Pr	OMe	H	H	AJ-76	D_3 (1)
Me	Pr	Pr	OMe	H	H	UH-232	D_3 (1)

R_1	R_2	R_3	R_4	R_5	name	mut. data
H	H	OH	OH	H	SKF-38393	$D_{1/2/5}$ (11)
Me	H	OH	Cl	H	SCH-23390 (*R*) SCH-23388 (*S*)	$D_{1/2/5}$ (38) D_1 (7)
Me	H	OH	I	H	SCH-23982	$D_{1/5}$ (4)
$CH_2CH{=}CH_2$	H	OH	OH	Cl	Cl-APB, SKF-82958	$D_{1/2}$ (9)
$CH_2CH{=}CH_2$	H	OH	OH	Br	Br-APB	D_2 (3)
H	OH	OH	OH	Cl	Fenoldopam, SKF-82526	$D_{2/5}$ (5)

R_1	R_2	R_3	name	mut. data
OH	H	H	m-Tyramine	D_2 (4)
H	OH	H	p-Tyramine	D_2 (4)
OH	OH	H	Dopamine	$D_{1/2/3/4/5}$ (64)
OMe	OH	H	3-methoxytyramine	D_2 (3)
OH	OH	OH	Norepinephrine, Noradrenaline	D_4 (3)

R	name	mut. data
Cl	CPPMA	$D_{2/4}$ (11)
I	L750,667	$D_{2/4}$ (7)

X	R	name	mut. data
CH	F	CP226269	D_4 (4)
N	H	ABT-724	D_4 (4)

R	name	mut. data
H	Spiperone	$D_{1/2/3}$ (54)
Me	N-methylspiperone	$D_{2/4}$ (30)

X	name	mut. data
O	FAUC329	D_3 (4)
S	CHEMBL550222	D_3 (4)

X	name	mut. data
O	FAUC321	$D_{2/3}$ (6)
S	FAUC335	$D_{2/3}$ (6)

Figure 15. continued

DOI: 10.1021/acs.jmedchem.8b00836
J. Med. Chem. 2019, 62, 3784−3839

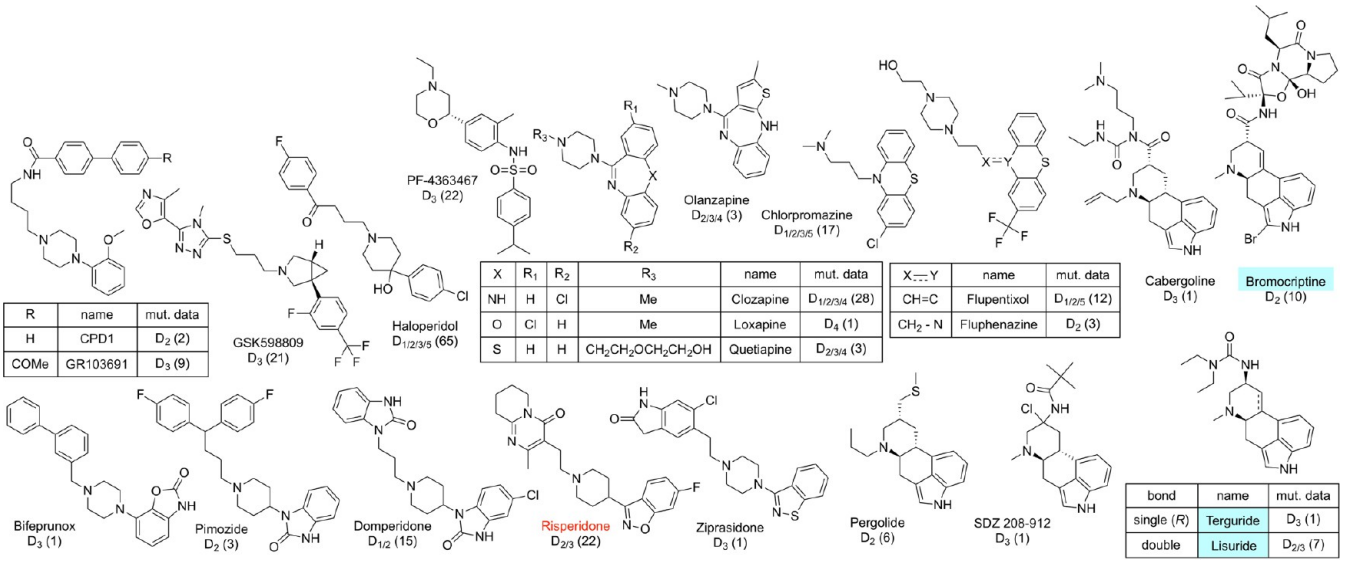

Figure 15. Dopamine receptor ligands used in mutation studies.[214−217,219−241] Cocrystallized ligands in the D_2, D_3, and D_4 structures shown in red. Chemically similar ligands to the cocrystallized ligands in dopamine receptor crystal structures indicated with orange background, chemically similar ligands to any cocrystallized ligand in aminergic receptor crystal structures indicated with a cyan background. Receptors with available mutation data for the specific ligand are indicated along with the number of data points in parentheses. A PDF version of the figure is provided in the Supporting Information.

subtypes are 0.3 and 0.1 Å, respectively. The average backbone RMSD for all dopamine receptors is 1.33 Å, with the largest difference of 2.3 Å between the risperidone-bound D_2 and the nemonapride-bound D_4 (Figures 3, 16, 20). In this case, the extracellular tips of helices TM4−7 are shifted about 2−2.5 Å relative to each other. D_3 and D_4 crystal structures show a similar binding mode of the benzamide ligands, however, as mentioned earlier, in D_4 an extra subpocket is opened between TM2 and TM3, and the extracellular tips of TM6 and TM7 are also shifted relative to each other by 2 and 1.2 Å, respectively. On the other hand, risperidone in D_2 opens a deep subpocket in the hydrophobic core of the receptor, reaching $I^{3\times40}$ as seen also in the methiothepin and ritanserin-bound serotonin crystal structures. Furthermore, the extracellular tip of TM5 is shifted 2.8 Å inward and the tip of TM6 4 Å outward in D_2 relative to the other dopamine receptors. In the amine pocket, $D^{3\times32}$ forms an ionic interaction with the amine group of basic ligands such as pyrrolidinylmethylbenzamide, aminotetralin, aryl-piperidine, and aryl-piperazine compounds, while residue $Y^{7\times42}$ stabilizes the conformation of $D^{3\times32}$ and residues $W^{6\times48}$ and $F^{6\times51}$ form cation−π interaction, consistent with mutation studies (section 6.3.1) and SAR studies, showing the essential role of the cationic properties of the amine group of most dopamine receptor ligands. The substituted benzamide moiety of the cocrystallized ligands eticlopride and nemonapride make hydrophobic interactions with $V^{3\times33}$, $C^{3\times36}$, $I^{45\times52}$, $F^{6\times51}$, $F^{6\times52}$, and $H^{6\times55}$ in $D_{2/3}$. Risperidone furthermore contacts $I^{3\times40}$, $F^{5\times47}$, and $F^{6\times44}$ in a deeper orthosteric binding pocket in D_2. Nemonapride forms an H-bond with $S192^{5\times43}$ and halogen bond with $S193^{5\times44}$ in D_3. The endogenous ligand, dopamine, potentially forms H-bond interactions with $T^{3\times37}$, $S^{5\times43}$, $S^{5\times44}$, and/or $S^{5\times461}$ in the major pocket between TM3−6 in dopamine receptors. Mutation studies demonstrate the important role of these hydrophobic and polar residues (section 6.3.2), and SAR studies demonstrate the preference of dopamine receptors for ligands with multiply substituted aromatic moieties binding this region. Ortho- and meta-substitution with hydrophobic substituents are beneficial on benzamide and aryl-piperazine ligands, such as in the privileged 2,3-dichlorophenylpiperazine scaffold and various phenol bioisosteres, are also employed mimicking the catecholamine group of the endogenous ligand. Interestingly, the mutation of $S^{5\times43}$, $S^{5\times44}$, $S^{5\times461}$, and $H/N^{6\times55}$ show highly ligand-dependent effects in D_{1-4}. In the D_3 crystal structure, an H-bond network is formed by $Y365^{7\times34}$, $H349^{6\times55}$, and the backbone of $I183^{45\times52}$, creating a lid over the major pocket, but there is a tunnel toward the minor pocket from the amine pocket. Only a few data points are available for the minor pocket and extracellular vestibule in combination with dualsteric ligands (e.g., for polar residues $E^{2\times64}$, $T^{7\times38}$, and hydrophobic residues $V^{2\times60}$, $L^{2\times63}$, and $Y/F^{7\times34}$). However, no data is yet available for $D/S^{7\times35}$ that potentially also forms H-bond interactions with ketone or heterocyclic amide groups of dualsteric ligands such as buspirone, aripiprazole, domperidone, haloperidol, and spiperone.

6.2. Chemical Space of Dopamine Receptor Ligands in Crystal Structures and Mutation Studies. The cocrystallized dopamine receptor ligands eticlopride (30 mutants), nemonapride (52 mutants), and risperidone (22 mutants) as well as close analogues raclopride (35 mutants, Figure 16), sulpiride (37 mutants), and the endogenous dopamine (64 mutants, Figure 16) have been extensively investigated in mutation studies of the dopamine D_1, D_2, D_3, and D_4 receptors covering 27 different residues in total (Figure 14). Seventeen of these residues line the binding site in the dopamine receptor crystal structures (Figure 3). Sixteen (12%) of the ligands investigated in mutation studies are chemically similar, and 12 (9%) are pharmacophorically similar to the cocrystallized ligands (Figure 15). All benzamide ligands (including analogues with noncyclic or a tropane basic moiety) have been investigated at 182 (20%) ligand−mutant combinations in total. Phenethylamine analogues have been investigated at 235 (28%) ligand−mutant combinations in total. Aryl-piperidine and aryl-piperazine ligands have been

DOI: 10.1021/acs.jmedchem.8b00836
J. Med. Chem. 2019, 62, 3784−3839

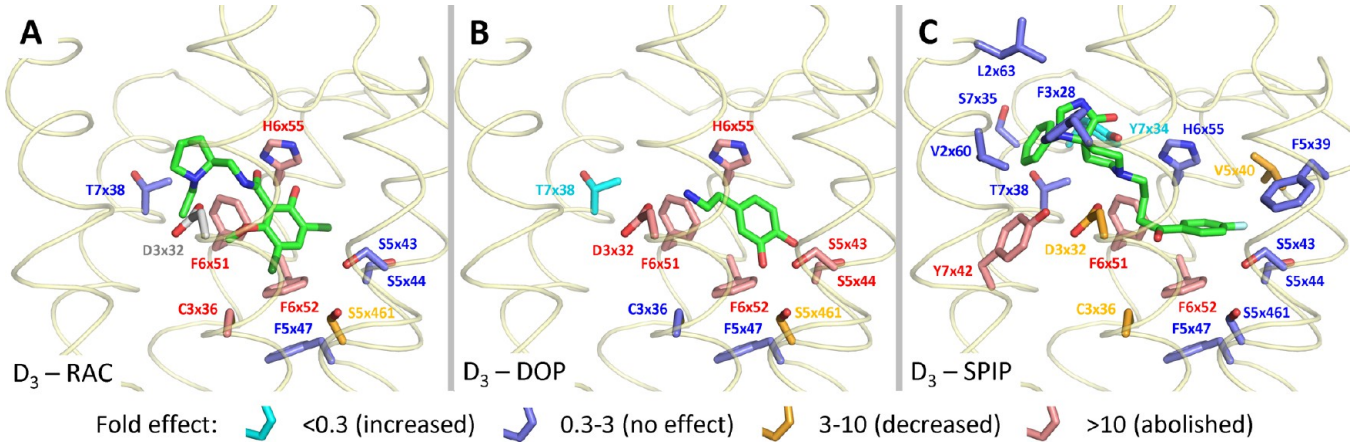

Figure 16. Dopamine receptor ligand binding modes and associated mutation data. (A) D_3 (PDB: 3PBL[38]) with docked raclopride, analogue of cocrystallized eticlopride, mutation effects mapped on structure for $D_{2/3}$-raclopride. (B) D_3 (PDB: 3PBL) with docked dopamine, mutation effects mapped on structure for $D_{2/3}$-dopamine. (C) D_3 (PDB: 3PBL) with docked spiperone, mutation effects mapped on structure for $D_{2/3}$-spiperone. See Figure 5 for color coding. Mutation effects for alanine mutants were used where available.

investigated at 169 (18%) ligand−mutant combinations in total. Most of these compounds do not share 2D chemical or 3D shape/pharmacophore-based similarity with the cocrystallized dopamine receptor ligands but represent combined ligand and receptor SAR data sets that provide detailed information on the structural determinants of dopamine receptor binding. Moreover, 10 ligands are chemically similar to cocrystallized ligands in serotonin and adrenergic receptor complexes, such as ergolines terguride, lisuride and bromocriptine, endogenous dopamine and noradrenaline, and aryl-piperazines with heterocyclic substitutions at the basic amine (e.g., CPPMA). Several nonselective aminergic receptor ligands, including clozapine, spiperone, chlorpromazine, lisuride, and haloperidol, have been investigated altogether at 98 different dopamine receptor mutants, as well as mutants at other receptor subfamilies (e.g., clozapine was used in serotonin, muscarinic, dopamine, and histamine receptor mutation studies), providing insights into the receptor specific determinants of binding of these ligands by different aminergic GPCRs.

6.3. Structural Determinants of Dopamine Receptor−Ligand Interactions. *6.3.1. Amine and Major Pocket Mutations in Dopamine Receptors.* Mutation of the conserved $D^{3\times32}$ to nonacidic residue alanine has only been tested for nemonapride and risperidone, where it abolished functional activity in both cases.[37] Mutation to glutamic acid ($D110^{3\times32}E$) has been shown to diminish binding for 9 of 12 ligands in the dopamine D_3 receptor, including the endogenous dopamine, 7-OH-DPAT, cyclohexene-amine agonists, and the dualsteric FAUC329, FAUC335, and spiperone (Figure 16) ligands, indicating that not only the ionic interaction with the anionic carboxylate group of $D^{3\times32}$ is required for ligand binding but also the size of the residue is of importance.[214,215] The $Y^{7\times42}F$ mutant in $D_{2/3}$ lacking a stabilizing H-bond interaction with $D^{3\times32}$ has no pronounced effect on the binding of orthosteric ligands such as the antagonists eticlopride, sulpiride, DO-710, and metoclopramide; however, it decreases binding of the antagonists nemonapride, flupentixol, and PF-4363467 with larger appendages on the basic amine and dualsteric ligands haloperidol, domperidone, spiperone, and GSK598809, suggesting that the H-bond between $Y^{7\times42}$ and $D^{3\times32}$ is important in shaping the secondary binding pocket in dopamine receptors.[216−218] Interestingly, D_1 and D_5 are among the few aminergic receptors (along with histamine H_3 and H_4) with a tryptophan at the 7×42 position. Mutation to the more abundant tyrosine in D_1 ($W^{7\times42}Y$) does not affect binding of three ligands including that of the endogenous dopamine.[219] There is also a difference at position 3×36 between D_1-like and D_2-like receptors. There is no mutation data available for this position in D_1 and D_5, where the residue is a serine, but there is data available for D_2 and D_3, where it is a cysteine. The $C118^{3\times36}A/M/S$ mutations in D_2 do not affect binding of dopamine and the orthosteric antagonists nemonapride and sulpiride, while the $C114^{3\times36}L/M/S$ mutation is detrimental to binding of 13 different ligands in the D_3 receptor, suggesting a differential role of this residue even in the two similar receptors.[37,218,220−223] Another difference in the amine pocket between the two families is $V/T^{7\times38}$. The $V317^{7\times38}T$ mutant in D_1 and the $T412^{7\times38}A/V$ mutants in D_2 do not have a significant effect on binding of 11 ligands but decrease binding of nemonapride and risperidone. In D_3, the $T369^{7\times38}V$ mutant again does not have an effect on binding of nine ligands but increases binding of the agonists dopamine and 7-OH-DPAT and the antagonist GR218231, possibly by enhancing hydrophobic complementarity with propyl groups of the two latter ligands. Finally, the $T^{7\times38}A$ mutant in D_4 has a ligand-dependent effect, decreasing binding of five investigated ligands (the hydroxyl group of butaclamol, the most affected ligand, possibly forms an H-bond with this residue) and increasing binding of six investigated ligands and does not have an effect on 12 other ligands. Even very similar ligands are differentially affected by this mutation; therefore, it is hypothesized that this mutation affects the dynamics of the binding pocket or the whole receptor rather than introducing local changes in the ligand environment. Mutations $T119^{3\times37}A$ and $I122^{3\times40}A$ located in the deep pocket induced by risperidone as expected affect risperidone binding but not that of nemonapride, which does not penetrate so deep in the binding site.[37] Disruption of the aromatic cage in the major pocket generally results in severe effects on ligand binding. The $F345^{6\times51}A/W$ mutation is equivocally detrimental to binding of 14 investigated ligands except spiperone in D_3.[37,214,224] The $F390^{6\times52}A/W$ mutant is similarly detrimental for seven different ligands in D_2.[37,224,225] Mutations of the hydrophobic residue at position 5×40 are only studied for 1−1 ligand in D_1

DOI: 10.1021/acs.jmedchem.8b00836
J. Med. Chem. 2019, 62, 3784−3839

and D_2, where it decreases binding, while in D_3 it showed less pronounced effects, possibly depending on how deep the specific ligands are able to penetrate in the binding site.[217,218] Mutation of hydrophobic residues on the other face of the cocrystallized ligand eticlopride I/V$^{3\times33}$, I/L/S$^{45\times52}$, and F/Y$^{5\times39}$ do not have a pronounced effect on the binding of ligands,[217,222] which is consistent with the location of this residue further away (~6Å from eticlopride) in the dopamine D_3 crystal structure than in other aminergic receptors. Polar residues in the major binding pocket S$^{5\times43}$, S$^{5\times44}$, and S$^{5\times461}$ have been mutated to alanine and evaluated for almost 70 ligands in D_{1-4}. These have been the most studied mutations in dopamine receptors, unsurprisingly, as these form crucial H-bond interactions with the catechol moiety of the endogenous ligand dopamine. The S$^{5\times43}$A and S$^{5\times44}$A mutants negatively affect binding of phenethylamine agonists with a *meta*-hydroxyl moiety (e.g., agonists dopamine, noradrenaline, dipropyl-6,7-ADTN, 7-OH-DPAT) but increase binding of halogen substituted eticlopride analogues (e.g., antagonists FLA-797, remoxipride, metoclopramide), suggesting that these serines interact with the meta position of the aromatic ring substitution.[226−235] This also suggests that eticlopride analogues with a methoxy instead of a hydroxyl group in the ortho position might have a flipped aromatic ring relative to the cocrystallized eticlopride. On the other hand, the S$^{5\times461}$A mutant affinities for phenethylamine agonists that contain a para-substituted hydroxyl group (dopamine, noradrenaline, dipropyl-5,6-ADTN) or other ligands containing a polar substituent at the corresponding position (BRL 25594, raclopride, sulpiride, domperidone) are affected by this mutation.[226−231,233,235] Finally, mutations in the polar lid formed above the major pocket by Y$^{7\times34}$, H$^{6\times55}$, and I$^{45\times52}$ also have ligand-dependent effects in dopamine receptors. The H$^{6\times55}$L mutation decreases binding of several eticlopride analogues but increases binding of benzamide-1, metoclopramide, and clebopride containing a *para*-NH_2 group, implying that these ligands move toward the extracellular space to accommodate the additional polar group.[236,237] The H$^{6\times55}$A/F furthermore increases binding of, e.g., the FAUC series of dualsteric ligands, possibly by creating space above the major pocket by reducing the size of the lid or by disrupting the H-bond network.[238] The Y$^{7\times34}$F/L/V mutants increase binding of spiperone and clozapine but decrease binding of risperidone, PF-4363467, and *N*-methylspiperone.[217,218,222]

6.3.2. Minor Pocket and Extracellular Vestibule Mutations in Dopamine Receptors. Relatively few mutation data points are available for the minor pocket and extracellular vestibule in dopamine receptors. The space between TM2 and TM7 is somewhat larger than in other aminergic receptors, and this pocket is hypothesized to be accessible by most dualsteric ligands, as seen in the D_2-risperidone complex (6CM4). Mutation of K81$^{2\times60}$ in D_1 has no effect on binding of small orthosteric ligands.[219] The V91$^{2\times60}$F mutation in D_2 increases binding of CPPMA, possibly by the additional aromatic stacking interaction,[222] and the reverse F91$^{2\times60}$V mutant in D_4 decreases binding of the closely related L750,667 by the loss of this stacking interaction.[239] In contrast, the V86$^{2\times60}$F mutation in D_3 (contacting the pyrrolidine ring of cocrystallized eticlopride) decreases binding of the dualsteric FAUC series of molecules, possibly by decreasing the size of the minor pocket, whereas these ligands are larger than CPPMA in D_2 and D_4.[215] Hydrophobic residues at positions 3×28 and 3×29 also contact the pyrrolidine ring of eticlopride but have only been mutated in other dopamine receptor subtypes. As mentioned in section 6.1, the benzyl moiety of nemonapride opens up a subpocket between TM2 and TM3 between L90$^{2\times59}$ and L111$^{3\times28}$ in D_4,[39] which probably does not exist in other dopamine receptor subtypes, as both of these residues are large aromatic ones. Indeed, the L90$^{2\times59}$W mutation in D_4 increases binding of the antagonists raclopride, OPC-4392, aripiprazole and *N*-methylspiperone, possibly by forcing L111$^{3\times28}$ to face the binding site as found in the D_4 crystal structure and increasing complementarity with ligands not containing overlapping moieties with the benzyl group of nemonapride. The F110$^{3\times28}$L mutation increases binding of the antagonist CPPMA and the V111$^{3\times29}$M mutation decreases binding of *N*-methylspiperone, possibly also by modulating the size of the minor pocket, but they do not have a significant effect on several other ligands in D_2.[222] Conversely, in D_4, the M112$^{3\times29}$V mutation increases the size of the minor pocket and thus increases binding of, e.g., raclopride, nafadotride, and A-69024.[239] Mutation of L$^{2\times63}$ and E$^{2\times64}$ has no significant effect on orthosteric ligand binding, e.g., that of eticlopride and PF-4363467, but has a pronounced, but varying (decreasing and increasing) effect on binding affinity for dualsteric risperidone, aripiprazole, *N*-methylspiperone, haloperidol, and GSK598809 in $D_{2/3/4}$.[37,218] The unique conformation seen for the conserved W100$^{23\times50}$ in ECL1 in the dopamine D_2 receptor justifies its large disruptive effect on dualsteric ligand binding in D_2.[37] However, mutations in other subtypes have not been performed, and thus its effect cannot be compared to cases when it is not contacting ligands. Only one data point is available for the S$^{7\times35}$D mutant in D_3 that mimics the D_1-like receptors, but it does not have any effect on spiperone binding. Finally, the mutation Y36$^{1\times39}$L/F is not involved in our binding site selection as this residue does not contact any cocrystallized ligands in aminergic receptor crystal structures, but it seems to be accessible in the minor pocket in the D_3 crystal structure. This mutation indeed does not have any effect on the investigated orthosteric ligands (agonists dopamine, 7-OH-DPAT, and antagonists GR218231, chlorpromazine, and raclopride) but decreases binding of dualsteric haloperidol and GSK598809.[218,237]

6.4. Structure-Based Extrapolation of Dopamine Receptor Mutation Effects. Mutation data predictions within the dopamine receptor family were performed for human data for the D_3 receptor with an available crystal structure. Retrospective predictions for dopamine receptor D_3 were performed with 0.78 accuracy. The initial 197 points used for extrapolation (14% of coverage) were predicted for 39% (77 points) in retrospective studies, and prospective analysis resulted in a heat map with 193 points (14% coverage). The heat maps referring to the original data set used for extrapolation, and the retrospective and prospective predictions are provided in the Supporting Information.

7. HISTAMINE RECEPTOR MUTATIONS

7.1. Structural Histamine Receptor−Ligand Interactions. Histamine receptors are activated by the small neurotransmitter histamine. In humans, there are four histamine receptor subtypes of which H_1 has been crystallized.[40] The doxepin bound H_1 (PDB: 3RZE[40]) crystal structure shows a binding mode of a tricyclic amine scaffold in the orthosteric pocket, covering residues in the amine pocket (D$^{3\times32}$, S$^{3\times36}$, W$^{6\times48}$, Y$^{6\times51}$, I$^{7\times38}$, Y$^{7\times42}$) and the major pocket of histamine receptors (Y$^{3\times33}$, T$^{3\times37}$, I$^{3\times40}$, W$^{4\times57}$, T$^{5\times43}$,

DOI: 10.1021/acs.jmedchem.8b00836
J. Med. Chem. 2019, 62, 3784−3839

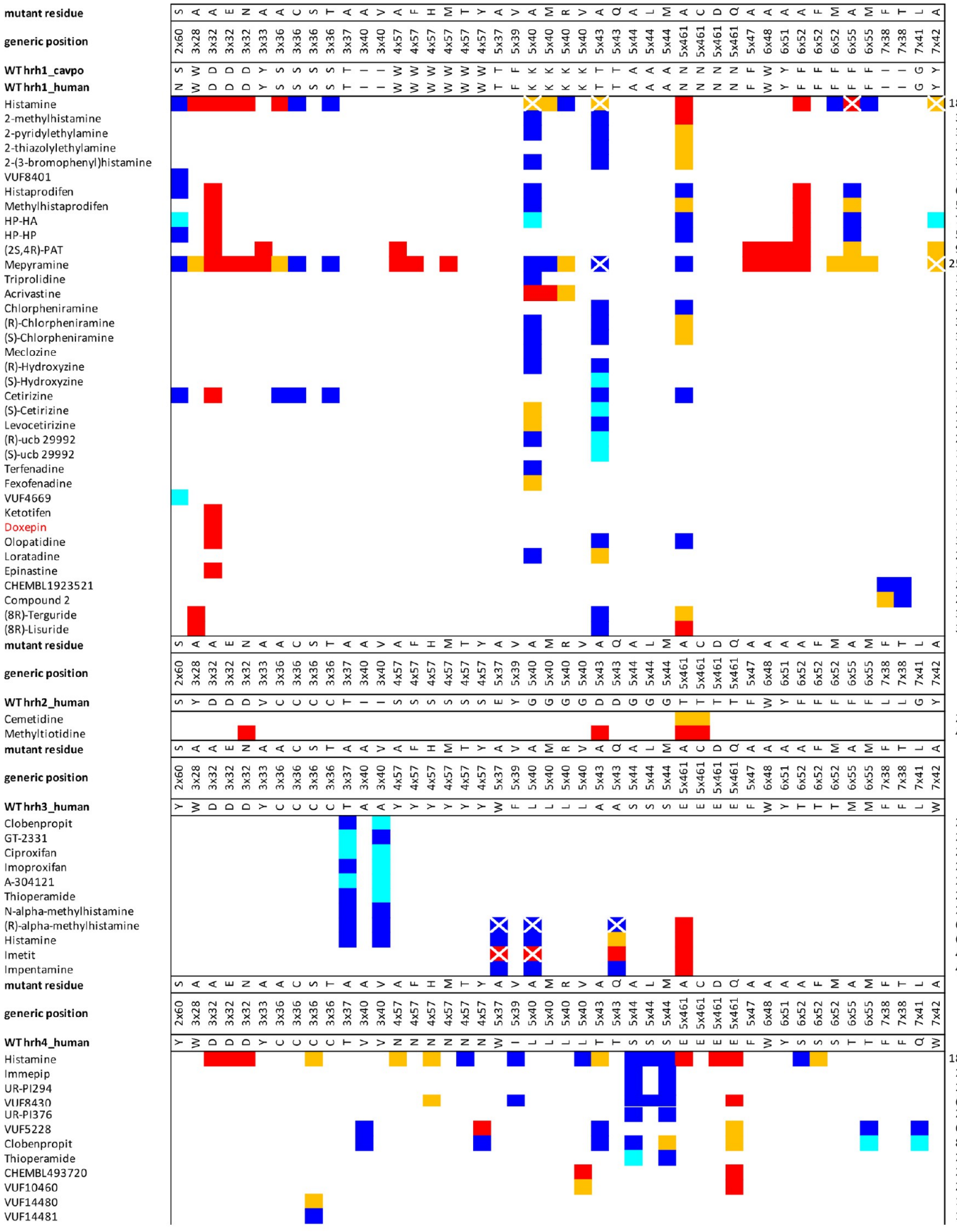

Figure 17. continued

DOI: 10.1021/acs.jmedchem.8b00836
J. Med. Chem. 2019, 62, 3784−3839

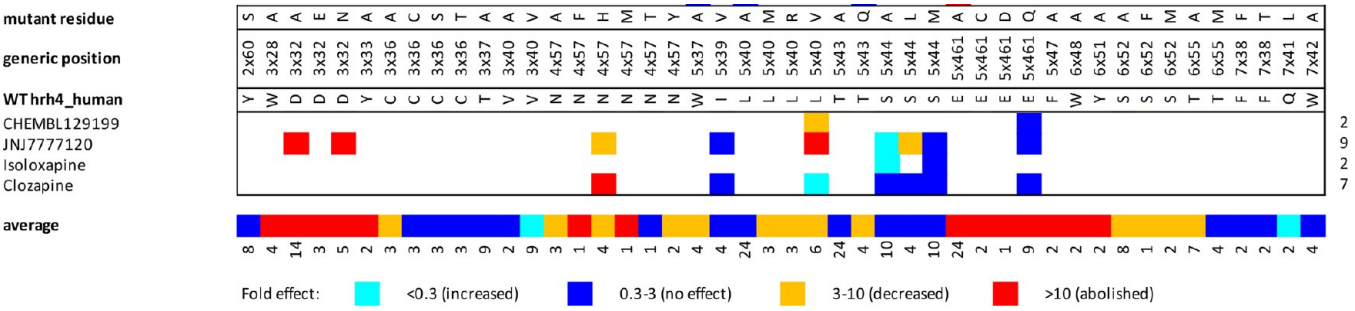

Figure 17. Histamine receptor mutation data.[107,242−250,252−259,261−265] Data is shown for the consensus binding pocket defined using structure-based generic position numbers from GPCRdb.[18] Wild-type residues for the orthologues involved in mutation studies, and the mutant residue are shown (note that only the mutations which have a data point shown in the table were actually carried out, the table is organized for comparability among orthologues). Ligands are grouped similarly as in Figure 18. When multiple data points were available for the specific mutant−ligand combination, the geometric mean of the fold effect values was used. See Figure 5 for color coding. Mutant numbers for each ligand and ligand numbers for each mutant are indicated in the right side and the bottom of the heat map, respectively. The average fold effect (geometric mean) for each mutant is also shown at the bottom of the heat map. PDF and Excel versions of the heat map are provided in the Supporting Information.

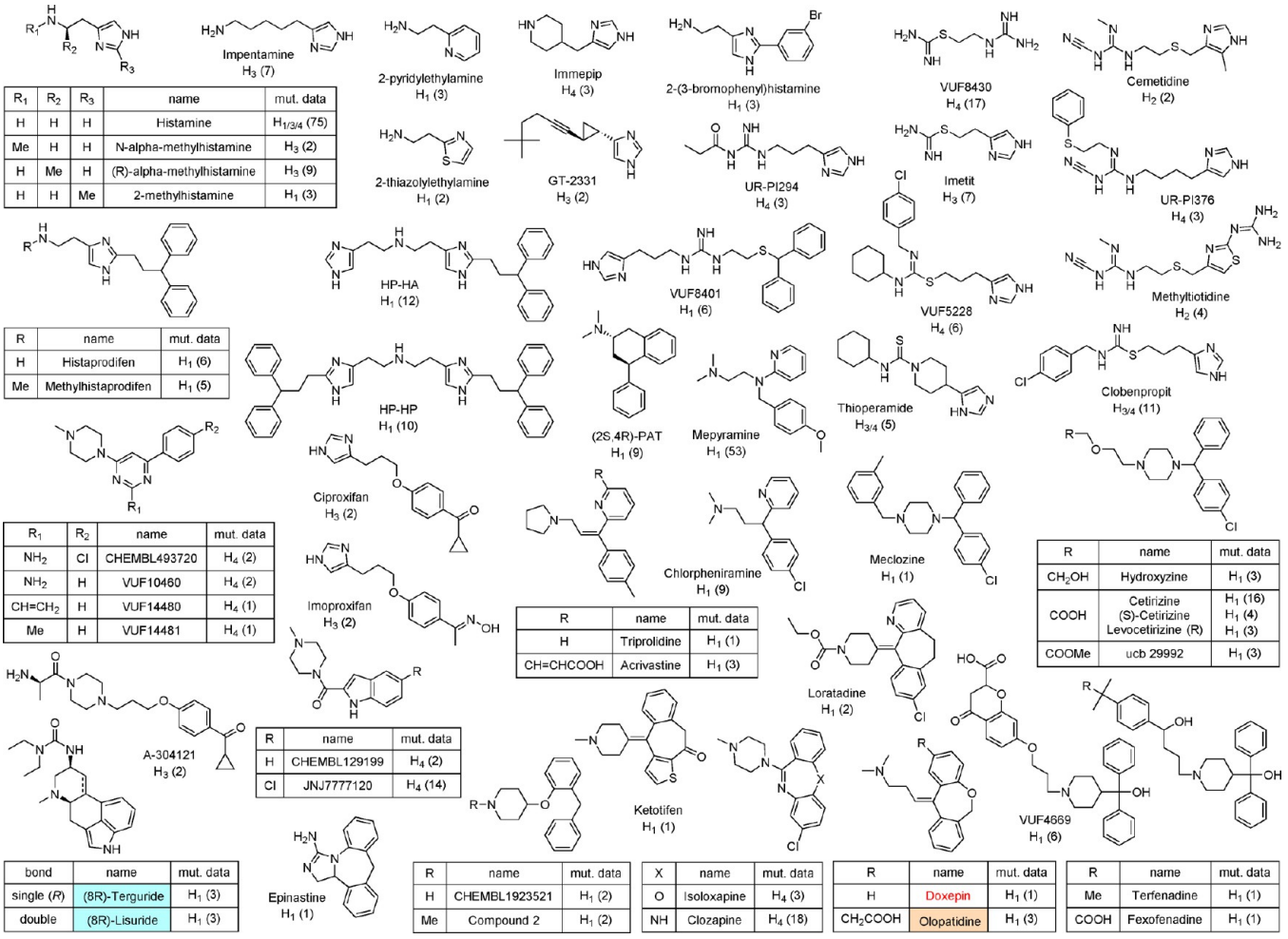

R_1	R_2	R_3	name	mut. data
H	H	H	Histamine	$H_{1/3/4}$ (75)
Me	H	H	N-alpha-methylhistamine	H_3 (2)
H	Me	H	(R)-alpha-methylhistamine	H_3 (9)
H	H	Me	2-methylhistamine	H_1 (3)

R	name	mut. data
H	Histaprodifen	H_1 (6)
Me	Methylhistaprodifen	H_1 (5)

R_1	R_2	name	mut. data
NH_2	Cl	CHEMBL493720	H_4 (2)
NH_2	H	VUF10460	H_4 (2)
$CH=CH_2$	H	VUF14480	H_4 (1)
Me	H	VUF14481	H_4 (1)

R	name	mut. data
H	CHEMBL129199	H_4 (2)
Cl	JNJ7777120	H_4 (14)

R	name	mut. data
H	Triprolidine	H_1 (1)
CH=CHCOOH	Acrivastine	H_1 (3)

R	name	mut. data
CH_2OH	Hydroxyzine	H_1 (3)
COOH	Cetirizine (S)-Cetirizine Levocetirizine (R)	H_1 (16) H_1 (4) H_1 (3)
COOMe	ucb 29992	H_1 (3)

bond	name	mut. data
single (*R*)	(8R)-Terguride	H_1 (3)
double	(8R)-Lisuride	H_1 (3)

R	name	mut. data
H	CHEMBL1923521	H_1 (2)
Me	Compound 2	H_1 (2)

X	name	mut. data
O	Isoloxapine	H_4 (3)
NH	Clozapine	H_4 (18)

R	name	mut. data
H	Doxepin	H_1 (1)
CH_2COOH	Olopatidine	H_1 (3)

R	name	mut. data
Me	Terfenadine	H_1 (1)
COOH	Fexofenadine	H_1 (1)

Figure 18. Histamine receptor ligands used in mutation studies.[107,242−250,252−259,261−265] The cocrystallized ligand in the H_1 structure is shown in red. Chemically similar ligands to the cocrystallized ligand in the histamine receptor crystal structure are indicated with orange background, and chemically similar ligands to any cocrystallized ligand in aminergic receptor crystal structures are indicated with a cyan background. Receptors with available mutation data for the specific ligand are indicated along with the number of data points in parentheses. A PDF version of the figure is provided in the Supporting Information.

$A^{5\times44}$, $N^{5\times461}$, $F^{5\times47}$, $F^{6\times44}$, $F^{6\times52}$, $F^{6\times55}$). The interaction patterns with different residues targeted in the minor pocket and extracellular vestibule ($Y^{2\times63}$, $W^{3\times28}$, $L^{3\times29}$, $E^{45\times51}$, $T^{45\times52}$, $I^{6\times58}$, $A^{6\times59}$, $E^{7\times31}$, $H^{7\times34}$, $M^{7\times35}$) by dualsteric ligands may furthermore modulate the ligand-dependent structure−affinity, −function, and −selectivity relationships of histamine receptors; however, relatively few bitopic ligands are yet available for this family. As only one crystal structure is publicly

DOI: 10.1021/acs.jmedchem.8b00836
J. Med. Chem. 2019, 62, 3784−3839

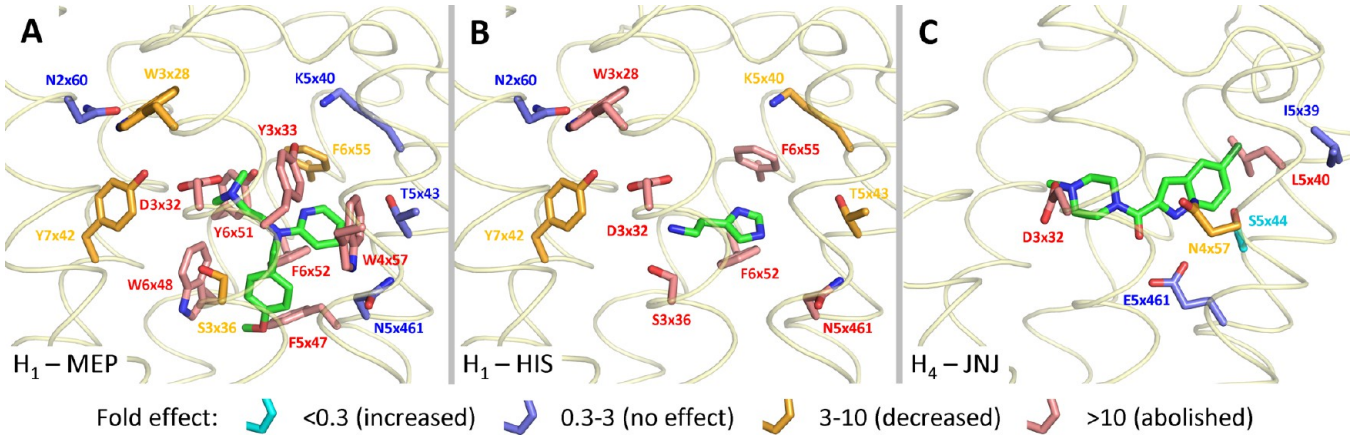

Figure 19. Histamine receptor ligand binding modes and associated mutation data. (A) H_1 (PDB: 3RZE[40]) with docked mepyramine, a ligand similar to cocrystallized doxepin, mutation effects mapped on structure for H_1-mepyramine. (B) H_1 (PDB: 3RZE) with docked histamine, mutation effects mapped on structure for H_1-histamine. (C) H_4 homology model from GPCRdb with docked JNJ7777120, mutation effects mapped on structure for H_4-JNJ7777120. See Figure 5 for color coding. Mutation effects for alanine mutants were used where available.

available to date for any histamine receptor, it was not possible to analyze variation in ligand binding modes of histamine receptors (Figures 3, 19, 20). In the amine pocket of histamine receptors, $D^{3\times32}$ forms an ionic interaction with the amine group of basic ligands, such as histamine derivatives, guanidine or isothiourea ligands, and tricyclic amines, while residues C/$S^{3\times36}$ and $Y^{7\times42}$ stabilize the conformation of $D^{3\times32}$ and residues $W^{6\times48}$ and $F^{6\times51}$ form cation−π interaction, consistent with mutation studies (section 7.3.1) and SAR studies, showing the essential role of the cationic properties of the amine group of histamine ligands. The dibenzoxepin scaffold of the cocrystallized ligand doxepin forms hydrophobic interactions with $Y^{3\times33}$, $I^{3\times40}$, $W^{4\times57}$, $F^{5\times47}$, $F^{6\times44}$, $W^{6\times48}$, $Y^{6\times51}$, $F^{6\times52}$, and $F^{6\times55}$ and forms a weak H-bond interaction with $T^{3\times37}$ in the major pocket between TM3−6. Mutation studies demonstrate the important role of these hydrophobic residues (section 7.3.2). and SAR studies demonstrate the preference of histamine receptors for ligands with butterfly shaped double aromatic moieties or small aromatic moieties with an optional polar H-bond interaction functionality, mimicking the imidazole group of the endogenous ligand. While in the H_1 receptor crystal structure, $N198^{5\times461}$ does not form a polar interaction with the doxepin ligand, but rather with $W158^{4\times57}$, it is most probable that the analogous $E^{5\times461}$ in H_3 and H_4 interacts with the endogenous histamine and is stabilized by Y/$N^{4\times57}$ from the adjacent helix. In the H_2 receptor, a similar network is possibly formed by $S150^{4\times57}$ and $T190^{5\times461}$. In all receptors, the mutation of N/T/$E^{5\times461}$ underlines the important role of this residue in recognizing histamine and histamine analogue ligands. No structural information is as of yet available on the interaction of minor/extracellular vestibule residues with dualsteric histamine ligands.

7.2. Chemical Space of Histamine Receptor Ligands in Crystal Structures and Mutation Studies. The cocrystallized histamine receptor ligand doxepin has not been utilized in mutation studies of histamine receptors; only one data point for this ligand at H^1 $D^{3\times32}$A is available.[242] The most investigated histamine ligand in mutation studies is mepyramine (53 mutants, Figure 19). The endogenous histamine itself has been extensively investigated (75 mutation data points, Figure 19) at receptors $H_{1/3/4}$ covering 33 different residues in total (Figure 17), 16 of which line the binding site in the H_1R crystal structure (Figure 3). The 21 other imidazole containing ligands cover altogether 105 (29%) of ligand mutant combinations. Only olopatadine of the ligands investigated in mutation studies is chemically substantially similar to the cocrystallized doxepin, and six (10%) ligands are pharmacophorically substantially similar to the cocrystallized ligand (Figure 18), covering altogether 25 (7%) ligand−mutant combinations. Although most compounds do not share 2D chemical or 3D shape/pharmacophore-based similarity with the cocrystallized histamine receptor ligand, they nevertheless represent combined ligand and receptor SAR data sets that provide detailed information on the structural determinants of histamine receptor binding. Terguride and lisuride are chemically similar to cocrystallized ligands in serotonin receptor complexes and were evaluated in mutation studies at serotonin and dopamine receptors as well. Trans-PAT, clozapine, and isoloxapine have also been investigated at serotonin, muscarinic acetylcholine, and dopamine receptor mutants, providing insights into the receptor specific determinants of binding of these ligands by different aminergic GPCRs.

7.3. Structural Determinants of Histamine Receptor−Ligand Interactions. *7.3.1. Amine and Major Pocket Mutations in Histamine Receptors.* Mutation of conserved $D^{3\times32}$ diminishes binding of agonists and antagonists to H_1 (cetirizine, doxepin, epinastine, histamine, histaprodifen, HP-HA, HP-HP, ketotifen, loratadine, mepyramine, methylhistaprodifen, olopatadine, (2*S*,4*R*)-PAT),[242−246] H_2 (methyltiotidine),[247] and H_4 (histamine, JNJ-7777120),[107,248] which is consistent with the role of $D107^{3\times32}$ in binding the cationic amine moiety of doxepin in the H_1 crystal structure (PDB: 3RZE[40]). Mutation of other residues lining the amine binding pocket, including I/L/$F^{7\times38}$, G/L/$Q^{7\times41}$, and Y/$W^{7\times42}$, show receptor and ligand-dependent effects.[246,249,250] The $Y458^{7\times42}$A mutant decreases the affinity of the endogenous agonist histamine, as well as the antagonists mepyramine, and (2*S*,4*R*)-PAT but increases the affinity of the large HP-HA agonist for H_1.[246,249] $Q347^{7\times41}$L mutant increases the affinity of partial agonist clobenpropit for H_4.[251] The $I454^{7\times38}$F mutation in H_1 only affects the benzylphenoxypiperidine antagonist compound 2 by reducing the space available for the methyl substituent on the basic amine group. Although in the H_1 crystal structure $S111^{3\times36}$ does not form a stabilizing H-bond with $D107^{3\times32}$, such a feature is seen in other aminergic

DOI: 10.1021/acs.jmedchem.8b00836
J. Med. Chem. 2019, 62, 3784−3839

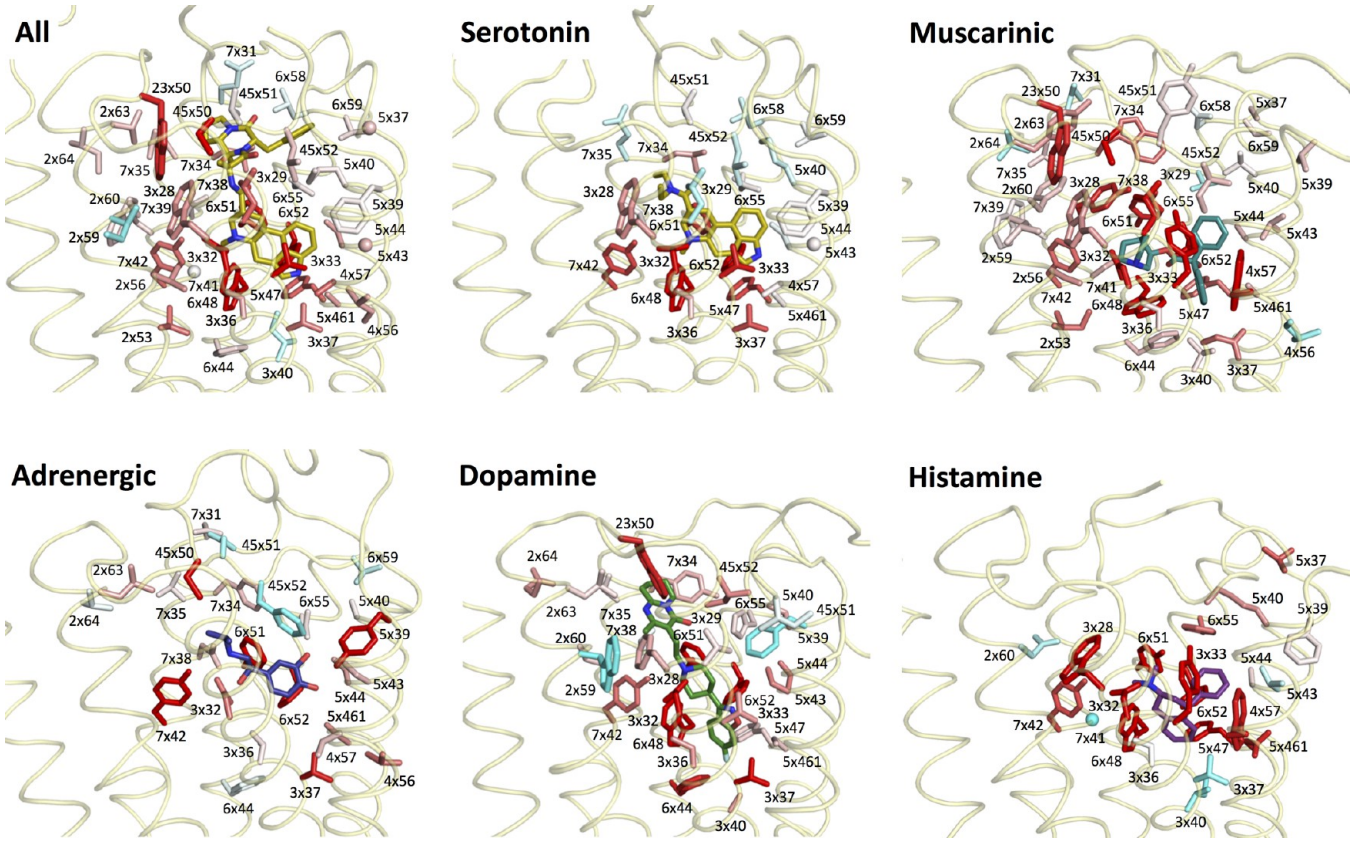

Figure 20. Interaction hotspots in aminergic receptors. Median fold effects in mutation studies for each generic position aggregated for all aminergic receptors and per subfamily mapped on example structures of the subfamilies. Color coding: cyan−white−red spectrum, where cyan, median fold effect effect <0.3 (increased); white, median fold effect = 1 (no effect) to red, median fold effect >10 (abolished). The structures depicted are: All, 5-HT_{2B} in complex with ergotamine (PDB: 4IB4[31]); serotonin, 5-HT_{2B} in complex with LSD (PDB: 5TVN[61]); muscarinic, M_2 in complex with QNB (PDB: 3UON[101]); adrenergic, β_1 in complex with isoprenaline (PDB: 2Y03[157]); dopamine, D_2 in complex with risperidone (PDB: 6CM4[37]); histamine, H_1 with docked (2*S*,4*R*)-PAT (PDB: 3RZE[40]).

receptors and may be hypothesized that it plays a role also in histamine receptor flexibility. Mutation of $S111^{3\times36}$ to alanine does reduce binding of histamine and mepyramine in H_1, but mutation to polar cysteine or threonine does not have an effect on binding of these ligands.[252] However, in H_4, the reverse $C98^{3\times36}S$ mutation reduces binding of histamine and the covalent partial agonist VUF14480, the more electron rich cysteine being more favorable for covalent interaction with the alkene moiety of the latter ligand.[253] Mutation of the hydrophobic residues interacting with doxepin in the H_1 crystal structure generally results in decreased or abolished ligand binding. The $Y^{3\times33}A$, $W^{4\times57}A/F/M$, $F^{5\times47}A$, $W^{6\times48}A$, and $Y^{6\times51}A$ mutants abolish binding of the antagonists (2*S*,4*R*)-PAT and mepyramine to H_1.[246,254] $F432^{6\times52}A$ and $F432^{6\times52}M$ mutants abolish binding of seven tested ligands to H_1.[245,246,254] The H_1 mimicking $S320^{6\times52}F$ mutant reduces binding of histamine to H_4, suggesting that the polar environment is more favorable for the small endogenous ligand to this receptor.[248] $F435^{6\times55}A$ and $F^{6\times55}M$ mutants decrease the affinity of 4 of the 7 tested ligands, but this mutation has a smaller effect than mutation of $F432^{6\times52}$.[245,246,254] The mouse and rat H_3 mimicking $A122^{3\times40}V$ mutant of human H_3 increases binding of a range of ligands, identifying this residue as a determinant of H_3 species differences.[255] The polar network between positions 4×57 and 5×461 seems to be important in all histamine receptors, but mutation data for residue 4×57 is only available for H_1 and H_4.[246,248,250,256] Mutation of $W157^{4\times57}$ to the aromatic phenylalanine is detrimental to binding of mepyramine, suggesting that the large size and/or H-bond donor capacity of this residue are essential for ligand binding. Mutation of $N147^{4\times57}$ in H_4 to dog H_4 ($N^{4\times57}H$) and/or H_3 ($N^{4\times57}Y$) mimicking residues reduces binding of histamine, VUF8430, VUF5228, JNJ7777120 (Figure 19), and clozapine, and this effect is proposed to be associated with the role of $N147^{4\times57}$ in positioning $E182^{5\times461}$ toward the H_4 ligand binding pocket. The $N198^{5\times461}A$ mutation in H_1, $T190^{5\times461}A/C$ in H_2, $E195^{5\times461}A$ in H_3, and $E182^{5\times461}A/D/Q$ in H_4 decrease or abolish binding of most of the tested ligands.[107,242,244,245,248,250,257−259] Although mutation data is not available in all receptors for all chemotypes, it seems that small ligands, such as histamine and other histamine derivatives, 2-pyridylethylamine, 2-thiazolylethylamine, guanidine, or isothiourea ligands are affected more by these mutations than ligands with double aromatic scaffolds such as histaprodifen, HP-HA, HP-HP, mepyramine, chlorphenirамine, cetirizine, olopatadine, and clozapine. Mutation studies based on a guinea pig H_1 homology model identified $K200^{5\times40}$ as an important interaction site for the zwitterionic ligands acrivastine, fexofenadine, and (to lesser extent) *S*-cetirizine.[254] This H_1-specific anion-binding subpocket, consisting of the residues $K179^{45\times49}$, $K190^{5\times40}$, and $H450^{7\times34}$, has indeed been confirmed by the H_1 crystal structure in which this pocket is occupied by a phosphate ion.[40] $L175^{5\times40}$ is an important interaction point for the chlorine substituents of indolecarbox-

DOI: 10.1021/acs.jmedchem.8b00836
J. Med. Chem. 2019, 62, 3784−3839

amide and aminopyrimidines in H_4 that forms a subpocket between the extracellular region of TM5 and ECL2, which determines subtle differences in SAR between these two ligand classes.[260] The same L175$^{5\times40}$ residue furthermore is an important molecular determinant of H_4 species selectivity that explains differences in binding affinities of JNJ7777120 and clozapine for human (L175$^{5\times40}$) and cynomolgus monkey (175V$^{5\times40}$) H_4 orthologues.[256] Stereoselective binding is observed for *R*- and *S*-cetirizine and *R*- and *S*-chlorphenirамine, where both the *R*-enantiomers have a higher affinity for H_1R. Interestingly, the T194$^{5\times43}$A mutant increases binding of *S*-cetirizine but not of *R*-cetirizine.[257,261] This stereoisomer-specific mutational effect can be explained by docking studies in the H_1 crystal structure, which indicate that only *S*-cetirizine is sterically hindered by T194$^{5\times43}$.[11]

7.3.2. Minor Pocket and Extracellular Vestibule Mutations in Histamine Receptors. Very few mutation data points are available for the minor pocket and extracellular vestibule in histamine receptors. For the other aminergic receptors, more or less indication is available for the existence of a secondary binding pocket either in the form of a characterized allosteric pocket (as in muscarinic acetylcholine receptors) or a transient secondary binding pocket (as in adrenergic receptors). For histamine receptors, however, no such information is yet available. The phosphate pocket seen in the H_1 crystal structure is located close to the orthosteric binding pocket, and other than zwitterionic antihistamines extending to this pocket, only a few dualsteric antihistamines are known. The guinea pig H_1 mimicking N84$^{2\times60}$S mutant of human H_1 does not affect binding of most tested ligands, except those of the large HP-HA (and to a lesser extent HP-HP) dimer and VUF4669 extending that far toward TM2.[249] The H_1 W103$^{3\times28}$A mutant decreases binding of histamine, mepyramine, and serotonin ligands (8*R*)-lisuride and (8*R*)-terguride, which contact the same residue in 5-HT receptors by analogy to the known 5-HT$_{2B}$-LSD crystal structure.[244] Finally, the S156$^{45.42}$A and F169$^{45.55}$V mutations in the ECL2 of the human H_4 receptor significantly decrease binding of several ligands (histamine, isoloxapine, clozapine, clobenpropit, mepyramine, and UR-PI376); however, related residues in the H_1 receptor seem not to be available for ligand contact, rather they probably affect the dynamics of ECL2 and association/dissociation of ligands.[256,262,263]

7.4. Structure-Based Extrapolation of Histamine Receptor Mutation Effects. Mutation data predictions within the histamine receptor family were performed for human data for the H_1 receptor with an available crystal structure. Results for H_1 receptor: initially 160 points could be used for mutation data extrapolation for 34 ligands at 33 mutants (14% coverage). In retrospective studies, 18% of the points (28 data points) were retrieved, and 885 points were predicted in prospective analysis leading to final 79% of coverage. Accuracy of the retrospective studies was 0.66. The heat maps referring to the original data set used for extrapolation, and the retrospective and prospective predictions are provided in the Supporting Information.

8. COMMON AND DIVERGENT DETERMINANTS OF AMINERGIC RECEPTOR MUTATION EFFECTS

8.1. Interaction Hotspots in Aminergic Receptors. When comparing the aggregated mutation data for each generic position in each aminergic receptor subfamily, many similarities but also some interesting differences may be found (Figure 20). The characteristic D$^{3\times32}$ has been mutated in all subfamilies, and its mutation is generally detrimental to ligand binding. However, in the adrenergic receptors this mutation results in smaller losses in ligand binding than in other aminergic receptors (3 vs 8−15 median fold effect), possibly because the other specific interactions with N$^{7\times38}$ and TM5 serines are still available. Mutation of Y$^{7\times42}$ in H-bond with D$^{3\times32}$ also reduces binding in most cases by destabilizing the interaction of basic amines with D$^{3\times32}$ (3−20 median fold effect). The C$^{45\times50}$ mutation is detrimental to ligand binding in all cases (13−22 median fold effect), but this is due to incomplete receptor folding by the loss of the key disulphide bridge. Residues of the hydrophobic core of the receptors at positions 3×33, 6×48, 6×51, and 6×52 were mutated in most subfamilies, and these mutations also abolish binding of most ligands (6−34 median fold effect). Mutations at other positions, however, had a larger variation in their elicited effects. From Figure 20, it can be seen that for serotonin receptors mutation of residues at the bottom of the binding site were more likely to cause a large decrease in ligand binding, while residues at the opening of the binding pocket even increased binding (median fold effect <1 for positions 3×29, 7×35, 5×40, 45×52, and 6×58). In muscarinic acetylcholine receptors, mutation of almost all residues resulted in loss of effect on average, a notable exception being the mutation of V$^{6\times55}$ (median fold effect 0.6), which is a polar residue in most other aminergic receptors but a hydrophobic one in the muscarinic acetylcholine receptors (N$^{6\times52}$ one helix turn down is the characteristic polar residue in these, which is a phenylalanine in most other receptors). In adrenergic receptors somewhat surprisingly, the mutation of TM5 serines considered to be important for catechol ligand binding and receptor activation resulted in median fold effects of 1.7−2.3, therefore it seems that the polar network of residues in adrenergic receptors can tolerate single mutations better than in other subfamilies. In dopamine receptors, mutation of relatively few residues resulted in high median fold effects. Furthermore, mutation at position 2×59 resulted in increased effects as outlined in section 6.3, and mutations of aromatic residues at 5×39 and 7×34 also resulted in increased ligand binding (median fold effect 0.3−0.4). Finally, in histamine receptors, mutation of most residues of the amine and the major pocket resulted in abolished ligand binding (median fold effects 3.2−20.0), but interestingly mutation of positions 3×37 and 3×40 deep in the binding pocket resulted in median fold effects 0.4−0.5, suggesting that ligands could be accommodated better in a larger and deeper binding pocket.

8.2. Differential Determinants of Endogenous Agonist Binding. Natural aminergic receptor agonists are proposed to interact with polar residues at positions 5×43 and/or 5×461, as shown in the $\beta_{1/2}$ and 5-HT$_{1B/2B}$ agonist bound crystal structures and supported by mutagenesis studies. Crystal structures and mutagenesis studies suggest that the catechol moieties of the chemically similar agonists epinephrine and dopamine adopt different binding modes in different adrenergic and dopamine receptors. Mutation studies indicate that both S$^{5\times43}$ and S$^{5\times461}$ play an important role in epinephrine and norepinephrine binding to α_{1B}, α_{2A}, and β_2, consistent with the β_2 crystal structure (PDB: 4LDO[165]) in which epinephrine forms hydrogen bonds with both S203$^{5\times43}$ and S207$^{5\times461}$. In contrast, mutagenesis studies also suggest that the catechol moiety of dopamine interacts with S195$^{5\times43}$ but not with S196$^{5\times461}$ in D_3.[233] In the other dopamine D_1, D_2,

DOI: 10.1021/acs.jmedchem.8b00836
J. Med. Chem. 2019, 62, 3784−3839

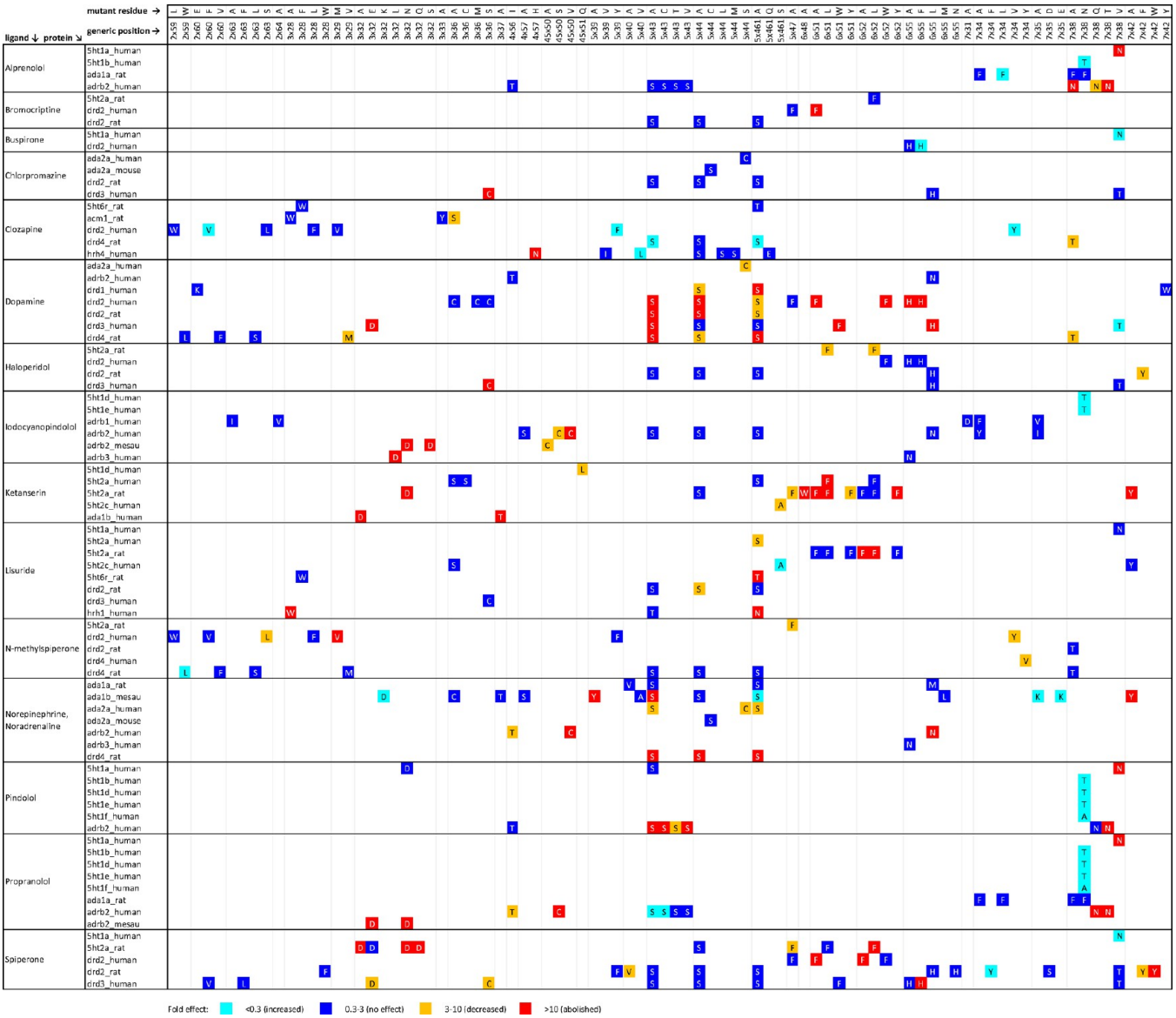

Figure 21. Mutation data for ligands with polypharmacological effects pooled for all tested mutants at all receptor subtypes. Data is shown for the consensus binding pocket defined using structure-based generic position numbers from GPCRdb. Wild-type residues for the specific receptor subtypes involved in mutation studies are indicated in the cells, and the mutant residues are shown in the header (note that only the mutations which have a data point shown in the table were actually carried out, the table is organized for comparability among all receptor subtypes). When multiple data points were available for the specific mutant−ligand combination, the geometric mean of the fold effect values was used. See Figure 5 for color coding.

and D_4 receptors, both $S^{5\times43}$ and $S^{5\times461}$ are important for dopamine binding, whereas mutation of $S187^{5\times43}$ and $S192^{5\times461}$ does not affect epinephrine and norepinephrine binding to rat α_{1A}. This comparative analysis of receptor mutation data indicates that there are subtle differences in the binding modes of dopamine and epinephrine/norepinephrine catechol between and within adrenergic and dopamine receptor subfamilies. This observation is further supported by the fact that the $N292^{6\times55}L$ mutation does not affect dopamine binding to β_2, whereas the homologous $H349^{6\times55}L$ mutation significantly decreases dopamine binding to D_3 (Figure 16). Several residues important for 5-HT recognition by serotonin receptors have been indicated in various docking studies. The crystal structures of 5-HT_{1B} and 5-HT_{2B} have enabled more detailed analysis of ligand−receptor interactions within this group of receptors. Polar interactions between the $D^{3\times32}$, $T^{3\times37}$, and $Y^{7\times42}$ residues have been detected, as well as nonpolar interactions between the indole ring of 5-HT and 5×43 and 5×461 residues (serine and alanine, and glycine and alanine for 5-HT_{1B} and 5-HT_{2B}, respectively).[30] These in silico results were supported by mutation studies: $D135^{3\times32}A$ mutation of 5-HT_{2B} leads to loss of the ability of 5-HT to bind to the receptor, K_D increased from 12 nM to over 10000 nM. Mutations of other residues do not lead to such significant changes: $T^{3\times37}A$ changed the pK_i of 5-HT from 8.09 to 6.75 for 5-HT_{1B} and from 8.41 to 6.35 for 5-HT_{2B}. The $A^{5\times461}S$ mutation changes the 5-HT affinity in different directions: from 8.09 to 7.85 pK_i modification for 5-HT_{1B} and from 8.41 to 8.44 for 5-HT_{2B}, whereas for $Y^{7\times42}A$ mutation, the pK_i change from 8.09 to 8.45 and 8.41 to 6.46 is detected for 5-HT_{1B} and 5-HT_{2B}, respectively. Other residues indicated by mutation studies as influencing 5-HT binding are 2×50, 3×36,

DOI: 10.1021/acs.jmedchem.8b00836
J. Med. Chem. 2019, 62, 3784−3839

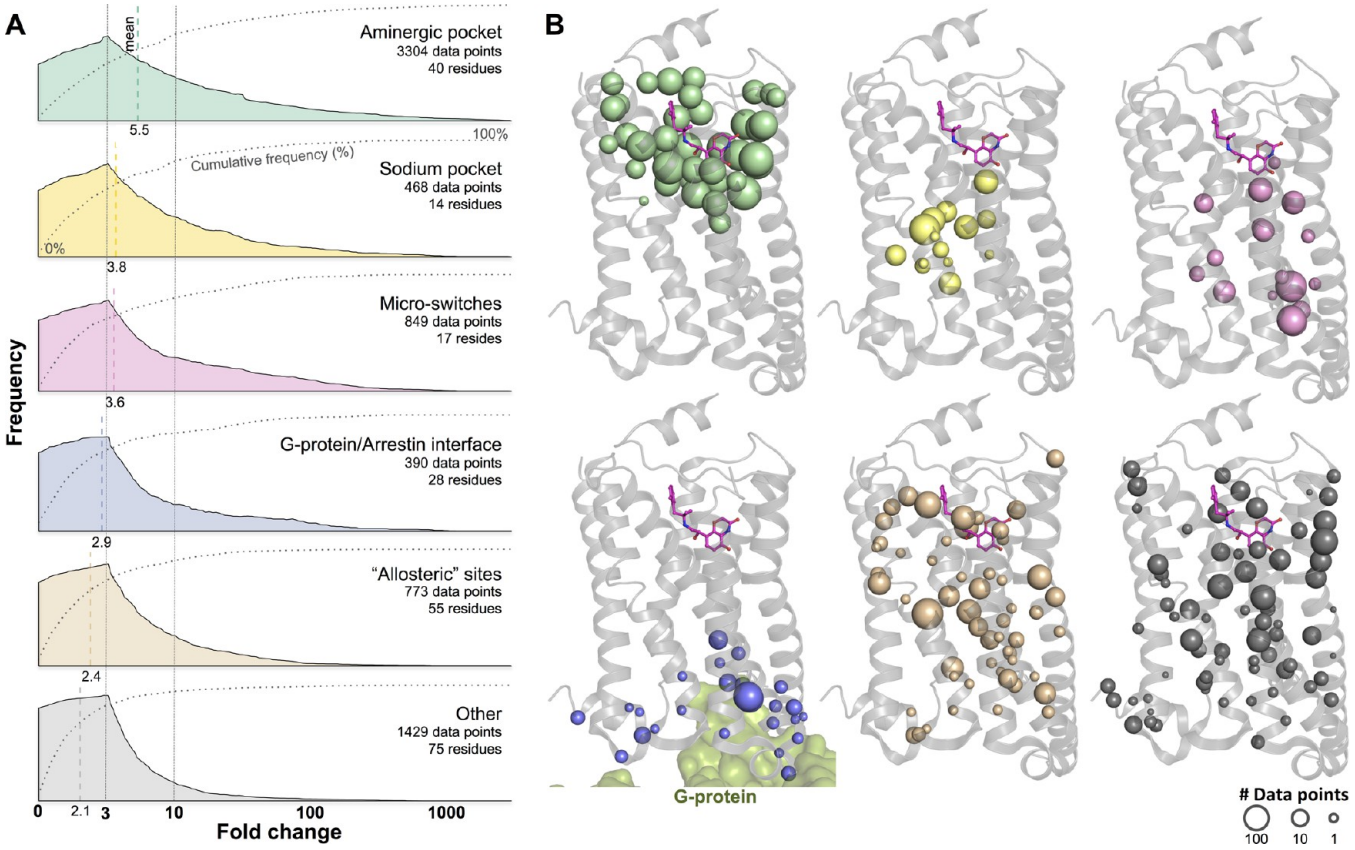

Figure 22. Distribution and fold effect of the collected mutation data points across the archetypical GPCR fold. (A) Distribution plots (frequency) of the fold effect of the collected data points categorized into the aminergic pocket, the sodium pocket, microswitches, the G protein and arrestin binding interface, "allosteric sites" (defined as all residue positions observed to interact with ligands in class A GPCR crystal structures outside of the aminergic pocket), and the other remaining mutation points ("Other"). The number of residues refer to the number of unique residue positions with available mutational data. (B) Visualization of the positions for the different mutation data points mapped onto the β_2 adrenoceptor crystal structure (PDB: 3SN6[167]) for each of the residues sets (except for "Other"). The spheres indicate the position of the residues and the size the number of data points (color-coding of the spheres corresponds to the color-coding in A. A partial surface of the G_s protein is shown in pale-green, and the agonist BI-167107 is shown in magenta sticks. For the "Other" group, only residues with a generic GPCRdb number are shown in the residue count in A and represented in B. However, all data points (including for positions without a generic GPCRdb number) are included in the frequency graph for "Other".

5×39, 5×49, 6×51, 6×52, 6×55, and 7×49. Studies of other serotonin receptor subtypes have indicated several further residues, mutation of which lead to significant change of 5-HT affinity, e.g., the 6×34 position that leads to increased 5-HT affinity after the substitution of WT residue ($C322^{6\times34}K$ mutation for 5-HT_{2A},[266] $S312^{6\times34}K$ for 5-HT_{2C},[267] and $A258^{6\times34}L$ for 5-HT_4[268]): from a K_i of ∼200 nM, it fell below 10 nM. On the other hand, both $D172^{3\times49}N$[74] and $S239^{5\times44}A$[92] substitutions in rat 5-HT_{2A} lead to much lower 5-HT affinity in competition studies. Also, the $F^{5\times48}A$ mutation of 5-HT_{2A} leads to over 10-fold lowering of 5-HT binding.[92] Deterioration of 5-HT affinity is also observed for mutants of, e.g., $D72^{2\times50}$ in 5-HT_6,[269] $T^{3\times36}$,[93] and $N279^{6\times55}$ in 5-HT_4,[76] and $Y358^{7\times42}$ in HT_{2C}.[95] Combined mutation and modeling studies indicate that histamine has similar binding modes in H_1, H_3, and H_4 by donating a hydrogen bond to $N^{5\times461}$ (in H_1)[243,245,257,258] or $E^{5\times461}$ (in H_3, H_4),[107,248,259] with its N^{τ} imidazole nitrogen atom, but adopts a different binding orientation in H_2 in which N^{τ} and N^{π} form hydrogen bonds with $D186^{5\times43}$ and $T190^{5\times461}$, respectively.[247] In H_3 and H_4, the negatively charged $E^{5\times461}$ can furthermore form a stronger ionic/hydrogen bond with N^{τ} than $N198^{5\times461}$ in H_1, explaining the higher affinity of histamine for H_3 and H_4 compared to H_1. Although there is a negatively charged aspartate at position 5×43 in H_2, it has been hypothesized that an increase in distance to the N^{τ} nitrogen atom might lead to the reduced affinity for this receptor compared to the H_3 and H_4.

8.3. Differential Determinants of Polypharmacological Ligand Binding. Mutation studies of ligands with various polypharmacological profiles reveal different effects upon particular residue mutations (Figure 21). For example, the mutation of serine from the position 5×43 in β_2 and 5-HT_{1A} leads to different changes in pindolol affinity (all mutations in β_2 (serine was substituted by threonine, cysteine, alanine, and valine) result in significant deterioration of pindolol binding, from 5- up to 68-fold[186]), whereas the $S199^{5\times43}A$ substitution in 5-HT_{1A} leads to ∼ 2 fold[68] change in the K_i of pindolol. Another example of a similar effect is the mutation of asparagine from position 7×38 in 5-HT_{1A} and β_2, although in this case, it is 5-HT_{1A} for which the effect upon mutation is more significant: the $N^{7\times38}V$ substitution leads to over 100-fold change of pindolol affinity to 5-HT_{1A},[69] while the $N312^{7\times38}Q$ in β_2 improves pindolol affinity (0.6 fold change) and $N312^{7\times39}T$ is connected with lower pindolol affinity (50-fold change).[176] Significant differences are also observed for lisuride binding upon mutation of the 5×461 position of different

DOI: 10.1021/acs.jmedchem.8b00836
J. Med. Chem. 2019, 62, 3784−3839

receptors. The S242$^{5\times461}$A substitution for 5-HT$_{2A}$[86] and T196$^{5\times461}$A for 5-HT$_6$[87] lead to loss of high lisuride affinity (6- and 34-fold of K_i change, respectively), whereas the A222$^{5\times461}$S mutant of 5-HT$_{2C}$[86] and S197$^{5\times461}$A mutant of D$_2$[230] lead to slight improvement in lisuride binding, 0.2 and 0.7 fold change, respectively. The D110$^{3\times32}$E mutation of D$_3$ is connected with three times lower spiperone binding,[214] whereas the same mutation in 5-HT$_{2A}$ does not influence spiperone affinity.[77] Different direction of changes in spiperone binding are also observed for position 6×51 in dopamine receptors: substitution of phenylalanine into alanine for D$_2$[244] changes the K_D of spiperone by 33 fold, whereas the F$^{6\times51}$W mutation only has a 2-fold decrease in spiperone binding affinity for D$_3$. Competition studies performed for 5-HT$_{2A}$−WT and after F$^{6\times51}$L mutation lead only to slight change in K_i values.[96] Clozapine also shows differential effects for mutation of residue position 5×461 at 5-HT$_6$ and D$_4$ receptors. While the mutation T$^{5\times461}$A in rat 5-HT$_6$ results in a mild loss of affinity of clozapine to the receptor[87] (K_i increasing from 16.6 to 44.1 nM), mutation of S$^{5\times461}$ to alanine in the rat D$_4$ receptor increases the affinity of the ligand[235] (K_i decreasing from 1.8 to 0.4 nM). Thus, it is seen that similar mutations can have largely differing effects in the binding sites of different aminergic receptors for ligands with different polypharmacological profiles. However, mutation data supporting the understanding of differential roles of these residues is scarce, as the sets of mutations and the sets of ligands used for different receptors have low overlap.

8.4. Mutation Effects Outside of the Consensus Binding Site. Of all 6692 annotated ligand−mutation pairs, half (50.4%) cover the aminergic pocket (residue positions defined in section 2.2). The other pairs are dispersed across the GPCR, but several of them target functional sites such as: (i) the coupling interface between GPCRs and G proteins and arrestins (5.9%), with positions 12×48, 12×49, 12×51, 1×60, 2×37, 2×38, 2×39, 2×40, 2×43, 34×50, 34×51, 34×52, 34×53, 34×54, 34×55, 34×56, 34×57, 3×49, 3×50, 3×53, 3×54, 3×55, 3×56, 4×38, 4×40, 5×61, 5×64, 5×65, 5×67, 5×68, 5×69, 5×71, 5×72, 5×74, 6×23, 6×24, 6×25, 6×26, 6×28, 6×29, 6×32, 6×33, 6×36, 6×37, 6×40, 7×56, 8×47, 8×48, 8×49, 8×50, 8×51, and 8×56, (ii) the sodium pocket (7.1%), with positions 1×50, 1×53, 2×46, 2×47, 2×49, 2×50, 3×39, 3×43, 6×44, 6×48, 7×45, 7×46, 7×49, 7×50, and 7×53, and (iii) microswitches (13.0%), with positions 3×40, 3×46, 3×49, 3×50, 5×47, 5×50, 5×58, 6×30, 6×34, 6×37, 6×44, 6×48, 6×50, 7×43, 7×49, 7×50, and 7×53, which are all residues involved in the (de)activation mechanism of GPCRs[270,271] (Figure 22). Mutations on these functional sites can influence the functional state of the receptor and thereby result in an change in ligand binding affinity. Apart from this, 11,8% of the mutations cover ligand-binding pocket positions outside the aminergic pocket but are observed in ligand binding in at least one class A GPCR crystal structure (an additional 55 generic positions). Effects on these positions could potentially indicate inhibitors binding to allosteric sites. However, it should be noted that some of these ligand binding residues and the functional sites can overlap. For example, residues interacting with the intracellular β_2 adrenoceptor inhibitor Cmpd-15 (as observed in the crystal structure 5X7D[163]) also overlap with the G protein and arrestin binding interface. Overall, mutations in the aminergic binding site have the largest effect (mean of 5.5-fold effect) on the binding affinity of ligands (Figure 22A). However, mutations in the sodium pocket, microswitches, and G protein and arrestin interface can also have a pronounced effect on ligand binding affinity. One example is the frequently mutated position 3×49 (123 data points), which is a well-known microswitch (in the DRY-motif) and residue contact within the G protein interface. Mutations at this position can result in a more than 100-fold increase in affinity as seen for example for isoproterenol at the β_2 adrenoceptor. Finally, it should be noted that in the present work, we have adopted the assumption that most of the ligands used in mutation studies in aminergic receptors bind the previously described consensus binding site. While this is probably a safe assumption for basic amine containing ligands, it is not unprecedented in the GPCR field that ligands formerly thought to bind the orthosteric site are shown to bind distinct allosteric sites in crystal structures. Putative muscarinic allosteric and dualsteric ligands binding to the ECV were indicated in section 4 and Figure 9. Similarly, the CXCR4 ligand IT1t was shown to bind only in the minor pocket/ECV. More surprisingly, the aforementioned β_2 adrenoceptor inhibitor Cmpd-15 was shown to bind intracellularly in the G protein-coupling interface, and also CCR2 and CCR9 chemokine receptor ligands CCR2-RA-[R] and vercirnon, respectively, were shown to occupy an intracellular pocket. Furthermore, in more and more GPCR structures extrahelical membrane exposed binding sites are also revealed, such as in FFA1, PAR2, P2Y$_1$, C5a$_1$, and class B receptors GCGR and GLP-1R (see Figure 22B).[10] Therefore, it cannot be ruled out that in some cases large mutation effects outside of the amine binding pocket indicate an alternative ligand binding mode. However, mutation data availability is often biased by the assumptions of functionally relevant residues of the receptors, and such interesting mutations may not have been performed at all.

8.5. Comparison of Mutation Effects in Binding and Functional Assays. As pointed out earlier, only radioligand competition, displacement, saturation, and kinetics data were collected for the present review (data types K_D and K_i). It is generally more straightforward to associate structural modifications to ligand binding than to functional effects of the ligands, although even the former can pose challenges as seen in the previous section. We did not aim to evaluate mutation effects on functional studies (such as data types IC$_{50}$ and EC$_{50}$) but investigated a few references, where both binding and functional effects were measured. Examples of mutational data referring to functional studies were provided for representatives of each receptor family. For serotonin receptors, the 5-HT$_{1B}$ case was considered,[271] and the mutational effects provided in this study were on similar level in comparison to the affinity binding data, with the majority of data points falling into second and third class of MUT/WT effect. A similar effect was observed for the dopamine receptor D$_1$.[272] The affinity data were only slightly affected by the mutations reported in the study (all data points were assigned to the second MUT/WT effect class), similarly to observations from the cAMP accumulation assay. Agonists of muscarinic acetylcholine M$_4$ receptor were also similarly affected by mutations in terms of ligand affinity and the functional effects examined falling into the first and the second effect classes.[120] Mutations also similarly affected affinity and functional studies for reported cases of adrenergic (first and second effect classes)[192] and histamine (second, third, and fourth effect classes)[254] receptors. Thus, from this small comparison, it seems that

DOI: 10.1021/acs.jmedchem.8b00836
J. Med. Chem. 2019, 62, 3784−3839

the observed binding and functional effects are not substantially different in aminergic GPCRs.

9. APPLICATIONS UTILIZING AMINERGIC GPCR MUTATION DATA

Using data from mutation studies have aided various efforts to understand GPCR structure and GPCR-ligand binding. Main types of applications include (i) structural modeling of GPCRs including the identification of residues crucial for proper folding, SCAM measurements for identifying residue orientations, and combined ligand/receptor SAR studies to uncover the structural determinants of GPCR ligand recognition, (ii) ligand discovery and design including enhanced binding mode prediction or virtual screening efficiency using, e.g., interaction filters derived from mutation studies, and design of ligands targeting specific binding pockets, displaying specific selectivity/polypharmacology profiles, or kinetics, (iii) chemical biology applications including the design of covalent binders to stabilize specific receptor conformations and design of mutant receptors with altered ligand recognition profiles (RASSLs or DREADDs). In the following, a few applications where using mutagenesis data played a crucial role are discussed.

9.1. Prediction of Aminergic GPCR Crystal Structures.

9.1.1. Substituted-Cysteine Accessibility to Probe the Ligand Binding Sites of Aminergic Receptors. Before the first experimental GPCR crystal structure was available, the substituted-cysteine accessibility method (SCAM) was used to map the surface of the binding site crevice, e.g., in the dopamine D_2 receptor.[273] In this method, each of the residues in the seven TMs is mutated to cysteine, one at a time. Then, the water accessibility of the engineered cysteines is determined through the effects of treatment with positively charged sulfhydryl reagents such as MTSEA. These reagents are more reactive with the thiolate anion than with the thiol, and only water-accessible cysteines are expected to be reactive with the reagents. It can be inferred that a wild-type residue is on the water-accessible surface if reaction of an MTS reagent with the corresponding engineered cysteine irreversibly alters radioligand binding. Furthermore, a residue can be inferred to face the binding-site crevice if the ligand is able to retard the reaction of the MTS reagents with the engineered cysteine. The amino acid residues inferred to form the surface of the binding-site crevice in the dopamine D_2 receptor from SCAM experiments were in good agreement with the highly homologous dopamine D_3 structure determined a decade later, including residues in all TMs. Later, cysteine mutation of the residues constituting ECL2 was also carried out, and the reaction of five of these mutants with sulfhydryl reagents inhibited antagonist binding and bound antagonist protected two, $I^{45\times52}C$ and to a lesser extent $N^{5\times36}C$, from reaction.[274] Ligand interaction with $I^{45\times52}$ was also confirmed by the D_3 crystal structure. Anomalous behavior of several cysteine substitutions in TM4 of the dopamine D_2 receptor ($W^{4\times50}C$, $F^{4\times54}C$, and $L^{4\times62}C$) also led to the hypothesis that TM4 forms an interface between two D_2 subunits.[275] Cross-linking at the naturally occurring $C^{4\times59}$ was completely prevented by mutating this residue to serine demonstrating that this cysteine at the extracellular end of TM4 is part of a symmetrical homodimer interface. The SCAM method was used to infer binding-site crevices of mu, delta, and kappa opioid receptors and the CB_2 cannabinoid receptor as well, later confirmed by the crystallographic structures of the opioid receptors and the CB_1 cannabinoid receptor.[276,277]

9.1.2. Predicting the Crystal Structure Coordinates of Aminergic Receptors. The strengths of using mutation study-based constraints in modeling structural GPCR−ligand interactions have been demonstrated in the GPCR Dock 2008,[20] 2010,[21] and 2013[22] assessments to predict the crystal structures of the A_{2A} adenosine receptor, the CXCR4 chemokine receptor, the dopamine D_3 receptor, serotonin 5-HT_{1B} and 5-HT_{2B} receptors, and the class F smoothened receptor. In the GPCR Dock 2010 challenge, at least five groups were reported to use mutagenesis data in binding pocket selection and deduction of key contacts for predicting the D_3-eticlopride and the CXCR4-IT1t complexes.[21] One of the top ranking groups in the challenge[25] used homology modeling of the D_3 receptor with the previously crystallized adrenergic β_2 as template. Then ss-TEA, a large-scale sequence alignment-based method, was used to score residues according to ligand binding probability based on the analysis of Shannon entropies of residue positions of a multiple sequence alignment of 7700 class A GPCR transmembrane domains.[278] The most important ligand interacting residues were predicted to be $D^{3\times32}$, $V^{3\times33}$, $S^{5\times43}$, $H^{6\times55}$, $Y^{7\times34}$, and $T^{7\times38}$, which were corroborated by mutation data and later confirmed by the crystal structure.[233,237] Ligand interactions were modeled using pharmacophore searches followed by flexible receptor docking. The structure-based pharmacophores were derived from the important ligand binding residues identified in the previous step using the Snooker program.[279] A donor and positive ionizable feature in the pharmacophore originated from $D^{3\times32}$, an acceptor feature from $T^{7\times38}$, and hydrophobic features from $F^{6\times51}$, $F^{6\times52}$, $H^{6\times55}$, and $F^{7\times34}$. The best model had TM and ligand RMSD of 2.0 and 2.1 Å, respectively, and predicted 57% of the correct ligand contacts. In the GPCR Dock 2013 challenge, the top ergotamine bound 5-HT_{1B} and 5-HT_{2B} models that most accurately predicted the ergotamine binding modes observed in the crystal structures were based on experimentally supported modeling constraints,[24] derived from homologous GPCR crystal structures, mutagenesis data, and ergotamine crystal structure information, including: (i) the conserved salt bridge between orthosteric ligands and $D^{3\times32}$ observed in all aminergic GPCR crystal structures, (ii) H-bond interactions between the indole nitrogen of ergotamine and the side chain of $S212^{5\times43}$ in 5-HT_{1B} and the backbone carbonyl of $G221^{5\times43}$ in 5-HT_{2B} based on β-adrenergic receptor mutation studies[186,280] and crystal structures,[155,167] showing that $S^{5\times43}$ is involved in agonist binding, and (iii) an internal hydrogen bond observed in the crystal structure of ergotamine. Retrospective evaluation showed that the combination of modeling constraints resulted in 5-HT_{1B} and 5-HT_{2B} models with improved ergotamine binding mode prediction and virtual ligand screening capabilities compared to models generated without constraints or with a single constraint. The interaction between $T^{3\times37}$ and the ergotamine indole observed in 5-HT_{1B} and 5-HT_{2B} crystal structures was not reflected by the limited effect of the $T^{3\times37}A$ mutation on ergotamine binding and was not predicted by the models. The 5-HT_{1B} crystal structure in complex with chemically similar LSD, however, confirmed the predicted interaction with $S^{5\times43}$, demonstrating the value of mutation data guided GPCR modeling. Despite these successful modeling cases, it has to be noted that the interpretation of mutation data is not always straightforward. As discussed in section 8.4, mutations outside of the ligand

DOI: 10.1021/acs.jmedchem.8b00836
J. Med. Chem. 2019, 62, 3784−3839

binding pocket may also result in high observed effects on ligand binding or functional alteration of the receptor. Abagyan et al. warn about the findings of the aforementioned GPCR Dock 2008[20] assessment. Site directed mutagenesis suggested at least 10 residues, in which mutations resulted in a complete loss or significant drop in ligand affinity. However, when the A_{2A} receptor crystal structure became available, only four of these residues were found to be in direct contact with the cocrystallized antagonist.[281] Carlsson et al. in their retrospective analysis of the GPCR Dock 2013[22] challenge also write that mutation effects should be interpreted and implemented very cautiously in model building.[24] Interpretation of such data might be biased by the availability of specific mutations, and often single mutation constraints are not sufficient to improve predictions. Furthermore, mutation effects may not be transferrable even to closely related GPCRs, and changes in ligand binding for mutants should not be considered to be sufficient evidence for a direct interaction with a specific residue (see the analysis in section 8.4 and Figure 22). However, the present review aims to provide comprehensive maps of residue mutations for a wide range of ligands, which in our view can largely increase the accuracy of ligand binding mode predictions.

9.2. Aminergic GPCR Ligand Discovery and Design.

9.2.1. Ligand Functional Effect Studies in β-Adrenergic Receptors. Modeling studies[282,283] based on the first antagonist bound β_2 adrenergic crystal structure demonstrated that customizing the orientation of the side chains of $S203^{5\times43}$ and $S207^{5\times461}$ based on agonist vs antagonist specific receptor mutation data[185−187,280] enabled the preferential scoring of β_2 adrenergic agonists over antagonists. Mutation of $S^{5\times43}$ affects the affinity of both β_2 adrenergic agonists adrenaline, synephrine, phenylephrine, and antagonists isoprenaline and derivatives, pindolol and propranolol, consistent with β-adrenergic crystal structures (PDB: 4LDO, adrenaline;[165] 2Y03, isoprenaline[157]), in which these ligands form H-bond interactions with $S^{5\times43}$. Mutation of $S^{5\times461}$ affects binding of full agonists (but not of antagonists), supporting the alternative rotameric state of this residue in the agonist bound β_2 adrenergic models and later confirmed by the full agonist bound β-adrenergic crystal structures in which the catechol or catechol-mimicking moieties of BI-167107 (PDB: 3P0G,[166] 3SN6,[167] 4LDE[165]), carmoterol (PDB: 2Y02), isoproterenol (PDB: 2Y03[157]), and FAUC50 (PDB: 3PDS[169]) containing two (or more) H-bond donors allows for an additional H-bond with $S^{5\times461}$.[170] Partial agonist dobutamine (PDB: 2Y00, 2Y01[157]) also has two H-bond donors that can interact with $S^{5\times43}$ and $S^{5\times461}$, but their interactions seem to be less optimal. The use of an interaction fingerprint (IFP) scoring method that determines ligand binding-mode similarity enabled: (i) the prediction of binding modes of β-adrenergic ligands for which crystal structures have not yet been solved, (ii) the selective identification and discrimination of agonists from antagonists in retrospective virtual screening studies, and (iii) the prospective identification of novel β_2 agonists.[170,282,284]

9.2.2. Histamine Receptor Selectivity and Binding Site Solvation. The symmetric distribution of complementary pharmacophore features in H_2, H_3, and H_4 binding sites (i.e., $D^{3\times32}$ in TM3 and $D^{5\times43}/E^{5\times461}$ in TM5) and of histamine receptor ligands that contain two basic groups, makes binding mode prediction challenging.[107,250,260,285−288] The binding modes of several H_4 ligands, including isothioureas, indolecarboxamides, and aminopyrimidines, in H_4 have been investigated by combining complementary in silico and in vitro approaches.[250,260] Extensive H_4 SAR, mutagenesis, docking, and MD simulation studies indicated that indolecarboxamides and aminopyrimidines form an H-bond with $D94^{3\times32}$ via their piperazine amine moiety while forming H-bond interactions with $E182^{5\times461}$ with their indole and aminopyrimidine groups, respectively, and interacting with $L175^{5\times40}$ with their chlorine substituent.[107,260] A comparable ligand-steered, experimentally supported protein-modeling approach combining 3D-QSAR, MD simulations, SAR, and mutagenesis studies indicated that clobenpropit can bind H_4 in two distinct binding modes (forming H-bonds with $D94^{3\times32}$ and $E182^{5\times461}$ with their imidazole and isothiourea groups). The addition of a cyclohexyl group to the clobenpropit isothiourea moiety, however, allows VUF5228 to adopt only one specific binding mode in the H_4 binding pocket, in which its imidazole interacts with $D94^{3\times32}$ and its isothiourea group interacts with $E182^{5\times461}$. Combined WaterFLAP calculations and site-directed mutagenesis studies indicated that optimal binding of the amine-binding region in H_1 is correlated with the presence of a trapped "unhappy" water and depends on the character of the residue on position 7×38,[251] a residue that is highly variable in aminergic GPCRs and has been previously related to stereoselective and subtype-selective binding. The additional *N*-methyl group of the tertiary amine compound 2 shields the H-bond formed with $D107^{3\times32}$ from bulk water and displaces the "unhappy" water that is trapped between $D107^{3\times32}$ and $I454^{7\times38}$ in the secondary amine VUF14544 bound H_1. The role of $I454^{7\times38}$ was confirmed by the fact that WT and $I454^{7\times38}$F mutant H_1 had a similarly increased affinity for compound 2 compared to VUF14544, whereas the $I454^{7\times38}$T mutant does not distinguish between these two ligands.

9.2.3. Mapping the Binding Modes of Bitopic and Allosteric Ligands. It has been postulated that several aminergic GPCRs possess a secondary binding pocket available for the binding of bitopic ligands, allosteric ligands, or transiently binding the orthosteric ligands during association and dissociation. In the case of the muscarinic M_2 receptor, existence of this binding pocket has been proven crystallographically in the ternary complex between M_2, the agonist iperoxo, and the positive allosteric modulator LY2119620 bound between the extracellular loops as described in section 4.1 (PDB: 4MQT).[34] Although mutation data for the cocrystallized allosteric modulator is not available, the congener LY2033298 was extensively studied in the M_4 receptor.[33] $W435^{7\times34}$ and $F186^{45\times51}$ were identified as crucial residues for binding of the allosteric modulator, their mutation to alanine completely abolishing binding. These residues form an aromatic sandwich with the allosteric modulator in the M_2 crystal structure. Molecular dynamics simulations have shown that first-generation muscarinic allosteric modulators possessing permanently charged ammonium groups also bind to this binding pocket in the M_2 receptor.[289] C_7/3-phth is anchored by two aromatic clusters, one formed by $W422^{7\times34}$ and $Y177^{45\times51}$ and the other by $Y80^{2\times60}$ and $Y83^{2\times63}$. A series of rationally designed mutations further strengthened the binding mode hypothesis from the simulations: $N410^{6\times58}$Y and $N419^{7\times31}$W further enhanced the cation−π interaction strength in the first center and $T423^{7\times35}$E and $T84^{2\times64}$D formed further favorable charge−charge interactions in the second center, thereby increasing the affinity of the allosteric modulator. On the contrary, the $N410^{x58}$K mutation in the first

DOI: 10.1021/acs.jmedchem.8b00836
J. Med. Chem. 2019, 62, 3784−3839

center and the Y80$^{2\times60}$K, Y83$^{2\times63}$K, and T423$^{7\times35}$K mutations in the second center introduced unfavorable charge repulsion, thereby decreasing the affinity of the allosteric modulator. Similarly, in the M_1 receptor, benzylquinolone carboxylic acid (BQCA), a selective M_1 positive allosteric modulator, was shown to bind in the extracellular pocket using mutagenesis experiments.[109] From alanine scanning Y85$^{2\times63}$ in TM2, Y179$^{45\times51}$ and F182 in ECL2, and E397$^{7\times31}$ and W400$^{7\times34}$ in TM7 were identified as residues that contribute to the BQCA binding pocket in M_1 as well as to the transmission of cooperativity with the orthosteric agonist carbachol. Combined SAR and mutagenesis studies also confirmed this binding pocket for benzoquinazolinone 12, a structural analogue of BQCA, that has a 50-fold increase in allosteric site affinity as compared with BQCA, while retaining a similar level of positive cooperativity with acetylcholine.[52] Alanine mutations of Y82$^{2\times60}$, Y85$^{2\times63}$, Y179$^{45\times51}$, and W$^{7\times34}$ largely decreased M_1 binding of benzoquinazolinone 12 and/or impaired cooperativity with the endogenous ligand. Conservative mutations of the aromatic residues and SAR of the ligand suggested that the tricyclic core of the PAM forms aromatic interactions with the TM2 residues while the pyrazolylpyridine pendant is sandwiched between Y$^{45\times51}$ and W$^{7\times34}$. Bitopic ligands of the $M_{1/2}$ receptors were synthesized by linking orthosteric moieties such as atropine, scopolamine, iperoxo, and isox (an oxidized derivative of iperoxo) with permanently charged allosteric tetraalkyl ammonium, phthalimide and naphthalimide derivatives.[290,291] Furthermore, the simple ligands TBPB and 77-LH-28-1 were also shown to act through a bitopic binding mechanism.[51] Combined mutagenesis experiments involving residues of the orthosteric (W$^{3\times28}$, D$^{3\times32}$, Y$^{3\times33}$, Y$^{6\times51}$) and allosteric (Y$^{2\times60}$, Y$^{2\times63}$, Y$^{45\times51}$, W$^{7\times34}$, E/T$^{7\times35}$) sites confirmed that these ligands interact with both binding pockets. A large number of bitopic ligands have been discovered for the dopamine D_2 and D_3 receptors. For example, SB269652 composed of an indole-2-carboxamide moiety linked to the dihydroisoquinoline orthosteric moiety, was demonstrated to adopt a bitopic binding pose at one protomer of a dopamine D_2 receptor dimer.[292] Additionally, this ligand was deconstructed to yield *N*-isopropyl-1*H*-indole-2-carboxamide, a negative allosteric modulator of the dopamine D_2 receptor.[241] Mutation of V91$^{2\times60}$A and E95$^{2\times64}$A were carried out, which reduced the affinity and/or negative cooperativity of the bitopic ligand SB269652, indicating that its indole-2-carboxamide moiety extends into the secondary pocket between the extracellular ends of TM2 and TM7. Furthermore, the V91$^{2\times60}$A mutation completely abolished the effect of the allosteric fragment *N*-isopropyl-1*H*-indole-2-carboxamide, indicating this residue as key for D_2 binding. On the other hand, the E95$^{2\times64}$A mutation caused a 100-fold increase in its affinity and a complete abolition of negative cooperativity with dopamine. These results suggested that the deconstructed fragment binds in the same region as within the parent compound; however, the different contribution of the different residues suggest a possibly different orientation of the fragment. Virtual fragment screening efforts targeting the allosteric binding site to identify bitopic/allosteric ligands of dopamine $D_{2/3}$ receptors also indicated the importance of interactions with the extracellular ends of TM2 and TM7. In one study, the hit fragments were linked to a nonselective orthosteric aryl-piperazine ligand, and it was shown that selectivity between dopamine receptor subtypes can be modulated in the secondary pocket suggesting interactions with the aforementioned E$^{2\times64}$ and Y/L$^{1\times39}$, S$^{7\times35}$, and T$^{7\times38}$.[293] In another study, hit fragments were shown to bind the D_3 receptor and displayed negative allosteric effects on dopamine binding. Identified interaction motifs included polar interactions with Y365$^{7\times34}$ hydroxyl and/or aromatic ring, polar interactions with S366$^{7\times35}$ and E$^{2\times64}$ side chains, and hydrogen bonding to the backbone amides of S192$^{5\times43}$, C181$^{45\times50}$, and I183$^{45\times52}$ in the ECL2.[294]

9.2.4. Halogen Bonding in Serotonin Receptor Ligand Design. Halogen atoms have been considered important for improving ligand binding to the protein for many years, although there are recent studies that specified their role as formation of a specific interaction, the halogen bond.[295,296] In line with recent studies on the importance of halogen bond formation in interaction of ligands with class A GPCRs, a series of long-chain arylpiperazine derivatives as new ligands of D_2 and 5-HT$_{1A}$/5-HT$_7$ receptors were designed and synthesized by linking 2,3-dichlorophenylpiperazin and piperidinylsulfonylquinoline moieties and identified as antagonist of the above-mentioned receptors and for which antipsychotic and antidepressant properties were indicated in in vivo models (MK-801-induced hyperlocomotor activity in mice and forced swim test (FST) in mice, respectively).[297] Molecular modeling studies supported the experimental results and indicated the halogen interactions in the formed ligand−receptor complexes. Introduction of a chlorine atom in the 4-position of phenyl piperazine compounds increased affinity to D_2 receptor in comparison to unsubstituted and 4-fluoro compounds due to postulated halogen interaction with S193$^{5\times43}$. Mutational data studies also indicated significant role of this residue in ligand−receptor affinity, with DNS, DNX, DHX, quinpirole, and dopamine leading to 4.5-, 32.5-, 15-, 2.8-, and 177.8-fold modification of K_i values to dopamine D_2.[227] Additionally, the shift of the chlorine atom from the 4- to the 3-position led to improvement in affinity for 5-HT$_{1A}$, 5-HT$_7$, and D_2. This effect was justified by the stabilization of the ligand−receptor complexes via V190$^{5\times40}$-mediated halogen bond in D_2 and T$^{5\times40}$ in 5-HT$_{1A}$ and 5-HT$_7$. However, introduction of a second chlorine atom in the 2-position of the phenylpiperazine ring, despite formation of additional halogen bond with H$^{6\times55}$, did not change affinities to the examined receptors in comparison to the respective 3-chloro counterparts. The role of H$^{6\times55}$ was also extensively examined in mutational studies for D_2 with 7-OH-DPAT and quinpirole as tested ligands, with significant reduction of affinity upon mutation.

9.2.5. Structural Determinants of Binding Kinetics in Aminergic Receptors. In the muscarinic M_3 receptor, mutation effects on the residence time vs the pK_i of tiotropium were strongly correlated, but mutation of some amino acids led to a disproportionately enhanced dissociation rate.[113] The most important residues deviating from linear behavior were N508$^{6\times52}$ forming concerted H-bonds with the ester and hydroxyl groups of the ligand in the orthosteric pocket, and the residues that form the "lid" above tiotropium, i.e., tyrosines Y149$^{3\times33}$, Y507$^{6\times51}$, and Y530$^{7\times38}$. Mutation of these residues to alanine accelerated the dissociation by up to 2 orders of magnitude and reduced the half-life from 24.5 h to between 17 s and 8.3 min. A tiotropium analogue lacking the hydroxyl group interacting with N$^{6\times52}$ was synthesized and evaluated against wild-type and the N508$^{6\times52}$A mutant receptor. In the mutant, neither tiotropium nor its analogue can interact with N$^{6\times52}$ and the ratios of the K_i values and the k_{off} values were in the same range. In the WT receptor, there was a stronger effect

DOI: 10.1021/acs.jmedchem.8b00836
J. Med. Chem. 2019, 62, 3784−3839

on the k_{off} ratios compared to the K_i ratios, thereby confirming the important H-bond interactions. The observation of the importance of the lid over the binding pocket on the dissociation kinetics led to an interpretation where these residues act as a mechanical barrier that keeps tiotropium in the binding pocket. Furthermore, mutation of $V^{6\times55}$ to alanine located in the exit channel did not reduce the affinity of tiotropium but the half-life was reduced to less than 10 h, indicating a further important role of this residue in controlling the dissociation of tiotropium. The recently solved crystal structure of the LSD-bound serotonin 5-HT_{2B} receptor revealed not only the unusual ligand orientation in the binding site but also explained the unexpectedly slow on- and off-rates at the 5-HT_{2B} and also the 5-HT_{2A} subtype.[61] The very slow dissociation rate (k_{off} = 0.022 ± 0.004 min^{-1}) was explained again as the formation of a "lid" over the ligand by residues 207−214 ($C^{45\times50}$ to $F^{5\times36}$) of the ECL2 that makes it more difficult for LSD to dissociate. In molecular dynamics simulations the lid occasionally moved to the side allowing LSD to start dissociation. The rationally designed $L^{45\times52}A$ mutant reduced the residence time of LSD from 46 to 4 min at the 5-HT_{2B} subtype and 221 to 50 min in the 5-HT_{2A} subtype. The mutated ECL2 also showed highly increased mobility in molecular dynamics simulations. In another study, analysis of access to the orthosteric binding sites in inactive- and active-state β_2 adrenoceptor structures provided a structural rationale for the slowing of agonist and antagonist association.[298] Intracellular binding of G protein or G protein mimicking nanobodies stabilizes a rearrangement of the cytoplasmic end of TM7 and ECL2 with $F193^{45\times52}$ and $Y308^{7\times34}$, moving 2−2.5Å closer to each other to form again a lid over the orthosteric ligand-binding site. $K305^{7\times31}$ also contributes to capping the orthosteric site by trading its salt bridge with $D^{45\times51}$ for an interaction with the backbone carbonyl of $F193^{45\times52}$. The $Y308^{7\times34}A$ mutant significantly diminished the capacity of the Nb80 nanobody to slow the association of DHAP (association half-time increased from 3.5 to 2.2 min in the presence of Nb80) and formoterol (association half-time increased from 2.6 to 1.3 min in the presence of Nb80). Furthermore, the mutation also enhances the extent of formoterol binding reflecting the capacity of the agonist formoterol to cooperatively stabilize Nb80 binding and vice versa. Finally, in the case of zwitterionic ligands of the histamine H_1 receptor, the effect of mutations on binding kinetics revealed specific interactions associated with controlling ligand dissociation rates.[261] Stereoisomers of cetirizine, levocetirizine, and *S*-cetirizine are selective antagonists of the H_1 receptor with high affinity and stereoselectivity (K_i values of 6, 3, and 100 nM, respectively). The differences in affinity come almost exclusively from the differences in the off-rate of the enantiomers (half-life 142 min compared to 6 min). In addition, hydroxyl or methyl ester analogues dissociate more rapidly, with half-times of 31 and 7 min, respectively. The importance of the carboxylic function of levocetirizine was further supported by the results from the $K190^{5\times40}A$ mutation. This mutation decreased the half-life of the levocetirizine complex to 13 min and reduced its affinity from 3 to 12 nM, whereas the affinity and dissociation kinetics of hydroxyl and methyl ester analogues were hardly affected. In addition to the aminergic receptor cases described above, site-directed mutagenesis studies have also been used to elucidate the structural determinants of receptor−ligand binding kinetics for several other GPCR subfamilies, including adenosine receptors (A_{2A})[299] and chemokine receptors (CCR5).[300]

9.3. Site-Directed Mutagenesis-Enabled Chemical Biology Studies of Aminergic GPCRs. Mutational studies are also important for studying the mechanisms of GPCR activation, enabling the construction of covalent ligands, stabilizing the active conformation of the protein, and allowing examination of its architecture in such activated states. Weichert et al. developed a series of covalently binding agents, derivatives of monoamine neurotransmitters noradrenaline, dopamine, serotonin, and histamine.[168] They overcome typical problems connected with obtaining stable ligand−protein complexes, that is, low binding affinity and rapid dissociation rate, features characteristic for endogenous ligands. Development of new covalent agents in the above-mentioned study followed the disulfide-based cross-linking methodology. Therefore, mutants of the considered proteins were constructed, e.g., $H^{2\times63}$ in the β_2 adrenergic receptor was substituted by cysteine, constructing an anchor for binding of covalent agonist FAUC50 via disulfide bridging. On the basis of the homology within the group of aminergic GPCRs, a general methodology of converting endogenous neurotransmitters into disulfide-functionalized, covalently binding molecules was developed (examples for dopamine receptor D_2, serotonin receptor 5-HT_{2A}, and histamine receptor H_1 were presented). Analogously, cysteine was introduced into position 2×63 of the dopamine D_2 receptor in replacement of leucine. The mutation of this residue was also earlier reported, where leucine was changed into serine.[222] Saturation experiments with *N*-methylspiperone revealed an almost 4-fold change of the K_D value, from 79 to 300 pM, whereas in radioligand competition studies, the K_i of CPPMA changed from 920 to 540 nM, and spiperone changed from 280 to 780 nM. Interestingly, Weichert et al. observed only subtle changes of ligand binding upon $T134^{2\times63}C$ mutation in 5-HT_{2A}, and only further mutation of $S131^{2\times60}$ into glycine led to a covalently bound ligand−receptor complex. In the case of histamine receptor H_1, the mutation $Y87^{2\times63}C$ led to the desired covalently bound ligand−receptor complex. Another study reported the development of a partial agonist of the histamine H_4 receptor (VUF14480), covalently bound to the protein, with the identification of cysteine in position 3×36 as the residue being an anchor point for the above-mentioned covalent bond.[253] This was confirmed by mutational studies, where the $C98^{3\times36}S$ substitution led to a decrease in pK_i values of VUF14480 from 6.3 to 5.8. An adverse effect of the cysteine substitution in 3×36 position was observed for another compound examined in this study, VUF14481, with the change in the pK_i from 6.4 to 6.8. Values of pK_i for the endogenous ligand, histamine, were 8.1 and 7.2, respectively, and K_D of 7 and 27 nM for wild-type and mutant receptor, respectively. Further examination of the structure and role of GPCRs is also possible with the construction of so-called receptors activated solely by synthetic ligands (RASSLs) and designer receptors exclusively activated by designer drugs (DREADDs). Bruysters et al. exploited the differences in binding pockets of different classes of H_1 receptor agonists and identified the first $G\alpha_{q/11}$-coupled RASSL.[252] The mutant human H_1 receptor with $F435^{6\times55}A$ replacement combined strongly decreased affinity (25-fold) and potency (200-fold) for the endogenous ligand histamine with improved affinities (up to 54-fold) and potencies (up to 2600-fold) for synthetic 2-phenylhistamine agonists. In another study, a human muscarinic acetylcholine M_3 receptor

DOI: 10.1021/acs.jmedchem.8b00836
J. Med. Chem. 2019, 62, 3784−3839

was constructed possessing a cyan fluorescent protein in place of the third intracellular loop and mutations at position 3×33 (replacement of tyrosine by cysteine) and/or 5×46 (glycine change into alanine) in the M_3-RASSL.[301] Mutation of position 3×33 in M_3 was also reported in the study of Tautermann et al. ($Y149^{3\times33}A$).[113] These changes had significant impact on the affinity of the examined ligands (eight different compounds were tested). For example, pK_i of tiotropium changed from 10.8 to 8.6 upon mutation and that of *N*-methylscopolamine from 9.8 to 7.9. The saturation studies performed on M_3 and M_3-RASSL revealed 100-fold difference in [^{3}H]QNB affinity: K_D of 75 nM for M_3 vs K_D of 7.9 nM for M_3-RASSL. Reduced affinity was also observed in competition studies with atropine: K_i of 47 nM vs K_i of 0.74 nM for M_3-RASSL and M_3, respectively. Further modification of the produced constructs by tagging at the N-terminus with an anti-VSV-G epitope and the 20 kDa SNAP-tag sequence led to K_D of 35 nM for M_3 and 1.4 nM for M_3-RASSL, and IC_{50} for atropine was 0.74 and 23 nM, respectively. However, despite the reduced affinity for muscarinic receptor antagonists, the M_3-RASSL stimulated by clozapine *N*-oxide produced similar response to acetylcholine at wild-type M_3 in functional studies. The in vivo behavior of designed muscarinic acetylcholine receptors has been recently investigated.[302]

CONCLUDING REMARKS

Aminergic GPCRs are implicated in various diseases and continue to be one of the most pursued drug targets. Mutagenesis studies in the past enabled the delineation and characterization of aminergic GPCR binding pockets and the unraveling of crucial protein−ligand interactions for the binding of endogenous and drug-like small molecule ligands as well as the studying of residue substitutions affecting signal transduction. With the elucidation of more than 50 aminergic GPCRs to date from the five major aminergic GPCR subfamilies (serotonin, muscarinic acetylcholine, adrenergic, dopamine, and histamine; note that trace amine receptors have not been investigated in mutation studies yet), this large body of mutagenesis data can now be analyzed in the light of experimentally determined ligand binding modes and can be used to guide computational binding mode prediction also for ligands that are dissimilar to the cocrystallized ones. Mutational studies in the postcrystallographic era have focused on the delineation of binding interactions of ligands with novel chemotypes and novel binding pockets (such as allosteric ligands) and uncovering the relationships between ligand SAR, residue substitutions, and the way these are translated to functional effects. Furthermore, the detailed structural understanding of protein−ligand interactions in aminergic GPCRs enables the directed design of mutants for specific chemical biology applications such as creating receptors with altered ligand binding profiles or enabling covalent modifications. Despite their already large contribution to understanding GPCR structure and function, mutagenesis experiments will continue to be indispensable for enabling crystallization of further receptor subtypes implicated in diseases or conveying drug side effects, studying binding pockets, and binding interactions of novel ligand chemotypes, improving the performance of computational methods for their prediction thereof, and understanding the signal transduction mechanisms in different GPCRs.

ASSOCIATED CONTENT

Supporting Information

The Supporting Information is available free of charge on the ACS Publications website at DOI: 10.1021/acs.jmedchem.8b00836.

Excel file of the aminergic GPCR mutation data (uploaded to Zenodo: 10.5281/zenodo.58104) and GPCRdb: http://gpcrdb.org) and KNIME workflow to analyze the mutation data set; heat maps used for mutation effect prediction, retrospective evaluation and prospective prediction heat maps; PyMOL sessions used to create Figures 3, 7, 10, 13, 16, 19, 20, and 22; PDF versions of Figures 5, 6, 8, 9, 11, 12, 14, 15, 17, and 18 are provided in the Supporting Information. (ZIP)

AUTHOR INFORMATION

Corresponding Author

*E-mail: Chris.DeGraaf@heptares.com. Phone: +44 (0)1223 949 100.

ORCID

Márton Vass: 0000-0003-1486-0063
Andrzej J. Bojarski: 0000-0003-1417-6333
Rob Leurs: 0000-0003-1354-2848
Albert J. Kooistra: 0000-0001-5514-6021
Chris de Graaf: 0000-0002-1226-2150

Author Contributions

⊥Márton Vass and Sabina Podlewska contributed equally.

Notes

The authors declare no competing financial interest.

Biographies

Márton Vass obtained his Ph.D. degree at the Budapest University of Technology and Economics on in silico methodologies aiding fragment-based drug discovery in 2014 while he was working as research scientist in the Lead Discovery Laboratory (CADD team) of Gedeon Richter Plc. a midsized specialty pharmaceutical R&D company in Budapest, where he was responsible for the computational support of medicinal chemistry projects in the CNS field (2011−2015). In 2015, Márton Vass started a postdoctoral fellowship in the Division Medicinal Chemistry at VU University Amsterdam on the 3D-e-Chem project developing open source integrated data analysis and modeling workflows for GPCR selectivity and polypharmacology prediction, virtual screening, drug repurposing, and mutation data analysis. In the group he also receives funding from the GPCR Consortium.

Sabina Podlewska obtained her M.Sc. degree at the Jagiellonian University, Faculty of Chemistry, in 2012. Thereafter she pursued her Ph.D. studies and obtained the degree in 2016 at the same faculty on the development of machine learning-based tools for computer-aided drug design. In 2015, she obtained scholarship by the Polish Ministry of Science and Higher Education for outstanding achievements for Ph.D. students. In the meantime (2010), she started a position in the Institute of Pharmacology, Polish Academy of Sciences, Department of Medicinal Chemistry where she works on in silico methods for the search of new serotonin receptor ligands, with special focus on machine learning-based approaches. Currently she runs her own grant on the search for new ligands of serotonin receptor 5-HT_7 with improved metabolic stability.

Iwan J. P. de Esch performed his Ph.D. research at Vrije Universiteit Amsterdam. He became a research associate in the drug design group at the University of Cambridge in 1998 and cofounded De Novo

DOI: 10.1021/acs.jmedchem.8b00836
J. Med. Chem. 2019, 62, 3784−3839

Pharmaceuticals in 2000. In 2003, Iwan de Esch returned to academia and is now full professor Biocomputational Chemistry for Drug Innovation at Vrije Universiteit Amsterdam. Prof. Dr. de Esch is cofounder of IOTA Pharmaceuticals and cofounder of Griffin Pharmaceuticals, contributing to the valorization of the fragment-based drug discovery and the GPCR research lines of the academic group. In 2011, de Esch was awarded the Galenus Research Prize for his work on fragment-based drug discovery, and since 2016 he is project leader of the European Union's Horizon2020 MSCA Programme ITN project FragNet.

Andrzej J. Bojarski obtained his Ph.D. degree in 1996 at the Faculty of Pharmacy Jagiellonian University Medical College on modeling interactions between arylpiperazine ligands and the 5-HT_{1A} receptor. His postdoctoral fellowships involved research in the Institut für Pharmazeutische Chemie Heinrich Heine Universität Düsseldorf (01.1999−07.1999) and in the Institute of Medicinal Chemistry University of Lausanne (10.1999−03.2000). He obtained habilitation in 2005 also at the Faculty of Pharmacy Jagiellonian University Medical College, and in 2013 he was appointed Full Professor. Since 2006, he has been head of the Department of Medicinal Chemistry Institute of Pharmacology, Polish Academy of Sciences, where he worked from 1992. His scientific achievements have been appreciated by many institutions, most recently by Minister of Health Group Awards for the best publications (2008, 2010).

Rob Leurs performed his Ph.D. research on G-protein coupled receptors at Vrije Universiteit Amsterdam. After a postdoctoral fellowship at INSERM, he was awarded with a Royal Netherlands Academy of Arts and Sciences fellowship. He was awarded the Galenus Research Prize (1997), the Organon Award for Pharmacology (2000), a Pfizer Academic Award (2001), a STW/NOW Pionieer grant (2001), and was appointed academy member of the Royal Netherlands Academy of Arts and Sciences (KNAW) (2016). Rob Leurs is full professor and head of the Division of Medicinal Chemistry at Vrije Universiteit Amsterdam and cofounder of Griffin Discoveries, a company that valorizes the GPCR expertise. Prof. Dr. Leurs is project leader of the EU FP7-funded project PDE4NPD, phosphodiesterase inhibitors for the treatment of neglected parasitic diseases.

Albert J. Kooistra obtained his B.Sc. degree in Telematics at the University of Twente, his M.Sc. degree (cum laude) in Bioinformatics and his Ph.D. in computational Medicinal Chemistry at the Vrije Universiteit Amsterdam. He performed his Ph.D. research (2010−2014) on virtual screening methodology development and structural chemogenomics analyses. As postdoctoral researcher, he implemented in silico approaches for knowledge and structure-based steering of medicinal chemistry efforts. In 2016, he joined the CMBI at the Radboud university medical center to collaborate within the 3D-e-Chem project developing new technologies for integrating ligand and protein data for structure-based prediction of ligand selectivity and polypharmacology. In 2018, he joined the group of Prof. Gloriam at the Department of Drug Design and Pharmacology of the University of Copenhagen as assistant professor.

Chris de Graaf performed his Ph.D. research at Vrije Universiteit Amsterdam on computational ligand binding mode and affinity predictions in Cytochrome P450 enzymes (2002−2006). As postdoctoral fellow with AstraZeneca Pharmaceuticals and Strasbourg University (Dr. Rognan), he worked on the development and application of novel GPCR modeling and virtual screening techniques (2006−2008). In 2009, Chris de Graaf was appointed assistant professor at VU University Amsterdam, where he developed structural cheminformatics and computational medicinal chemistry methods to complement synthetic medicinal chemistry and molecular pharmacology studies in drug discovery research projects. Since 2018, Dr. De Graaf is Head of Computational Chemistry at Sosei Heptares in Cambridge, UK, leading the development and application of computer-assisted drug design approaches for GPCR structure-based drug discovery.

■ ACKNOWLEDGMENTS

This research was financially supported by The Netherlands eScience Center (NLeSC)/NWO (Enabling Technologies project: 3D-e-Chem, grant 027.014.201) to C.d.G., The Netherlands Organization for Scientific Research (NWO CW TOP-PUNT grant 718.014.002, 7 ways to 7TMR modulation (7-to-7), to R.L.). S.P., M.V., I.J.P.d.E., R.L, A.J.K., A.J.B., and C.d.G. participated in the European Cooperation in Science and Technology Action CM1207 [GPCR-Ligand Interactions, Structures, and Transmembrane Signalling: A European Research Network (GLISTEN)]. S.P. received funding from the National Science Centre, Poland within the grant HARMONIA 7: 2015/18/M/NZ7/00377. The authors are thankful to Stefan Verhoeven and Ross McGuire for technical assistance with the 3D-e-Chem KNIME nodes and workflows.

■ ABBREVIATIONS USED

DREADD, designer receptor exclusively activated by designer drugs; ECFP, extended connectivity fingerprint; FST, forced swim test; GPCR, G protein-coupled receptor; IFP, interaction fingerprint; MACCS, molecular access system (fingerprint type); MD, molecular dynamics; RASSL, receptor activated solely by synthetic ligand; RMSD, root-mean-square deviation (of atomic positions); SAR, structure−activity relationship; SCAM, substituted cysteine accessibility method; SDM, site-directed mutagenesis; TM, transmembrane (helix); WT, wild-type.

■ REFERENCES

(1) Santos, R.; Ursu, O.; Gaulton, A.; Bento, A. P.; Donadi, R. S.; Bologa, C. G.; Karlsson, A.; Al-Lazikani, B.; Hersey, A.; Oprea, T. I.; Overington, J. P. A comprehensive map of molecular drug targets. *Nat. Rev. Drug Discovery* **2017**, *16*, 19−34.

(2) Cherezov, V.; Rosenbaum, D. M.; Hanson, M. A.; Rasmussen, S. G.; Thian, F. S.; Kobilka, T. S.; Choi, H. J.; Kuhn, P.; Weis, W. I.; Kobilka, B. K.; Stevens, R. C. High-resolution crystal structure of an engineered human beta2-adrenergic G protein-coupled receptor. *Science* **2007**, *318*, 1258−1265.

(3) Robertson, N.; Jazayeri, A.; Errey, J.; Baig, A.; Hurrell, E.; Zhukov, A.; Langmead, C. J.; Weir, M.; Marshall, F. H. The properties of thermostabilised G protein-coupled receptors (StaRs) and their use in drug discovery. *Neuropharmacology* **2011**, *60*, 36−44.

(4) Tate, C. G. A crystal clear solution for determining G-protein-coupled receptor structures. *Trends Biochem. Sci.* **2012**, *37*, 343−352.

(5) Chun, E.; Thompson, A. A.; Liu, W.; Roth, C. B.; Griffith, M. T.; Katritch, V.; Kunken, J.; Xu, F.; Cherezov, V.; Hanson, M. A.; Stevens, R. C. Fusion partner toolchest for the stabilization and crystallization of G protein-coupled receptors. *Structure* **2012**, *20*, 967−976.

(6) Rosenbaum, D. M.; Cherezov, V.; Hanson, M. A.; Rasmussen, S. G.; Thian, F. S.; Kobilka, T. S.; Choi, H. J.; Yao, X. J.; Weis, W. I.; Stevens, R. C.; Kobilka, B. K. GPCR engineering yields high-resolution structural insights into beta2-adrenergic receptor function. *Science* **2007**, *318*, 1266−1273.

(7) Steyaert, J.; Kobilka, B. K. Nanobody stabilization of G protein-coupled receptor conformational states. *Curr. Opin. Struct. Biol.* **2011**, *21*, 567−572.

DOI: 10.1021/acs.jmedchem.8b00836
J. Med. Chem. 2019, 62, 3784−3839

(8) Piscitelli, C. L.; Kean, J.; de Graaf, C.; Deupi, X. A molecular pharmacologist's guide to G protein-coupled receptor crystallography. *Mol. Pharmacol.* **2015**, *88*, 536−551.
(9) Bento, A. P.; Gaulton, A.; Hersey, A.; Bellis, L. J.; Chambers, J.; Davies, M.; Kruger, F. A.; Light, Y.; Mak, L.; McGlinchey, S.; Nowotka, M.; Papadatos, G.; Santos, R.; Overington, J. P. The ChEMBL bioactivity database: An update. *Nucleic Acids Res.* **2014**, *42*, D1083−1090.
(10) Vass, M.; Kooistra, A. J.; Yang, D.; Stevens, R. C.; Wang, M. W.; de Graaf, C. Chemical diversity in the G protein-coupled receptor superfamily. *Trends Pharmacol. Sci.* **2018**, *39*, 494−512.
(11) Kooistra, A. J.; Kuhne, S.; de Esch, I. J.; Leurs, R.; de Graaf, C. A structural chemogenomics analysis of aminergic GPCRs: Lessons for histamine receptor ligand design. *Br. J. Pharmacol.* **2013**, *170*, 101−126.
(12) Munk, C.; Harpsøe, K.; Hauser, A. S.; Isberg, V.; Gloriam, D. E. Integrating structural and mutagenesis data to elucidate GPCR ligand binding. *Curr. Opin. Pharmacol.* **2016**, *30*, 51−58.
(13) Jespers, W.; Schiedel, A. C.; Heitman, L. H.; Cooke, R. M.; Kleene, L.; van Westen, G. J. P.; Gloriam, D. E.; Muller, C. E.; Sotelo, E.; Gutierrez-de-Teran, H. Structural mapping of adenosine receptor mutations: Ligand binding and signaling mechanisms. *Trends Pharmacol. Sci.* **2018**, *39*, 75−89.
(14) Beukers, M. W.; Kristiansen, K.; Ijzerman, A. P.; Edvardsen, O. TinyGRAP database: A bioinformatics tool to mine G-protein-coupled receptor mutant data. *Trends Pharmacol. Sci.* **1999**, *20*, 475−477.
(15) Isberg, V.; Mordalski, S.; Munk, C.; Rataj, K.; Harpsøe, K.; Hauser, A. S.; Vroling, B.; Bojarski, A. J.; Vriend, G.; Gloriam, D. E. GPCRdb: An information system for G protein-coupled receptors. *Nucleic Acids Res.* **2016**, *44*, D356−D364.
(16) Isberg, V.; Mordalski, S.; Munk, C.; Rataj, K.; Harpsøe, K.; Hauser, A. S.; Vroling, B.; Bojarski, A. J.; Vriend, G.; Gloriam, D. E. GPCRdb: An information system for G protein-coupled receptors. *Nucleic Acids Res.* **2017**, *45*, 2936.
(17) Pandy-Szekeres, G.; Munk, C.; Tsonkov, T. M.; Mordalski, S.; Harpsøe, K.; Hauser, A. S.; Bojarski, A. J.; Gloriam, D. E. GPCRdb in 2018: Adding GPCR structure models and ligands. *Nucleic Acids Res.* **2018**, *46*, D440−D446.
(18) Isberg, V.; de Graaf, C.; Bortolato, A.; Cherezov, V.; Katritch, V.; Marshall, F. H.; Mordalski, S.; Pin, J. P.; Stevens, R. C.; Vriend, G.; Gloriam, D. E. Generic GPCR residue numbers - aligning topology maps while minding the gaps. *Trends Pharmacol. Sci.* **2015**, *36*, 22−31.
(19) Kufareva, I.; Ilatovskiy, A. V.; Abagyan, R. Pocketome: An encyclopedia of small-molecule binding sites in 4D. *Nucleic Acids Res.* **2012**, *40*, D535−540.
(20) Michino, M.; Abola, E.; participants, G. D.; Brooks, C. L., 3rd; Dixon, J. S.; Moult, J.; Stevens, R. C. Community-wide assessment of GPCR structure modelling and ligand docking: GPCR Dock 2008. *Nat. Rev. Drug Discovery* **2009**, *8*, 455−463.
(21) Kufareva, I.; Rueda, M.; Katritch, V.; Stevens, R. C.; Abagyan, R. participants, G. D. Status of GPCR modeling and docking as reflected by community-wide GPCR Dock 2010 assessment. *Structure* **2011**, *19*, 1108−1126.
(22) Kufareva, I.; Katritch, V.; Stevens, R. C.; Abagyan, R. Advances in GPCR modeling evaluated by the GPCR Dock 2013 assessment: Meeting new challenges. *Structure* **2014**, *22*, 1120−1139.
(23) Bhattacharya, S.; Lam, A. R.; Li, H.; Balaraman, G.; Niesen, M. J.; Vaidehi, N. Critical analysis of the successes and failures of homology models of G protein-coupled receptors. *Proteins: Struct., Funct., Genet.* **2013**, *81*, 729−739.
(24) Rodriguez, D.; Ranganathan, A.; Carlsson, J. Strategies for improved modeling of GPCR-drug complexes: Blind predictions of serotonin receptors bound to ergotamine. *J. Chem. Inf. Model.* **2014**, *54*, 2004−2021.
(25) Roumen, L.; Sanders, M. P. A.; Vroling, B.; De Esch, I. J. P.; De Vlieg, J.; Leurs, R.; Klomp, J. P. G.; Nabuurs, S. B.; De Graaf, C. In silico veritas: The pitfalls and challenges of predicting GPCR-ligand interactions. *Pharmaceuticals* **2011**, *4*, 1196−1215.
(26) Marcou, G.; Rognan, D. Optimizing fragment and scaffold docking by use of molecular interaction fingerprints. *J. Chem. Inf. Model.* **2007**, *47*, 195−207.
(27) Aminergic G protein-coupled receptor (GPCR) mutation data set. In Zenodo; Zenodo, 2016; DOI: DOI: 10.5281/zenodo.58104.
(28) The Uniprot Consortium. UniProt: A hub for protein information. *Nucleic Acids Res.* **2015**, *43*, D204−D212.
(29) Ballesteros, J. A.; Weinstein, H. Integrated methods for the construction of three-dimensional models and computational probing of structure-function relations in G protein-coupled receptors. *Methods Neurosci.* **1995**, *25*, 366−428.
(30) Wang, C.; Jiang, Y.; Ma, J.; Wu, H.; Wacker, D.; Katritch, V.; Han, G. W.; Liu, W.; Huang, X. P.; Vardy, E.; McCorvy, J. D.; Gao, X.; Zhou, X. E.; Melcher, K.; Zhang, C.; Bai, F.; Yang, H.; Yang, L.; Jiang, H.; Roth, B. L.; Cherezov, V.; Stevens, R. C.; Xu, H. E. Structural basis for molecular recognition at serotonin receptors. *Science* **2013**, *340*, 610−614.
(31) Wacker, D.; Wang, C.; Katritch, V.; Han, G. W.; Huang, X. P.; Vardy, E.; McCorvy, J. D.; Jiang, Y.; Chu, M.; Siu, F. Y.; Liu, W.; Xu, H. E.; Cherezov, V.; Roth, B. L.; Stevens, R. C. Structural features for functional selectivity at serotonin receptors. *Science* **2013**, *340*, 615−619.
(32) Peng, Y.; McCorvy, J. D.; Harpsøe, K.; Lansu, K.; Yuan, S.; Popov, P.; Qu, L.; Pu, M.; Che, T.; Nikolajsen, L. F.; Huang, X. P.; Wu, Y.; Shen, L.; Bjorn-Yoshimoto, W. E.; Ding, K.; Wacker, D.; Han, G. W.; Cheng, J.; Katritch, V.; Jensen, A. A.; Hanson, M. A.; Zhao, S.; Gloriam, D. E.; Roth, B. L.; Stevens, R. C.; Liu, Z. J. 5-HT2C receptor structures reveal the structural basis of GPCR polypharmacology. *Cell* **2018**, *172*, 719−730.
(33) Thal, D. M.; Sun, B.; Feng, D.; Nawaratne, V.; Leach, K.; Felder, C. C.; Bures, M. G.; Evans, D. A.; Weis, W. I.; Bachhawat, P.; Kobilka, T. S.; Sexton, P. M.; Kobilka, B. K.; Christopoulos, A. Crystal structures of the M1 and M4 muscarinic acetylcholine receptors. *Nature* **2016**, *531*, 335−340.
(34) Kruse, A. C.; Ring, A. M.; Manglik, A.; Hu, J.; Hu, K.; Eitel, K.; Hubner, H.; Pardon, E.; Valant, C.; Sexton, P. M.; Christopoulos, A.; Felder, C. C.; Gmeiner, P.; Steyaert, J.; Weis, W. I.; Garcia, K. C.; Wess, J.; Kobilka, B. K. Activation and allosteric modulation of a muscarinic acetylcholine receptor. *Nature* **2013**, *504*, 101−106.
(35) Kruse, A. C.; Hu, J.; Pan, A. C.; Arlow, D. H.; Rosenbaum, D. M.; Rosemond, E.; Green, H. F.; Liu, T.; Chae, P. S.; Dror, R. O.; Shaw, D. E.; Weis, W. I.; Wess, J.; Kobilka, B. K. Structure and dynamics of the M3 muscarinic acetylcholine receptor. *Nature* **2012**, *482*, 552−556.
(36) Miller-Gallacher, J. L.; Nehme, R.; Warne, T.; Edwards, P. C.; Schertler, G. F.; Leslie, A. G.; Tate, C. G. The 2.1 A resolution structure of cyanopindolol-bound beta1-adrenoceptor identifies an intramembrane Na+ ion that stabilises the ligand-free receptor. *PLoS One* **2014**, *9*, e92727.
(37) Wang, S.; Che, T.; Levit, A.; Shoichet, B. K.; Wacker, D.; Roth, B. L. Structure of the D2 dopamine receptor bound to the atypical antipsychotic drug risperidone. *Nature* **2018**, *555*, 269−273.
(38) Chien, E. Y.; Liu, W.; Zhao, Q.; Katritch, V.; Han, G. W.; Hanson, M. A.; Shi, L.; Newman, A. H.; Javitch, J. A.; Cherezov, V.; Stevens, R. C. Structure of the human dopamine D3 receptor in complex with a D2/D3 selective antagonist. *Science* **2010**, *330*, 1091−1095.
(39) Wang, S.; Wacker, D.; Levit, A.; Che, T.; Betz, R. M.; McCorvy, J. D.; Venkatakrishnan, A. J.; Huang, X. P.; Dror, R. O.; Shoichet, B. K.; Roth, B. L. D4 dopamine receptor high-resolution structures enable the discovery of selective agonists. *Science* **2017**, *358*, 381−386.
(40) Shimamura, T.; Shiroishi, M.; Weyand, S.; Tsujimoto, H.; Winter, G.; Katritch, V.; Abagyan, R.; Cherezov, V.; Liu, W.; Han, G. W.; Kobayashi, T.; Stevens, R. C.; Iwata, S. Structure of the human histamine H1 receptor complex with doxepin. *Nature* **2011**, *475*, 65−70.
(41) Kooistra, A. J.; Vass, M.; McGuire, R.; Leurs, R.; de Esch, I. J.; Vriend, G.; Verhoeven, S.; de Graaf, C. 3D-e-Chem: Structural

DOI: 10.1021/acs.jmedchem.8b00836
J. Med. Chem. 2019, 62, 3784−3839

cheminformatics workflows for computer-aided drug discovery. *ChemMedChem* **2018**, *13*, 614−626.
(42) McGuire, R.; Verhoeven, S.; Vass, M.; Vriend, G.; de Esch, I. J.; Lusher, S. J.; Leurs, R.; Ridder, L.; Kooistra, A. J.; Ritschel, T.; de Graaf, C. 3D-e-Chem-VM: Structural cheminformatics research infrastructure in a freely available virtual machine. *J. Chem. Inf. Model.* **2017**, *57*, 115−121.
(43) Berthold, M. R.; Cebron, N.; Dill, F.; Gabriel, T. R.; Kötter, T.; Meinl, T.; Ohl, P.; Sieb, C.; Thiel, K.; Wiswedel, B. KNIME: The Konstanz Information Miner. In *Data Analysis, Machine Learning and Applications*, Springer: Berlin Heidelberg, 2007; pp 319−326.
(44) Kim, S.; Thiessen, P. A.; Bolton, E. E.; Chen, J.; Fu, G.; Gindulyte, A.; Han, L.; He, J.; He, S.; Shoemaker, B. A.; Wang, J.; Yu, B.; Zhang, J.; Bryant, S. H. PubChem Substance and Compound databases. *Nucleic Acids Res.* **2016**, *44*, D1202−1213.
(45) Granas, C.; Nordvall, G.; Larhammar, D. Site-directed mutagenesis of the human 5-HT1B receptor. *Eur. J. Pharmacol.* **1998**, *349*, 367−375.
(46) Granas, C.; Nordquist, J.; Mohell, N.; Larhammar, D. Site-directed mutagenesis of the 5-HT1B receptor increases the affinity of 5-HT for the agonist low-affinity conformation and reduces the intrinsic activity of 5-HT. *Eur. J. Pharmacol.* **2001**, *421*, 69−76.
(47) Parker, E. M.; Grisel, D. A.; Iben, L. G.; Shapiro, R. A. A single amino acid difference accounts for the pharmacological distinctions between the rat and human 5-hydroxytryptamine1B receptors. *J. Neurochem.* **1993**, *60*, 380−383.
(48) Oksenberg, D.; Marsters, S. A.; O'Dowd, B. F.; Jin, H.; Havlik, S.; Peroutka, S. J.; Ashkenazi, A. A single amino-acid difference confers major pharmacological variation between human and rodent 5-HT1B receptors. *Nature* **1992**, *360*, 161−163.
(49) Wurch, T.; Colpaert, F. C.; Pauwels, P. J. Chimeric receptor analysis of the ketanserin binding site in the human 5-Hydroxytryptamine1D receptor: importance of the second extracellular loop and fifth transmembrane domain in antagonist binding. *Mol. Pharmacol.* **1998**, *54*, 1088−1096.
(50) Johnson, M. P.; Loncharich, R. J.; Baez, M.; Nelson, D. L. Species variations in transmembrane region V of the 5-hydroxytryptamine type 2A receptor alter the structure-activity relationship of certain ergolines and tryptamines. *Mol. Pharmacol.* **1994**, *45*, 277−286.
(51) Keov, P.; Lopez, L.; Devine, S. M.; Valant, C.; Lane, J. R.; Scammells, P. J.; Sexton, P. M.; Christopoulos, A. Molecular mechanisms of bitopic ligand engagement with the M1 muscarinic acetylcholine receptor. *J. Biol. Chem.* **2014**, *289*, 23817−23837.
(52) Abdul-Ridha, A.; Lane, J. R.; Mistry, S. N.; Lopez, L.; Sexton, P. M.; Scammells, P. J.; Christopoulos, A.; Canals, M. Mechanistic insights into allosteric structure-function relationships at the M1 muscarinic acetylcholine receptor. *J. Biol. Chem.* **2014**, *289*, 33701−33711.
(53) Matsui, H.; Lazareno, S.; Birdsall, N. J. Probing of the location of the allosteric site on m1 muscarinic receptors by site-directed mutagenesis. *Mol. Pharmacol.* **1995**, *47*, 88−98.
(54) Zhu, J.; Taniguchi, T.; Takauji, R.; Suzuki, F.; Tanaka, T.; Muramatsu, I. Inverse agonism and neutral antagonism at a constitutively active alpha-1a adrenoceptor. *Br. J. Pharmacol.* **2000**, *131*, 546−552.
(55) Berman, H. M.; Westbrook, J.; Feng, Z.; Gilliland, G.; Bhat, T. N.; Weissig, H.; Shindyalov, I. N.; Bourne, P. E. The Protein Data Bank. *Nucleic Acids Res.* **2000**, *28*, 235−242.
(56) *Calculator*, 15.11.9.0; ChemAxon Ltd: Budapest, 2015.
(57) *Corina*, 3.49; Molecular Networks GmbH: Erlangen, Germany, 2011.
(58) Korb, O.; Stutzle, T.; Exner, T. E. PLANTS: Application of ant colony optimization to structure-based drug design. *Ant Colony Optimization and Swarm Intelligence, Proceedings* **2006**, *4150*, 247−258.
(59) Korb, O.; Stutzle, T.; Exner, T. E. Empirical scoring functions for advanced protein-ligand docking with PLANTS. *J. Chem. Inf. Model.* **2009**, *49*, 84−96.
(60) Liu, W.; Wacker, D.; Gati, C.; Han, G. W.; James, D.; Wang, D.; Nelson, G.; Weierstall, U.; Katritch, V.; Barty, A.; Zatsepin, N. A.; Li, D.; Messerschmidt, M.; Boutet, S.; Williams, G. J.; Koglin, J. E.; Seibert, M. M.; Wang, C.; Shah, S. T.; Basu, S.; Fromme, R.; Kupitz, C.; Rendek, K. N.; Grotjohann, I.; Fromme, P.; Kirian, R. A.; Beyerlein, K. R.; White, T. A.; Chapman, H. N.; Caffrey, M.; Spence, J. C.; Stevens, R. C.; Cherezov, V. Serial femtosecond crystallography of G protein-coupled receptors. *Science* **2013**, *342*, 1521−1524.
(61) Wacker, D.; Wang, S.; McCorvy, J. D.; Betz, R. M.; Venkatakrishnan, A. J.; Levit, A.; Lansu, K.; Schools, Z. L.; Che, T.; Nichols, D. E.; Shoichet, B. K.; Dror, R. O.; Roth, B. L. Crystal structure of an LSD-bound human serotonin receptor. *Cell* **2017**, *168*, 377−389.
(62) Ishchenko, A.; Wacker, D.; Kapoor, M.; Zhang, A.; Han, G. W.; Basu, S.; Patel, N.; Messerschmidt, M.; Weierstall, U.; Liu, W.; Katritch, V.; Roth, B. L.; Stevens, R. C.; Cherezov, V. Structural insights into the extracellular recognition of the human serotonin 2B receptor by an antibody. *Proc. Natl. Acad. Sci. U. S. A.* **2017**, *114*, 8223−8228.
(63) Yin, W.; Zhou, X. E.; Yang, D.; de Waal, P. W.; Wang, M.; Dai, A.; Cai, X.; Huang, C.-Y.; Liu, P.; Wang, X.; Yin, Y.; Liu, B.; Zhou, Y.; Wang, J.; Liu, H.; Caffrey, M.; Melcher, K.; Xu, Y.; Wang, M.-W.; Xu, H. E.; Jiang, Y. Crystal structure of the human 5-HT1B serotonin receptor bound to an inverse agonist. *Cell Discovery* **2018**, *4*, 12.
(64) *The Serotonin Receptors: From Molecular Pharmacology to Human Therapeutics*; The Receptors; Roth, B. L., Ed.; Humana Press, 2006.
(65) Durant, J. L.; Leland, B. A.; Henry, D. R.; Nourse, J. G. Reoptimization of MDL keys for use in drug discovery. *J. Chem. Inf. Comput. Sci.* **2002**, *42*, 1273−1280.
(66) Rogers, D.; Hahn, M. Extended-connectivity fingerprints. *J. Chem. Inf. Model.* **2010**, *50*, 742−754.
(67) Hawkins, P. C.; Skillman, A. G.; Nicholls, A. Comparison of shape-matching and docking as virtual screening tools. *J. Med. Chem.* **2007**, *50*, 74−82.
(68) Ho, B. Y.; Karschin, A.; Branchek, T.; Davidson, N.; Lester, H. A. The role of conserved aspartate and serine residues in ligand binding and in function of the 5-HT1A receptor: A site-directed mutation study. *FEBS Lett.* **1992**, *312*, 259−262.
(69) Guan, X. M.; Peroutka, S. J.; Kobilka, B. K. Identification of a single amino acid residue responsible for the binding of a class of beta-adrenergic receptor antagonists to 5-hydroxytryptamine1A receptors. *Mol. Pharmacol.* **1992**, *41*, 695−698.
(70) Kuipers, W.; Link, R.; Standaar, P. J.; Stoit, A. R.; Van Wijngaarden, I.; Leurs, R.; Ijzerman, A. P. Study of the interaction between aryloxypropanolamines and Asn386 in helix VII of the human 5-hydroxytryptamine1A receptor. *Mol. Pharmacol.* **1997**, *51*, 889−896.
(71) Adham, N.; Tamm, J. A.; Salon, J. A.; Vaysse, P. J.; Weinshank, R. L.; Branchek, T. A. A single point mutation increases the affinity of serotonin 5-HT1D alpha, 5-HT1D beta, 5-HT1E and 5-HT1F receptors for beta-adrenergic antagonists. *Neuropharmacology* **1994**, *33*, 387−391.
(72) Braden, M. R.; Parrish, J. C.; Naylor, J. C.; Nichols, D. E. Molecular interaction of serotonin 5-HT2A receptor residues Phe339(6.51) and Phe340(6.52) with superpotent N-benzyl phenethylamine agonists. *Mol. Pharmacol.* **2006**, *70*, 1956−1964.
(73) Christopher, J. A.; Brown, J.; Dore, A. S.; Errey, J. C.; Koglin, M.; Marshall, F. H.; Myszka, D. G.; Rich, R. L.; Tate, C. G.; Tehan, B.; Warne, T.; Congreve, M. Biophysical fragment screening of the beta1-adrenergic receptor: Identification of high affinity arylpiperazine leads using structure-based drug design. *J. Med. Chem.* **2013**, *56*, 3446−3455.
(74) Wang, C. D.; Gallaher, T. K.; Shih, J. C. Site-directed mutagenesis of the serotonin 5-hydroxytrypamine2 receptor: Identification of amino acids necessary for ligand binding and receptor activation. *Mol. Pharmacol.* **1993**, *43*, 931−940.
(75) Boess, F. G.; Monsma, F. J., Jr.; Sleight, A. J. Identification of residues in transmembrane regions III and VI that contribute to the

DOI: 10.1021/acs.jmedchem.8b00836
J. Med. Chem. 2019, 62, 3784−3839

ligand binding site of the serotonin 5-HT6 receptor. *J. Neurochem.* **1998**, *71*, 2169−2177.
(76) Mialet, J.; Dahmoune, Y.; Lezoualc'h, F.; Berque-Bestel, I.; Eftekhari, P.; Hoebeke, J.; Sicsic, S.; Langlois, M.; Fischmeister, R. Exploration of the ligand binding site of the human 5-HT(4) receptor by site-directed mutagenesis and molecular modeling. *Br. J. Pharmacol.* **2000**, *130*, 527−538.
(77) Kristiansen, K.; Kroeze, W. K.; Willins, D. L.; Gelber, E. I.; Savage, J. E.; Glennon, R. A.; Roth, B. L. A highly conserved aspartic acid (Asp-155) anchors the terminal amine moiety of tryptamines and is involved in membrane targeting of the 5-HT(2A) serotonin receptor but does not participate in activation via a "salt-bridge disruption" mechanism. *J. Pharmacol. Exp. Ther.* **2000**, *293*, 735−746.
(78) Manivet, P.; Schneider, B.; Smith, J. C.; Choi, D. S.; Maroteaux, L.; Kellermann, O.; Launay, J. M. The serotonin binding site of human and murine 5-HT2B receptors: Molecular modeling and site-directed mutagenesis. *J. Biol. Chem.* **2002**, *277*, 17170−17178.
(79) Joubert, L.; Claeysen, S.; Sebben, M.; Bessis, A. S.; Clark, R. D.; Martin, R. S.; Bockaert, J.; Dumuis, A. A 5-HT4 receptor transmembrane network implicated in the activity of inverse agonists but not agonists. *J. Biol. Chem.* **2002**, *277*, 25502−25511.
(80) Harris, R. N., 3rd; Stabler, R. S.; Repke, D. B.; Kress, J. M.; Walker, K. A.; Martin, R. S.; Brothers, J. M.; Ilnicka, M.; Lee, S. W.; Mirzadegan, T. Highly potent, non-basic 5-HT6 ligands. Site mutagenesis evidence for a second binding mode at 5-HT6 for antagonism. *Bioorg. Med. Chem. Lett.* **2010**, *20*, 3436−3440.
(81) Claeysen, S.; Joubert, L.; Sebben, M.; Bockaert, J.; Dumuis, A. A single mutation in the 5-HT4 receptor (5-HT4-R D100(3.32)A) generates a Gs-coupled receptor activated exclusively by synthetic ligands (RASSL). *J. Biol. Chem.* **2003**, *278*, 699−702.
(82) Rivail, L.; Giner, M.; Gastineau, M.; Berthouze, M.; Soulier, J. L.; Fischmeister, R.; Lezoualc'h, F.; Maigret, B.; Sicsic, S.; Berque-Bestel, I. New insights into the human 5-HT4 receptor binding site: Exploration of a hydrophobic pocket. *Br. J. Pharmacol.* **2004**, *143*, 361−370.
(83) Impellizzeri, A. A.R.; Pappalardo, M.; Basile, L.; Manfra, O.; Andressen, K. W.; Krobert, K. A.; Messina, A.; Levy, F. O.; Guccione, S. Identification of essential residues for binding and activation in the human 5-HT7(a) serotonin receptor by molecular modeling and site-directed mutagenesis. *Front. Behav. Neurosci.* **2015**, *9*, 92.
(84) Choudhary, M. S.; Sachs, N.; Uluer, A.; Glennon, R. A.; Westkaemper, R. B.; Roth, B. L. Differential ergoline and ergopeptine binding to 5-hydroxytryptamine2A receptors: Ergolines require an aromatic residue at position 340 for high affinity binding. *Mol. Pharmacol.* **1995**, *47*, 450−457.
(85) Hirst, W. D.; Abrahamsen, B.; Blaney, F. E.; Calver, A. R.; Aloj, L.; Price, G. W.; Medhurst, A. D. Differences in the central nervous system distribution and pharmacology of the mouse 5-hydroxytryptamine-6 receptor compared with rat and human receptors investigated by radioligand binding, site-directed mutagenesis, and molecular modeling. *Mol. Pharmacol.* **2003**, *64*, 1295−1308.
(86) Almaula, N.; Ebersole, B. J.; Ballesteros, J. A.; Weinstein, H.; Sealfon, S. C. Contribution of a helix 5 locus to selectivity of hallucinogenic and nonhallucinogenic ligands for the human 5-hydroxytryptamine2A and 5-hydroxytryptamine2C receptors: Direct and indirect effects on ligand affinity mediated by the same locus. *Mol. Pharmacol.* **1996**, *50*, 34−42.
(87) Boess, F. G.; Monsma, F. J., Jr.; Meyer, V.; Zwingelstein, C.; Sleight, A. J. Interaction of tryptamine and ergoline compounds with threonine 196 in the ligand binding site of the 5-hydroxytryptamine6 receptor. *Mol. Pharmacol.* **1997**, *52*, 515−523.
(88) Córdova-Sintjago, T. C.; Liu, Y.; Booth, R. G. Molecular interactions of agonist and inverse agonist ligands at serotonin 5-HT2C G protein-coupled receptors: Computational ligand docking and molecular dynamics studies validated by experimental mutagenesis results. *Mol. Phys.* **2015**, *113*, 348−358.
(89) Wurch, T.; Pauwels, P. J. Coupling of canine serotonin 5-HT(1B) and 5-HT(1D) receptor subtypes to the formation of inositol phosphates by dual interactions with endogenous G(i/o) and recombinant G(alpha15) proteins. *J. Neurochem.* **2000**, *75*, 1180−1189.
(90) Pregenzer, J. F.; Alberts, G. L.; Im, W. B.; Slightom, J. L.; Ennis, M. D.; Hoffman, R. L.; Ghazal, N. B.; TenBrink, R. E. Differential pharmacology between the guinea-pig and the gorilla 5-HT1D receptor as probed with isochromans (5-HT1D-selective ligands). *Br. J. Pharmacol.* **1999**, *127*, 468−472.
(91) Granas, C.; Larhammar, D. Identification of an amino acid residue important for binding of methiothepin and Sumatriptan to the human 5-HT(1B) receptor. *Eur. J. Pharmacol.* **1999**, *380*, 171−181.
(92) Shapiro, D. A.; Kristiansen, K.; Kroeze, W. K.; Roth, B. L. Differential modes of agonist binding to 5-hydroxytryptamine(2A) serotonin receptors revealed by mutation and molecular modeling of conserved residues in transmembrane region 5. *Mol. Pharmacol.* **2000**, *58*, 877−886.
(93) Pellissier, L. P.; Sallander, J.; Campillo, M.; Gaven, F.; Queffeulou, E.; Pillot, M.; Dumuis, A.; Claeysen, S.; Bockaert, J.; Pardo, L. Conformational toggle switches implicated in basal constitutive and agonist-induced activated states of 5-hydroxytryptamine-4 receptors. *Mol. Pharmacol.* **2009**, *75*, 982−990.
(94) de la Fuente, T.; Martin-Fontecha, M.; Sallander, J.; Benhamu, B.; Campillo, M.; Medina, R. A.; Pellissier, L. P.; Claeysen, S.; Dumuis, A.; Pardo, L.; Lopez-Rodriguez, M. L. Benzimidazole derivatives as new serotonin 5-HT6 receptor antagonists. Molecular mechanisms of receptor inactivation. *J. Med. Chem.* **2010**, *53*, 1357−1369.
(95) Canal, C. E.; Cordova-Sintjago, T. C.; Villa, N. Y.; Fang, L. J.; Booth, R. G. Drug discovery targeting human 5-HT(2C) receptors: Residues S3.36 and Y7.43 impact ligand-binding pocket structure via hydrogen bond formation. *Eur. J. Pharmacol.* **2011**, *673*, 1−12.
(96) Choudhary, M. S.; Craigo, S.; Roth, B. L. A single point mutation (Phe340→Leu340) of a conserved phenylalanine abolishes 4-[125I]iodo-(2,5-dimethoxy)phenylisopropylamine and [3H]-mesulergine but not [3H]ketanserin binding to 5-hydroxytryptamine2 receptors. *Mol. Pharmacol.* **1993**, *43*, 755−761.
(97) Glennon, R. A.; Dukat, M.; Westkaemper, R. B.; Ismaiel, A. M.; Izzarelli, D. G.; Parker, E. M. The binding of propranolol at 5-hydroxytryptamine1D beta T355N mutant receptors may involve formation of two hydrogen bonds to asparagine. *Mol. Pharmacol.* **1996**, *49*, 198−206.
(98) Almaula, N.; Ebersole, B. J.; Zhang, D.; Weinstein, H.; Sealfon, S. C. Mapping the binding site pocket of the serotonin 5-hydroxytryptamine2A receptor. Ser3.36(159) provides a second interaction site for the protonated amine of serotonin but not of lysergic acid diethylamide or bufotenin. *J. Biol. Chem.* **1996**, *271*, 14672−14675.
(99) Parker, E. M.; Izzarelli, D. G.; Lewis-Higgins, L.; Palmer, D.; Shapiro, R. A. Two amino acid differences in the sixth transmembrane domain are partially responsible for the pharmacological differences between the 5-HT1D beta and 5-HT1E 5-hydroxytryptamine receptors. *J. Neurochem.* **1996**, *67*, 2096−2103.
(100) Roth, B. L.; Shoham, M.; Choudhary, M. S.; Khan, N. Identification of conserved aromatic residues essential for agonist binding and second messenger production at 5-hydroxytryptamine2A receptors. *Mol. Pharmacol.* **1997**, *52*, 259−266.
(101) Haga, K.; Kruse, A. C.; Asada, H.; Yurugi-Kobayashi, T.; Shiroishi, M.; Zhang, C.; Weis, W. I.; Okada, T.; Kobilka, B. K.; Haga, T.; Kobayashi, T. Structure of the human M2 muscarinic acetylcholine receptor bound to an antagonist. *Nature* **2012**, *482*, 547−551.
(102) Thorsen, T. S.; Matt, R.; Weis, W. I.; Kobilka, B. K. Modified T4 lysozyme fusion proteins facilitate G protein-coupled receptor crystallogenesis. *Structure* **2014**, *22*, 1657−1664.
(103) Bakker, R. A.; Nicholas, M. W.; Smith, T. T.; Burstein, E. S.; Hacksell, U.; Timmerman, H.; Leurs, R.; Brann, M. R.; Weiner, D. M. In vitro pharmacology of clinically used central nervous system-active drugs as inverse H(1) receptor agonists. *J. Pharmacol. Exp. Ther.* **2007**, *322*, 172−179.
(104) Manfra, O.; Van Craenenbroeck, K.; Skieterska, K.; Frimurer, T.; Schwartz, T. W.; Levy, F. O.; Andressen, K. W. Downregulation of

DOI: 10.1021/acs.jmedchem.8b00836
J. Med. Chem. 2019, 62, 3784−3839

5-HT7 serotonin receptors by the atypical antipsychotics clozapine and olanzapine. Role of motifs in the C-terminal domain and interaction with GASP-1. *ACS Chem. Neurosci.* **2015**, *6*, 1206−1218.
(105) Faron-Gorecka, A.; Gorecki, A.; Kusmider, M.; Wasylewski, Z.; Dziedzicka-Wasylewska, M. The role of D1-D2 receptor heterodimerization in the mechanism of action of clozapine. *Eur. Neuropsychopharmacol.* **2008**, *18*, 682−691.
(106) Spalding, T. A.; Ma, J. N.; Ott, T. R.; Friberg, M.; Bajpai, A.; Bradley, S. R.; Davis, R. E.; Brann, M. R.; Burstein, E. S. Structural requirements of transmembrane domain 3 for activation by the M1 muscarinic receptor agonists AC-42, AC-260584, clozapine, and N-desmethylclozapine: Evidence for three distinct modes of receptor activation. *Mol. Pharmacol.* **2006**, *70*, 1974−1983.
(107) Jongejan, A.; Lim, H. D.; Smits, R. A.; de Esch, I. J.; Haaksma, E.; Leurs, R. Delineation of agonist binding to the human histamine H4 receptor using mutational analysis, homology modeling, and ab initio calculations. *J. Chem. Inf. Model.* **2008**, *48*, 1455−1463.
(108) Mitchelson, F. J. The pharmacology of McN-A-343. *Pharmacol. Ther.* **2012**, *135*, 216−245.
(109) Abdul-Ridha, A.; Lopez, L.; Keov, P.; Thal, D. M.; Mistry, S. N.; Sexton, P. M.; Lane, J. R.; Canals, M.; Christopoulos, A. Molecular determinants of allosteric modulation at the M1 muscarinic acetylcholine receptor. *J. Biol. Chem.* **2014**, *289*, 6067−6079.
(110) Hulme, E. C.; Curtis, C. A.; Page, K. M.; Jones, P. G. The role of charge interactions in muscarinic agonist binding, and receptor-response coupling. *Life Sci.* **1995**, *56*, 891−898.
(111) Page, K. M.; Curtis, C. A.; Jones, P. G.; Hulme, E. C. The functional role of the binding site aspartate in muscarinic acetylcholine receptors, probed by site-directed mutagenesis. *Eur. J. Pharmacol., Mol. Pharmacol. Sect.* **1995**, *289*, 429−437.
(112) Schwarz, R. D.; Spencer, C. J.; Jaen, J. C.; Mirzadegan, T.; Moreland, D.; Tecle, H.; Thomas, A. J. Mutations of aspartate 103 in the Hm2 receptor and alterations in receptor binding properties of muscarinic agonists. *Life Sci.* **1995**, *56*, 923−929.
(113) Tautermann, C. S.; Kiechle, T.; Seeliger, D.; Diehl, S.; Wex, E.; Banholzer, R.; Gantner, F.; Pieper, M. P.; Casarosa, P. Molecular basis for the long duration of action and kinetic selectivity of tiotropium for the muscarinic M3 receptor. *J. Med. Chem.* **2013**, *56*, 8746−8756.
(114) Leach, K.; Davey, A. E.; Felder, C. C.; Sexton, P. M.; Christopoulos, A. The role of transmembrane domain 3 in the actions of orthosteric, allosteric, and atypical agonists of the M4 muscarinic acetylcholine receptor. *Mol. Pharmacol.* **2011**, *79*, 855−865.
(115) Lu, Z. L.; Hulme, E. C. The functional topography of transmembrane domain 3 of the M1 muscarinic acetylcholine receptor, revealed by scanning mutagenesis. *J. Biol. Chem.* **1999**, *274*, 7309−7315.
(116) Gregory, K. J.; Hall, N. E.; Tobin, A. B.; Sexton, P. M.; Christopoulos, A. Identification of orthosteric and allosteric site mutations in M2 muscarinic acetylcholine receptors that contribute to ligand-selective signaling bias. *J. Biol. Chem.* **2010**, *285*, 7459−7474.
(117) Goodwin, J. A.; Hulme, E. C.; Langmead, C. J.; Tehan, B. G. Roof and floor of the muscarinic binding pocket: Variations in the binding modes of orthosteric ligands. *Mol. Pharmacol.* **2007**, *72*, 1484−1496.
(118) Wess, J.; Nanavati, S.; Vogel, Z.; Maggio, R. Functional role of proline and tryptophan residues highly conserved among G protein-coupled receptors studied by mutational analysis of the m3 muscarinic receptor. *EMBO J.* **1993**, *12*, 331−338.
(119) Lu, Z. L.; Saldanha, J. W.; Hulme, E. C. Transmembrane domains 4 and 7 of the M(1) muscarinic acetylcholine receptor are critical for ligand binding and the receptor activation switch. *J. Biol. Chem.* **2001**, *276*, 34098−34104.
(120) Nawaratne, V.; Leach, K.; Felder, C. C.; Sexton, P. M.; Christopoulos, A. Structural determinants of allosteric agonism and modulation at the M4 muscarinic acetylcholine receptor: Identification of ligand-specific and global activation mechanisms. *J. Biol. Chem.* **2010**, *285*, 19012−19021.
(121) Wess, J.; Gdula, D.; Brann, M. R. Site-directed mutagenesis of the m3 muscarinic receptor: Identification of a series of threonine and tyrosine residues involved in agonist but not antagonist binding. *EMBO J.* **1991**, *10*, 3729−3734.
(122) Hou, X.; Wehrle, J.; Menge, W.; Ciccarelli, E.; Wess, J.; Mutschler, E.; Lambrecht, G.; Timmerman, H.; Waelbroeck, M. Influence of monovalent cations on the binding of a charged and an uncharged ('carbo'-)muscarinic antagonist to muscarinic receptors. *Br. J. Pharmacol.* **1996**, *117*, 955−961.
(123) Bourdon, H.; Trumpp-Kallmeyer, S.; Schreuder, H.; Hoflack, J.; Hibert, M.; Wermuth, C. G. Modelling of the binding site of the human m1 muscarinic receptor: Experimental validation and refinement. *J. Comput.-Aided Mol. Des.* **1997**, *11*, 317−332.
(124) Ward, S. D.; Curtis, C. A.; Hulme, E. C. Alanine-scanning mutagenesis of transmembrane domain 6 of the M(1) muscarinic acetylcholine receptor suggests that Tyr381 plays key roles in receptor function. *Mol. Pharmacol.* **1999**, *56*, 1031−1041.
(125) Vogel, W. K.; Sheehan, D. M.; Schimerlik, M. I. Site-directed mutagenesis on the m2 muscarinic acetylcholine receptor: The significance of Tyr403 in the binding of agonists and functional coupling. *Mol. Pharmacol.* **1997**, *52*, 1087−1094.
(126) Mosser, V. A.; Amana, I. J.; Schimerlik, M. I. Kinetic analysis of M2 muscarinic receptor activation of Gi in Sf9 insect cell membranes. *J. Biol. Chem.* **2002**, *277*, 922−931.
(127) Huang, X. P.; Nagy, P. I.; Williams, F. E.; Peseckis, S. M.; Messer, W. S., Jr Roles of threonine 192 and asparagine 382 in agonist and antagonist interactions with M1 muscarinic receptors. *Br. J. Pharmacol.* **1999**, *126*, 735−745.
(128) Bluml, K.; Mutschler, E.; Wess, J. Functional role in ligand binding and receptor activation of an asparagine residue present in the sixth transmembrane domain of all muscarinic acetylcholine receptors. *J. Biol. Chem.* **1994**, *269*, 18870−18876.
(129) Spalding, T. A.; Burstein, E. S.; Henderson, S. C.; Ducote, K. R.; Brann, M. R. Identification of a ligand-dependent switch within a muscarinic receptor. *J. Biol. Chem.* **1998**, *273*, 21563−21568.
(130) Hulme, E. C.; Lu, Z. L.; Bee, M. S. Scanning mutagenesis studies of the M1 muscarinic acetylcholine receptor. *Recept. Channels* **2003**, *9*, 215−228.
(131) Heitz, F.; Holzwarth, J. A.; Gies, J. P.; Pruss, R. M.; Trumpp-Kallmeyer, S.; Hibert, M. F.; Guenet, C. Site-directed mutagenesis of the putative human muscarinic M2 receptor binding site. *Eur. J. Pharmacol.* **1999**, *380*, 183−195.
(132) Schmidt, C.; Li, B.; Bloodworth, L.; Erlenbach, I.; Zeng, F. Y.; Wess, J. Random mutagenesis of the M3 muscarinic acetylcholine receptor expressed in yeast. Identification of point mutations that "silence" a constitutively active mutant M3 receptor and greatly impair receptor/G protein coupling. *J. Biol. Chem.* **2003**, *278*, 30248−30260.
(133) Kappel, K.; Miao, Y.; McCammon, J. A. Accelerated molecular dynamics simulations of ligand binding to a muscarinic G-protein-coupled receptor. *Q. Rev. Biophys.* **2015**, *48*, 479−487.
(134) Drubbisch, V.; Lameh, J.; Philip, M.; Sharma, Y. K.; Sadee, W. Mapping the ligand binding pocket of the human muscarinic cholinergic receptor Hm1: Contribution of tyrosine-82. *Pharm. Res.* **1992**, *9*, 1644−1647.
(135) Lebon, G.; Langmead, C. J.; Tehan, B. G.; Hulme, E. C. Mutagenic mapping suggests a novel binding mode for selective agonists of M1 muscarinic acetylcholine receptors. *Mol Pharmacol.* **2009**, *75*, 331−341.
(136) Avlani, V. A.; Langmead, C. J.; Guida, E.; Wood, M. D.; Tehan, B. G.; Herdon, H. J.; Watson, J. M.; Sexton, P. M.; Christopoulos, A. Orthosteric and allosteric modes of interaction of novel selective agonists of the M1 muscarinic acetylcholine receptor. *Mol. Pharmacol.* **2010**, *78*, 94−104.
(137) Suga, H.; Sawyer, G. W.; Ehlert, F. J. Mutagenesis of nucleophilic residues near the orthosteric binding pocket of M1 and M2 muscarinic receptors: Effect on the binding of nitrogen mustard analogs of acetylcholine and McN-A-343. *Mol. Pharmacol.* **2010**, *78*, 745−755.

DOI: 10.1021/acs.jmedchem.8b00836
J. Med. Chem. 2019, 62, 3784−3839

(138) Huang, X. P.; Prilla, S.; Mohr, K.; Ellis, J. Critical amino acid residues of the common allosteric site on the M2 muscarinic acetylcholine receptor: More similarities than differences between the structurally divergent agents gallamine and bis(ammonio)alkane-type hexamethylene-bis-[dimethyl-(3-phthalimidopropyl)ammonium]-dibromide. *Mol. Pharmacol.* **2005**, *68*, 769−778.
(139) Valant, C.; Gregory, K. J.; Hall, N. E.; Scammells, P. J.; Lew, M. J.; Sexton, P. M.; Christopoulos, A. A novel mechanism of G protein-coupled receptor functional selectivity. Muscarinic partial agonist McN-A-343 as a bitopic orthosteric/allosteric ligand. *J. Biol. Chem.* **2008**, *283*, 29312−29321.
(140) Scarselli, M.; Li, B.; Kim, S. K.; Wess, J. Multiple residues in the second extracellular loop are critical for M3 muscarinic acetylcholine receptor activation. *J. Biol. Chem.* **2007**, *282*, 7385−7396.
(141) Ellis, J.; Seidenberg, M. Site-directed mutagenesis implicates a threonine residue in TM6 in the subtype selectivities of UH-AH 37 and pirenzepine at muscarinic receptors. *Pharmacology* **2000**, *61*, 62−69.
(142) Dowling, M. R.; Willets, J. M.; Budd, D. C.; Charlton, S. J.; Nahorski, S. R.; Challiss, R. A. A single point mutation (N514Y) in the human M3 muscarinic acetylcholine receptor reveals differences in the properties of antagonists: Evidence for differential inverse agonism. *J. Pharmacol. Exp. Ther.* **2006**, *317*, 1134−1142.
(143) Gnagey, A. L.; Seidenberg, M.; Ellis, J. Site-directed mutagenesis reveals two epitopes involved in the subtype selectivity of the allosteric interactions of gallamine at muscarinic acetylcholine receptors. *Mol. Pharmacol.* **1999**, *56*, 1245−1253.
(144) Allman, K.; Page, K. M.; Curtis, C. A.; Hulme, E. C. Scanning mutagenesis identifies amino acid side chains in transmembrane domain 5 of the M(1) muscarinic receptor that participate in binding the acetyl methyl group of acetylcholine. *Mol. Pharmacol.* **2000**, *58*, 175−184.
(145) Krejci, A.; Tucek, S. Changes of cooperativity between N-methylscopolamine and allosteric modulators alcuronium and gallamine induced by mutations of external loops of muscarinic M(3) receptors. *Mol. Pharmacol.* **2001**, *60*, 761−767.
(146) Huang, X. P.; Williams, F. E.; Peseckis, S. M.; Messer, W. S., Jr Differential modulation of agonist potency and receptor coupling by mutations of Ser388Tyr and Thr389Pro at the junction of transmembrane domain VI and the third extracellular loop of human M(1) muscarinic acetylcholine receptors. *Mol. Pharmacol.* **1999**, *56*, 775−783.
(147) Savarese, T. M.; Wang, C. D.; Fraser, C. M. Site-directed mutagenesis of the rat m1 muscarinic acetylcholine receptor. Role of conserved cysteines in receptor function. *J. Biol. Chem.* **1992**, *267*, 11439−11448.
(148) Bee, M. S.; Hulme, E. C. Functional analysis of transmembrane domain 2 of the M1 muscarinic acetylcholine receptor. *J. Biol. Chem.* **2007**, *282*, 32471−32479.
(149) Stewart, G. D.; Sexton, P. M.; Christopoulos, A. Prediction of functionally selective allosteric interactions at an M3 muscarinic acetylcholine receptor mutant using Saccharomyces cerevisiae. *Mol. Pharmacol.* **2010**, *78*, 205−214.
(150) Suga, H.; Ehlert, F. J. Effects of asparagine mutagenesis of conserved aspartic acids in helix 2 (D2.50) and 3 (D3.32) of M1-M4 muscarinic receptors on the irreversible binding of nitrogen mustard analogs of acetylcholine and McN-A-343. *Biochemistry* **2013**, *52*, 4914−4928.
(151) Spalding, T. A.; Burstein, E. S.; Wells, J. W.; Brann, M. R. Constitutive activation of the m5 muscarinic receptor by a series of mutations at the extracellular end of transmembrane 6. *Biochemistry* **1997**, *36*, 10109−10116.
(152) Sato, T.; Baker, J.; Warne, T.; Brown, G. A.; Leslie, A. G.; Congreve, M.; Tate, C. G. Pharmacological analysis and structure determination of 7-methylcyanopindolol-bound beta1-adrenergic receptor. *Mol. Pharmacol.* **2015**, *88*, 1024−1034.
(153) Warne, T.; Edwards, P. C.; Leslie, A. G.; Tate, C. G. Crystal structures of a stabilized beta1-adrenoceptor bound to the biased agonists bucindolol and carvedilol. *Structure* **2012**, *20*, 841−849.
(154) Moukhametzianov, R.; Warne, T.; Edwards, P. C.; Serrano-Vega, M. J.; Leslie, A. G.; Tate, C. G.; Schertler, G. F. Two distinct conformations of helix 6 observed in antagonist-bound structures of a beta1-adrenergic receptor. *Proc. Natl. Acad. Sci. U. S. A.* **2011**, *108*, 8228−8232.
(155) Warne, T.; Serrano-Vega, M. J.; Baker, J. G.; Moukhametzianov, R.; Edwards, P. C.; Henderson, R.; Leslie, A. G.; Tate, C. G.; Schertler, G. F. Structure of a beta1-adrenergic G-protein-coupled receptor. *Nature* **2008**, *454*, 486−491.
(156) Leslie, A. G.; Warne, T.; Tate, C. G. Ligand occupancy in crystal structure of beta1-adrenergic G protein-coupled receptor. *Nat. Struct. Mol. Biol.* **2015**, *22*, 941−942.
(157) Warne, T.; Moukhametzianov, R.; Baker, J. G.; Nehme, R.; Edwards, P. C.; Leslie, A. G.; Schertler, G. F.; Tate, C. G. The structural basis for agonist and partial agonist action on a beta(1)-adrenergic receptor. *Nature* **2011**, *469*, 241−244.
(158) Wacker, D.; Fenalti, G.; Brown, M. A.; Katritch, V.; Abagyan, R.; Cherezov, V.; Stevens, R. C. Conserved binding mode of human beta2 adrenergic receptor inverse agonists and antagonist revealed by X-ray crystallography. *J. Am. Chem. Soc.* **2010**, *132*, 11443−11445.
(159) Zou, Y.; Weis, W. I.; Kobilka, B. K. N-terminal T4 lysozyme fusion facilitates crystallization of a G protein coupled receptor. *PLoS One* **2012**, *7*, e46039.
(160) Huang, C. Y.; Olieric, V.; Ma, P.; Howe, N.; Vogeley, L.; Liu, X.; Warshamanage, R.; Weinert, T.; Panepucci, E.; Kobilka, B.; Diederichs, K.; Wang, M.; Caffrey, M. In meso in situ serial X-ray crystallography of soluble and membrane proteins at cryogenic temperatures. *Acta Crystallogr D Struct Biol* **2016**, *72*, 93−112.
(161) Ma, P.; Weichert, D.; Aleksandrov, L. A.; Jensen, T. J.; Riordan, J. R.; Liu, X.; Kobilka, B. K.; Caffrey, M. The cubicon method for concentrating membrane proteins in the cubic mesophase. *Nat. Protoc.* **2017**, *12*, 1745−1762.
(162) Staus, D. P.; Strachan, R. T.; Manglik, A.; Pani, B.; Kahsai, A. W.; Kim, T. H.; Wingler, L. M.; Ahn, S.; Chatterjee, A.; Masoudi, A.; Kruse, A. C.; Pardon, E.; Steyaert, J.; Weis, W. I.; Prosser, R. S.; Kobilka, B. K.; Costa, T.; Lefkowitz, R. J. Allosteric nanobodies reveal the dynamic range and diverse mechanisms of G-protein-coupled receptor activation. *Nature* **2016**, *535*, 448−452.
(163) Liu, X.; Ahn, S.; Kahsai, A. W.; Meng, K. C.; Latorraca, N. R.; Pani, B.; Venkatakrishnan, A. J.; Masoudi, A.; Weis, W. I.; Dror, R. O.; Chen, X.; Lefkowitz, R. J.; Kobilka, B. K. Mechanism of intracellular allosteric beta2AR antagonist revealed by X-ray crystal structure. *Nature* **2017**, *548*, 480−484.
(164) Hanson, M. A.; Cherezov, V.; Griffith, M. T.; Roth, C. B.; Jaakola, V. P.; Chien, E. Y.; Velasquez, J.; Kuhn, P.; Stevens, R. C. A specific cholesterol binding site is established by the 2.8 A structure of the human beta2-adrenergic receptor. *Structure* **2008**, *16*, 897−905.
(165) Ring, A. M.; Manglik, A.; Kruse, A. C.; Enos, M. D.; Weis, W. I.; Garcia, K. C.; Kobilka, B. K. Adrenaline-activated structure of beta2-adrenoceptor stabilized by an engineered nanobody. *Nature* **2013**, *502*, 575−579.
(166) Rasmussen, S. G.; Choi, H. J.; Fung, J. J.; Pardon, E.; Casarosa, P.; Chae, P. S.; Devree, B. T.; Rosenbaum, D. M.; Thian, F. S.; Kobilka, T. S.; Schnapp, A.; Konetzki, I.; Sunahara, R. K.; Gellman, S. H.; Pautsch, A.; Steyaert, J.; Weis, W. I.; Kobilka, B. K. Structure of a nanobody-stabilized active state of the beta(2) adrenoceptor. *Nature* **2011**, *469*, 175−180.
(167) Rasmussen, S. G.; DeVree, B. T.; Zou, Y.; Kruse, A. C.; Chung, K. Y.; Kobilka, T. S.; Thian, F. S.; Chae, P. S.; Pardon, E.; Calinski, D.; Mathiesen, J. M.; Shah, S. T.; Lyons, J. A.; Caffrey, M.; Gellman, S. H.; Steyaert, J.; Skiniotis, G.; Weis, W. I.; Sunahara, R. K.; Kobilka, B. K. Crystal structure of the beta2 adrenergic receptor-Gs protein complex. *Nature* **2011**, *477*, 549−555.
(168) Weichert, D.; Kruse, A. C.; Manglik, A.; Hiller, C.; Zhang, C.; Hubner, H.; Kobilka, B. K.; Gmeiner, P. Covalent agonists for

DOI: 10.1021/acs.jmedchem.8b00836
J. Med. Chem. 2019, 62, 3784−3839

studying G protein-coupled receptor activation. *Proc. Natl. Acad. Sci. U. S. A.* **2014**, *111*, 10744−10748.
(169) Rosenbaum, D. M.; Zhang, C.; Lyons, J. A.; Holl, R.; Aragao, D.; Arlow, D. H.; Rasmussen, S. G.; Choi, H. J.; Devree, B. T.; Sunahara, R. K.; Chae, P. S.; Gellman, S. H.; Dror, R. O.; Shaw, D. E.; Weis, W. I.; Caffrey, M.; Gmeiner, P.; Kobilka, B. K. Structure and function of an irreversible agonist-beta(2) adrenoceptor complex. *Nature* **2011**, *469*, 236−240.
(170) Kooistra, A. J.; Leurs, R.; de Esch, I. J.; de Graaf, C. Structure-based prediction of G protein-coupled receptor ligand function: A beta-adrenoceptor case study. *J. Chem. Inf. Model.* **2015**, *55*, 1045−1061.
(171) Strader, C. D.; Gaffney, T.; Sugg, E. E.; Candelore, M. R.; Keys, R.; Patchett, A. A.; Dixon, R. A. Allele-specific activation of genetically engineered receptors. *J. Biol. Chem.* **1991**, *266*, 5−8.
(172) Strader, C. D.; Sigal, I. S.; Candelore, M. R.; Rands, E.; Hill, W. S.; Dixon, R. A. Conserved aspartic acid residues 79 and 113 of the beta-adrenergic receptor have different roles in receptor function. *J. Biol. Chem.* **1988**, *263*, 10267−10271.
(173) Strader, C. D.; Sigal, I. S.; Register, R. B.; Candelore, M. R.; Rands, E.; Dixon, R. A. Identification of residues required for ligand binding to the beta-adrenergic receptor. *Proc. Natl. Acad. Sci. U. S. A.* **1987**, *84*, 4384−4388.
(174) Takahashi, K.; Hossain, M.; Ahmed, M.; Bhuiyan, M. A.; Ohnuki, T.; Nagatomo, T. Asp125 and Thr130 in transmembrane domain 3 are major sites of alpha1b-adrenergic receptor antagonist binding. *Biol. Pharm. Bull.* **2007**, *30*, 1891−1894.
(175) Porter, J. E.; Hwa, J.; Perez, D. M. Activation of the alpha1b-adrenergic receptor is initiated by disruption of an interhelical salt bridge constraint. *J. Biol. Chem.* **1996**, *271*, 28318−28323.
(176) Suryanarayana, S.; Kobilka, B. K. Amino acid substitutions at position 312 in the seventh hydrophobic segment of the beta 2-adrenergic receptor modify ligand-binding specificity. *Mol. Pharmacol.* **1993**, *44*, 111−114.
(177) Sugimoto, Y.; Fujisawa, R.; Tanimura, R.; Lattion, A. L.; Cotecchia, S.; Tsujimoto, G.; Nagao, T.; Kurose, H. Beta(1)-selective agonist (−)-1-(3,4-dimethoxyphenetylamino)-3-(3,4-dihydroxy)-2-propanol [(−)-RO363] differentially interacts with key amino acids responsible for beta(1)-selective binding in resting and active states. *J. Pharmacol. Exp. Ther.* **2002**, *301*, 51−58.
(178) Chen, S.; Xu, M.; Lin, F.; Lee, D.; Riek, P.; Graham, R. M. Phe310 in transmembrane VI of the alpha1B-adrenergic receptor is a key switch residue involved in activation and catecholamine ring aromatic bonding. *J. Biol. Chem.* **1999**, *274*, 16320−16330.
(179) Greasley, P. J.; Fanelli, F.; Rossier, O.; Abuin, L.; Cotecchia, S. Mutagenesis and modelling of the alpha(1b)-adrenergic receptor highlight the role of the helix 3/helix 6 interface in receptor activation. *Mol. Pharmacol.* **2002**, *61*, 1025−1032.
(180) Tehan, B. G.; Bortolato, A.; Blaney, F. E.; Weir, M. P.; Mason, J. S. Unifying family A GPCR theories of activation. *Pharmacol. Ther.* **2014**, *143*, 51−60.
(181) Chen, S.; Lin, F.; Xu, M.; Riek, R. P.; Novotny, J.; Graham, R. M. Mutation of a single TMVI residue, Phe(282), in the beta(2)-adrenergic receptor results in structurally distinct activated receptor conformations. *Biochemistry* **2002**, *41*, 6045−6053.
(182) Hwa, J.; Graham, R. M.; Perez, D. M. Identification of critical determinants of alpha 1-adrenergic receptor subtype selective agonist binding. *J. Biol. Chem.* **1995**, *270*, 23189−23195.
(183) Wang, C. D.; Buck, M. A.; Fraser, C. M. Site-directed mutagenesis of alpha 2A-adrenergic receptors: Identification of amino acids involved in ligand binding and receptor activation by agonists. *Mol. Pharmacol.* **1991**, *40*, 168−179.
(184) Rudling, J. E.; Kennedy, K.; Evans, P. D. The effect of site-directed mutagenesis of two transmembrane serine residues on agonist-specific coupling of a cloned human alpha2A-adrenoceptor to adenylyl cyclase. *Br. J. Pharmacol.* **1999**, *127*, 877−886.
(185) Kikkawa, H.; Kurose, H.; Isogaya, M.; Sato, Y.; Nagao, T. Differential contribution of two serine residues of wild type and constitutively active beta2-adrenoceptors to the interaction with beta2-selective agonists. *Br. J. Pharmacol.* **1997**, *121*, 1059−1064.
(186) Liapakis, G.; Ballesteros, J. A.; Papachristou, S.; Chan, W. C.; Chen, X.; Javitch, J. A. The forgotten serine. A critical role for Ser-2035.42 in ligand binding to and activation of the beta 2-adrenergic receptor. *J. Biol. Chem.* **2000**, *275*, 37779−37788.
(187) Sato, T.; Kobayashi, H.; Nagao, T.; Kurose, H. Ser203 as well as Ser204 and Ser207 in fifth transmembrane domain of the human beta2-adrenoceptor contributes to agonist binding and receptor activation. *Br. J. Pharmacol.* **1999**, *128*, 272−274.
(188) Cavalli, A.; Fanelli, F.; Taddei, C.; De Benedetti, P. G.; Cotecchia, S. Amino acids of the alpha1B-adrenergic receptor involved in agonist binding: Differences in docking catecholamines to receptor subtypes. *FEBS Lett.* **1996**, *399*, 9−13.
(189) Pauwels, P. J.; Colpaert, F. C. Disparate ligand-mediated Ca(2+) responses by wild-type, mutant Ser(200)Ala and Ser(204)Ala alpha(2A)-adrenoceptor: G(alpha15) fusion proteins: evidence for multiple ligand-activation binding sites. *Br. J. Pharmacol.* **2000**, *130*, 1505−1512.
(190) Ambrosio, C.; Molinari, P.; Cotecchia, S.; Costa, T. Catechol-binding serines of beta(2)-adrenergic receptors control the equilibrium between active and inactive receptor states. *Mol. Pharmacol.* **2000**, *57*, 198−210.
(191) Cockcroft, V.; Frang, H.; Pihlavisto, M.; Marjamaki, A.; Scheinin, M. Ligand recognition of serine-cysteine amino acid exchanges in transmembrane domain 5 of alpha2-adrenergic receptors by UK 14,304. *J. Neurochem.* **2000**, *74*, 1705−1710.
(192) Peltonen, J. M.; Nyronen, T.; Wurster, S.; Pihlavisto, M.; Hoffren, A. M.; Marjamaki, A.; Xhaard, H.; Kanerva, L.; Savola, J. M.; Johnson, M. S.; Scheinin, M. Molecular mechanisms of ligand-receptor interactions in transmembrane domain V of the alpha2A-adrenoceptor. *Br. J. Pharmacol.* **2003**, *140*, 347−358.
(193) Salminen, T.; Varis, M.; Nyronen, T.; Pihlavisto, M.; Hoffren, A. M.; Lonnberg, T.; Marjamaki, A.; Frang, H.; Savola, J. M.; Scheinin, M.; Johnson, M. S. Three-dimensional models of alpha-(2A)-adrenergic receptor complexes provide a structural explanation for ligand binding. *J. Biol. Chem.* **1999**, *274*, 23405−23413.
(194) Wieland, K.; Zuurmond, H. M.; Krasel, C.; Ijzerman, A. P.; Lohse, M. J. Involvement of Asn-293 in stereospecific agonist recognition and in activation of the beta 2-adrenergic receptor. *Proc. Natl. Acad. Sci. U. S. A.* **1996**, *93*, 9276−9281.
(195) Frang, H.; Cockcroft, V.; Karskela, T.; Scheinin, M.; Marjamaki, A. Phenoxybenzamine binding reveals the helical orientation of the third transmembrane domain of adrenergic receptors. *J. Biol. Chem.* **2001**, *276*, 31279−31284.
(196) Hamaguchi, N.; True, T. A.; Saussy, D. L., Jr.; Jeffs, P. W. Phenylalanine in the second membrane-spanning domain of alpha 1A-adrenergic receptor determines subtype selectivity of dihydropyridine antagonists. *Biochemistry* **1996**, *35*, 14312−14317.
(197) Hamaguchi, N.; True, T. A.; Goetz, A. S.; Stouffer, M. J.; Lybrand, T. P.; Jeffs, P. W. Alpha 1-adrenergic receptor subtype determinants for 4-piperidyl oxazole antagonists. *Biochemistry* **1998**, *37*, 5730−5737.
(198) Zhao, M. M.; Hwa, J.; Perez, D. M. Identification of critical extracellular loop residues involved in alpha 1-adrenergic receptor subtype-selective antagonist binding. *Mol. Pharmacol.* **1996**, *50*, 1118−1126.
(199) Isogaya, M.; Yamagiwa, Y.; Fujita, S.; Sugimoto, Y.; Nagao, T.; Kurose, H. Identification of a key amino acid of the beta2-adrenergic receptor for high affinity binding of salmeterol. *Mol. Pharmacol.* **1998**, *54*, 616−622.
(200) Kikkawa, H.; Isogaya, M.; Nagao, T.; Kurose, H. The role of the seventh transmembrane region in high affinity binding of a beta 2-selective agonist TA-2005. *Mol. Pharmacol.* **1998**, *53*, 128−134.
(201) Marjamaki, A.; Frang, H.; Pihlavisto, M.; Hoffren, A. M.; Salminen, T.; Johnson, M. S.; Kallio, J.; Javitch, J. A.; Scheinin, M. Chloroethylclonidine and 2-aminoethyl methanethiosulfonate recognize two different conformations of the human alpha(2A)-adrenergic receptor. *J. Biol. Chem.* **1999**, *274*, 21867−21872.

DOI: 10.1021/acs.jmedchem.8b00836
J. Med. Chem. 2019, 62, 3784−3839

(202) Waugh, D. J.; Gaivin, R. J.; Zuscik, M. J.; Gonzalez-Cabrera, P.; Ross, S. A.; Yun, J.; Perez, D. M. Phe-308 and Phe-312 in transmembrane domain 7 are major sites of alpha 1-adrenergic receptor antagonist binding. Imidazoline agonists bind like antagonists. *J. Biol. Chem.* **2001**, *276*, 25366−25371.
(203) Link, R.; Daunt, D.; Barsh, G.; Chruscinski, A.; Kobilka, B. Cloning of two mouse genes encoding alpha 2-adrenergic receptor subtypes and identification of a single amino acid in the mouse alpha 2-C10 homolog responsible for an interspecies variation in antagonist binding. *Mol. Pharmacol.* **1992**, *42*, 16−27.
(204) Lei, B.; Morris, D. P.; Smith, M. P.; Svetkey, L. P.; Newman, M. F.; Rotter, J. I.; Buchanan, T. A.; Beckstrom-Sternberg, S. M.; Green, E. D.; Schwinn, D. A. Novel human alpha1a-adrenoceptor single nucleotide polymorphisms alter receptor pharmacology and biological function. *Naunyn-Schmiedeberg's Arch. Pharmacol.* **2005**, *371*, 229−239.
(205) Ahmed, M.; Hossain, M.; Bhuiyan, M. A.; Ishiguro, M.; Tanaka, T.; Muramatsu, I.; Nagatomo, T. Mutational analysis of the alpha 1a-adrenergic receptor binding pocket of antagonists by radioligand binding assay. *Biol. Pharm. Bull.* **2008**, *31*, 598−601.
(206) Dohlman, H. G.; Caron, M. G.; DeBlasi, A.; Frielle, T.; Lefkowitz, R. J. Role of extracellular disulfide-bonded cysteines in the ligand binding function of the beta 2-adrenergic receptor. *Biochemistry* **1990**, *29*, 2335−2342.
(207) Fraser, C. M. Site-directed mutagenesis of beta-adrenergic receptors. Identification of conserved cysteine residues that independently affect ligand binding and receptor activation. *J. Biol. Chem.* **1989**, *264*, 9266−9270.
(208) Green, S. A.; Cole, G.; Jacinto, M.; Innis, M.; Liggett, S. B. A polymorphism of the human beta 2-adrenergic receptor within the fourth transmembrane domain alters ligand binding and functional properties of the receptor. *J. Biol. Chem.* **1993**, *268*, 23116−23121.
(209) Noda, K.; Saad, Y.; Graham, R. M.; Karnik, S. S. The high affinity state of the beta 2-adrenergic receptor requires unique interaction between conserved and non-conserved extracellular loop cysteines. *J. Biol. Chem.* **1994**, *269*, 6743−6752.
(210) Hwa, J.; Graham, R. M.; Perez, D. M. Chimeras of alpha1-adrenergic receptor subtypes identify critical residues that modulate active state isomerization. *J. Biol. Chem.* **1996**, *271*, 7956−7964.
(211) Hwa, J.; Gaivin, R.; Porter, J. E.; Perez, D. M. Synergism of constitutive activity in alpha 1-adrenergic receptor activation. *Biochemistry* **1997**, *36*, 633−639.
(212) Gros, J.; Manning, B. S.; Pietri-Rouxel, F.; Guillaume, J. L.; Drumare, M. F.; Strosberg, A. D. Site-directed mutagenesis of the human beta3-adrenoceptor−transmembrane residues involved in ligand binding and signal transduction. *Eur. J. Biochem.* **1998**, *251*, 590−596.
(213) Marjamaki, A.; Pihlavisto, M.; Cockcroft, V.; Heinonen, P.; Savola, J. M.; Scheinin, M. Chloroethylclonidine binds irreversibly to exposed cysteines in the fifth membrane-spanning domain of the human alpha2A-adrenergic receptor. *Mol. Pharmacol.* **1998**, *53*, 370−376.
(214) Dorfler, M.; Tschammer, N.; Hamperl, K.; Hubner, H.; Gmeiner, P. Novel D3 selective dopaminergics incorporating enyne units as nonaromatic catechol bioisosteres: Synthesis, bioactivity, and mutagenesis studies. *J. Med. Chem.* **2008**, *51*, 6829−6838.
(215) Ehrlich, K.; Gotz, A.; Bollinger, S.; Tschammer, N.; Bettinetti, L.; Harterich, S.; Hubner, H.; Lanig, H.; Gmeiner, P. Dopamine D2, D3, and D4 selective phenylpiperazines as molecular probes to explore the origins of subtype specific receptor binding. *J. Med. Chem.* **2009**, *52*, 4923−4935.
(216) Daniell, S. J.; Strange, P. G.; Naylor, L. H. Site-directed mutagenesis of Tyr417 in the rat D2 dopamine receptor. *Biochem. Soc. Trans.* **1994**, *22*, 144S.
(217) Lan, H.; DuRand, C. J.; Teeter, M. M.; Neve, K. A. Structural determinants of pharmacological specificity between D(1) and D(2) dopamine receptors. *Mol. Pharmacol.* **2006**, *69*, 185−194.
(218) Ferruz, N.; Doerr, S.; Vanase-Frawley, M. A.; Zou, Y.; Chen, X.; Marr, E. S.; Nelson, R. T.; Kormos, B. L.; Wager, T. T.; Hou, X.; Villalobos, A.; Sciabola, S.; De Fabritiis, G. Dopamine D3 receptor antagonist reveals a cryptic pocket in aminergic GPCRs. *Sci. Rep.* **2018**, *8*, 897.
(219) Tomic, M.; Seeman, P.; George, S. R.; O'Dowd, B. F. Dopamine D1 receptor mutagenesis: Role of amino acids in agonist and antagonist binding. *Biochem. Biophys. Res. Commun.* **1993**, *191*, 1020−1027.
(220) Javitch, J. A.; Li, X.; Kaback, J.; Karlin, A. A cysteine residue in the third membrane-spanning segment of the human D2 dopamine receptor is exposed in the binding-site crevice. *Proc. Natl. Acad. Sci. U. S. A.* **1994**, *91*, 10355−10359.
(221) Javitch, J. A.; Fu, D.; Chen, J.; Karlin, A. Mapping the binding-site crevice of the dopamine D2 receptor by the substituted-cysteine accessibility method. *Neuron* **1995**, *14*, 825−831.
(222) Simpson, M. M.; Ballesteros, J. A.; Chiappa, V.; Chen, J.; Suehiro, M.; Hartman, D. S.; Godel, T.; Snyder, L. A.; Sakmar, T. P.; Javitch, J. A. Dopamine D4/D2 receptor selectivity is determined by A divergent aromatic microdomain contained within the second, third, and seventh membrane-spanning segments. *Mol. Pharmacol.* **1999**, *56*, 1116−1126.
(223) Alberts, G. L.; Pregenzer, J. F.; Im, W. B. Contributions of cysteine 114 of the human D3 dopamine receptor to ligand binding and sensitivity to external oxidizing agents. *Br. J. Pharmacol.* **1998**, *125*, 705−710.
(224) Cho, W.; Taylor, L. P.; Mansour, A.; Akil, H. Hydrophobic residues of the D2 dopamine receptor are important for binding and signal transduction. *J. Neurochem.* **1995**, *65*, 2105−2115.
(225) Tschammer, N.; Dorfler, M.; Hubner, H.; Gmeiner, P. Engineering a GPCR-ligand pair that simulates the activation of D(2L) by Dopamine. *ACS Chem. Neurosci.* **2010**, *1*, 25−35.
(226) Pollock, N. J.; Manelli, A. M.; Hutchins, C. W.; Steffey, M. E.; MacKenzie, R. G.; Frail, D. E. Serine mutations in transmembrane V of the dopamine D1 receptor affect ligand interactions and receptor activation. *J. Biol. Chem.* **1992**, *267*, 17780−17786.
(227) Fowler, J. C.; Bhattacharya, S.; Urban, J. D.; Vaidehi, N.; Mailman, R. B. Receptor conformations involved in dopamine D(2L) receptor functional selectivity induced by selected transmembrane-5 serine mutations. *Mol. Pharmacol.* **2012**, *81*, 820−831.
(228) Cox, B. A.; Henningsen, R. A.; Spanoyannis, A.; Neve, R. L.; Neve, K. A. Contributions of conserved serine residues to the interactions of ligands with dopamine D2 receptors. *J. Neurochem.* **1992**, *59*, 627−635.
(229) Wiens, B. L.; Nelson, C. S.; Neve, K. A. Contribution of serine residues to constitutive and agonist-induced signaling via the D2S dopamine receptor: Evidence for multiple, agonist-specific active conformations. *Mol. Pharmacol.* **1998**, *54*, 435−444.
(230) Wilcox, R. E.; Huang, W. H.; Brusniak, M. Y.; Wilcox, D. M.; Pearlman, R. S.; Teeter, M. M.; DuRand, C. J.; Wiens, B. L.; Neve, K. A. CoMFA-based prediction of agonist affinities at recombinant wild type versus serine to alanine point mutated D2 dopamine receptors. *J. Med. Chem.* **2000**, *43*, 3005−3019.
(231) Woodward, R.; Coley, C.; Daniell, S.; Naylor, L. H.; Strange, P. G. Investigation of the role of conserved serine residues in the long form of the rat D2 dopamine receptor using site-directed mutagenesis. *J. Neurochem.* **1996**, *66*, 394−402.
(232) Neve, K. A.; Wiens, B. L. Four ways of being an agonist: Multiple sequence determinants of efficacy at D2 dopamine receptors. *Biochem. Soc. Trans.* **1995**, *23*, 112−116.
(233) Sartania, N.; Strange, P. G. Role of conserved serine residues in the interaction of agonists with D3 dopamine receptors. *J. Neurochem.* **1999**, *72*, 2621−2624.
(234) Kortagere, S.; Cheng, S. Y.; Antonio, T.; Zhen, J.; Reith, M. E.; Dutta, A. K. Interaction of novel hybrid compounds with the D3 dopamine receptor: Site-directed mutagenesis and homology modeling studies. *Biochem. Pharmacol.* **2011**, *81*, 157−163.
(235) Cummings, D. F.; Ericksen, S. S.; Goetz, A.; Schetz, J. A. Transmembrane segment five serines of the D4 dopamine receptor uniquely influence the interactions of dopamine, norepinephrine, and Ro10−4548. *J. Pharmacol. Exp. Ther.* **2010**, *333*, 682−695.

DOI: 10.1021/acs.jmedchem.8b00836
J. Med. Chem. 2019, 62, 3784−3839

(236) Woodward, R.; Daniell, S. J.; Strange, P. G.; Naylor, L. H. Structural studies on D2 dopamine receptors: Mutation of a histidine residue specifically affects the binding of a subgroup of substituted benzamide drugs. *J. Neurochem.* **1994**, *62*, 1664−1669.
(237) Lundstrom, K.; Turpin, M. P.; Large, C.; Robertson, G.; Thomas, P.; Lewell, X. Q. Mapping of dopamine D3 receptor binding site by pharmacological characterization of mutants expressed in CHO cells with the Semliki Forest virus system. *J. Recept. Signal Transduction Res.* **1998**, *18*, 133−150.
(238) Tschammer, N.; Bollinger, S.; Kenakin, T.; Gmeiner, P. Histidine 6.55 is a major determinant of ligand-biased signaling in dopamine D2L receptor. *Mol. Pharmacol.* **2011**, *79*, 575−585.
(239) Schetz, J. A.; Benjamin, P. S.; Sibley, D. R. Nonconserved residues in the second transmembrane-spanning domain of the D(4) dopamine receptor are molecular determinants of D(4)-selective pharmacology. *Mol. Pharmacol.* **2000**, *57*, 144−152.
(240) Ericksen, S. S.; Cummings, D. F.; Teer, M. E.; Amdani, S.; Schetz, J. A. Ring substituents on substituted benzamide ligands indirectly mediate interactions with position 7.39 of transmembrane helix 7 of the D4 dopamine receptor. *J. Pharmacol. Exp. Ther.* **2012**, *342*, 472−485.
(241) Mistry, S. N.; Shonberg, J.; Draper-Joyce, C. J.; Klein Herenbrink, C.; Michino, M.; Shi, L.; Christopoulos, A.; Capuano, B.; Scammells, P. J.; Lane, J. R. Discovery of a novel class of negative allosteric modulator of the dopamine D2 receptor through fragmentation of a bitopic ligand. *J. Med. Chem.* **2015**, *58*, 6819−6843.
(242) Nonaka, H.; Otaki, S.; Ohshima, E.; Kono, M.; Kase, H.; Ohta, K.; Fukui, H.; Ichimura, M. Unique binding pocket for KW-4679 in the histamine H1 receptor. *Eur. J. Pharmacol.* **1998**, *345*, 111−117.
(243) Ohta, K.; Hayashi, H.; Mizuguchi, H.; Kagamiyama, H.; Fujimoto, K.; Fukui, H. Site-directed mutagenesis of the histamine H1 receptor: Roles of aspartic acid107, asparagine198 and threonine194. *Biochem. Biophys. Res. Commun.* **1994**, *203*, 1096−1101.
(244) Bakker, R. A.; Weiner, D. M.; ter Laak, T.; Beuming, T.; Zuiderveld, O. P.; Edelbroek, M.; Hacksell, U.; Timmerman, H.; Brann, M. R.; Leurs, R. 8R-lisuride is a potent stereospecific histamine H1-receptor partial agonist. *Mol. Pharmacol.* **2004**, *65*, 538−549.
(245) Bruysters, M.; Pertz, H. H.; Teunissen, A.; Bakker, R. A.; Gillard, M.; Chatelain, P.; Schunack, W.; Timmerman, H.; Leurs, R. Mutational analysis of the histamine H1-receptor binding pocket of histaprodifens. *Eur. J. Pharmacol.* **2004**, *487*, 55−63.
(246) Cordova-Sintjago, T. C.; Fang, L.; Bruysters, M.; Leurs, R.; Booth, R. G. Molecular determinants of ligand binding at the human histamine H1 receptor: Site-directed mutagenesis results analyzed with ligand docking and molecular dynamics studies at H1 homology and crystal structure models. *J. Chem. Pharm. Res.* **2012**, *4*, 2937−2951.
(247) Gantz, I.; DelValle, J.; Wang, L. D.; Tashiro, T.; Munzert, G.; Guo, Y. J.; Konda, Y.; Yamada, T. Molecular basis for the interaction of histamine with the histamine H2 receptor. *J. Biol. Chem.* **1992**, *267*, 20840−20843.
(248) Shin, N.; Coates, E.; Murgolo, N. J.; Morse, K. L.; Bayne, M.; Strader, C. D.; Monsma, F. J., Jr Molecular modeling and site-specific mutagenesis of the histamine-binding site of the histamine H4 receptor. *Mol. Pharmacol.* **2002**, *62*, 38−47.
(249) Bruysters, M.; Jongejan, A.; Gillard, M.; van de Manakker, F.; Bakker, R. A.; Chatelain, P.; Leurs, R. Pharmacological differences between human and guinea pig histamine H1 receptors: Asn84 (2.61) as key residue within an additional binding pocket in the H1 receptor. *Mol. Pharmacol.* **2005**, *67*, 1045−1052.
(250) Istyastono, E. P.; Nijmeijer, S.; Lim, H. D.; van de Stolpe, A.; Roumen, L.; Kooistra, A. J.; Vischer, H. F.; de Esch, I. J.; Leurs, R.; de Graaf, C. Molecular determinants of ligand binding modes in the histamine H(4) receptor: Linking ligand-based three-dimensional quantitative structure-activity relationship (3D-QSAR) models to in silico guided receptor mutagenesis studies. *J. Med. Chem.* **2011**, *54*, 8136−8147.
(251) Kuhne, S.; Kooistra, A. J.; Bosma, R.; Bortolato, A.; Wijtmans, M.; Vischer, H. F.; Mason, J. S.; de Graaf, C.; de Esch, I. J.; Leurs, R. Identification of ligand binding hot spots of the histamine H1 receptor following structure-based fragment optimization. *J. Med. Chem.* **2016**, *59*, 9047−9061.
(252) Jongejan, A.; Bruysters, M.; Ballesteros, J. A.; Haaksma, E.; Bakker, R. A.; Pardo, L.; Leurs, R. Linking agonist binding to histamine H1 receptor activation. *Nat. Chem. Biol.* **2005**, *1*, 98−103.
(253) Nijmeijer, S.; Engelhardt, H.; Schultes, S.; van de Stolpe, A. C.; Lusink, V.; de Graaf, C.; Wijtmans, M.; Haaksma, E. E.; de Esch, I. J.; Stachurski, K.; Vischer, H. F.; Leurs, R. Design and pharmacological characterization of VUF14480, a covalent partial agonist that interacts with cysteine 98(3.36) of the human histamine H(4) receptor. *Br. J. Pharmacol.* **2013**, *170*, 89−100.
(254) Wieland, K.; Laak, A. M.; Smit, M. J.; Kuhne, R.; Timmerman, H.; Leurs, R. Mutational analysis of the antagonist-binding site of the histamine H(1) receptor. *J. Biol. Chem.* **1999**, *274*, 29994−30000.
(255) Yao, B. B.; Hutchins, C. W.; Carr, T. L.; Cassar, S.; Masters, J. N.; Bennani, Y. L.; Esbenshade, T. A.; Hancock, A. A. Molecular modeling and pharmacological analysis of species-related histamine H(3) receptor heterogeneity. *Neuropharmacology* **2003**, *44*, 773−786.
(256) Lim, H. D.; de Graaf, C.; Jiang, W.; Sadek, P.; McGovern, P. M.; Istyastono, E. P.; Bakker, R. A.; de Esch, I. J.; Thurmond, R. L.; Leurs, R. Molecular determinants of ligand binding to H4R species variants. *Mol. Pharmacol.* **2010**, *77*, 734−743.
(257) Leurs, R.; Smit, M. J.; Tensen, C. P.; Ter Laak, A. M.; Timmerman, H. Site-directed mutagenesis of the histamine H1-receptor reveals a selective interaction of asparagine207 with subclasses of H1-receptor agonists. *Biochem. Biophys. Res. Commun.* **1994**, *201*, 295−301.
(258) Moguilevsky, N.; Varsalona, F.; Guillaume, J. P.; Noyer, M.; Gillard, M.; Daliers, J.; Henichart, J. P.; Bollen, A. Pharmacological and functional characterisation of the wild-type and site-directed mutants of the human H1 histamine receptor stably expressed in CHO cells. *J. Recept. Signal Transduction Res.* **1995**, *15*, 91−102.
(259) Uveges, A. J.; Kowal, D.; Zhang, Y.; Spangler, T. B.; Dunlop, J.; Semus, S.; Jones, P. G. The role of transmembrane helix 5 in agonist binding to the human H3 receptor. *J. Pharmacol. Exp. Ther.* **2002**, *301*, 451−458.
(260) Schultes, S.; Engelhardt, H.; Roumen, L.; Zuiderveld, O. P.; Haaksma, E. E.; de Esch, I. J.; Leurs, R.; de Graaf, C. Combining quantum mechanical ligand conformation analysis and protein modeling to elucidate GPCR-ligand binding modes. *ChemMedChem* **2013**, *8*, 49−53.
(261) Gillard, M.; Van Der Perren, C.; Moguilevsky, N.; Massingham, R.; Chatelain, P. Binding characteristics of cetirizine and levocetirizine to human H(1) histamine receptors: Contribution of Lys(191) and Thr(194). *Mol. Pharmacol.* **2002**, *61*, 391−399.
(262) Lim, H. D.; Jongejan, A.; Bakker, R. A.; Haaksma, E.; de Esch, I. J.; Leurs, R. Phenylalanine 169 in the second extracellular loop of the human histamine H4 receptor is responsible for the difference in agonist binding between human and mouse H4 receptors. *J. Pharmacol. Exp. Ther.* **2008**, *327*, 88−96.
(263) Wifling, D.; Loffel, K.; Nordemann, U.; Strasser, A.; Bernhardt, G.; Dove, S.; Seifert, R.; Buschauer, A. Molecular determinants for the high constitutive activity of the human histamine H4 receptor: Functional studies on orthologues and mutants. *Br. J. Pharmacol.* **2015**, *172*, 785−798.
(264) Schultes, S.; Nijmeijer, S.; Engelhardt, H.; Kooistra, A. J.; Vischer, H. F.; de Esch, I. J.; Haaksma, E.; Leurs, R.; de Graaf, C. Mapping histamine H4 receptor−ligand binding modes. *MedChemComm* **2013**, *4*, 193−204.
(265) Leurs, R.; Smit, M. J.; Meeder, R.; Ter Laak, A. M.; Timmerman, H. Lysine200 located in the fifth transmembrane domain of the histamine H1 receptor interacts with histamine but not with all H1 agonists. *Biochem. Biophys. Res. Commun.* **1995**, *214*, 110−117.
(266) Egan, C. T.; Herrick-Davis, K.; Teitler, M. Creation of a constitutively activated state of the 5-hydroxytryptamine2A receptor

DOI: 10.1021/acs.jmedchem.8b00836
J. Med. Chem. 2019, 62, 3784−3839

by site-directed mutagenesis: Inverse agonist activity of antipsychotic drugs. *J. Pharmacol. Exp. Ther.* **1998**, *286*, 85−90.
(267) Herrick-Davis, K.; Egan, C.; Teitler, M. Activating mutations of the serotonin 5-HT2C receptor. *J. Neurochem.* **1997**, *69*, 1138−1144.
(268) Claeysen, S.; Sebben, M.; Becamel, C.; Bockaert, J.; Dumuis, A. Novel brain-specific 5-HT4 receptor splice variants show marked constitutive activity: Role of the C-terminal intracellular domain. *Mol. Pharmacol.* **1999**, *55*, 910−920.
(269) Zhang, J.; Shen, C. P.; Xiao, J. C.; Lanza, T. J.; Lin, L. S.; Francis, B. E.; Fong, T. M.; Chen, R. Z. Effects of mutations at conserved TM II residues on ligand binding and activation of mouse 5-HT6 receptor. *Eur. J. Pharmacol.* **2006**, *534*, 77−82.
(270) Venkatakrishnan, A. J.; Deupi, X.; Lebon, G.; Tate, C. G.; Schertler, G. F.; Babu, M. M. Molecular signatures of G-protein-coupled receptors. *Nature* **2013**, *494*, 185−194.
(271) Venkatakrishnan, A. J.; Deupi, X.; Lebon, G.; Heydenreich, F. M.; Flock, T.; Miljus, T.; Balaji, S.; Bouvier, M.; Veprintsev, D. B.; Tate, C. G.; Schertler, G. F.; Babu, M. M. Diverse activation pathways in class A GPCRs converge near the G-protein-coupling region. *Nature* **2016**, *536*, 484−487.
(272) Jensen, A. A.; Pedersen, U. B.; Kiemer, A.; Din, N.; Andersen, P. H. Functional importance of the carboxyl tail cysteine residues in the human D1 dopamine receptor. *J. Neurochem.* **1995**, *65*, 1325−1331.
(273) Ballesteros, J. A.; Shi, L.; Javitch, J. A. Structural mimicry in G protein-coupled receptors: Implications of the high-resolution structure of rhodopsin for structure-function analysis of rhodopsin-like receptors. *Mol. Pharmacol.* **2001**, *60*, 1−19.
(274) Shi, L.; Javitch, J. A. The second extracellular loop of the dopamine D2 receptor lines the binding-site crevice. *Proc. Natl. Acad. Sci. U. S. A.* **2004**, *101*, 440−445.
(275) Guo, W.; Shi, L.; Javitch, J. A. The fourth transmembrane segment forms the interface of the dopamine D2 receptor homodimer. *J. Biol. Chem.* **2003**, *278*, 4385−4388.
(276) Xu, W.; Li, J.; Chen, C.; Huang, P.; Weinstein, H.; Javitch, J. A.; Shi, L.; de Riel, J. K.; Liu-Chen, L. Y. Comparison of the amino acid residues in the sixth transmembrane domains accessible in the binding-site crevices of mu, delta, and kappa opioid receptors. *Biochemistry* **2001**, *40*, 8018−8029.
(277) Nebane, N. M.; Hurst, D. P.; Carrasquer, C. A.; Qiao, Z.; Reggio, P. H.; Song, Z. H. Residues accessible in the binding-site crevice of transmembrane helix 6 of the CB2 cannabinoid receptor. *Biochemistry* **2008**, *47*, 13811−13821.
(278) Sanders, M. P.; Fleuren, W. W.; Verhoeven, S.; van den Beld, S.; Alkema, W.; de Vlieg, J.; Klomp, J. P. ss-TEA: Entropy based identification of receptor specific ligand binding residues from a multiple sequence alignment of class A GPCRs. *BMC Bioinf.* **2011**, *12*, 332.
(279) Sanders, M. P.; Verhoeven, S.; de Graaf, C.; Roumen, L.; Vroling, B.; Nabuurs, S. B.; de Vlieg, J.; Klomp, J. P. Snooker: A structure-based pharmacophore generation tool applied to class A GPCRs. *J. Chem. Inf. Model.* **2011**, *51*, 2277−2292.
(280) Strader, C. D.; Candelore, M. R.; Hill, W. S.; Sigal, I. S.; Dixon, R. A. Identification of two serine residues involved in agonist activation of the beta-adrenergic receptor. *J. Biol. Chem.* **1989**, *264*, 13572−13578.
(281) Katritch, V.; Rueda, M.; Lam, P. C.; Yeager, M.; Abagyan, R. GPCR 3D homology models for ligand screening: Lessons learned from blind predictions of adenosine A2a receptor complex. *Proteins: Struct., Funct., Genet.* **2010**, *78*, 197−211.
(282) de Graaf, C.; Rognan, D. Selective structure-based virtual screening for full and partial agonists of the beta2 adrenergic receptor. *J. Med. Chem.* **2008**, *51*, 4978−4985.
(283) Katritch, V.; Reynolds, K. A.; Cherezov, V.; Hanson, M. A.; Roth, C. B.; Yeager, M.; Abagyan, R. Analysis of full and partial agonists binding to beta2-adrenergic receptor suggests a role of transmembrane helix V in agonist-specific conformational changes. *J. Mol. Recognit.* **2009**, *22*, 307−318.
(284) Kooistra, A. J.; Vischer, H. F.; McNaught-Flores, D.; Leurs, R.; de Esch, I. J.; de Graaf, C. Function-specific virtual screening for GPCR ligands using a combined scoring method. *Sci. Rep.* **2016**, *6*, 28288.
(285) Ishikawa, M.; Watanabe, T.; Kudo, T.; Yokoyama, F.; Yamauchi, M.; Kato, K.; Kakui, N.; Sato, Y. Investigation of the histamine H3 receptor binding site. Design and synthesis of hybrid agonists with a lipophilic side chain. *J. Med. Chem.* **2010**, *53*, 6445−6456.
(286) Kiss, R.; Noszal, B.; Racz, A.; Falus, A.; Eros, D.; Keseru, G. M. Binding mode analysis and enrichment studies on homology models of the human histamine H4 receptor. *Eur. J. Med. Chem.* **2008**, *43*, 1059−1070.
(287) Lorenzi, S.; Mor, M.; Bordi, F.; Rivara, S.; Rivara, M.; Morini, G.; Bertoni, S.; Ballabeni, V.; Barocelli, E.; Plazzi, P. V. Validation of a histamine H3 receptor model through structure-activity relationships for classical H3 antagonists. *Bioorg. Med. Chem.* **2005**, *13*, 5647−5657.
(288) Schlegel, B.; Laggner, C.; Meier, R.; Langer, T.; Schnell, D.; Seifert, R.; Stark, H.; Holtje, H. D.; Sippl, W. Generation of a homology model of the human histamine H(3) receptor for ligand docking and pharmacophore-based screening. *J. Comput.-Aided Mol. Des.* **2007**, *21*, 437−453.
(289) Dror, R. O.; Green, H. F.; Valant, C.; Borhani, D. W.; Valcourt, J. R.; Pan, A. C.; Arlow, D. H.; Canals, M.; Lane, J. R.; Rahmani, R.; Baell, J. B.; Sexton, P. M.; Christopoulos, A.; Shaw, D. E. Structural basis for modulation of a G-protein-coupled receptor by allosteric drugs. *Nature* **2013**, *503*, 295−299.
(290) Bock, A.; Bermudez, M.; Krebs, F.; Matera, C.; Chirinda, B.; Sydow, D.; Dallanoce, C.; Holzgrabe, U.; De Amici, M.; Lohse, M. J.; Wolber, G.; Mohr, K. Ligand binding ensembles determine graded agonist efficacies at a G protein-coupled receptor. *J. Biol. Chem.* **2016**, *291*, 16375−16389.
(291) Schmitz, J.; van der Mey, D.; Bermudez, M.; Klockner, J.; Schrage, R.; Kostenis, E.; Trankle, C.; Wolber, G.; Mohr, K.; Holzgrabe, U. Dualsteric muscarinic antagonists−orthosteric binding pose controls allosteric subtype selectivity. *J. Med. Chem.* **2014**, *57*, 6739−6750.
(292) Lane, J. R.; Donthamsetti, P.; Shonberg, J.; Draper-Joyce, C. J.; Dentry, S.; Michino, M.; Shi, L.; Lopez, L.; Scammells, P. J.; Capuano, B.; Sexton, P. M.; Javitch, J. A.; Christopoulos, A. A new mechanism of allostery in a G protein-coupled receptor dimer. *Nat. Chem. Biol.* **2014**, *10*, 745−752.
(293) Vass, M.; Agai-Csongor, E.; Horti, F.; Keseru, G. M. Multiple fragment docking and linking in primary and secondary pockets of dopamine receptors. *ACS Med. Chem. Lett.* **2014**, *5*, 1010−1014.
(294) Lane, J. R.; Chubukov, P.; Liu, W.; Canals, M.; Cherezov, V.; Abagyan, R.; Stevens, R. C.; Katritch, V. Structure-based ligand discovery targeting orthosteric and allosteric pockets of dopamine receptors. *Mol. Pharmacol.* **2013**, *84*, 794−807.
(295) Clark, T.; Hennemann, M.; Murray, J. S.; Politzer, P. Halogen bonding: The sigma-hole. Proceedings of "Modeling interactions in biomolecules II", Prague, September 5th-9th, 2005. *J. Mol. Model.* **2007**, *13*, 291−296.
(296) Wilcken, R.; Zimmermann, M. O.; Lange, A.; Zahn, S.; Boeckler, F. M. Using halogen bonds to address the protein backbone: A systematic evaluation. *J. Comput.-Aided Mol. Des.* **2012**, *26*, 935−945.
(297) Partyka, A.; Kurczab, R.; Canale, V.; Satala, G.; Marciniec, K.; Pasierb, A.; Jastrzebska-Wiesek, M.; Pawlowski, M.; Wesolowska, A.; Bojarski, A. J.; Zajdel, P. The impact of the halogen bonding on D2 and 5-HT1A/5-HT7 receptor activity of azinesulfonamides of 4-[(2-ethyl)piperidinyl-1-yl]phenylpiperazines with antipsychotic and antidepressant properties. *Bioorg. Med. Chem.* **2017**, *25*, 3638−3648.
(298) DeVree, B. T.; Mahoney, J. P.; Velez-Ruiz, G. A.; Rasmussen, S. G.; Kuszak, A. J.; Edwald, E.; Fung, J. J.; Manglik, A.; Masureel, M.; Du, Y.; Matt, R. A.; Pardon, E.; Steyaert, J.; Kobilka, B. K.; Sunahara, R. K. Allosteric coupling from G protein to the agonist-binding pocket in GPCRs. *Nature* **2016**, *535*, 182−186.

DOI: 10.1021/acs.jmedchem.8b00836
J. Med. Chem. 2019, 62, 3784−3839

(299) Segala, E.; Guo, D.; Cheng, R. K.; Bortolato, A.; Deflorian, F.; Dore, A. S.; Errey, J. C.; Heitman, L. H.; Izjerman, A. P.; Marshall, F. H.; Cooke, R. M. Controlling the Dissociation of Ligands from the Adenosine A2A Receptor through Modulation of Salt Bridge Strength. *J. Med. Chem.* **2016**, *59*, 6470−6479.
(300) Swinney, D. C.; Beavis, P.; Chuang, K. T.; Zheng, Y.; Lee, I.; Gee, P.; Deval, J.; Rotstein, D. M.; Dioszegi, M.; Ravendran, P.; Zhang, J.; Sankuratri, S.; Kondru, R.; Vauquelin, G. A study of the molecular mechanism of binding kinetics and long residence times of human CCR5 receptor small molecule allosteric ligands. *Br. J. Pharmacol.* **2014**, *171*, 3364−3375.
(301) Alvarez-Curto, E.; Prihandoko, R.; Tautermann, C. S.; Zwier, J. M.; Pediani, J. D.; Lohse, M. J.; Hoffmann, C.; Tobin, A. B.; Milligan, G. Developing chemical genetic approaches to explore G protein-coupled receptor function: Validation of the use of a receptor activated solely by synthetic ligand (RASSL). *Mol. Pharmacol.* **2011**, *80*, 1033−1046.
(302) Gomez, J. L.; Bonaventura, J.; Lesniak, W.; Mathews, W. B.; Sysa-Shah, P.; Rodriguez, L. A.; Ellis, R. J.; Richie, C. T.; Harvey, B. K.; Dannals, R. F.; Pomper, M. G.; Bonci, A.; Michaelides, M. Chemogenetics revealed: DREADD occupancy and activation via converted clozapine. *Science* **2017**, *357*, 503−507.

DOI: 10.1021/acs.jmedchem.8b00836
J. Med. Chem. 2019, 62, 3784−3839